

**Partial Nitrification Processes for Ammonium Rich Sludge Thickening Lagoon  
Supernatant Treatment**

Yanxi Shao

A thesis submitted in partial fulfillment of the requirements for the degree of

Doctor of Philosophy

in Environmental Engineering

Department of Civil and Environmental Engineering

University of Alberta

© Yanxi Shao, 2018

## **Abstract**

In wastewater treatment, nitrogen removal is becoming increasingly challenging to meet the more stringent standards and regulations. At local wastewater treatment plant, nitrogen removal is challenging when the plant was experiencing shock loadings. Thus, improving the nitrogen removal is urgently needed at the wastewater treatment plant. It is found that more than 30% of the total nitrogen loading to the plant is contributed by returning the high ammonia strength lagoon supernatant separating from the anaerobically digested sludge. Technology improvement facilitates the nitrogen removal efficiency. Nitrogen is conventionally removed through complete nitrification processes. However, the processes may consume a large amount of oxygen to treat high ammonia strength wastewater. In this case, a more sustainable treatment using partial nitrification is preferred. The first part of this thesis was testing the applicability of integrated fixed film activated sludge (IFAS) technology to handle the shock loading conditions. The second part of this thesis focused on investigating the applicability of the IFAS technology in treating the high ammonia strength supernatant.

Complete nitrification was employed for low strength wastewater treatment. The complete nitrification oxidized ammonium to nitrite by ammonia oxidizing bacteria (AOB), and further to nitrate by nitrite oxidizing bacteria (NOB). For the partial nitrification, the process oxidized the ammonium to nitrite, instead of nitrate. The partial nitrification process saved 25% of the oxygen requirement, as compared to the complete nitrification process. If combining the partial nitrification with the denitrification process, the combined processes can even save 40% of carbon sources requirement for the denitrification.

In the first part of this thesis study, a bench top IFAS reactor was operated to investigate the ammonium removal efficiency and the stability of IFAS reactor in response to sudden operational condition changes. Suspended flocs and attached biofilm were the two major biomass aggregates in the IFAS reactors, the differences of the microbial structure and biodegradation kinetics of these two aggregates were explained in detail.

The second part of this study investigated the impact of ammonium concentration on the establishment of partial nitrification microbial community in an integrated fixed-film activated sludge (IFAS) reactor. Partial nitrification was achieved successfully under room temperature when the  $\text{NH}_4^+$ -N concentration in the feeding was greater than 400 mg/L. The ammonium nitrogen concentration in the digested sludge supernatant determined the free ammonia concentration, which was identified as the key controlling factor for the partial nitrification process. Molecular analysis confirmed that AOB abundance increased and NOB number reduced at high ammonium loading conditions. Compared with biofilm, suspended sludge played a major role in ammonium removal, which contributed to 66% total ammonium conversion. The impacts of feed water characteristics, including the ammonium concentration and the percentage of raw digested sludge liquor supernatant in the feed, on microbial population dynamics and nitrification kinetics were elucidated. It was observed that increased ammonium concentration in the reactor feed led to the enhanced specific ammonium conversion and nitrite accumulation rates but reduced microbial community diversity. The increased raw supernatant percentage reduced specific ammonium conversion and nitrite accumulation rates and led to an increased microbial community diversity. Microbial community structures varied significantly in suspended flocs and in attached biofilm.

The production and composition of extracellular polymeric substances (EPS) were important parameters of bioreactor performance. The characteristics of EPS from nitrification- and nitrification- dominant processes in the IFAS reactors were compared. The results showed that the

loosely bound EPS (LB-EPS) mainly consisted of polysaccharides, while tightly bound EPS (TB-EPS) were composed of polysaccharides and protein in variable ratios. The quantitative polymerase chain reaction and EPS composition analysis (X-ray photoelectron spectroscopy and three-dimensional excitation and emission matrix fluorescence) demonstrated that the microbial community structure determined the TB-EPS composition. Higher abundance of AOB was related to higher amide or amine like substances content and more aromatic and tryptophan protein like substances in TB-EPS. The decrease of heterotrophic bacteria and nitrite oxidizing bacteria correlated to a decreased hydrocarbon-like substance and humic acid like substances in the TB-EPS. Quartz crystal microbalance with dissipation studies demonstrated that the adsorption of TB-EPS to solid surface was stronger and less reversible as compared to the LB-EPS, which emphasized the importance of protein in cell adhesion.

# Preface

This thesis is an original work by Yanxi Shao. All of the studies conducted in this thesis was designed and planned by me and supervised by Professor Yang Liu at the University of Alberta and Mr. Abdul Mohammed from EPCOR Water Services Inc. All the research work was conducted by me except the following contribution from collaborators and coauthors:

## Chapter 3:

Professor Yang Liu, Dr. Yijing Shi and Mr. Abdul Mohammed contributed to the research planning; and Professor Yang Liu contributed to the manuscript edits.

## Chapter 4:

Professor Yang Liu and Mr. Abdul Mohammed contributed to the research planning; Mr. Sen Yang provided help with the sampling; and Professor Yang Liu contributed to the manuscript edits.

## Chapter 5:

Professor Yang Liu and Mr. Abdul Mohammed contributed to the research planning; Anna P. Florentino helped with the data analysis; and Professor Yang Liu, Ian Buchanan, and Mr. Abdul Mohammed contributed to the manuscript edits.

## Chapter 6:

Professor Yang Liu and Dr. Huixin Zhang contributed to the research planning; and Professor Yang Liu, Ian Buchanan, and Mr. Abdul Mohammed contributed to the manuscript edits.

## Chapter 7:

Professor Yang Liu and Mr. Abdul Mohammed contributed to the research planning.

*To my dear parents*

*Jiawen Shao*

*Fangying Wang*

*And to my beloved husband*

*Dr. Fan Xie*

# Acknowledgements

There are a number of people without whose support this thesis might not have been written, and to whom I want to express my sincere appreciation.

First of all, I want to thank my supervisors, Dr. Yang Liu and Mr. Abdul Mohammed. I am very lucky having both of them as my friends and supervisors over the past 5 years. They always provide clear guidance and generous support throughout my program. They lead me on a way to become a critical thinker and researcher.

I would like to thank the postdoctoral fellows in my research group. Dr. Yijing shi and Dr. Zhiya Sheng, Dr. Huixin Zhang and Dr. Anna P. Florentino, they all provided valuable suggestions and help during my research.

I would also like to thank my friends and colleagues, and technicians in my department: Sen Yang, Kingsley Nze, Chen Liang, Yupeng Zhao, and all my other colleagues for their generous support and understanding.

This project was supported by EPCOR Water Services Inc., the Natural Sciences and Engineering Research Council of Canada (NSERC) Collaborative Research and Development Grant in Strategies to Improve Ammonia Removal from Ammonia-Rich Sludge Liquor in Canada, NSERC Industrial Postgraduate Scholarship (IPS) program and Alberta Innovates.

## TABLE OF CONTENTS

CHAPTER 1. INTRODUCTION AND OBJECTIVES.....	1
1.1. Background and research motivation.....	1
1.2. Scope of research and objectives.....	3
1.3. Thesis organization.....	7
1.4. References.....	8
CHAPTER 2. LITERATURE REVIEW .....	9
2.1. Complete nitrification process partial nitrification process .....	9
2.1.1 Concepts and biochemistry .....	9
2.1.2 Nitrifying organisms .....	10
2.1.3 Achieving partial nitrification .....	13
2.1.3.1. Temperature .....	13
2.1.3.2. Dissolved oxygen (DO) .....	14
2.1.3.3. Free ammonia (FA), free nitrous acid (FNA), and free hydroxylamine (FH).....	14
2.1.3.4. pH .....	15
2.1.3.5. Operational mode.....	16
2.2. Denitritation process .....	16
2.3. Nitrous oxide production.....	18
2.4. Integrated fixed film activated sludge (IFAS) technology .....	20
2.5. Other partial nitrification related technologies.....	22
2.6. References.....	27
CHAPTER 3. WASTEWATER AMMONIA REMOVAL USING AN INTEGRATED FIXED-	



FILM ACTIVATED SLUDGE-SEQUENCING BATCH BIOFILM REACTOR (IFAS-SBR): COMPARISON OF SUSPENDED FLOCS AND ATTACHED BIOFILM.....	38
3.1. Introduction.....	38
3.2. Method and Material.....	40
3.2.1. Reactor operation.....	40
3.2.2. Biodegradation kinetics .....	42
3.2.3. Biomass in activated sludge and biofilm.....	42
3.2.4. Extracellular polymeric substance (EPS) analysis.....	43
3.2.5. q-PCR analysis.....	43
3.2.6. Statistical analysis.....	44
3.3. Results and Discussion.....	45
3.3.1. Reactor performance.....	45
3.3.2. Biomass concentrations .....	47
3.3.3. Effects of the C/N ratio on nitrifying bacteria.....	49
3.3.4. Ammonium removal kinetics.....	54
3.3.5. COD removal kinetics .....	57
3.3.6. EPS production.....	57
3.3.7. EPS composition.....	59
3.4. Conclusions .....	61
3.5. References.....	62
CHAPTER 4. IMPACTS OF AMMONIUM LOADING ON NITRITATION STABILITY AND MICROBIAL COMMUNITY DYNAMICS IN THE INTEGRATED FIXED-FILM ACTIVATED SLUDGE SEQUENCING BATCH REACTOR (IFAS-SBR) .....	68
4.1. Introduction.....	68

4.2. Methods and materials.....	70
4.2.1. Reactor operation.....	70
4.2.2. Analytical methods.....	71
4.2.3. DNA extraction and molecular microbiology analysis.....	72
4.2.4. Batch test and kinetics analysis .....	73
4.2.5. Statistical analysis .....	74
4.3. Results and Discussion.....	74
4.3.1. Reactor performance results.....	74
4.3.2. Impact of ammonia loading on ammonia conversion kinetics.....	78
4.3.3. Ammonium removal by biofilms and flocs.....	79
4.3.4. Microbial community analysis-qPCR .....	82
4.3.5. Microbial community analysis-next generation sequencing.....	85
4.4. Conclusions .....	87
4.5. References.....	87
CHAPTER 5. MICROBIAL POPULATION DYNAMICS IN A PARTIAL NITRIFICATION REACTOR TREATING HIGH AMMONIA STRENGTH SUPERNATANT FROM ANAEROBICALLY DIGESTED SLUDGE: ROLE OF THE FEED WATER CHARACTERISTICS.....	
5.1. Introduction .....	93
5.2. Methodology.....	95
5.2.1. Digested sludge supernatant collection.....	95
5.2.2. Reactors operation .....	96
5.2.3. Analytical methods.....	97
5.2.4. Cycle tests for nitrogen removal kinetics .....	98

5.2.5. DNA extraction and sequencing .....	98
5.2.6. Data analysis .....	98
5.3. Results and Discussion .....	99
5.3.1. Digested sludge supernatant characteristics.....	99
5.3.2. Reactor performance .....	100
5.3.3. Microbial community composition analysis.....	101
5.3.3.1. The taxonomic classification of sequencing data at the phylum level....	101
5.3.3.2 The diversity analysis.....	103
5.3.3.3. The canonical correspondence analysis (CCA) analysis .....	104
5.3.4. The impact of feed characteristics on nitrogen removal kinetics and the microbial community structure .....	109
5.3.5. The comparison of ammonia oxidizing bacteria (AOB) in the flocs and biofilm ..	111
5.4. Conclusions .....	112
5.5. References.....	113
CHAPTER 6. COMPARISON OF MICROBIAL COMMUNITY AND EXTRACELLULAR POLYMERIC SUBSTANCE (EPS) IN NITRIFICATION AND NITRITATION BIOREACTORS .....	118
6.1. Introduction.....	118
6.2. Methods and materials.....	120
6.2.1. Reactor operation and DNA extraction.....	120
6.2.2. EPS extraction .....	121
6.2.3. X-ray photoelectron spectroscopy analysis.....	121
6.2.4. Three-dimensional excitation and emission matrix fluorescence analysis .....	122

6.2.5. Quartz crystal microbalance with dissipation (QCM-D) analysis.....	122
6.2.6. Statistical analysis .....	123
6.3. Results and discussions.....	124
6.3.1. Reactor performance .....	124
6.3.2. Microbial community structure analysis.....	124
6.3.3. EPS production and characteristics.....	125
6.3.3.1. Colorimetric data analyses.....	125
6.3.3.2. X-ray photoelectron spectroscopy data analysis.....	127
6.3.3.3. Three-dimensional excitation and emission matrix fluorescence data analysis.....	129
6.3.4. Adsorption of EPS components to solid surface .....	131
6.4. Conclusions.....	134
6.5. References.....	134
CHAPTER 7. DENITRITATION AND COMBINED SYSTEM OF PARTIAL NITRIFICATION- DENITRITATION WITH ALKALINITY RECOVERY .....	138
7.1. Introduction.....	138
7.2. Methodology.....	140
7.2.1. Analytical methods.....	140
7.2.2. Alkalinity deficiency test.....	140
7.2.3. Denitrification kinetics determination .....	141
7.2.4. Combined partial nitrification-denitrification cycle test.....	142
7.3. Results and discussions.....	143
7.3.1. The impact of alkalinity deficiency on the partial nitrification .....	143
7.3.2 The denitrification kinetics .....	145

7.3.3. The cycle test for the combined partial nitrification and denitrification system.....	146
7.4. Conclusion .....	148
7.5. References.....	149
CHAPTER 8. CONCLUSIONS AND RECOMMENDATIONS .....	151
8.1. Thesis overview .....	151
8.2. Conclusion .....	152
8.3. Recommendations.....	154
BIBLIOGRAPHY .....	156
APPENDICES.....	179
Appendix-A.....	179
Appendix-B.....	188
Appendix-C.....	202

## LIST OF TABLES

**Table 2.1.** The comparison of fixed and mobile media.

**Table 3.1.** Primers required for q-PCR analysis and target genes.

**Table 3.2.** MLSS, MLVSS and TSS, VSS on biofilm.

**Table 4.1.** Operational parameters of the reactor

**Table 4.2.** Quantification of functional genes per mg biomass in the sludge and biofilm

**Table 5.1.** Feeding strategy for the reactor.

**Table 5.2.** Comparison of the reported ranges of heavy metals inhibition threshold in literature and heavy metals concentrations measured in this study.

**Table 5.3.** The diversity analysis of flocs and biofilm samples.

**Table 6.1.** The 3D-EEM fluorescence spectrum parameters for TB-EPS samples from nitrification and nitritation conditions.

**Table 7.1.** the changes in  $\text{NH}_4^+\text{-N}$ ,  $\text{NO}_2^-\text{-N}$ , Alkalinity and COD concentrations during the reaction in the combined system.

## LIST OF FIGURES

**Figure 1.1.** Schemes of wastewater treatment process in Gold Bar Wastewater treatment plant.

**Figure 1.2.** The fluctuation of the average BOD5 concentration in the raw wastewater entering the Gold Bar wastewater treatment plant during the year of 2016.

**Figure 1.3.** the organization of the studies covered in this thesis.

**Figure 2.1.** Schematic diagram of nitrification processes. AMO is the ammonia mono-oxygenase; HAO is the hydroxylamine oxidoreductase; and NOR is the nitrite oxidoreductase.

**Figure 2.2.** The impact of temperature on the growth rate of AOB and NOB. The red dashed line refers to the common temperature range for partial nitrification. The green dashed line refers to the turn over temperature for the AOB to grow faster than NOB. This figure is after Choi, (2007).

**Figure 2.3.** Schematic diagram of denitrification and denitritation processes. Nar is the nitrate reductase; Nir is the nitrite reductase; Nor is the nitric oxide reductase; and Nos is the nitrous oxide reductase(adapted from Bothe et al., (2007)). Per gCODrequired/g Nreduced for denitrification and denitritation are shown in boxes.

**Figure 2.4.** The schematic diagram for N<sub>2</sub>O production pathways. Cu-enzyme is a Cu containing enzyme(Bartossek et al., 2012; Walker et al., 2010). Other enzymes were previous defined in Figure 2.1 and Figure 2.3. blue arrow represents the process mediated by NOB, orange arrows show the process mediated in AOA, green arrows show the process mediated in AOB and the red arrows are for processes mediated by heterotrophic denitrifiers. The dashed arrows indicate the process is abiotic process.

**Figure 2.5.** The distribution of AOB and anammox in the small and big flocs from the CANON system.

**Figure 3.1.** IFAS-SBR configuration and sequences for one cycle.

**Figure 3.2.** (a) Influent and effluent concentrations of ammonia nitrogen, nitrate nitrogen, and COD; solid triangle and square represent ammonia and COD concentrations in influent, empty triangle, square, and circles show ammonia nitrogen, COD, and nitrate nitrogen in effluent. (b), (c), and (d) are boxplots that show the COD and ammonia nitrogen removal percentage in Phase 1 (C/N = 10:1), Phase 2 (C/N=5:1), and Phase 3 (C/N = 3:1), respectively. In all boxplots, the bottom of each box shows the first quartile of the dataset, the bold line at the center represents the second quartile (median) of the data points, and the top line of the box is the third quartile of the dataset.

**Figure 3.3.** Percentage of active biomass in biofilm and activated sludge during three phases.

**Figure 3.4.** (a) Percentage of amoA (AOB gene) gene in total bacteria on biofilm and activated sludge during three phases. (b) Two NOB genera genes in total bacteria on both biofilm and activated sludge during three phases. Phase 2 and Phase 3 are divided into three stages: beginning, intermediate, and stable. Beginning stage samples were collected 1 day after the change of C/N ratio, intermediate stage samples were collected in the middle of the phase, and stable stage samples were collected at the end of the phase. In (b), NSR gene is commonly found in *Nitrospira* spp. and nitro gene is commonly found in *Nitrobacter* spp. Error bars show the standard deviations.

**Figure 3.5.** (a) amoA gene (AOB gene) recovery in Phase 2; (b) NOB genes recovery in Phase 2. (c) amoA gene recovery in Phase 3; (d) NOB genes recovery in Phase 3. The blue lines with diamonds display the percentage of NOB and AOB genes over total genes in biofilm, and the red lines with squares display the percentages of NOB and AOB genes over total genes in activated sludge. Horizontal axis displays the days after the C/N ratio changes, and the vertical axis indicates the percentage of nitrifiers genes over total genes in activated sludge and biofilm. Error bars show the standard deviations.

**Figure 3.6.** Cycle tests for ammonia and COD removal: (a) Ammonium nitrogen removal during



one cycle; line with circles displays the phase1 data, line with squares displays the phase2 data, and line with triangles displays phase3 data. (b) COD removal during one cycle. The reaction time in one cycle is 230 minutes. Sampling points are at  $t = 0$  min, 5 min, 10 min, 15 min, 25 min, 35 min, 50 min, 65 min, 95 min, 125 min, 185 min, and the end of the cycle ( $t = 230$  min), line with circles displays the phase1 data, line with squares displays the phase2 data, and line with triangles displays phase3 data.

**Figure 3.7.** (a) EPS protein and polysaccharide content per gVSS for both biofilm biomass and activated sludge in three different C/N conditions. In Phase1 the C/N = 10:1, in Phase 2 the C/N = 5:1, and in Phase 3, the C/N = 3:1. (b) Polysaccharide/protein ratio in EPS for both biofilm biomass and activated sludge under three different C/N conditions. PN and PS refer to protein and polysaccharide, respectively. Error bars show the standard deviations.

**Figure 4.1.** IFAS-SBR reactor performance in the reactor during reactor operation. (a) shows the influent and effluent water quality along time. Ammonium nitrogen concentrations in the reactor feed in different phases are listed on top of the figure and each phase is divided by dashed lines. (b) shows the average effluent quality and the ammonium removal and nitrite accumulation efficiency during the stable phase (last 10 days) of each stage.

**Figure 4.2.** The impact of ammonium nitrogen concentration on the nitrite accumulation rate and the ammonium removal rate.

**Figure 4.3.** Batch tests results show the conversion of nitrogen species by different biomass aggregates: (a) oxidation of ammonium, (b) accumulation of nitrite in the same batch test. Control groups are the no biofilm and no sludge groups. The attached biofilm means the test with biofilm only. The suspended sludge represents the test with suspended sludge only, and the suspended sludge + attached biofilm means the group with both the suspended sludge and attached biofilm.

**Figure 4.4.** Figure (a) gives the specific ammonium-N biodegradation rates and biosorption

capacity of suspended sludge and attached biofilm. Figure (b) shows the two mechanisms (biodegradation and biosorption) of ammonium reduction and the contributions from sludge and biofilm through these two mechanisms.

**Figure 4.5.** (a) shows the comparison of microbial community before (100mg/L condition) and after partial nitrification establishment and in the seed sludge from Gold Bar wastewater treatment plant. Genus at a relative abundance <1% were removed from the figure. Highlighted areas represent *Nitrosomonas* (orange) and *Nitrospira* (Blue), which were the major nitrifiers in the reactor. (b) gives the microbial community richness analysis. R1AS100 represented the community in the sludge that collected under 100mg/L condition (before partial nitrification); R1AS800 indicated the community in the sludge that collected under 800mg/L condition (partial nitrification); R1B100 corresponded to the community in the biofilm under 100mg/L condition (before partial nitrification); R1B800 indicated the community in the biofilm collected under 800mg/L condition (partial nitrification); and the seed represented the community in the seed sludge.

Figure 5.1. The relative abundance of sequences at phylum level in biofilm (a) and suspended flocs (b) of reactor 1. Phyla with relative abundance <1% are not shown in the figure.

**Figure 5.2.** Canonical correspondence analysis (CCA) analysis of Miseq sequencing data of flocs (a) and biofilm (b). The red vectors represent the environmental variables that affected the microbial community structure. The length of the vectors indicated the strength of the relationship between these variables and the community structure. The green triangles in the plot represent the samples. The circles represent the genus in the community. Genera in Bacteroidetes are colored with orange, and Genera in Proteobacteria are colored in green. Genera in the other phylum are not colored. Genera with relative abundance <1% were not shown in the plot.

**Figure 5.3.** (a) The change of specific ammonia conversion and nitrite accumulation rate during three different stages: complete nitrification (stage 1), partial nitrification (stage 5), and partial

nitrification when the fed was raw supernatant (stage 9). (b) The AOB and NOB functional genes copies/ mg biomass in both suspended flocs and attached biofilm during these three stages measured by qPCR. (c) The relative abundance of Nitrosomonas in % in both flocs and biofilm samples measured by MiSeq analysis.

**Figure 5.4.** The distribution of AOB functional genes in the flocs and the biofilm under various feed conditions.

**Figure 6.1.** Abundance of functional genes in the suspended flocs and biofilm samples under nitrification and nitritation conditions. The grid patterned blocks represent the AOB functional genes; the slash patterned blocks represent the NOB functional genes.

**Figure 6.2.** The characteristics of EPS samples collected from suspended flocs and biofilm under nitrification-dominant and nitritation-dominant conditions. (a) the results for TB-EPS and LB-EPS of suspended flocs and biofilm from nitrification (left) and nitritation dominant (right) conditions Figure (b) indicates the percentages of substances containing different functional groups in the EPS samples based on the X-ray photoelectron spectroscopy results; the solid fill shows the percentage containing C-C(-H) bonds, thick slashes pattern shows the percentage containing C-O(-N) bonds, the thin slash pattern shows the percentage containing C=O bonds, and the light grey solid pattern shows the percentage containing O=C-OH bonds.

**Figure 6.3.** 3D-EEM data for biofilm and flocs TB-EPS from nitritation and nitrification dominant conditions.

**Figure 6.4.** the QCMD data for LB-EPS and TB-EPS sample from biofilm that collected under nitritation dominant condition. The deviation of the frequency line (blue line) from the center line (dashed horizontal line) demonstrated the adsorption capacity of EPS samples on to solid surface.

**Figure 6.5.** The frequency changes for five trials with glucose and BSA (as EPS surrogates for polysaccharides and proteins) at different ratios (from left to right: 1. Glucose only; 2. Glucose:

BSA=3:1; 3. Glucose: BSA=1:1; Glucose: BSA=1:3; and BSA only). The blue boxed represent the residual attached mass after the NaCl solution wash and water wash. The dark orange parts represent the mass released during the NaCl wash, and the light orange parts represent the mass released during the water wash.

**Figure 7.1.** the set-up of the denitrification batch test. D1 and D2 are duplicates.

**Figure 7.2.** The inhibition of alkalinity shortage on the partial nitrification process. The blue shaded area is the inhibition area and the orange shaded area indicates the complete stop of partial nitrification. The green shaded area is the optimal pH range for AOB.

**Figure 7.3.** The kinetics of denitrification. (a) demonstrated the nitrite-nitrogen concentration changes; (b)demonstrated the nitrate-nitrogen changes; (c) and (d) demonstrated the COD concentration changes; and (e) the nitrous oxide content in the headspace.

**Figure 7.4.** the sequences of combined nitrification denitrification system.

## LIST OF ABBREVIATIONS

AMO	ammonia mono-oxygenase
amoA	ammonia monooxygenase subunit A gene
ANOVA	analysis of variance
AOA	ammonia oxidizing archaea
AOB	ammonia oxidizing bacteria
ATP	adenosine triphosphate
BNR	biological nutrient removal
BOD	biological oxygen demand
BSA	bovine serum albumin
C/N	carbon/nitrogen ratio
CANDO	coupled aerobic-anoxic nitrous decomposition operation
CANON	completely autotrophic nitrogen removal over nitrite
CAS	conventional activated sludge
CCA	canonical correspondence analysis
COD	chemical oxygen demand
DEMON	de-ammonification
DNRA	dissimilatory nitrate reduction to ammonia
DO	dissolved oxygen
EEM	excitation-emission matrix
EPS	extracellular polymeric substances
FA	free ammonia
FH	free hydroxylamine
FISH	fluorescence in situ hybridization

FNA	free nitrous acid
FRI	fluorescence regional integration
GC-ECD	gas chromatography-electron capture detector
GHG	greenhouse gas
HAO	hydroxylamine oxidoreductase
HRT	hydraulic retention time
IFAS	integrated fixed film activated sludge
LB-EPS	lightly bounded extracellular polymeric substances
MBBR	moving bed biofilm reactor
ML	million litres
MLSS	mixed liquor suspended solids
MLVSS	mixed liquor volatile suspended solids
N-AOM	denitrification, anammox and nitrite dependent-oxidation of methane
N	nitrogen
NGS	next generation sequencing
NOB	nitrite oxidizing bacteria
NOR	nitrite oxidoreductase
NOR	nitrite oxidoreductase
OLAND	oxygen-Limited Autotrophic Nitrification–Denitrification
PBS	phosphate buffered saline
PHB	poly-hydroxybutyrate
PS/PN	polysaccharide/protein
QCM-D	quartz crystal microbalance with dissipation
qPCR	quantitative polymerase chain reaction

S-EPS	soluble extracellular polymeric substances
SBR	sequencing batch reactor
SHARON	single reactor system for high ammonia removal over nitrite process
SRT	solids retention time
SVI	settling volume index
TB-EPS	tightly bounded extracellular polymeric substances
TOC	total organic carbon
TSS	total suspended solids
VFA	volatile fatty acid
WWTP	wastewater treatment plant
XPS-X	X-ray photoelectron spectroscopy

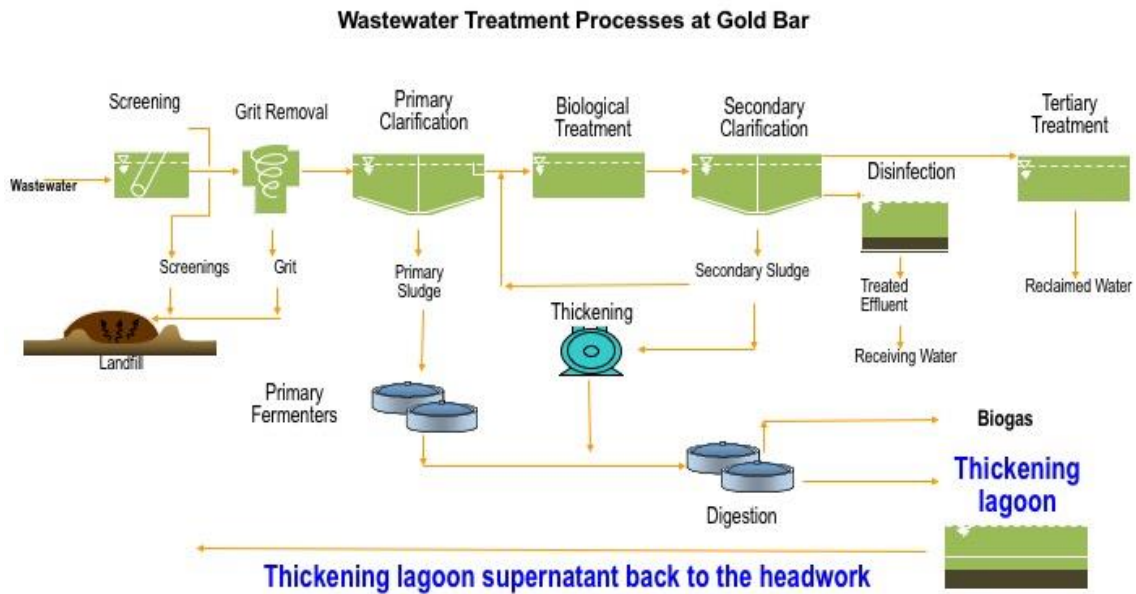
## CHAPTER 1. INTRODUCTION AND OBJECTIVES

### 1.1. Background and motivations

Nitrogen (N) is an essential element for microorganism growth. Together with Phosphorus (P), high concentration of N in the water body will lead to the eutrophication (U.S.EPA, 2007). Also, high concentration of ammonium in water bodies will lead to the acute death of fishes and the other aquatic lives. In other cases, the ammonium nitrogen also will lead to the acidification of soil and break the balance of the ecosystem. The ammonium nitrogen concentration in the domestic wastewater that enters the local wastewater treatment plant is around 30mg/L to 50mg/L. Based on the surface water quality guideline for use in Alberta (Alberta et al., 1999), the total nitrogen and limit is 1.0mg/L. It is important to remove the N in the municipal wastewater before disposal into natural water reservoirs.

Gold Bar Wastewater treatment plant (WWTP) is located at Edmonton, Alberta, Canada. The treated wastewater discharge from Gold Bar is one of the three major contributors (the other two are combined sewer overflow and storm water outfalls) of pollutants to the North Saskatchewan River. According to the Approval to Operate (#361975-00-00), the limits for ammonium-N in the treated water are 5mg/L in the summer and 10mg/L in the winter. There was round 101,475 million litres (ML) of wastewater conveyed to the plant in the year of 2016 (EPCOR Water Services Inc., 2017). The plant achieved the limits required by Alberta Environment and Parks. However, as the population in the city of Edmonton expands and the standards for the effluent quality become more and more stringent, the Gold Bar WWTP is seeking ways to improve the nitrogen removal efficiency to better service the communities. The schematic diagram for the wastewater treatment processes at the Gold Bar WWTP was shown in Figure 1.1.





**Figure 1.1.** The wastewater treatment processes at Gold Bar treatment plant.

Nitrification and denitrification processes are the most conventional processes to remove the ammonium from the wastewater. Nitrification composes of two steps: the oxidation of ammonia to nitrite which is mediated by the ammonia oxidizing bacterium (AOB) and the conversion of nitrite to nitrate by the nitrite oxidizing bacterium (NOB). Both the AOB and NOB are autotrophs which utilize inorganic compounds for growth and energy production. Denitrification process refers the conversion from nitrate to nitrite and further to nitrogen gas. The denitrification process is usually carried out by denitrifiers. Most of the denitrifiers are heterotrophic bacteria that utilized the organics as carbon source for energy production and growth. At most of the conventional wastewater treatment plants (WWTPs), biological nutrient removal (BNR) systems are designed to remove nitrogen and phosphorous in wastewater (Jeyanayagam, 2005). In the aerobic sections of a BNR system, nitrifiers (AOB and NOB) conduct the nitrification processes. In the anoxic sections of a BNR system, denitrifiers carry out the denitrification processes with the addition of

external carbon sources. In terms of the nitrogen removal, the nitrification process is the rate limiting step, and thus the nitrification efficiency is critical to the success of a BNR system.

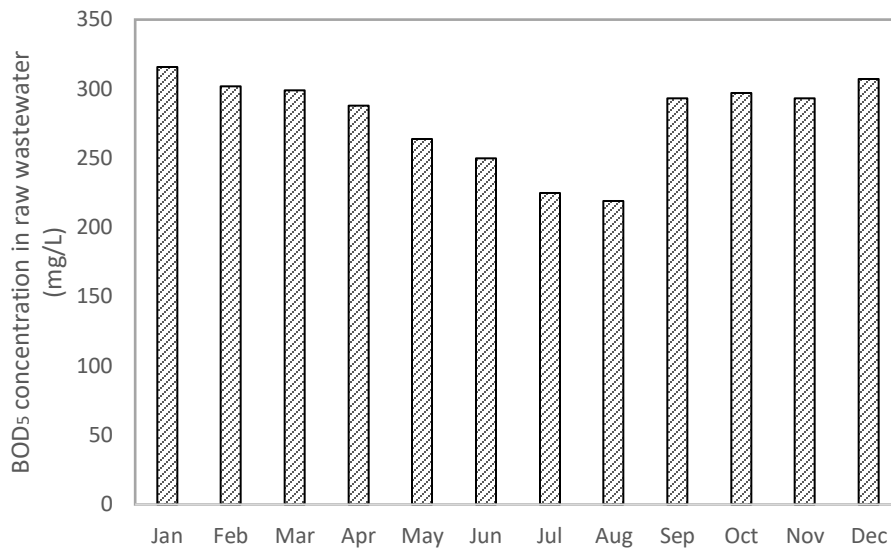
As the standards for the effluent from the wastewater treatment plant are becoming more and more stringent and the population of the city is expanding, there is an urgent need for the plants to improve the nitrification efficiency.

## **1.2. Scope of research and objectives**

In order to improve the nitrogen removal efficiency of the municipal wastewater, an integrated fixed-film activated sludge (IFAS) technology was proposed for mainstream biological treatment. The IFAS technology integrated the biofilm supporting carriers into the conventional activated sludge (CAS) system to provide surfaces the organisms can grow on and provide longer solids retention time (SRT) for the organisms, especially for the slow growers.

IFAS technology had been well studied for the improvement of the mainstream treatment. However, it was hypothesised that the organic carbon loading had an impact on the nitrification efficiency. According to the BOD<sub>5</sub> concentration in the influent entering the WWTP (Figure 1.2.), a fluctuation in the BOD<sub>5</sub> during the year of 2016 was observed. To investigate the nitrogen removal efficiency under different BOD<sub>5</sub> loading, a project focusing on the stability of the IFAS reactor under different organic loading was brought out. The main objectives of this study included:

1. To investigate the nitrogen and COD removal efficiency under different organic loading;
2. To compare the microbial community in suspended flocs and attached biofilm;
3. To investigate the extracellular polymeric substance (EPS) dynamics under different organic loadings.



**Figure 1.2.** The fluctuation of the average BOD<sub>5</sub> concentration in the raw wastewater entering the Gold Bar wastewater treatment plant during the year of 2016 (data obtained from EPCOR Water Services Inc., 2017).

Tracing back to the sources of the nitrogen, the thickening lagoon supernatant was a big contributor of nitrogen entering the plant. As shown in Figure 1.1. the thickening lagoon was designed for the storage of digested sludge from the anaerobic digester. The solids in the sludge would get settled and the supernatant was pumped back to the headworks. The supernatant only accounted for 1% of the total flow entered the plant. But due to the high ammonium content (800-1200mg/L NH<sub>4</sub><sup>+</sup>-N) in the supernatant, it accounted for more than 30% of nitrogen loading entering the plant. This might lead to a consequence that during extreme conditions (like the shocking loading period) the nitrogen removal became challenging in the mainstream treatment. In this scenario, a side stream treatment for the lagoon supernatant was proposed. The conventional way to remove the ammonium nitrogen was through complete nitrification. However, the complete nitrification consumed large amount of oxygen which elevated the energy input and cost for maintenance. The partial nitrification was suggested for the treatment of high ammonium strength wastewater because it saved up to 25% of the oxygen that required

for ammonia oxidation. Partial nitrification was easily achievable under high temperature 30-35 °C. But heating up reactor to such high temperature demanded high energy input. It might be more economically feasible and energy saving if achieving partial nitrification under lower temperature (20-21°C). Moreover, combining the partial nitrification with the denitrification process would also reduce the external carbon addition by 40% for complete nitrogen removal. Moreover, the lagoon supernatant was alkalinity deficient. Large amount of external alkalinity addition would elevate the chemical cost for future application in larger scale reactors. The denitrification process turned out to be an alkalinity producing process and could also be a potential source of alkalinity to support the partial nitrification process. Considering all the possibilities, a study on the treatment of the high ammonium strength lagoon supernatant using partial nitrification and denitrification processes was also included in this project. This study was separated into three sections based on the processes involved: the partial nitrification, the denitrification process, and the combined partial nitrification and denitrification in one reactor. The objectives in the first section included:

1. To test the feasibility of the partial nitrification process in treating high ammonium strength wastewater;
2. To elucidate the kinetics and stability of the partial nitrification process;
3. To investigate the impact of feeding water characteristics on the performance of the reactor and the microbial community dynamics in suspended flocs and attached biofilm;
4. To compare the EPS from complete and partial nitrification processes.

The partial nitrification process converted the ammonium to nitrite, and the denitrification process converted the nitrite to nitrogen gas with the addition of organic carbon. The process was carried out by heterotrophic denitrifiers. By combining the partial nitrification and the denitrification

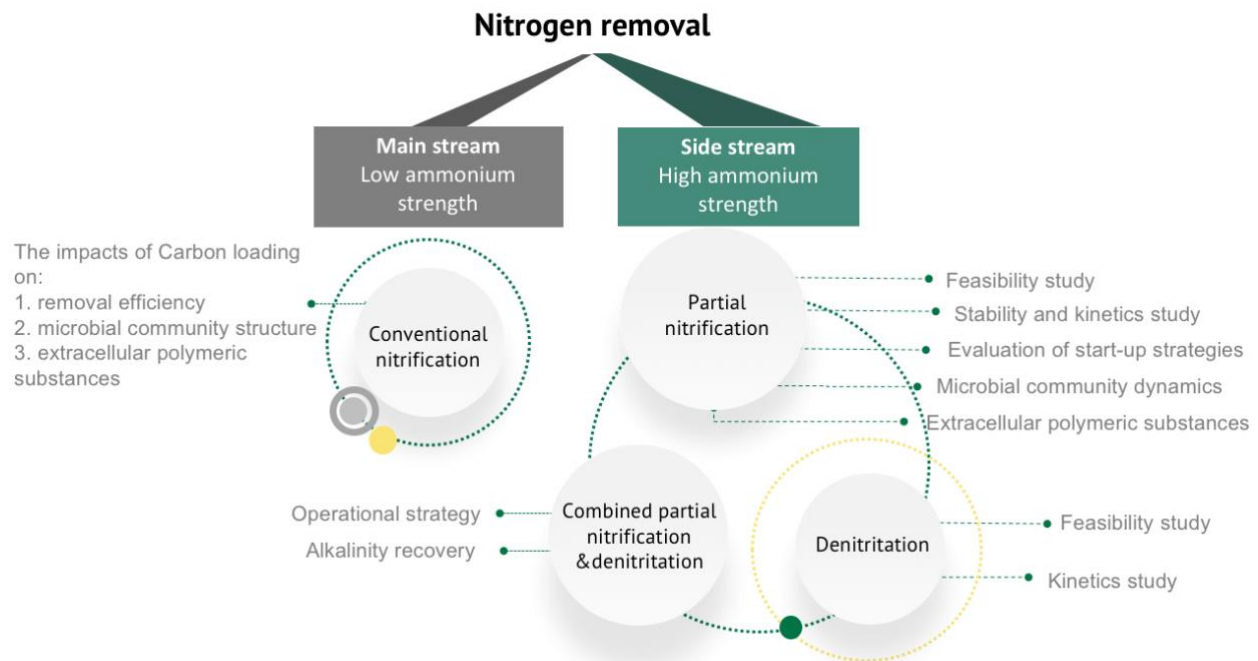
processes, we could achieve complete nitrogen removal from ammonium to nitrogen gas. The main goals for this section of study included:

1. To test the feasibility of denitritation process treating the effluent from the partial nitrification reactors.
2. To calculate the removal kinetics and use the kinetics for future reactor design.

When the partial nitrification was applied to treat the high ammonium strength lagoon supernatant, the deficiency of alkalinity in the raw supernatant would cease the partial nitrification. Alkalinity that recovered from the denitritation process could be utilized for the nitrification process if operation mode was well designed. Based on this, the objectives for the third section of study included:

1. To test the feasibility of the combined partial nitrification-denitritation system
2. To monitor the nitrogen species conversion during the treatment
3. To calculate the alkalinity recovery and the organic carbon addition during the treatment.

The following flowchart summarized the organization of this thesis and the objectives for each part of studies (Figure 1.3).



**Figure 1.3.** the organization of the studies covered in this thesis.

### **1.3. Thesis organization**

The structure of this thesis is listed below:

Chapter 1 is a general introduction of the nitrogen removal in local wastewater treatment and the challenges the plant is facing. The motivations and objectives for the project are well described in this chapter.

Chapter 2 is a literature review of the work that had been in the field of nitrogen removal. More specifically, the nitrogen removal processes (including conventional nitrification, partial nitrification, denitrification, anammox) and the microorganisms that mediated the processes are well discussed in this chapter. The technologies that applied in this study are also reviewed.

Chapter 3 is based on a published paper. This chapter elucidates the impacts of C/N ratio on the performance; the bacterial community structure in both the suspended flocs and attached biofilm; and the EPS characteristics of the integrated fixed-film activated sludge (IFAS) reactor that operated under sequencing batch mode.

Chapter 4 is based on a published paper. This chapter elucidates the establishment and the performance of the partial nitrification reactor treating synthetic high ammonium strength wastewater.

Chapter 5 investigates the impacts of feed characteristics, including the ammonium concentration and the raw lagoon supernatant percentage in the feed, on the microbial community dynamics and the nitrogen removal kinetics in partial nitrification reactor.

Chapter 6 characterizes and compares the tightly bounded extracellular polymeric substance (TB-EPS) from the complete and partial nitrification processes. The contribution of EPS components to the adsorption to solid surface is also studied in this chapter.

Chapter 7 demonstrates the inhibitory effect on partial nitrification by the alkalinity shortage in the lagoon supernatant. To solve the problem, an innovative design of a combined partial nitrification and denitrification system, which would recover the alkalinity from the denitrification process, is proposed in this chapter.

Chapter 8 presents the general conclusion and recommendations for the future studies.

The appendix includes supporting information for different chapters.

#### **1.4. References**

Alberta, Water Management Division, Alberta, Environmental Sciences Division, 1999. Surface water quality guidelines for use in Alberta. Alberta Environment, Environmental Sciences Division, Edmonton.

EPCOR Water Services Inc., 2017. Gold Bar Wastewater Treatment Plant 2016 Wastewater Treatment Annual Report.

Jeyanayagam, S., 2005. True confessions of the biological nutrient removal process. Fla. Water Resour. J. 37–46.

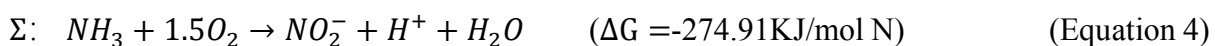
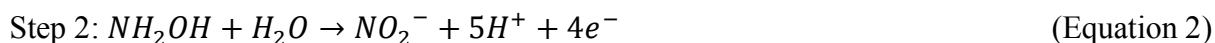
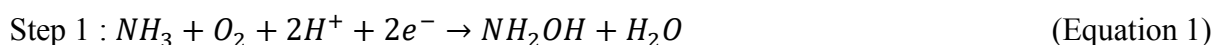
U.S.EPA, 2007. Biological nutrient removal processes and cost

## CHAPTER 2. LITERATURE REVIEW

### 2.1. Complete nitrification and partial nitrification

#### 2.1.1. Concepts and biochemistry

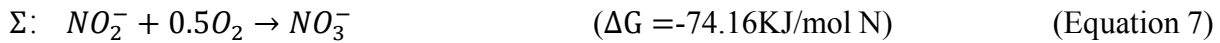
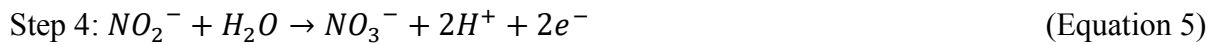
Complete nitrification refers to the biological oxidation of ammonia to nitrate. The complete nitrification was also known as the conventional nitrification. It has been conventionally applied in the WWTPs for the ammonium oxidation in the secondary biological treatment reactors. It involves two steps, The oxidation of ammonia to nitrite and the oxidation of nitrite to nitrate. The oxidation of ammonia to nitrite is usually carried out by ammonia oxidizing bacteria (AOB). The second step is carried out by the nitrite oxidizing bacteria (NOB). The complete nitrification is practical for the mainstream low ammonia strength wastewater treatment. However, for the high ammonia strength wastewater, the application of complete nitrification will consume huge amount of oxygen. Considering the economy feasibility, using partial nitrification would be more applicable for the treatment of high ammonium strength wastewater. Partial nitrification refers to the first step of ammonia oxidation. It is also known as the nitritation process. The nitrite, instead of nitrate is the end product of the oxidation. By stopping the reaction at nitrite, the partial nitrification could save up to 25% of the oxygen and lower the cost of operation. The partial nitrification consist of three sub-processes (Bai et al., 2012; Sinha and Annachhatre, 2007):





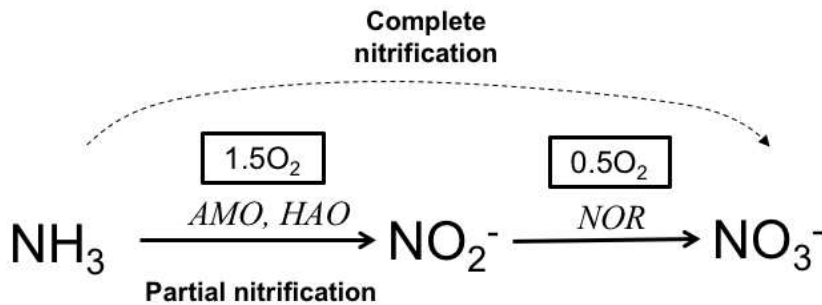
Step 1 is the oxidation of ammonia to hydroxylamine (Eq.1). The membrane bound ammonia mono-oxygenase (AMO) is the enzyme functioning in this process. The step 2 is the oxidation of hydroxylamine to nitrite (Eq.2). Hydroxylamine oxidoreductase (HAO) is the enzyme functioning in Step 2. Combining the three sub steps, we get the oxidation of the ammonia to nitrite equation (Eq.4). The combined process is an energy generating process. It is also a rate limiting step for the complete nitrification.

The oxidation of nitrite to nitrate is also known as the nitrataion process. Two sub steps are included in this process.



Compared to the oxidation of ammonia, oxidation of nitrite releases less energy and happens faster.

The enzyme functioning in this step is the membrane bound nitrite oxidoreductase (NOR). Figure 2.1 below demonstrated the two steps in nitrification processes and the enzymes and oxygen requirements for each step.



**Figure 2.1.** Schematic diagram of nitrification processes. AMO is the ammonia mono-oxygenase; HAO is the hydroxylamine oxidoreductase; and NOR is the nitrite oxidoreductase.

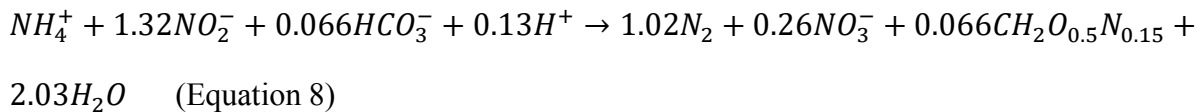
### 2.1.2 Nitrifying organisms

Nitrifying organisms are playing important roles in the global nitrogen cycle. Understanding the microorganisms in the engineered systems becomes more and more important in the field of wastewater treatment. As mentioned in previous section, the oxidation of ammonia is commonly implemented by the AOB. Most of the AOB belong to the *β-Proteobacteria*. Among the AOBs, the family of *Nitrosomonas* is the dominant family. *Nitrosomonas europaea* / *N. mobilis* lineage was the dominant *Nitrosomonas* detected in the WWTP (Koops et al., 2006). *N. europaea* was extensively detected in a WWTP treating low strength domestic wastewater, while *N. mobilis* was detected in a WWTP treating industrial wastewater, revealing its tolerance to high salinity (Prosser et al., 2014). Researchers also detected a high amount of *Nitrosomonas oligotropha* in laboratory scale experiments treating industrial wastewater with high heavy metals content (Stehr et al., 1995). Another genera of AOB, *Nitrospira sp.*, was seldom found in laboratory scale reactors, and rarely found in a full scale WWTP (Prosser et al., 2014).

It was commonly believed that AOB was the only ammonia oxidizer until the recent discovery of ammonia oxidizing archaea (AOA)(Francis et al., 2005; Treusch et al., 2005). Like AOB, AOA was also found to carry the genes encode the subunit A of AMO (Treusch et al., 2005). The difference between the AOA and AOB is that they used different pathways for the production of nitrite from hydroxylamine. Specifically,  $\text{NH}_3$  is oxidized to hydroxylamine with the facilitation of ammonia mono-oxygenase (AMO); the hydroxylamine is further oxidized to nitrite with the facilitation of the hydroxylamine oxidoreductase (HAO) in the AOB. But AOA is lack of (HAO). The oxidation of hydroxylamine in AOA is carried out through the reaction of hydroxylamine with  $\text{NO}$  and  $\text{H}_2\text{O}$  that facilitated by the Cu- containing enzyme (Bartossek et al., 2012, 2010; Kozlowski et al., 2016; Walker et al., 2010). Moreover, the AOA was found to be more vulnerable to toxic compounds than the AOB. Higher abundance of AOA than AOB was found in natural

environments, but not in the industrial WWTP (Adair and Schwartz, 2008; Bai et al., 2012; Francis et al., 2005; He et al., 2007; Leininger et al., 2006; Wuchter et al., 2006; Zhang et al., 2008).

Another interesting group of ammonia oxidizer is named anammox bacteria (Strous et al., 1999). The anammox bacteria is known as anaerobic ammonia oxidizer. Unlike AOB or AOA, the anammox bacteria uses both nitrite and ammonia as substrates to produce nitrogen gas under anaerobic condition, and the metabolic pathway for anammox process is elucidated in Equation 8. The anammox based ammonia removal system was developed in Delft University of Technology.



The anammox process is a promising process as it requires no external carbon addition for complete nitrogen removal. However, the start-up time of anammox reactor was around 10 months or longer (Rikmann et al., 2018), except for cases that enriched anammox sludge was used as seed and system was well controlled (Christensson et al., 2013; Kowalski et al., 2018).

More recently, the discovery of comammox, which is known as complete nitrifier, was discovered (Daims et al., 2015; van Kessel et al., 2015). The comammox bacteria would oxidize the ammonium all the way to nitrate in a single cell. The discovery of comammox refreshed our knowledge about the roles the organisms played in the nitrogen cycle. Upon date, only one species of comammox, named *Candidatus Nitrospira inopinata*, was cultured (Daims et al., 2015).

For the nitrite oxidizing bacteria (NOB), was widely spread in the *Proteobacteria*. The most common genus found were *Nitrospira* and *Nitrobacter*. The *Nitrospira* belongs to the class of *Nitrospirae*, and *Nitrobacter* belongs to the  $\alpha$ -*Proteobacteria*. Researchers had found that these

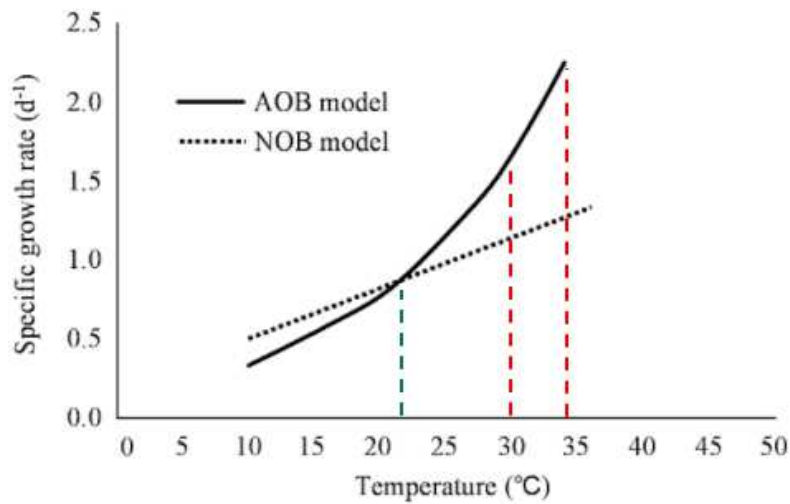
*Nitrobacter* has lower affinity towards the nitrite than the *Nitrospira*. *Nitrobacter* would compete over *Nitrospira* when the substrate is abundant, and vice versus (Nogueira and Melo, 2006). More interesting, the Comammox bacteria discovered so far all fall in the genera of *Nitrospira* (Daims et al., 2015).

### 2.1.3 Achieving partial nitrification

The key to achieve partial nitrification was to eliminate the NOB bacteria while proliferate the AOB in the same system. It had been well studied that temperature, low DO, short HRT and inhibitors would be the factors affecting the growth of NOB. the impacts of these factors will be well illustrated in the following paragraphs.

#### 2.1.3.1 Temperature

AOB competes over NOB under high temperature as the specific growth rate of AOB is higher than NOB under such temperature range (Figure 2.2). Literature pointed out 20-25° is turnover temperature for AOB to grow faster than the NOB (Hellings et al., 1998; Peng and Zhu, 2006). The commonly use temperature range for partial nitrification technologies is from 30 to 35 °C to ensure the elimination of NOB and the proliferation of AOB (Hellings et al., 1998; Mulder et al., 2001; Nhu Hien et al., 2017; Zhang et al., 2010). However, partial nitrification was achievable under low temperature if other operational parameters was well controlled, for example dissolved oxygen (DO), solid retention time (SRT), intermittent aeration pattern, inhibitors etc.



**Figure 2.2.** The impact of temperature on the growth rate of AOB and NOB. The red dashed line refers to the common temperature range for partial nitrification. The green dashed line refers to the turn over temperature for the AOB to grow faster than NOB. This figure is after Choi (2007).

### 2.1.3.2 Dissolved oxygen (DO)

It was reported that the DO half saturation coefficient of AOB is 0.2-0.4 mg/L, and the value for NOB is 1.2-1.5 mg/L (Picioreanu et al., 1997), indicating that the AOB has a higher affinity towards DO. The AOB could compete over NOB under low DO environment (Peng et al., 2004). Previous studies reported that maintaining solution DO below 1mg/L was critical for achieving partial nitrification (Sinha and Annachhatre, 2007; Tokutomi, 2004). However, some researchers also reported a DO level greater than 1mg/L for optimal nitrification. For instance, Ciudad et al.(2005) found that nitrification was achieved at a DO level of 1.4mg/L. Peng and Zhu (2006) suggested a DO ranging from 0.5mg/L to 1.5mg/L was suitable for partial nitrification. Ge et al. (2014) reported that 1.5-2.0 mg/L DO was the optimal range for their reactors. These results underlined that the DO in a range of 0.5 to 2.0 mg/L might be the optimal range for partial nitrification.

### 2.1.3.3 Free ammonia (FA), free nitrous acid (FNA), and free hydroxylamine (FH)

Anthonisen et al. (1976) conducted a classic study on the inhibition of NOB and AOB by the FA and FNA. They proposed two equations (Eq. 9&10) for the calculations of FA and FNA based on the ammonium-N concentration, nitrite -N concentration, the temperature, and pH.

$$\text{FA as } NH_3(\text{mg/L}) = \frac{17}{14} \times \frac{\text{total ammonia as N}(\text{mg/L}) \times 10^{pH}}{K_b / K_w + 10^{pH}} \quad (\text{Equation 9})$$

Where  $K_b / K_w = e^{(6344/273 + ^\circ\text{C})}$

$$\text{FNA as } HNO_2(\text{mg/L}) = \frac{46}{14} \times \frac{NO_2^- - N(\text{mg/L})}{K_a \times 10^{pH}} \quad (\text{Equation 10})$$

Where  $K_a = e^{(-2300/273 + ^\circ\text{C})}$

The reported inhibition range of FA on the NOB and AOB are 0.1-1.0 mg/L and 10-150mg/l, respectively. Moreover, the inhibition range of FNA on the NOB and AOB is 0.22-2.8 mg/L (Anthonisen et al., 1976). Then, the mechanism for FA inhibition on NOB was found. FA is a competitive inhibitor of nitrite oxidoreductase (NOR) (Yang and Alleman, 1992). Further, the inhibition mechanism of FNA was found. A proton donated by FNA interferes with the pH gradient for ATP synthesis (Glass et al., 1997). Up to now, FA and FNA were still reported as the most effective inhibitors on NOB (Hellings et al., 1998; Nhat et al., 2017; Wang and Gao, 2016). Free hydroxylamine (FH) is an intermediate of nitrification. Scientists reported that the hydroxylamine has an irreversible inhibition effect on the NOB under anoxic condition (Hao and Chen, 1994; Stüven et al., 1992). FH exhibits acute toxicity to NOB and contributes to the nitrite build up and achievement of partial nitrification.

### 2.1.3.4 pH

The growth range for pure AOB and NOB cultures are 5.8 to 8.5 and 6.5 to 8.5, respectively (Princic et al., 1998). It was reported that when pH under 6.5 or higher than 8.9, the inhibition of nitrification was detected (Ruiz et al., 2003). Other reports demonstrated that the optimum range for AOB was 7.5 to 8.0 or 7.4-7.8 (Claros et al., 2013), and for NOB was 7.6 to 7.8 (American Water Works Association, 2006). In this case, using pH control only to eliminate NOB seems impossible. It was also suggested that the pH was related with the FA and FNA concentrations (Anthonisen et al., 1976); and further influence the partial nitrification (Peng and Zhu, 2006) as mentioned in the previous section.

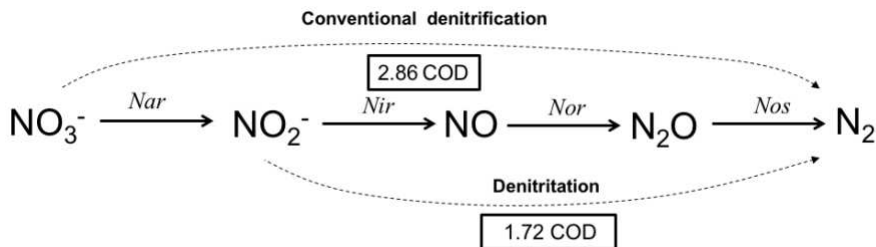
#### 2.1.3.5 Operational mode

It was reported that the partial nitrification was easily achievable if the reactor was operated under sequencing batch mode. A review survey revealed that more than half of the full-scale partial nitrification/anammox applications were operated under the sequencing batch reactor (SBR) mode, followed by the granular sludge application and moving bed biofilm reactor (MBBR) (Lackner et al., 2014). It had been demonstrated that the SBR was favorable for the establishment of partial nitrification-denitrification for following reasons: 1) the SRT in the SBR was long and led to a significant increase of internal decay, which provided the denitrification process with external organic carbon source (Gustavsson, 2010); 2) the SRT was usually started with a feeding phase under anoxic condition, the hydroxylamine formed under this condition proposed a potent inhibition on the NOB, which might also contribute to the establishment of partial nitrification (Peng and Zhu, 2006); 3) the length of the SRT was easily controlled (EPA, 1999); and 4) the required volume of an SBR was smaller than the continuous flow reactor, which lowered the capital cost for installation. However, some studies showed a higher process stability and reaction rate in

the continuous flow reactor. For full-scale applications in the future, the cost of different operation mode and reaction rate should be considered.

## 2.2 Denitrification process

Conventional denitrification process is described as the conversion from  $NO_3^-$  to  $N_2$  by heterotrophic bacteria. The process actually involves the conversions from nitrate to nitrite, nitrite to  $NO$ , and further to  $N_2O$  and  $N_2$  (Figure 2.3). Each sub-step of the process was facilitated by different types of microbial enzymes.



**Figure 2.3.** Schematic diagram of denitrification and denitrification processes. *Nar* is the nitrate reductase; *Nir* is the nitrite reductase; *Nor* is the nitric oxide reductase; and *Nos* is the nitrous oxide reductase (adapted from Bothe et al., (2007)). Per  $gCOD_{required}/g N_{reduced}$  for denitrification and denitrification are shown in boxes.

Generally, the heterotrophic denitrifying bacteria produce all the enzymes for denitrification, while the other organisms produce one or some of the enzymes. Heterotrophic denitrifiers usually carried out the reduction of nitrate to nitrite. In some cases, the bacteria mediating dissimilatory nitrate reduction to ammonia (DNRA) could also reduce the nitrate. Besides, the nitrite oxidoreductase can reduce nitrate to nitrite under anoxic condition (Freitag et al., 1987), indicating the potential of NOB to reduce nitrate. The reduction of nitrite to nitric oxide is the central step for denitrification because it is an essential step for the energy conservation for denitrification, anammox and nitrite

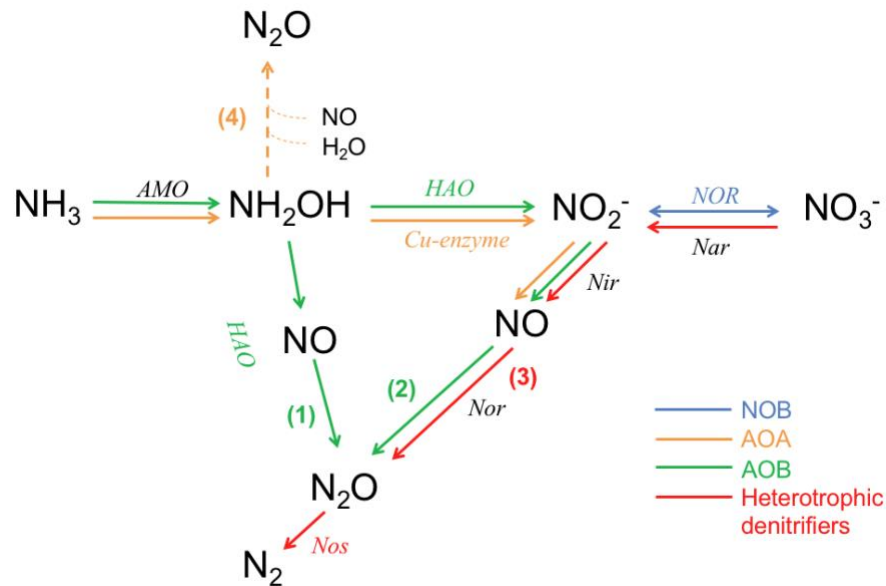


dependent-oxidation of methane (N-AOM) (Schreiber et al., 2012). Organisms capable of mediating this step include heterotrophic denitrifiers, DNRA, anammox, N-AOM bacteria, AOB and NOB. The next step is the reduction of NO to N<sub>2</sub>O, which is also an energy conservation step, but for denitrification only. Except for the anammox organisms, all the other organisms involved in the reduction of nitrite to nitric oxide can perform this step. The last step of denitrification is the reduction from nitrous oxide to nitrogen gas. This step is facilitated by the nitrous oxide reductase (Nos). The nos gene clusters that encode the Nos enzyme are only found in denitrifiers. It leads to the consequence that organisms having nir and nor genes but lacking nos gene will release NO or N<sub>2</sub>O during the denitrification processes (Stein and Klotz, 2016). The accumulation of NO in the reactor will reduce the denitrification rate, although the inhibition mechanism is not confirmed yet (Fux et al., 2006; Gustavsson, 2010). The inhibition of N<sub>2</sub>O on the denitrification has not been reported yet. However, the emission of N<sub>2</sub>O will lead to a series of environmental issues, which will be further discussed in next section.

External carbon sources are needed for the denitrification process. Traditionally, methanol was used as a cost-effective external carbon source (Hellings et al., 1998). Later, the biofuel industry by-products were used as a more cost-effective COD alternative (Mulder et al., 2006). Phenol (Queiroz et al., 2011; Ramos et al., 2016), sodium acetate, glucose, glycerol (Kulikowska and Bernat, 2013), starch, and ethanol were also utilized as carbon sources for the denitrification process. Other options include the COD-rich condensate from sludge drying (Mulder et al., 2006), the volatile fatty acid (VFA) (Scherson et al., 2014). Denitrifying organisms have different preference and utilization efficiency for different carbon sources (Güven, 2009). The selection of COD sources depended on the scale of application, the availability of carbon sources, the utilization efficiency and the budget for chemical cost.

### 2.3. Nitrous oxide production

Nitrous oxide is a type of greenhouse gas (GHG). It has 200 to 300 times GHG potential than CO<sub>2</sub>. The release of N<sub>2</sub>O needs to be well monitored and controlled at plants. The biological nitrous oxide production was concluded through two major pathways: the incomplete denitrification (heterotrophic), and the nitrifiers denitrification and oxidation of hydroxylamine (autotrophic). Moreover, the nitrous oxide formed through the abiotic reaction of NH<sub>2</sub>OH with NO<sub>2</sub><sup>-</sup> (Duan et al., 2017). Also, scientists revealed that the nitrous oxide production pathways by AOB and AOA are different recently. Briefly, the production of N<sub>2</sub>O by AOB was through the enzymatical nitrifiers denitrification, but the production of N<sub>2</sub>O by AOA was through the non-enzyme driven hybrid formation through the reaction of NH<sub>2</sub>OH with NO and H<sub>2</sub>O (Kozłowski et al., 2016). Combining the information above, there are four different pathways for N<sub>2</sub>O production (Figure 2.4).



**Figure 2.4.** The schematic diagram for N<sub>2</sub>O production pathways. Cu-enzyme is a Cu containing enzyme (Bartossek et al., 2012; Walker et al., 2010). Other enzymes were previously defined in Figure 2.1 and Figure 2.3. blue arrow represents the process mediated by NOB, orange arrows show the process mediated in AOA, green arrows show the process mediated in AOB and the red

arrows are for processes mediated by heterotrophic denitrifiers. The dashed arrows indicate the process is abiotic process.

The major contributor to  $N_2O$  producer during nitrification-denitrification processes was debatable (Massara et al., 2017). Incomplete heterotrophic denitrification was reported as the biggest contributor to the nitrous oxide production in a case study treating landfill leachate (Gabarró et al., 2014) and in a batch experiment (Domingo-Félez et al., 2017). Other studies claimed the nitrifiers denitrification under low DO condition was the major contributor for  $N_2O$  and they suggested that avoiding excessive nitrite after nitrification and maintain the DO at 1.5mg/L would reduce the  $N_2O$  production (Desloover et al., 2012; Frison et al., 2015). The bright side of  $N_2O$  was that it could be used as an oxidant for engines in high-performance vehicles or rocket motors. Scientists had explored a new technology to recover the  $N_2O$  from the denitrification process. Scherson et al. (2014) introduced a new technology named “CANDO”, which recovered  $N_2O$  from denitrification process and then combusted  $N_2O$  with  $CH_4$  to improve the energy generating efficiency from the combustion.

Overall, future works are required to understand the  $N_2O$  production pathways in depth and validate the contribution of different pathways to the overall  $N_2O$  production.


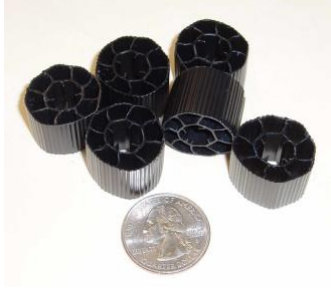
#### **2.4.Integrated fixed film activated sludge (IFAS) technology**

Date back to 18 years ago, rope-like Ringlece integrated fixed-film media was employed by Randall and Sen (Randall and Sen, 1996) in municipal wastewater reclamation facility, Anne Arundel County, Maryland, USA. They proved that the integrated fixed-film activated sludge (IFAS) is a promising technology that capable of enhancing the nitrogen removal without the additional construction of reaction tanks. It saved millions of dollars for the projected construction

cost. The key for the IFAS technology was to combine the attached biofilm and the suspended sludge in the same reactor. In this way, the SRT was extended and the autotrophic nitrifiers could be retained in the system.

There are two major types of media incorporated into the IFAS systems: the fixed media and mobile media. The fixed media refers to the media that are fixed in place in the reactor, for example the rope-like media mentioned above. However, the rope-like media turned out to face serious operational problem, such as the unwanted worm bloom (Copithron et al., 2006). The worm bloom would lead to the collapse of the whole system. To solve the problem, more and more advanced media had been invented, for example, web-like fixed media (BioWeb®), plastic sheets-like tricking filters had been employed in IFAS technology. The structured plastic sheets designed with specific aeration system had been proved to control the growth of red worms. The mobile media refers the media that are mobile and free moving in the IFAS reactor, instead of being fixed in place in the reactor. The foam pads and sponge were the first type of market available mobile media. The foam pads were marketed as CAPTOR technology by Simons-Hartley Ltd. The Foam pads with a specific density of about 0.95g/mL were placed in the reactor in a free-floating fashion with a screen used for media retention (Metcalf and Eddy, 2003). Air knives were used for screen cleaning. Pads were withdrawn and cleaned by a pad cleaner. The sponge media was developed by Linde AG. Compared to foams pads, the sponge blocks were more heterogeneous in shape and size. Same as foams, retention screens are required to prevent the loss of media (Metcalf and Eddy, 2003). However, the frequent replacement of foam pads and sponge due to the fragility of these mobile media raised the cost of long-term operation. A new rigid type of mobile media was marketed by AnoxKaldnes. This rigid, polyethylene media had a life of more than 10 years, according to the practical experience. Further, no backwash of the media was required because the

media was self-maintained. Retention screens were still required. The advantages and disadvantages of the fixed and mobile media are listed in the following table.

<b>Table 2.1. The comparison of fixed and mobile media.</b> Figures adapted from Johnson et al. (2005) and Ye et al. (2010).		
	<b>Fixed</b>	<b>Mobile</b>
		
<b>Advantages</b>	<p>High surface area provided high efficiency</p> <p>Low cost</p> <p>Low land requirement</p> <p>Upgrade the existing system without construction of extra reaction tanks</p> <p>Enhanced activated sludge activities</p> <p>Less sludge production</p> <p>Easy, quick and inexpensive installation</p> <p>Can use existing aeration system</p> <p>No in-basin screen needed</p>	<p>Easy installation</p> <p>Not subject to the growth of red worms</p> <p>High rate of bio-kinetics with less production of sludge</p> <p>Enhance nutrient removal performance without additional construction of reaction tanks</p>
<b>Disadvantages</b>	<p>-Subject to unwanted growth of red worms, in case of worm bloom, chlorinate RAS and anoxic treatment is needed.</p> <p>-Periodic cleaning for specific types of fixed media</p> <p>-Locations of aeration system and media module need to be justified to meet the removal efficiency goal</p> <p>The durability of the media material need to be considered</p>	<p>-Retention screen required</p> <p>Maintenance issues with huge number of carriers</p> <p>-Finer influent screening required</p> <p>-Subject to filamentous organisms growth</p> <p>-Air knives required for screen cleaning</p> <p>-Typically required coarse bubble diffusers</p> <p>-Insufficient mixing in the reactor</p> <p>-Relatively high cost, if consider the modifying construction</p>

Till now, the IFAS technology improved notably. The technology had been applied into wastewater treatment of different scales world widely (Borchert et al., 2011; Johnson et al., 2005; Johnson and McQuarrie, 2002; Ye et al., 2010, 2009).

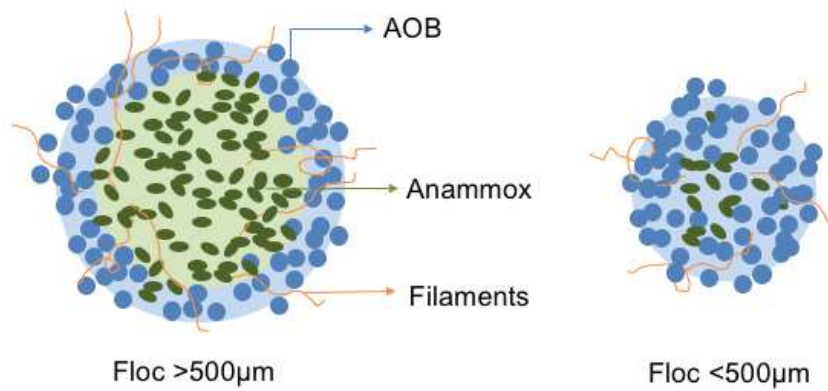
The mobile media was selected for this study to test the feasibility and stability of IFAS reactor in the mainstream wastewater treatment through complete nitrification-denitrification and the side-stream treatment through the partial nitrification-denitrification.

## **2.5. Other partial nitrification related technologies**

Regarding the application of partial nitrification process in the treatment of high ammonia strength wastewater, there are several technologies available. The first well-known technology is called “Single reactor system for High Ammonia Removal Over Nitrite process (SHARON)”. The SHARON process was first developed using a bench top reactor by the Delft University of Technology and later applied in full-scale Dokhaven WWTP at Rotterdam (Hellings et al., 1998). The SHARON process was operated under high temperature (35°C) in order to proliferate the AOB and eliminate the NOB. The SHARON process can be combined with the denitrification process or the anammox process.

The CANON process refers to the completely autotrophic nitrogen removal over nitrite. This technology was also developed at Delft University of Technology and was based on the presence of nitrifying and anammox bacteria in the flocs (Nielsen et al., 2005; Sliekers et al., 2003). The processes in their studies was flocs based or granular sludge based. Spatial separation of organisms and processes was discovered. Under oxygen limited conditions, ammonia was oxidized to nitrite by nitrifying bacteria resided on the outer layer of big flocs (>500µm in diameter), and then nitrite reacted together with the remaining ammonia to form nitrogen gas by anammox bacteria that lived

in the internal layer of the flocs. More interesting, they also found the nitrification was carried out mainly by the small flocs (<500µm in diameter) in the reactor, and the anammox activity was carried out by the big flocs. Figure 2.5 demonstrates the spatial distribution of AOB and anammox in the flocs of different sizes from the CANON system.



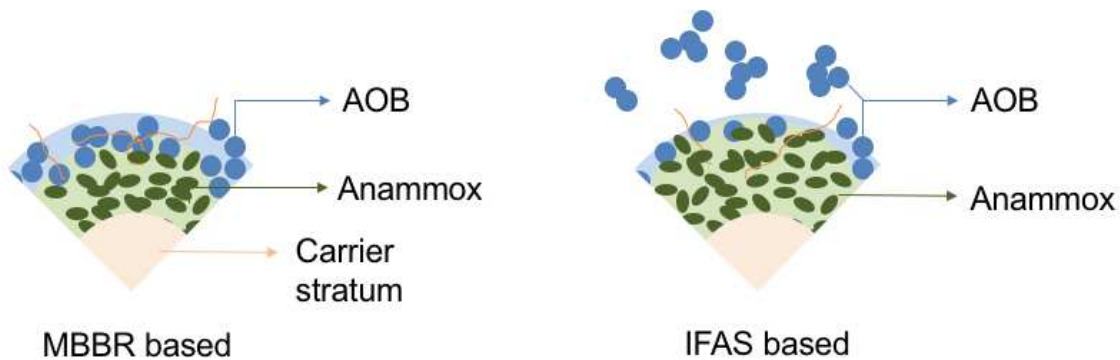
**Figure 2.5.** The distribution of AOB and anammox in the small and big flocs from the CANON system.

The OLAND technology is short for the oxygen limited autotrophic nitrification denitrification. This technology was developed in the Laboratory of Microbial Ecology in Gent (Verstraete and Philips 1998). Kuai and Verstraete (1998) were the first to introduce the term OLAND. At first, this process was believed to attribute to nitrifiers, but further investigation showed that anammox bacteria were also responsible for ammonium nitrogen removal. That make the OLAND and CANON are quite similar. But some scientists still believed that the OLAND technology took advantages of the denitrification activity of the aerobic nitrifiers (Ahn 2006). Generally, two steps were involved in this technology: ammonium oxidation to nitrite and nitrite reduction to nitrogen gas all by nitrifying bacteria.

The DEMON system had ammonia-oxidizing bacteria (AOB) in it, which converted half the ammonia to nitrite. A second anaerobic biological process used the anammox bacteria to convert the nitrite and remaining ammonia directly into nitrogen gas. The theory behind this technology

was similar to the CANON and OLAND technology. But the true key to the process success was the patented control strategy and patent pending biomass separation device, which enriched the specialized slowly growing biomass. This enhanced process robustness and treatment capacity (Nifong et al., 2013).

ANITA™Mox technology was marketed by Veolia Water Technologies. The first full-scale application was in Malmo, Sweden. This technology can be operated under MBBR or IFAS based. For MBBR based system, a biofilm stratification concept was used, similar to the CANON technology. While the concept for this IFAS based system was the separation of AOB in the sludge and anammox organisms attached on the biofilm. The IFAS based system turned out to be three times faster than the MBBR system (Lemaire et al., 2013). The concepts for the IFAS based and MBBR based systems were compared in Figure 2.6. The company brings out a new seeding strategy called “BioFarm”. This BioFarm is well maintained anammox reactor and filled with K5 carrier to support the growth of anammox. For new ANITA™Mox installations, BioFarm provides 3% to 15% of the carriers to the new reactors. This idea can shorten the reactor start-up time from 9-12 months to 2-5 months (Christensson et al., 2013, 2011).



**Figure 2.6.** the comparison between the MBBR and IFAS based ANITA™Mox systems.

Another new innovative technology that take advantages of partial nitrification process is called coupled aerobic-anoxic nitrous decomposition operation (CANDO). This technology was



developed by Stanford University (Scherson et al., 2014). The technology is divided into three major parts: 1) partial nitrification from ammonia to nitrite, 2) recovery of nitrous oxide gas from the partial denitrification of nitrite; and 3)  $N_2O$  conversion to  $N_2$  with energy recovery by either the catalytic decomposition to  $N_2$  and  $O_2$  or the use of  $N_2O$  to oxidize biogas  $CH_4$ . As the first and the third steps were previously established under full scale, the major breakthrough of Scherson et al.'s study was the nitrous oxide recovery strategy, in which they found that decoupled dosing of carbon sources and nitrite can maximize the production of nitrous oxide. Adding acetate in to the bioreactor under anaerobic condition increases the poly-hydroxybutyrate (PHB) production in the cells. After, nitrite is added to the reactor and reacts with PHB to form  $N_2O$ .

A floc-based four stages hybrid system named new activated sludge (NAS<sup>®</sup>) was developed by Colson, The Netherlands. This hybrid system consists of partial nitrification, anammox, denitrification, and nitrification processes. It is designed to treat the effluent from the digested food-processing wastewater to dischargeable level (Desloover et al., 2011; Lackner et al., 2014).

The technology for partial nitrification is improving and developing. Even though the anammox become a hotspot recently, the un-stability and long starting up time of anammox reactors are still big challenges for applications. Considering this, the partial nitrification and denitrification are chosen as the main subjects for this study due to the fast start-up, stability and high biodegradation efficiency of partial nitrification and denitrification.

As mentioned before, the IFAS based reactors were used in this study. A small bench top IFAS reactor (1L) was used to test the stability of complete nitrification-denitrification processes under different C/N ratio. Two more bench top IFAS reactors (6L each) were operated to test the feasibility of partial nitrification for the treatment of high ammonia strength lagoon supernatant.

These two reactors were operated under sequencing batch mode as the partial nitrification was easily achievable under the sequencing batch mode.

## 2.6. References

- Adair, K.L., Schwartz, E., 2008. Evidence that Ammonia-Oxidizing Archaea are More Abundant than Ammonia-Oxidizing Bacteria in Semiarid Soils of Northern Arizona, USA. *Microb. Ecol.* 56, 420–426. <https://doi.org/10.1007/s00248-007-9360-9>
- Ahn, Y.-H., 2006. Sustainable nitrogen elimination biotechnologies: A review. *Process Biochem.* 41, 1709–1721. <https://doi.org/10.1016/j.procbio.2006.03.033>
- American Water Works Association (Ed.), 2006. Fundamentals and control of nitrification in chloraminated drinking water distribution systems, 1st ed. ed, AWWA manual. American Water Works Association, Denver, CO.
- Anthonisen, A.C., Loehr, R.C., Prakasam, T.B.S., Srinath, E.G., 1976. Inhibition of Nitrification by Ammonia and Nitrous Acid. *J. Water Pollut. Control Fed.* 48, 835–852.
- Bai, Y., Sun, Q., Wen, D., Tang, X., 2012. Abundance of ammonia-oxidizing bacteria and archaea in industrial and domestic wastewater treatment systems. *FEMS Microbiol. Ecol.* 80, 323–330. <https://doi.org/10.1111/j.1574-6941.2012.01296.x>
- Bartossek, R., Nicol, G.W., Lanzen, A., Klenk, H.-P., Schleper, C., 2010. Homologues of nitrite reductases in ammonia-oxidizing archaea: diversity and genomic context: Nitrite reductase of soil archaea. *Environ. Microbiol.* 12, 1075–1088. <https://doi.org/10.1111/j.1462-2920.2010.02153.x>
- Bartossek, R., Spang, A., Weidler, G., Lanzen, A., Schleper, C., 2012. Metagenomic Analysis of Ammonia-Oxidizing Archaea Affiliated with the Soil Group. *Front. Microbiol.* 3. <https://doi.org/10.3389/fmicb.2012.00208>

- Borchert, J., Hubbell, S., Rupp, H., 2011. Demonstration of IFAS Technology for Cold Temperature Nitrification in Lagoon WWTFs at Clare and Ludington, Michigan. Proc. Water Environ. Fed. 2011, 5257–5264. <https://doi.org/10.2175/193864711802765705>
- Bothe, H., Ferguson, S.J., Newton, W.E. (Eds.), 2007. Biology of the nitrogen cycle, 1st ed. ed. Elsevier, Amsterdam ; Boston.
- Choi, E., 2007. Piggery waste management: towards a sustainable future. IWA Publ, London.
- Christensson, M., Ekström, S., Chan, A.A., Le Vaillant, E., Lemaire, R., 2013. Experience from start-ups of the first ANITA Mox Plants. Water Sci. Technol. 67, 2677. <https://doi.org/10.2166/wst.2013.156>
- Christensson, M., Ekström, S., Lemaire, R., Le Vaillant, E., Bundgaard, E., Chauzy, J., Stålhandske, L., Hong, Z., Ekenberg, M., 2011. ANITA™ Mox – A BioFarm Solution for Fast Start-up of Deammonifying MBBRs. Proc. Water Environ. Fed. 2011, 265–282. <https://doi.org/10.2175/193864711802639309>
- Ciudad, G., Rubilar, O., Muñoz, P., Ruiz, G., Chamy, R., Vergara, C., Jeison, D., 2005. Partial nitrification of high ammonia concentration wastewater as a part of a shortcut biological nitrogen removal process. Process Biochem. 40, 1715–1719. <https://doi.org/10.1016/j.procbio.2004.06.058>
- Claros, J., Jiménez, E., Aguado, D., Ferrer, J., Seco, A., Serralta, J., 2013. Effect of pH and HNO<sub>2</sub> concentration on the activity of ammonia-oxidizing bacteria in a partial nitritation reactor. Water Sci. Technol. 67, 2587. <https://doi.org/10.2166/wst.2013.132>
- Copithron, R.R., Sturdevant, J., Farren, G., Sen, D., 2006. Case study of an IFAS system-Over 10 years of experience. Water Environ. Fund.
- Daims, H., Lebedeva, E.V., Pjevac, P., Han, P., Herbold, C., Albertsen, M., Jehmlich, N., Palatinszky, M., Vierheilig, J., Bulaev, A., Kirkegaard, R.H., von Bergen, M., Rattei, T., Bendinger, B., Nielsen, P.H., Wagner, M., 2015. Complete nitrification by Nitrospira bacteria. Nature 528, 504–509. <https://doi.org/10.1038/nature16461>

- Desloover, J., De Clippeleir, H., Boeckx, P., Du Laing, G., Colsen, J., Verstraete, W., Vlaeminck, S.E., 2011. Floc-based sequential partial nitrification and anammox at full scale with contrasting N<sub>2</sub>O emissions. *Water Res.* 45, 2811–2821. <https://doi.org/10.1016/j.watres.2011.02.028>
- Desloover, J., Vlaeminck, S.E., Clauwaert, P., Verstraete, W., Boon, N., 2012. Strategies to mitigate N<sub>2</sub>O emissions from biological nitrogen removal systems. *Curr. Opin. Biotechnol.* 23, 474–482. <https://doi.org/10.1016/j.copbio.2011.12.030>
- Domingo-Félez, C., Pellicer-Nàcher, C., Petersen, M.S., Jensen, M.M., Plósz, B.G., Smets, B.F., 2017. Heterotrophs are key contributors to nitrous oxide production in activated sludge under low C-to-N ratios during nitrification-Batch experiments and modeling: N<sub>2</sub>O Production in Nitrifying Batch Experiments. *Biotechnol. Bioeng.* 114, 132–140. <https://doi.org/10.1002/bit.26062>
- Duan, H., Ye, L., Erler, D., Ni, B.-J., Yuan, Z., 2017. Quantifying nitrous oxide production pathways in wastewater treatment systems using isotope technology – A critical review. *Water Res.* 122, 96–113. <https://doi.org/10.1016/j.watres.2017.05.054>
- EPA, 1999. Wastewater Technology Fact Sheet Sequencing Batch Reactors.
- Francis, C.A., Roberts, K.J., Beman, J.M., Santoro, A.E., Oakley, B.B., 2005. Ubiquity and diversity of ammonia-oxidizing archaea in water columns and sediments of the ocean. *Proc. Natl. Acad. Sci.* 102, 14683–14688. <https://doi.org/10.1073/pnas.0506625102>
- Freitag, A., Rudert, M., Bock, E., 1987. Growth of *Nitrobacter* by dissimilatory nitrate reduction. *FEMS Microbiol. Lett.* 48, 105–109. <https://doi.org/10.1111/j.1574-6968.1987.tb02524.x>
- Frison, N., Chiumenti, A., Katsou, E., Malamis, S., Bolzonella, D., Fatone, F., 2015. Mitigating off-gas emissions in the biological nitrogen removal via nitrite process treating anaerobic effluents. *J. Clean. Prod.* 93, 126–133. <https://doi.org/10.1016/j.jclepro.2015.01.017>

- Fux, C., Velten, S., Carozzi, V., Solley, D., Keller, J., 2006. Efficient and stable nitrification and denitrification of ammonium-rich sludge dewatering liquor using an SBR with continuous loading. *Water Res.* 40, 2765–2775. <https://doi.org/10.1016/j.watres.2006.05.003>
- Gabarró, J., González-Cárcamo, P., Rusalleda, M., Ganigué, R., Gich, F., Balaguer, M.D., Colprim, J., 2014. Anoxic phases are the main N<sub>2</sub>O contributor in partial nitrification reactors treating high nitrogen loads with alternate aeration. *Bioresour. Technol.* 163, 92–99. <https://doi.org/10.1016/j.biortech.2014.04.019>
- Ge, S., Peng, Y., Qiu, S., Zhu, A., Ren, N., 2014. Complete nitrogen removal from municipal wastewater via partial nitrification by appropriately alternating anoxic/aerobic conditions in a continuous plug-flow step feed process. *Water Res.* 55, 95–105. <https://doi.org/10.1016/j.watres.2014.01.058>
- Glass, C., Silverstein, J., Oh, J., 1997. Inhibition of Denitrification in Activated Sludge by Nitrite. *Water Environ. Res.* 69, 1086–1093.
- Gustavsson, D.J.I., 2010. Biological sludge liquor treatment at municipal wastewater treatment plants – a review. *Vatten* 66, 179–192.
- Güven, D., 2009. Effects of Different Carbon Sources on Denitrification Efficiency Associated with Culture Adaptation and C/N Ratio. *CLEAN - Soil Air Water* 37, 565–573. <https://doi.org/10.1002/clen.200800198>
- Hao, O.J., Chen, J.M., 1994. Factors Affecting Nitrite Buildup in Submerged Filter System. *J. Environ. Eng.* 120, 1298–1307. [https://doi.org/10.1061/\(ASCE\)0733-9372\(1994\)120:5\(1298\)](https://doi.org/10.1061/(ASCE)0733-9372(1994)120:5(1298))
- He, J., Shen, J., Zhang, L., Zhu, Y., Zheng, Y., Xu, M., Di, H., 2007. Quantitative analyses of the abundance and composition of ammonia-oxidizing bacteria and ammonia-oxidizing archaea of a Chinese upland red soil under long-term fertilization practices. *Environ. Microbiol.* 9, 2364–2374. <https://doi.org/10.1111/j.1462-2920.2007.01358.x>

- Hellinga, C., Schellen, A., Mulder, J., Vanloosdrecht, M., Heijnen, J., 1998. The sharon process: An innovative method for nitrogen removal from ammonium-rich waste water. *Water Sci. Technol.* 37, 135–142. [https://doi.org/10.1016/S0273-1223\(98\)00281-9](https://doi.org/10.1016/S0273-1223(98)00281-9)
- Johnson, T.L., McQuarrie, J.P., 2002. IFAS BNR Full-scale Design and Performance Challenges. *Proc. Water Environ. Fed.* 2002, 214–226. <https://doi.org/10.2175/193864702784249105>
- Johnson, T.L., Wallis-Lage, C.L., Shaw, A.R., McQuarrie, J.P., 2005. IFAS OPTIONS – WHICH ONE IS RIGHT FOR YOUR PROJECT? *Proc. Water Environ. Fed.* 2005, 6290–6300. <https://doi.org/10.2175/193864705783815069>
- Koops, H.-P., Purkhold, U., Pommerening-Röser, A., Timmermann, G., Wagner, M., 2006. The Lithoautotrophic Ammonia-Oxidizing Bacteria, in: Dworkin, M., Falkow, S., Rosenberg, E., Schleifer, K.-H., Stackebrandt, E. (Eds.), *The Prokaryotes*. Springer New York, New York, NY, pp. 778–811. [https://doi.org/10.1007/0-387-30745-1\\_36](https://doi.org/10.1007/0-387-30745-1_36)
- Kowalski, M.S., Devlin, T.R., Oleszkiewicz, J.A., 2018. Start-up and long-term performance of anammox moving bed biofilm reactor seeded with granular biomass. *Chemosphere* 200, 481–486. <https://doi.org/10.1016/j.chemosphere.2018.02.130>
- Kozłowski, J.A., Stieglmeier, M., Schleper, C., Klotz, M.G., Stein, L.Y., 2016. Pathways and key intermediates required for obligate aerobic ammonia-dependent chemolithotrophy in bacteria and Thaumarchaeota. *ISME J.* 10, 1836–1845. <https://doi.org/10.1038/ismej.2016.2>
- Kuai, L., Verstraete, W., 1998. Ammonium Removal by the Oxygen-Limited Autotrophic Nitrification-Denitrification System. *Appl. Environ. Microbiol.* 64, 4500–4506.
- Kulikowska, D., Bernat, K., 2013. Nitritation–denitritation in landfill leachate with glycerine as a carbon source. *Bioresour. Technol.* 142, 297–303. <https://doi.org/10.1016/j.biortech.2013.04.119>

- Lackner, S., Gilbert, E.M., Vlaeminck, S.E., Joss, A., Horn, H., van Loosdrecht, M.C.M., 2014. Full-scale partial nitrification/anammox experiences – An application survey. *Water Res.* 55, 292–303. <https://doi.org/10.1016/j.watres.2014.02.032>
- Leininger, S., Urich, T., Schloter, M., Schwark, L., Qi, J., Nicol, G.W., Prosser, J.I., Schuster, S.C., Schleper, C., 2006. Archaea predominate among ammonia-oxidizing prokaryotes in soils. *Nature* 442, 806–809. <https://doi.org/10.1038/nature04983>
- Lemaire, R., Thesing, G., Christensson, M., Zhao, H., Liviano, I., 2013. Experience from Start-up and Operation of Deammonification MBBR Plants, and Testing of a New Deammonification IFAS Configuration. *Proc. Water Environ. Fed.* 2013, 1926–1947. <https://doi.org/10.2175/193864713813673857>
- Massara, T.M., Malamis, S., Guisasola, A., Baeza, J.A., Noutsopoulos, C., Katsou, E., 2017. A review on nitrous oxide (N<sub>2</sub>O) emissions during biological nutrient removal from municipal wastewater and sludge reject water. *Sci. Total Environ.* 596–597, 106–123. <https://doi.org/10.1016/j.scitotenv.2017.03.191>
- Metcalf, Eddy, 2003. *Wastewater Engineering, Treatment and Reuse*, 4th ed. McGraw-Hill, New York.
- Mulder, J.W., Duin, J.O.J., Goverde, J., Poiesz, W.G., van Veldhuizen, H.M., van Kempen, R., Roeleveld, P., 2006. Full-Scale Experience with the Sharon Process through the Eyes of the Operators. *Proc. Water Environ. Fed.* 2006, 5256–5270. <https://doi.org/10.2175/193864706783763444>
- Mulder, J.W., van Loosdrecht, M.C., Hellinga, C., van Kempen, R., 2001. Full-scale application of the SHARON process for treatment of rejection water of digested sludge dewatering. *Water Sci. Technol. J. Int. Assoc. Water Pollut. Res.* 43, 127–134.
- Nhat, P.T., Biec, H.N., Van, T.T.T., Tuan, D.V., Trung, N.L.H., Nghi, V.T.K., Dan, N.P., 2017. Stability of partial nitrification in a sequencing batch reactor fed with high ammonium

- strength old urban landfill leachate. *Int. Biodeterior. Biodegrad.* 124, 56–61. <https://doi.org/10.1016/j.ibiod.2017.06.017>
- Nhu Hien, N., Van Tuan, D., Nhat, P.T., Thi Thanh Van, T., Van Tam, N., Xuan Que, V.O.N., Phuoc Dan, N., 2017. Application of Oxygen Limited Autotrophic Nitrification/Denitrification (OLAND) for anaerobic latex processing wastewater treatment. *Int. Biodeterior. Biodegrad.* 124, 45–55. <https://doi.org/10.1016/j.ibiod.2017.07.009>
- Nielsen, M., Bollmann, A., Sliemers, O., Jetten, M., Schmid, M., Strous, M., Schmidt, I., Larsen, L.H., Nielsen, L.P., Revsbech, N.P., 2005. Kinetics, diffusional limitation and microscale distribution of chemistry and organisms in a CANON reactor. *FEMS Microbiol. Ecol.* 51, 247–256. <https://doi.org/10.1016/j.femsec.2004.09.003>
- Nifong, A., Nelson, A., Johnson, C., Bott, C.B., 2013. Performance of a Full-Scale Sidestream DEMON® Deammonification Installation. *Proc. Water Environ. Fed.* 2013, 3686–3709. <https://doi.org/10.2175/193864713813685700>
- Nogueira, R., Melo, L.F., 2006. Competition between *Nitrospira* spp. and *Nitrobacter* spp. in nitrite-oxidizing bioreactors. *Biotechnol. Bioeng.* 95, 169–175. <https://doi.org/10.1002/bit.21004>
- Peng, Y., Zhu, G., 2006. Biological nitrogen removal with nitrification and denitrification via nitrite pathway. *Appl. Microbiol. Biotechnol.* 73, 15–26. <https://doi.org/10.1007/s00253-006-0534-z>
- Peng, Y.Z., Chen, Y., Peng, C.Y., Liu, M., Wang, S.Y., Song, X.Q., Cu, Y.W., 2004. Nitrite accumulation by aeration controlled in sequencing batch reactors treating domestic wastewater. *Water Sci. Technol. J. Int. Assoc. Water Pollut. Res.* 50, 35–43.
- Picioreanu, C., Van Loosdrecht, M.C.M., Heijnen, J.J., 1997. Modelling the effect of oxygen concentration on nitrite accumulation in a biofilm airlift suspension reactor, in: Harremoes, P. (Ed.), *Biofilm Systems*. Presented at the WATER SCIENCE AND TECHNOLOGY, Pergamon, pp. 147–156.



- Princic, null, Mahne, null, Megusar, null, Paul, null, Tiedje, null, 1998. Effects of pH and oxygen and ammonium concentrations on the community structure of nitrifying bacteria from wastewater. *Appl. Environ. Microbiol.* 64, 3584–3590.
- Prosser, J.I., Head, I.M., Stein, L.Y., 2014. The Family Nitrosomonadaceae, in: Rosenberg, E., DeLong, E.F., Lory, S., Stackebrandt, E., Thompson, F. (Eds.), *The Prokaryotes*. Springer Berlin Heidelberg, Berlin, Heidelberg, pp. 901–918. [https://doi.org/10.1007/978-3-642-30197-1\\_372](https://doi.org/10.1007/978-3-642-30197-1_372)
- Queiroz, L.M., Aun, M.V., Morita, D.M., Alem Sobrinho, P., 2011. Biological nitrogen removal over nitritation/denitritation using phenol as carbon source. *Braz. J. Chem. Eng.* 28, 197–207. <https://doi.org/10.1590/S0104-66322011000200004>
- Ramos, C., Suárez-Ojeda, M.E., Carrera, J., 2016. Denitritation in an anoxic granular reactor using phenol as sole organic carbon source. *Chem. Eng. J.* 288, 289–297. <https://doi.org/10.1016/j.cej.2015.11.099>
- Randall, C.W., Sen, D., 1996. Full scale evaluation of an integrated fixed-film activated sludge (IFAS) process for enhanced nitrogen removal. *Water Sci. Technol.* 33, 155–161.
- Rikmann, E., Zekker, I., Tenno, T., Saluste, A., Tenno, T., 2018. Inoculum-free start-up of biofilm- and sludge-based deammonification systems in pilot scale. *Int. J. Environ. Sci. Technol.* 15, 133–148. <https://doi.org/10.1007/s13762-017-1374-3>
- Ruiz, G., Jeison, D., Chamy, R., 2003. Nitrification with high nitrite accumulation for the treatment of wastewater with high ammonia concentration. *Water Res.* 37, 1371–1377. [https://doi.org/10.1016/S0043-1354\(02\)00475-X](https://doi.org/10.1016/S0043-1354(02)00475-X)
- Scherson, Y.D., Woo, S.-G., Criddle, C.S., 2014. Production of Nitrous Oxide From Anaerobic Digester Centrate and Its Use as a Co-oxidant of Biogas to Enhance Energy Recovery. *Environ. Sci. Technol.* 48, 5612–5619. <https://doi.org/10.1021/es501009j>
- Schreiber, F., Wunderlin, P., Udert, K.M., Wells, G.F., 2012. Nitric oxide and nitrous oxide turnover in natural and engineered microbial communities: biological pathways, chemical

- reactions, and novel technologies. *Front. Microbiol.* 3. <https://doi.org/10.3389/fmicb.2012.00372>
- Sinha, B., Annachhatre, A.P., 2007. Partial nitrification—operational parameters and microorganisms involved. *Rev. Environ. Sci. Biotechnol.* 6, 285–313. <https://doi.org/10.1007/s11157-006-9116-x>
- Sliekers, A.O., Third, K., Abma, W., Kuenen, J., Jetten, M.S., 2003. CANON and Anammox in a gas-lift reactor. *FEMS Microbiol. Lett.* 218, 339–344. [https://doi.org/10.1016/S0378-1097\(02\)01177-1](https://doi.org/10.1016/S0378-1097(02)01177-1)
- Stehr, G., S. Zörner, B. Böttcher, H. P. Koops, 1995. Exopolymers: An Ecological Characteristic of a Floc-Attached, Ammonia-Oxidizing Bacterium. *Microb. Ecol.* 115.
- Stein, L.Y., Klotz, M.G., 2016. The nitrogen cycle. *Curr. Biol.* 26, R94–R98. <https://doi.org/10.1016/j.cub.2015.12.021>
- Strous, M., Fuerst, J.A., Kramer, E.H.M., Logemann, S., Muyzer, G., van de Pas-Schoonen, K.T., Webb, R., Kuenen, J.G., Jetten, M.S.M., 1999. Missing lithotroph identified as new planctomycete. *Nature* 400, 446–449. <https://doi.org/10.1038/22749>
- Stüven, R., Vollmer, M., Bock, E., 1992. The impact of organic matter on nitric oxide formation by *Nitrosomonas europaea*. *Arch. Microbiol.* 158. <https://doi.org/10.1007/BF00276306>
- Tokutomi, T., 2004. Operation of a nitrite-type airlift reactor at low DO concentration. *Water Sci. Technol. J. Int. Assoc. Water Pollut. Res.* 49, 81–88.
- Treusch, A.H., Leininger, S., Kletzin, A., Schuster, S.C., Klenk, H.-P., Schleper, C., 2005. Novel genes for nitrite reductase and Amo-related proteins indicate a role of uncultivated mesophilic crenarchaeota in nitrogen cycling: Role of mesophilic crenarchaeota in nitrogen cycling. *Environ. Microbiol.* 7, 1985–1995. <https://doi.org/10.1111/j.1462-2920.2005.00906.x>

- van Kessel, M.A.H.J., Speth, D.R., Albertsen, M., Nielsen, P.H., Op den Camp, H.J.M., Kartal, B., Jetten, M.S.M., Lücker, S., 2015. Complete nitrification by a single microorganism. *Nature* 528, 555–559. <https://doi.org/10.1038/nature16459>
- Verstraete, W., Philips, S., 1998. Nitrification-denitrification processes and technologies in new contexts. *Environ. Pollut.* 102, 717–726. [https://doi.org/10.1016/S0269-7491\(98\)80104-8](https://doi.org/10.1016/S0269-7491(98)80104-8)
- Walker, C.B., de la Torre, J.R., Klotz, M.G., Urakawa, H., Pinel, N., Arp, D.J., Brochier-Armanet, C., Chain, P.S.G., Chan, P.P., Gollabgir, A., Hemp, J., Hugler, M., Karr, E.A., Konneke, M., Shin, M., Lawton, T.J., Lowe, T., Martens-Habbena, W., Sayavedra-Soto, L.A., Lang, D., Sievert, S.M., Rosenzweig, A.C., Manning, G., Stahl, D.A., 2010. *Nitrosopumilus maritimus* genome reveals unique mechanisms for nitrification and autotrophy in globally distributed marine crenarchaea. *Proc. Natl. Acad. Sci.* 107, 8818–8823. <https://doi.org/10.1073/pnas.0913533107>
- Wang, X., Gao, D., 2016. In-situ restoration of one-stage partial nitrification-anammox process deteriorated by nitrate build-up via elevated substrate levels. *Sci. Rep.* 6. <https://doi.org/10.1038/srep37500>
- Wuchter, C., Abbas, B., Coolen, M.J.L., Herfort, L., van Bleijswijk, J., Timmers, P., Strous, M., Teira, E., Herndl, G.J., Middelburg, J.J., Schouten, S., Sinninghe Damste, J.S., 2006. Archaeal nitrification in the ocean. *Proc. Natl. Acad. Sci.* 103, 12317–12322. <https://doi.org/10.1073/pnas.0600756103>
- Yang, L., Alleman, J.E., 1992. Investigation of batch-wise nitrite build-up by an enriched nitrification culture. *Water Sci. Technol.* 26, 997–1005.
- Ye, J., Chestna, K.L., Kulick, F.M., Rotherme, B., 2010a. Full Scale Implementation, Operation, and Performance of a Structured Sheet Media IFAS System. *Proc. Water Environ. Fed.* 2010, 2555–2565. <https://doi.org/10.2175/193864710798170522>

- Ye, J., Kulick, F.M., McDowell, C.S., 2010b. Effective Biofilm Control on High Surface Density Vertical-Flow Structured Sheet Media for Submerged Applications. *Proc. Water Environ. Fed.* 2010, 4200–4220. <https://doi.org/10.2175/193864710798182402>
- Ye, J., McDowell, C.S., Koch, K., Koch, K., Kulick, F.M., Rothermel, B.C., 2009. Pilot Testing of Structured Sheet Media IFAS for Wastewater Biological Nutrient Removal (BNR). *Proc. Water Environ. Fed.* 2009, 4427–4442. <https://doi.org/10.2175/193864709793954015>
- Zhang, C.L., Ye, Q., Huang, Z., Li, W., Chen, J., Song, Z., Zhao, W., Bagwell, C., Inskip, W.P., Ross, C., Gao, L., Wiegel, J., Romanek, C.S., Shock, E.L., Hedlund, B.P., 2008. Global Occurrence of Archaeal amoA Genes in Terrestrial Hot Springs. *Appl. Environ. Microbiol.* 74, 6417–6426. <https://doi.org/10.1128/AEM.00843-08>
- Zhang, Z., Chen, S., Wu, P., Lin, L., Luo, H., 2010. Start-up of the Canon process from activated sludge under salt stress in a sequencing batch biofilm reactor (SBBR). *Bioresour. Technol.* 101, 6309–6314. <https://doi.org/10.1016/j.biortech.2010.03.040>

# **CHAPTER 3. WASTEWATER AMMONIUM REMOVAL USING AN INTEGRATED FIXED-FILM ACTIVATED SLUDGE-SEQUENCING BATCH BIOFILM REACTOR (IFAS-SBR): COMPARISON OF SUSPENDED FLOCS AND ATTACHED BIOFILM<sup>1</sup>**

## **3.1. Introduction**

Nitrogen (N) and phosphorous (P) are essential elements for microorganism growth. High concentrations of N and P in a water body will lead to eutrophication, posing threats to aquatic life (U.S. EPA, 2007). Also, a high free ammonia concentration in water is toxic to aquatic life. High ammonium concentration will lead to a high free ammonia concentration under high pH condition. Therefore, it is important to remove N and P from wastewater before releasing it into natural water reservoirs, thus nitrification efficiency is critical to the success of secondary biological wastewater treatment.

Integrated fixed-film activated sludge (IFAS) technology was developed to improve the efficiency of biological nutrient removal (BNR) in wastewater treatment plants worldwide. In the IFAS configuration, biocarriers are integrated into conventional activated sludge reactors to provide surface area for the bacterial attachment and growth. Biocarriers can also provide a longer solids retention time (SRT), as compared to the conventional activated sludge process, to facilitate slow growing nitrifying growth and promote nitrification (Kim et al., 2011; Onnis-Hayden et al., 2007). The potential effects of IFAS reactors on nutrient removal enhancement, especially nitrogen removal, had been extensively studied (Copithron et al., 2006; Johnson et al., 2005; Johnson and McQuarrie, 2002; Onnis-Hayden et al., 2011). Two main types of IFAS media that are commercially available: fixed and mobile media. The mobile media was used for this

---

<sup>1</sup>This chapter has been published: Shao, Y., Shi, Y., Mohammed, A., Liu, Y., 2017. Wastewater ammonia removal using an integrated fixed-film activated sludge-sequencing batch biofilm reactor (IFAS-SBR): Comparison of suspended flocs and attached biofilm. *International Biodeterioration & Biodegradation* 116, 38–47.

study as it facilitate high oxygen and nutrient transfer in reactors (Ye et al., 2009). Compared with continuous flow reactors, the operation of sequencing batch reactor (SBR) is more flexible. For full-scale application of SBR, parameters (like pH, concentrations of substrates, and dissolved oxygen) could be monitored by online analyzers. Biodegradation processes can be easily controlled by adjusting the timers or programed controllers. No clarifier is needed for SBR since the sedimentation will take place in the reactor itself (U.S. EPA, 1999). In this study, A combined IFAS and SBR technology was applied. The combination could improve the nitrification efficiency of conventional SBR and reduced the capital cost of upgrading existing reaction tanks.

Previous researchers suggested that the operational conditions of wastewater treatment reactors, including temperature, pH, and carbon/nitrogen (C/N) ratio, would affect the composition of the bacterial community (Bassin et al., 2012; Xia et al., 2008). The C/N ratio significantly affects the growth of and competition between heterotrophic and autotrophic nitrifying bacteria. The chemical oxygen demand (COD) represents the carbon source and energy source for heterotrophic bacteria. Nitrification is composed of two steps. Ammonium is used by autotrophic ammonia oxidizing bacteria (AOB) to produce nitrite in the first step of nitrification. In the second step of nitrification, nitrite is oxidized to nitrate by nitrite oxidizing bacteria (NOB). When heterotrophic bacteria are present in a reactor, a high COD will promote the growth of heterotrophs and increase the competition between heterotrophs and autotrophic nitrifying bacteria for space and oxygen, affecting the nitrification efficiency negatively (Bassin et al., 2012; Kim et al., 2011; Onnis-Hayden et al., 2011). However, the acclimation of heterotrophic bacteria on the support media in a reactor can also facilitate the biofilm development of nitrifying bacteria. Extracellular polymeric substances (EPS, also known as “slime”) are high molecular weight substances secreted by bacteria that enhance the attachment of bacteria to the support media. Heterotrophic bacteria produce high quantities of EPS, whereas nitrifiers are slow growing bacteria that usually lack EPS (Furumai and

Rittmann, 1994; Tsuneda et al., 2001). Bassin et al. (2012) found that the EPS secreted by a large amount of heterotrophic bacteria enhanced the biofilm accumulation of nitrifying bacteria during a reactor startup stage.

To promote the efficiency of biological wastewater treatment using IFAS technology, it is important to understand how the bacterial community changes in response to different operational conditions (Xia et al., 2008). Attached biofilm and suspended flocs are two major bacterial aggregates in an IFAS reactor. However, few studies have focused on bacterial community changes in both attached and suspended phases of a bioreactor and the related EPS production in response to different organic loadings. This study investigates the bacterial community compositional differences in biofilm and suspended activated sludge under different organic loadings in a bench scale IFAS reactor. The nitrifying activities of bacteria in both phases were analyzed with emphasis on comparing the impact of the organic loading on both suspended and attached phases that including (1) bacterial community dynamics—i.e., the distribution of AOB, NOB, and heterotrophic bacteria; (2) EPS production dynamics; and (3) nitrification and COD removal efficiency. The design of this experiment provides guidelines for a full-scale application of IFAS. The comparison between suspended flocs and attached biofilm enables a better understanding of the stability of these two aggregates in response to operational condition changes.

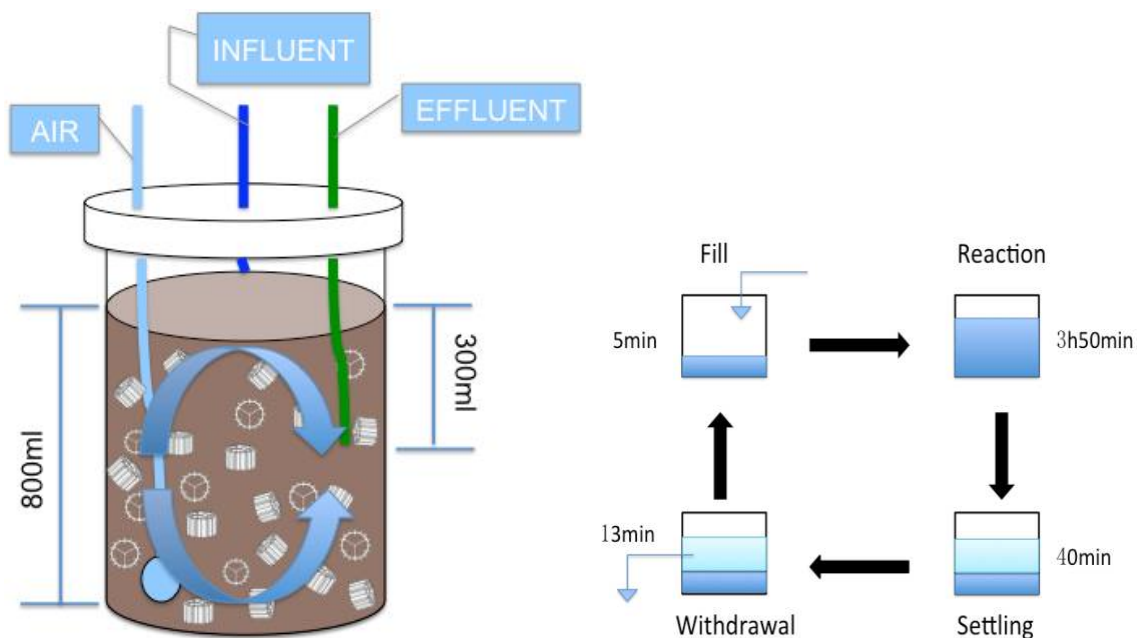
## **3.2. Method and Material**

### **3.2.1. Reactor operation**

One reactor (800 mL) was operated in sequencing batch mode with decreasing COD concentration in influent over time from September to December 2014. Synthetic wastewater (see Appendix A for recipe) was used as reactor influent (Zeng et al., 2003). Ammonium-nitrogen concentration in the influent was kept at around 50mg/L. As the COD concentration decreased and the ammonium

nitrogen did not change, the C/N ratios were 10:1 in Phase 1, 5:1 in Phase 2, and 3:1 in Phase 3. Sodium acetate was used as carbon source to adjust the C/N ratio.

Each cycle of the sequencing batch reactor (SBR) was 4 hours and 48 minutes, which included 5 min of feeding, 3 h and 50 min of reaction, 40 min of settling, and 13 min of fluid withdrawal (Figure 3.1). The volume exchange ratio was about 37.5%. The hydraulic retention time was 12 h and 48 min. The reactor was filled with polyethylene carriers 50% by volume (Bioflow 9) (RVT Process Equipment GmbH Company). The carriers were cylindrical with 9 mm diameter, 7 mm height, and a specific area of 800 m<sup>2</sup>/m<sup>3</sup>. The carrier density was 145 kg/m<sup>3</sup>, which is lighter than water. The low density enabled carriers to suspend and circulate in the reactor. Before Phase 1, the carriers were cultivated for one month to develop the biofilm. Air was pumped and diffused to the bottom of the reactor to provide oxygen to the reactor and drive carriers to flow throughout the reactor. The dissolved oxygen (DO) level in the reactor was maintained at 7–8 mg/L in all phases.



**Figure 3.1.** IFAS-SBR configuration and sequences for one cycle.



Reactor influent and effluent were sampled every day (or every two days when the bioreactor stabilized). The system was considered stable if the effluent characteristics and mixed liquid volatile suspended solids (MLVSS) were unchanged for one week. All samples were filtered (0.45  $\mu\text{m}$  pore) before being analyzed for COD,  $\text{NH}_4^+\text{-N}$ ,  $\text{NO}_3^-\text{-N}$ ,  $\text{NO}_2^-\text{-N}$  concentrations with reagent kits (methods 8000, 10205, 10206, 10207, respectively, Hach Company, Loveland, Colorado) within 2 hours of collection.

### 3.2.2. Biodegradation kinetics

To better understand nitrification activities, SBR cycle tests were conducted at the end of each phase. Mixed liquid samples were collected at the start of the reaction (0 min) and 5, 10, 15, 25, 35, 50, 65, 95, 125, 185 min, and the end of the reaction (230 min). The pH of the samples was measured at the sample collection points. Samples were centrifuged at 3000 g for 1 min, filtered (0.45  $\mu\text{m}$  pore), and analyzed for COD and  $\text{NH}_4^+\text{-N}$ . The  $\text{NH}_4^+\text{-N}$  uptake rate was determined as the linear regression of  $\text{NH}_4^+\text{-N}$  concentration over time divided by the VSS in the system (Bassin et al., 2012).

### 3.2.3. Biomass in activated sludge and biofilm

To determine growth in the suspended phase, mixed liquor suspended solids (MLSS) and MLVSS were measured at the end of each C/N ratio conditions using *Standard Methods 2540B* (APHA, 2011). The biomass attached to carriers was measured using standard methods with modifications. Briefly, five carriers were gently rinsed with demineralized water to remove loosely attached

biomass, then soaked with 25 mL ultrapure water in polyethylene centrifuge tubes. Carriers were sonicated for 10 min, then vortexed at maximum speed for one minute to detach biofilm from the carriers. The detached biofilm was measured using *Standard Methods* 2540B (APHA, 2011). The biofilm TSS and VSS were measured using *Standard Methods* 2540E (APHA, 2011).

#### 3.2.4. Extracellular polymeric substance (EPS) analysis

EPS in the activated sludge was extracted using the formaldehyde–NaOH method with modifications (Liu and Fang, 2002). 10 mL sludge was collected in a 15 mL polyethylene centrifuge tube and 0.06 mL of 36.5% formaldehyde was added to the tube. The tube contents were mixed by inversion for several times and stored at 4 °C for one hour. After one hour, the solution was mixed with 4 mL 1 N NaOH and stored at 4 °C for three hours. The tubes were then centrifuged at 6000 g for 20 minutes and the supernatant was collected, filtered (0.22 µm pore), and dialysed for 24 hours. To extract biofilm EPS, carriers were sonicated in ultrapure water for 10 min, then the liquid mixture was treated with the method described above. Polysaccharides in the EPS were analyzed by methods developed by DuBois et al., (1956). EPS protein content was determined using a Coomassie (Bradford) Protein Assay Kit from Thermo Scientific (Bradford, 1976). EPS production per biomass was calculated by dividing the EPS production by the VSS in the biofilm and the VSS in the activated sludge, separately.

#### 3.2.5. q-PCR analysis

Duplicate DNA samples were collected at the end of Phase 1, and the beginning, middle, and end of Phase 2 and Phase 3. Biomass DNA was extracted with MO BIO PowerSoil® DNA Isolation

Kits (MoBio Laboratories Inc, Carlsbad, California). Total bacteria, AOB, NOB, and denitrification bacteria were analyzed by qPCR (Bio-Rad Laboratories (Canada) Ltd., Mississauga, Ontario). Information about the primers and target genes is provided in Table 3.1. To identify AOB, primer sets amoA-1F and amoA-2R-TC targeted the gene encoding subunit A of ammonia monooxygenase (amoA) only in betaproteobacteria (Risgaard-Petersen et al., 2004). To identify NOB, the 16S rRNA gene of *Nitrobacter* spp. and *Nitrospira* spp. were targeted by corresponding primer sets. Details about denitrification primers and target genes are included in the supporting material (Appendix B-2).

**Table 3.1. Primers required for q-PCR analysis and target genes.**

	Primer	Nucleotides sequence 5'-3'	Target	References
<b>AOB</b>	amoA-1F	GGGGTTTCTACTGGTGGT	amoA gene of betaproteobacteria AOB	Risgaard-Petersen et al. 2004
	amoA-2R-TC	CCCCTCTGCAAAGCCTTCTTC		
<b>NOB</b>	Nitro 1198f	ACCCCTAGCAAATCTCAAAAAACCG	<i>Nitrobacter</i> spp. 16S rDNA	Y. M. Kim et al. 2011
	Nitro 1423r	CTTACCCCCAGTCGCTGACC	Nitrospira spp. 16S rDNA	
	NSR 1113f	CCTGCTTTCAGTTGCTACCG		
<b>Denitrifier</b>	NSR 1264r	GTTTGCAGCGCTTTGTACCG	nosZ gene          nirS gene       narG gene    nirK gene	
	nosZ 2F	CGCRACGGCAASAAGGTSMSST		
	nosZ 2R	CAK RTG CAK SGC RTG GCA GAA		
	nirS 1f	TACCACCCSGARCCGCGGT		
	nirS 3r	GCCGCCGTCTRTGVAGGAA		
	narG 1960m2f	TAYGTSGGGCAGGARAAACTG		
	narG 2050m2r	CGTAGAAGAAGCTGGTGCTGTT		
	nirK876	ATYGGCGGVCA YGGCGA		
	nirK1040	GCCTCGATCAGRTTTRTGTT		
	<b>Total bacteria</b>	341f		
	907r	CCGTCAATT CMT TTG AGT TT		

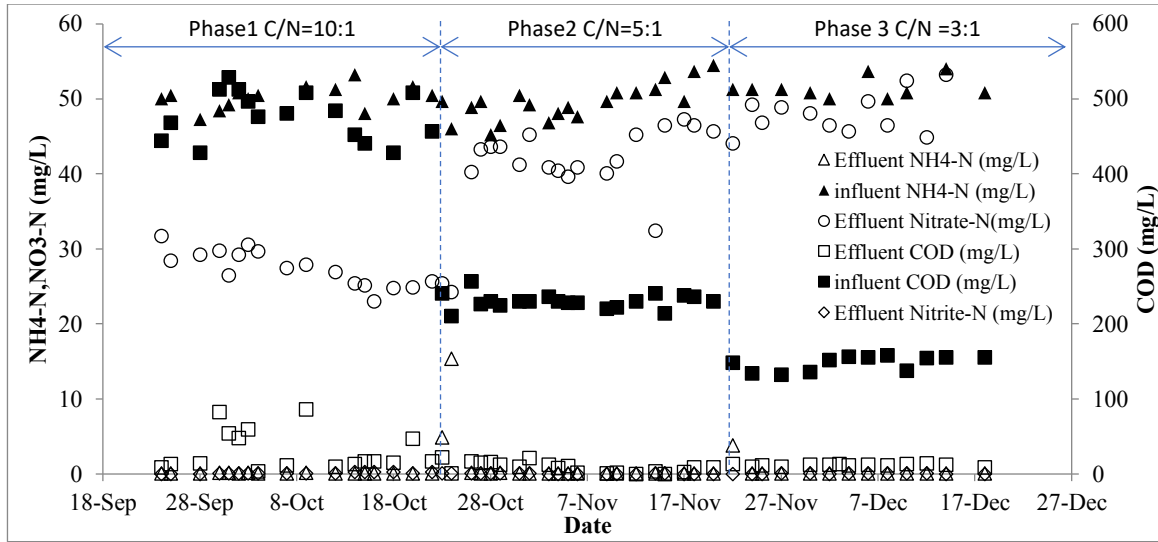
### 3.2.6. Statistical analysis

COD and  $\text{NH}_4^+\text{-N}$  removal percentages during the three phases were analyzed with single factor analysis of variance (ANOVA) with R-programming software and reported as p-values; a p-value smaller than 0.05 suggested that the difference was statistically significant. Other results from different phases are also analyzed with single factor ANOVA to determine the statistically significant differences.

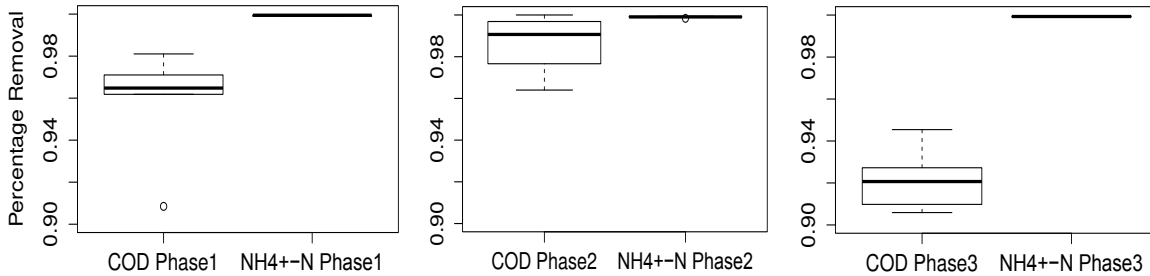
## 3.3. Results and Discussion

### 3.3.1. Reactor performance

Figure 3.2 shows that during stable stages (the end of each phase), the COD in the effluent was around 10 –20 mg/L and the  $\text{NH}_4^+\text{-N}$  concentration was lower than 0.1 mg/L. COD removal was  $95.9 \pm 2.6\%$ ,  $98.6 \pm 1.5\%$ , and  $92.2 \pm 1.6\%$  in Phase 1, Phase 2, and Phase 3, respectively. The COD concentrations in the influent were different in all three phases, which affected the percent COD removal.  $\text{NH}_4^+\text{-N}$  removal was  $99.93 \pm 0.03\%$  in Phase 1,  $99.90 \pm 0.04\%$  in Phase 2, and  $99.93 \pm 0.004\%$  in Phase 3. The ANOVA test showed that in the three phases the COD removal percentages were statistically different from each other (F critical = 15.99,  $p < 0.0002$ ), whereas  $\text{NH}_4^+\text{-N}$  removal percentages were not statistically different (F critical = 1.596,  $p = 0.24$ ). The  $\text{NH}_4^+\text{-N}$  removal efficiency did not change over the three phases while COD removal reached a peak of  $98.6 \pm 1.5\%$  in Phase 2. These data indicate that an IFAS-SBR is a good option for  $\text{NH}_4^+\text{-N}$  and COD removal from municipal wastewater under all C/N ratio conditions tested in this study.



(a)



(b)

(c)

(d)

**Figure 3.2.** (a) Influent and effluent concentrations of ammonia nitrogen, nitrate nitrogen, and COD; solid triangle and square represent ammonia and COD concentrations in influent, empty triangle, square, and circles show ammonia nitrogen, COD, and nitrate nitrogen in effluent. (b), (c), and (d) are boxplots that show the COD and ammonia nitrogen removal percentage in Phase 1 (C/N = 10:1), Phase 2 (C/N=5:1), and Phase 3 (C/N = 3:1), respectively. In all boxplots, the bottom of each box shows the first quartile of the dataset, the bold line at the center represents the second quartile (median) of the data points, and the top line of the box is the third quartile of the dataset.

Based on nitrogen balance of the system illustrated by Haandel and Lubbe (2012) , the nitrogen balance equation for stabilized system can be described below by Equation 3.1. No organic nitrogen was added into the influent.

Molecular nitrogen gas ( $N_2$ )= $(NH_4^+-N_{in} - NH_4^+-N_{ef} - NO_2^--N_{ef} - NO_3^--N_{ef}) \times 37.5\%V$   
(Equation 3.1)

The unit for  $N_2$  is mg,  $NH_4^+-N_{in}$ ,  $NH_4^+-N_{ef}$ ,  $NO_2^--N_{ef}$ , and  $NO_3^--N_{ef}$  are the concentrations of ionized nitrogen species in the reactor.  $V$  is the volume of the reactor, and 37.5% is the volume exchange ratio of the reaction. Detailed derivation processes of the equation are included in Appendix A-2).

The effluent nitrate concentration was slightly less than 30 mg  $NO_3^-$ -N /L in Phase 1 and rose to 40–50 mg  $NO_3^-$ -N/L in Phase 2 and Phase 3. Hereby the denitrification activities exist in the reactors. The denitrification activities were the strongest in Phase1 when C/N ratio was 10:1(Fig.3.2). The production of nitrogen gas decreased as the C/N ratio decreased. This might be related to the decrease of organic carbon in influent that inhibited the growth of heterotrophic denitrifiers. Denitrification processes might happen during 40 minute settling stage when aeration stopped to facilitate sludge settling, and anoxic condition was created. In addition, the inner layer of activated sludge flocs and deeper layer of the biofilms might also be anoxic for denitrification (Huang et al., 2015).

### 3.3.2. Biomass concentrations

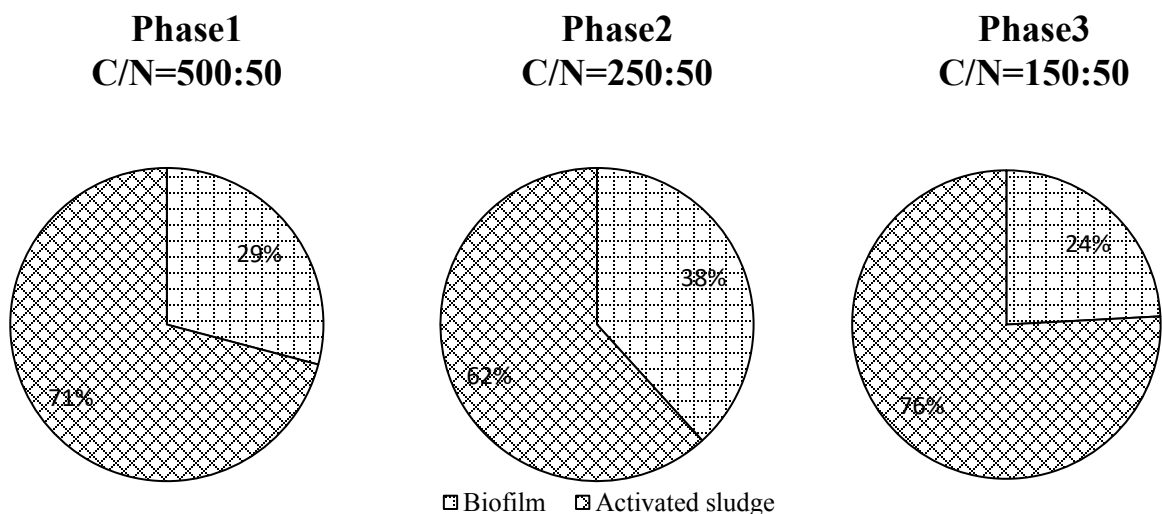
For better comparison between suspended flocs and biofilm, the biomass data were expressed in per reactor basis. As the C/N ratio decreased along the three phases, the biofilm biomass decreased from 619.2 mg VSS in Phase 1, 540mg in Phase 2 to 225.6 mg VSS per reactor in Phase 3. The activated sludge biomass decreased from 1664 mg MLVSS per reactor in Phase 1, 942.5mg in

Phase 2 to 812.5 mg MLVSS per reactor in Phase 3 (Table 3.2). This observation could be explained by a shortage of organic carbon in the reactor. Lack of substrate could lead to the decrease of biomass (Brdjanovic et al. 1998). Further, as shown in Figure 3.3, the biomass percentage in activated sludge (71%, 62%, and 76% in Phases 1, 2, and 3, respectively) was greater than that in biofilm (29%, 38%, and 24% in Phases 1, 2, and 3, respectively) under all three C/N ratios.

		Phase1	Phase2	Phase3
		C/N=10:1	C/N=5:1	C/N=3:1
<b>Biofilm</b>	TSS (mg/reactor)	792.0	612	259.2
	VSS (mg/reactor)	619.2	540	225.6
	VSS/TSS	0.780	0.876	0.833
<b>Activated sludge</b>	MLSS (mg/reactor)	1664	942.5	812.5
	MLVSS (mg/reactor)	1508	871	708.5
	MLVSS/MLSS	0.862	0.92	0.872

When the biomass percentages of all three phases were compared, the activated sludge was the most dominant in Phase 3, and the least dominant in Phase 2. It is possible that when the C/N ratio decreased from 10:1 to 5:1, biomass in the activated sludge came out with the effluent quickly right after the condition changes. The other contributor to the decrease of active biomass in the sludge might be the endogenous decay, which might be caused by the decrease of C/N ratio. The decrease of biomass in the biofilm indicated a sloughing of biomass from biofilm. An increase in the percentage of the biofilm biomass over the whole system during the condition changes indicated a higher stability in biofilm than in activated sludge and underline the advantage of IFAS application over conventional activated sludge in response to a sudden C/N ratio change from 10:1 to 5:1.

However, when the C/N ratio further decreased from 5:1 to 3:1, an interesting phenomenon was observed. Instead of the fast wash-out of activated sludge, more biomass detached from the biofilm (Table 3.2). As mentioned before, heterotrophic bacteria detachment of heterotrophic bacteria in the deeper biofilm layer might intensify the detachment of nitrifying bacteria. As a result, the biomass of activated sludge over total biomass in the reactor was the highest in Phase 3. In this case, the activated sludge is a more favorable habitat for bacteria. Under this condition ( $C/N < 5:1$ ), the detachment of biofilm might somehow attribute to the increasing share of activated sludge biomass. This process has been observed by other researchers and was defined as a “seeding” process (Bella et al., 2014; Di Trapani et al., 2013).



**Figure 3.3.** Percentage of active biomass in biofilm and activated sludge during three phases.

### 3.3.3. Effects of the C/N ratio on nitrifying bacteria

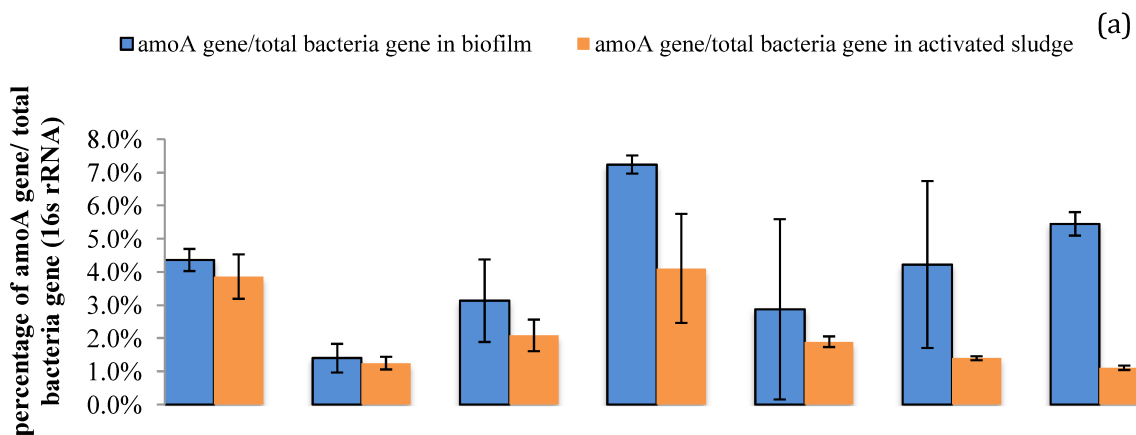
Nitrifying bacteria displayed different retention behaviors in biofilm and activated sludge. Figure 3.4 shows that gene copies/total gene copies of AOB (*amoA* genes) and NOB (Nitro and NSR genes) were higher in biofilm (1.5–7.7% for AOB and 4.2–10.9% for NOB) than in activated

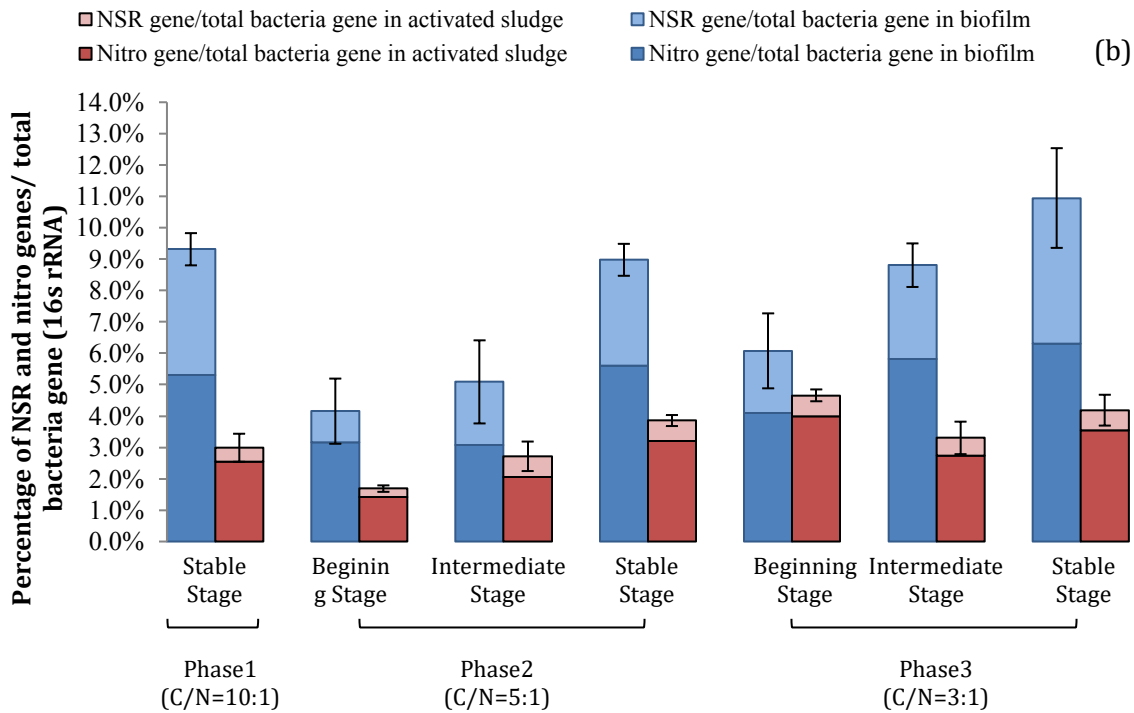


sludge (1.1–4.0% for AOB and 1.7–4.7% for NOB). Although the gene copy/total gene copies were higher for NOB than for AOB in biofilm, it is too harsh to conclude that NOBs have a greater affinity than AOB to biofilm. It is because the gene copy numbers in cells are variable. In another words, the gene copies/total gene copies ratio was not representative of the percentage of a specific bacterial population in total bacteria (Kim et al., 2011). However, the gene copy/total gene copies percentage was still a comparable parameter for differ conditions. Higher percentages of AOB and NOB gene copies/total gene copies in biofilm than in activated sludge suggests that the nitrifiers preferred to stay in attached biofilm rather than in suspended flocs. It is known that biofilm provides a longer SRT than the flocs, and therefore promotes the growth of slow growing nitrifying bacteria(Choi et al., 2014; Kim et al., 2011). It has also been reported that heterotrophic bacteria tend to stay in the suspended flocs rather than in biofilm because they have more contact with organic carbon and oxygen in suspended flocs than in biofilm. Furthermore, alternative aerobic and anaerobic conditions provided by suspended sludge favour the metabolism of certain heterotrophic bacteria, such as phosphorus accumulating organisms (Onnis-Hayden et al., 2011).

The two main types of nitrifying bacteria behaved differently in different bacterial aggregates. NOB genes (Nitro and NSR) were present in a higher percentage than AOB (*amoA*) genes in biofilm. Similar results were discovered in Kim et al. (2011). However, in a study that used specific fluorescence in situ hybridization (FISH) technology (Mahendran et al., 2012) to measure the abundance of bacteria, the relative abundance of AOB was found to be higher than that of NOB in biofilm as compared to the suspended flocs in IFAS reactors. In Mahendran et al's (2012) study, two types of AOB, *nitrosomonas spp.* and *betaproteobacterial* AOB, were measured. The discrepancy between these studies might attribute to different detection and quantification techniques being used.

In terms of the response to the C/N ratio changes, the nitrifying bacteria also reacted differently in different bacterial aggregates. As shown in Figure 3.4, when the reactor faced a sudden decrease in the C/N ratio, the percentages of AOB and NOB genes over total genes in activated sludge and in biofilm quickly dropped and then slowly recovered in around three weeks. For instance, when C/N ratio changed from Phase 1 (10:1) to Phase 2 (5:1), the percentage of AOB genes in biofilm dropped from  $4.4 \pm 0.3\%$  to  $1.4 \pm 0.4\%$ , and this value gradually increased to  $7.2 \pm 0.3\%$  during Phase 2 and then dropped again to  $2.9 \pm 2.7\%$  when C/N ratio changed from 5:1 (Phase 2) to 3:1 (Phase 3). The sudden reduction of AOB and NOB genes can be explained by the fact that the reactor is sensitive towards C/N ratio changes. The dramatic decreases in nitrifying organisms and subsequent recovery of nitrifying community after the decrease of C/N ratio indicated that every decrease of C/N ratio was a new start of bacterial community reconstruction.



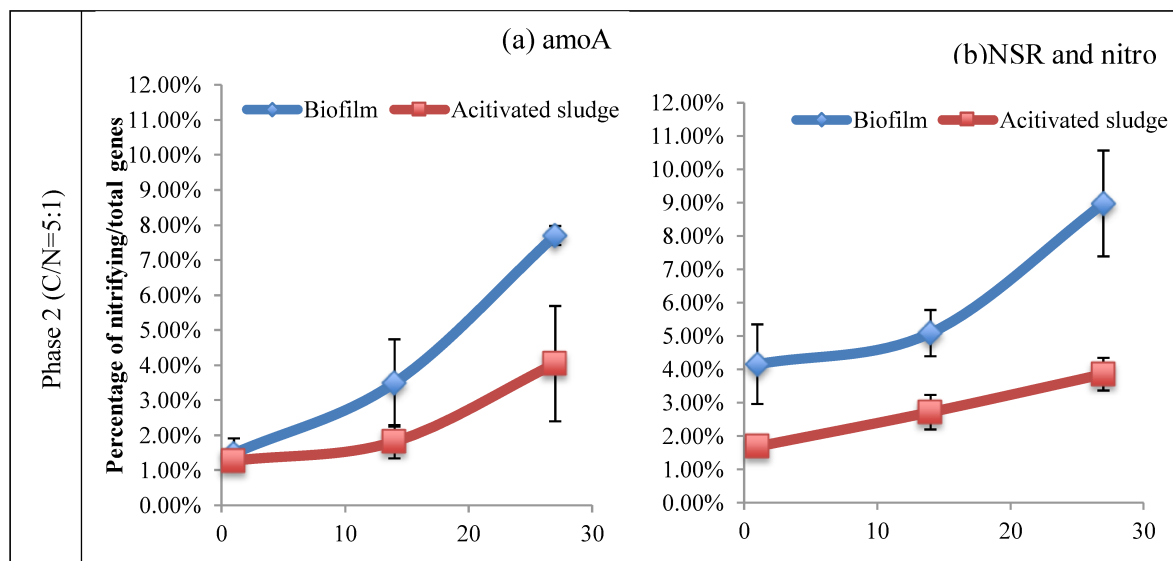


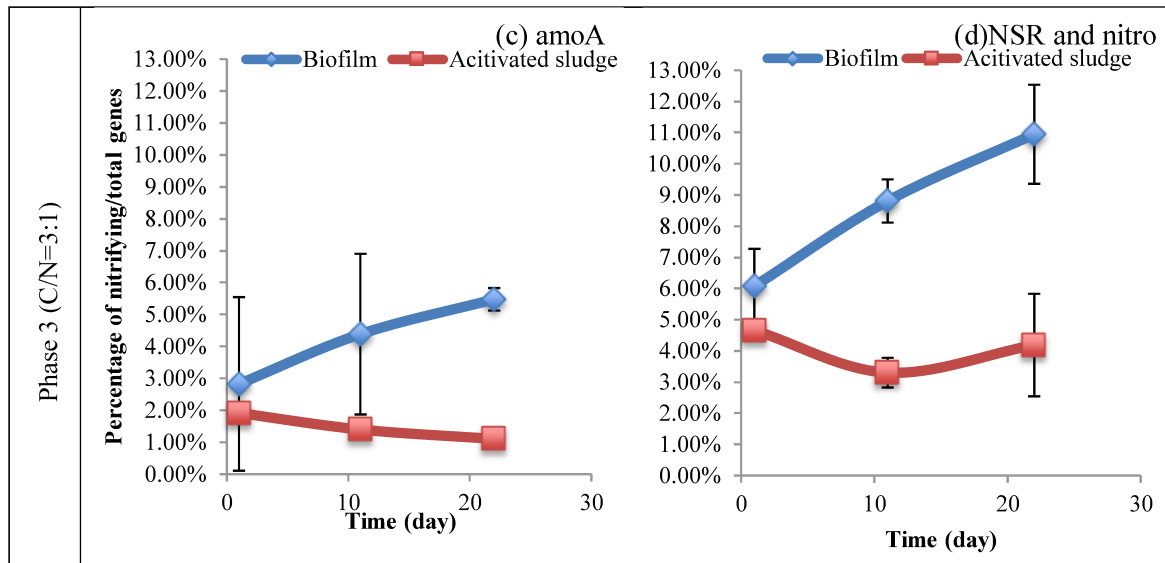
**Figure 3.4.** (a) Percentage of amoA (AOB gene) gene in total bacteria on biofilm and activated sludge during three phases. (b) Two NOB genera genes in total bacteria on both biofilm and activated sludge during three phases. Phase 2 and Phase 3 are divided into three stages: beginning, intermediate, and stable. Beginning stage samples were collected 1 day after the change of C/N ratio, intermediate stage samples were collected in the middle of the phase, and stable stage samples were collected at the end of the phase. In (b), NSR gene is commonly found in *Nitrospira spp.* and nitro gene is commonly found in *Nitrobacter spp.* Error bars show the standard deviations.

The percentage of AOB genes in biofilm was highest in Phase 2 ( $7.2 \pm 0.3\%$ ), compared to Phase 1 ( $4.4 \pm 0.3\%$ ) and Phase 3 ( $5.4 \pm 0.4\%$ ) ( $P=0.0001$ ,  $P<0.05$ ). In activated sludge, the AOB gene percentages were similar in Phase 1 and Phase 2 ( $3.9 \pm 0.7\%$  and  $4.1 \pm 1.6\%$ ) and dropped to  $1.1 \pm 0.1\%$  in Phase 3 ( $P=0.0044$ ,  $P<0.05$ ). In this case, the Phase 2 seems to be the optimal condition for AOB. For NOBs, the percentage in biofilm was the highest in Phase 3 ( $10.9 \pm 1.6\%$ ), while

Phase 2 ( $9.0 \pm 0.5\%$ ) and Phase 1 ( $9.3 \pm 0.5\%$ ) had similar percentage ( $P=6.38 \times 10^{-4}$ ,  $P < 0.05$ ). In suspended activated sludge, the percentages of NOBs slightly increased (from  $3.0 \pm 0.4\%$  in Phase 1,  $3.9 \pm 0.2\%$  in Phase 2, to  $4.2 \pm 0.5\%$  in Phase 3,  $P=4.77 \times 10^{-3}$ ,  $P < 0.05$ ) as C/N ratio decreased.

The recovery of AOB and NOB genes in biofilm and activated sludge responded differently to different C/N ratios. As shown in Figure 3.5, both NOB and AOB recovered faster in biofilm than in activated sludge, which may be explained by a more favorable environment provided for nitrifying bacteria (Onnis-Hayden et al., 2007). The faster recovery rate in biofilm indicates a more resilient nature of the biofilm community compared to the activated sludge population. Further, comparing the recovery rate under Phase 2 and 3, it is obvious that the recovery rate of nitrifiers decreased when the C/N ratio decreased (Figure 3.5). Based on the results, the lower C/N ratio had effects on the recovery of nitrifiers.





**Figure 3.5.** (a) amoA gene (AOB gene) recovery in Phase 2; (b) NOB genes recovery in Phase2. (c) amoA gene recovery in Phase 3; (d) NOB genes recovery in Phase 3. The blue lines with diamonds display the percentage of NOB and AOB genes over total genes in biofilm, and the red lines with squares display the percentages of NOB and AOB genes over total genes in activated sludge. Horizontal axis displays the days after the C/N ratio changes, and the vertical axis indicates the percentage of nitrifiers genes over total genes in activated sludge and biofilm. Error bars show the standard deviations.

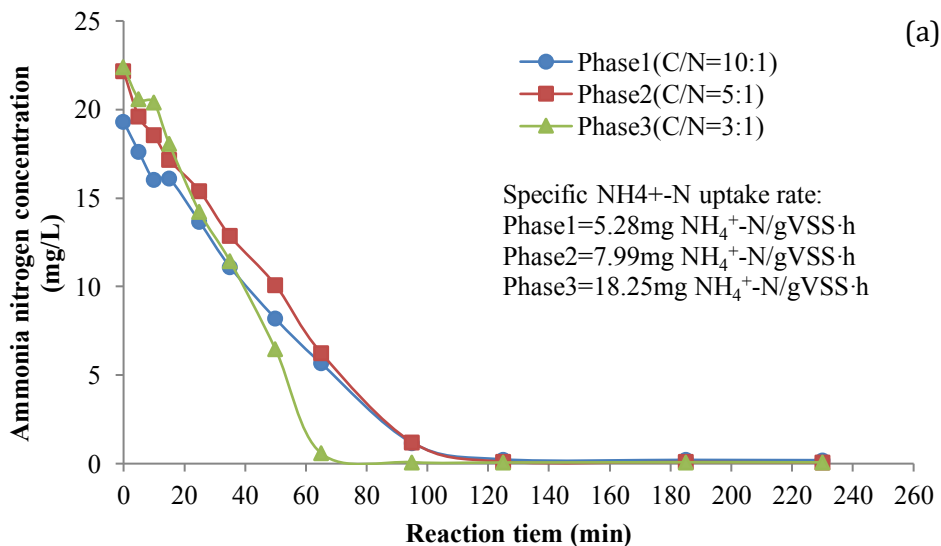
In addition, AOB and NOB showed different recovery behavior in response to C/N ratio changes. When the C/N ratio was 5:1, the recovery of AOB was faster than the recovery of NOB in both biofilm and activated sludge (Figure3. 5a&b). However, when the C/N ratio was only 3:1, recovery rate of AOB was slower than NOB in biofilm, and even shows a decreasing trend in the activated sludge flocs. This difference proved, again, condition of Phase2 (C/N=5:1) was a favorable living condition for AOB. Unlike AOB, the low C/N ratio showed a negative effect on the recovery of NOB right after the condition change, but after longer time operation, the percentage of NOBs in

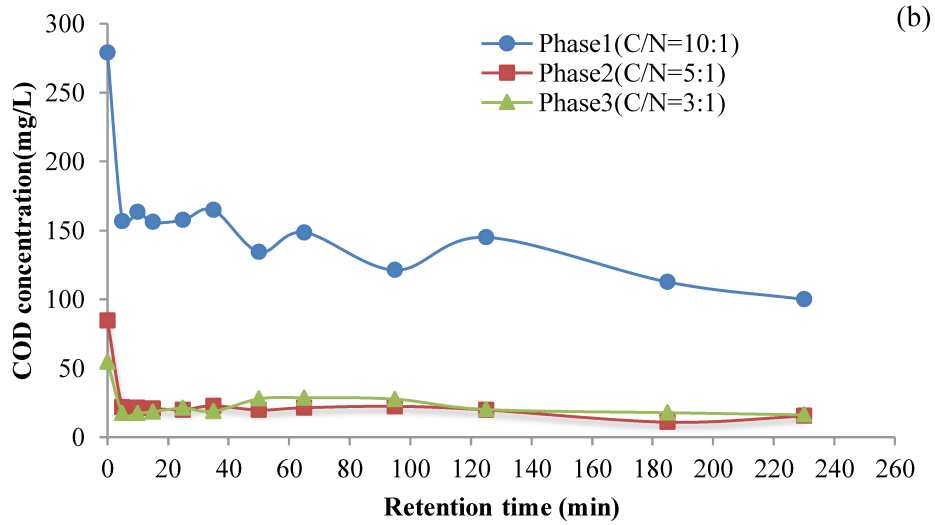
activated sludge flocs recovered. It suggested that NOB in activated sludge flocs had the ability to thrive under really low C/N condition. Researcher had found that the development of nitrifying biofilm could be very slow in the absence of organic compounds (Tsuneda et al., 2001). It is because nitrifying bacteria cannot form biofilm due to a lack of EPS production. The EPS produced by heterotrophic bacteria was usually utilized by autotrophs for biofilm development (Bassin et al., 2012). In addition, previous studies showed that aerobic nitrifying bacteria usually reside on the outer layer of the biofilm or floc, whereas heterotrophic bacteria (i.e., denitrifiers) usually reside on the anoxic layer of the biofilm under the outer oxic layer (Feng et al., 2011). Detachment of the inner layer of biofilm might have led to the sloughing off of AOB in the outer oxic layer, leading to the decrease of recovery rates for nitrifying bacteria in Phase 3.

#### 3.3.4. Ammonium removal

The  $\text{NH}_4^+\text{-N}$  concentration at beginning of the cycle ( $t = 0$  min) varied from 19.32 to 22.4 mg/L (Figure 3.6). In Phase 1 and Phase 2, ammonium was almost completely removed at  $t = 110$  min. In Phase 3, ammonium was completely removed at  $t = 70$  min (Figure 3.6a). The specific  $\text{NH}_4^+\text{-N}$  uptake rate increased as the C/N ratio decreased. The specific ammonium uptake rate was 5.28 mg  $\text{NH}_4^+\text{-N/gVSS}\cdot h$  in Phase 1, 7.99 mg  $\text{NH}_4\text{-N/gVSS}\cdot h$  in Phase 2, and 18.25 mg  $\text{NH}_4\text{-N/gVSS}\cdot h$  in Phase 3. A decrease in the C/N ratio might have led to a decrease in heterotrophic bacteria due to a decrease in carbon source, causing the autotrophic nitrifiers to be more competitive than the heterotrophic bacteria for space and oxygen (Lee, 2004), and further led to the increase of specific ammonium uptake rate. However, the total biomass decreased in both biofilm and activated sludge in response to a decrease in the C/N ratio. This indicates that the total biomass concentration is not the limiting factor that affects the nitrification efficiency. The reduced biomass in the reactor may

have enhanced the oxygen diffusion and materials transfer in these microbial aggregates (flocs and biofilm). Oxygen diffusion would have a greater effect on the biofilm than on the activated sludge. The diffusion resistance across the biofilm resulted in an up to 10 times higher half saturation coefficient ( $K_o$ ) of oxygen in biofilm than in activated sludge ( $K_o = 0.4\text{mg/L}$ ). The higher the half saturation coefficient of oxygen, the lower would be the transport of oxygen in the biofilm. The diffusion resistance led to a DO concentration decrease in a shallow penetration depth of biofilm (Pérez et al., 2005; Stricker et al., 2009; Zhou et al., 2012). The reduced biofilm thickness at a low C/N ratio could result in enhanced oxygen penetration into the deep layer of the biofilm (Zhou et al., 2012), promoting ammonium nitrogen oxidation and nitrite oxidation in the biofilm. An increase in the ammonium uptake rate from Phase 1 to Phase 3 might be the result of more efficient nitrification activities in the biofilm. Moreover, as mentioned in section 3.2.1., a “seeding” effect reported implied a detachment of nitrifiers from biofilm to the mixed liquor, which would also enhance the nitrification activities in the mixed liquor (Bella et al., 2014; Di Trapani et al., 2013).





**Figure 3.6.** Cycle tests for ammonia and COD removal: (a) Ammonium nitrogen removal during one cycle; line with circles displays the phase1 data, line with squares displays the phase2 data, and line with triangles displays phase3 data. (b) COD removal during one cycle. The reaction time in one cycle is 230 minutes. Sampling points are at  $t = 0$  min, 5 min, 10 min, 15 min, 25 min, 35 min, 50 min, 65 min, 95 min, 125 min, 185 min, and the end of the cycle ( $t = 230$  min), line with circles displays the phase1 data, line with squares displays the phase2 data, and line with triangles displays phase3 data.

### 3.3.5. COD removal kinetics

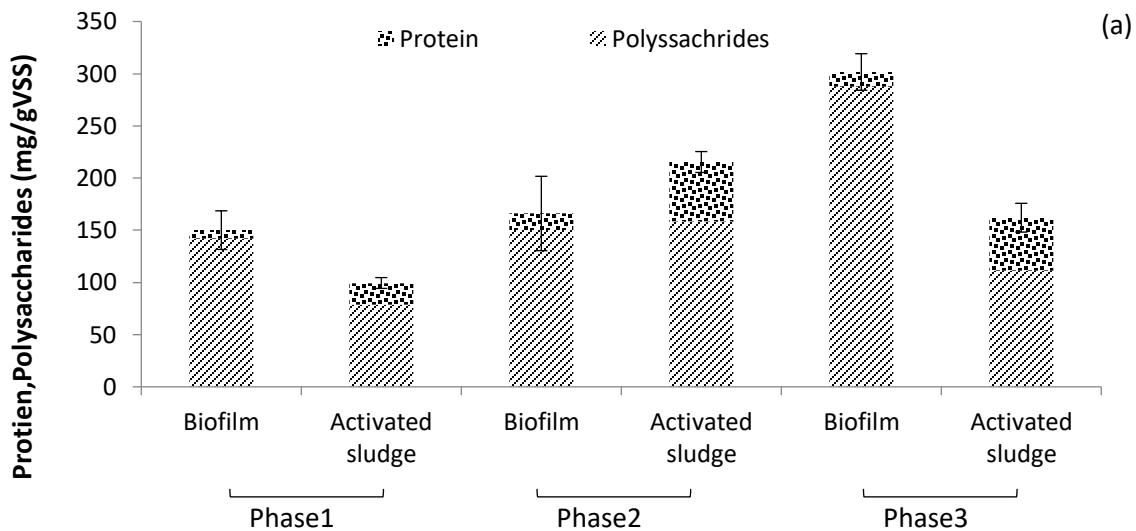
COD uptake curves were displayed in Figure 3.6b. The COD concentration dropped dramatically in the first 5 minutes of the cycle and fluctuated gently as the cycle continued. This behavior might be caused by the biosorption activity of the EPS outside the cells (Wei and Hong, 2010). Similar fast biosorption activity had been reported (Esparza-Soto and Westerhoff, 2003). Results showed that the COD concentration at the end of the reaction cycle was still higher than the effluent COD concentration (i.e., after settling). This could be explained by an additional COD removal by

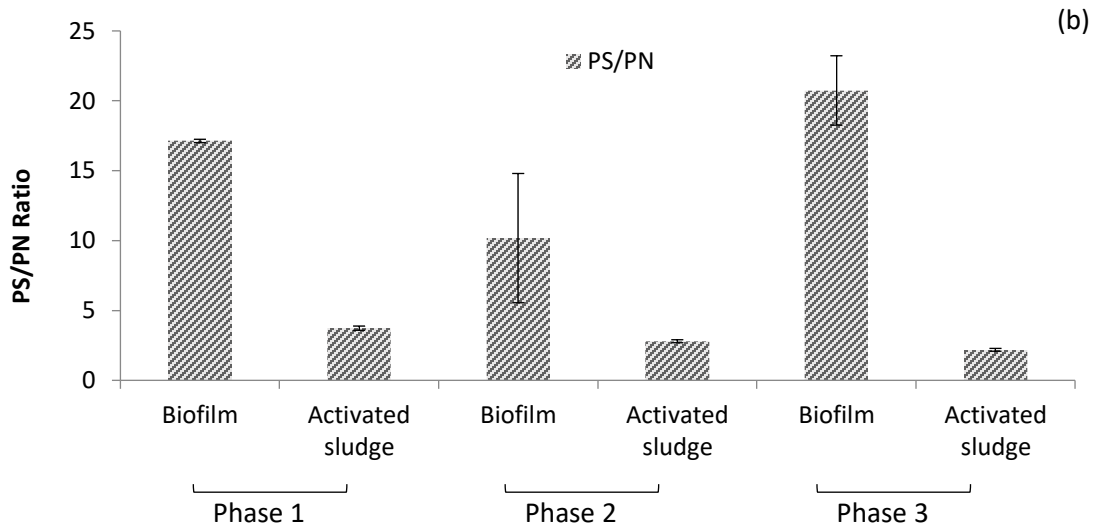


denitrifiers during the settling stage. During the settling, there is no aeration and the resulting anoxic environment encourages denitrification activities.

### 3.3.6. EPS production

EPS is a slime-like substance exuded by bacterial cells which changes the surficial properties of the cellular surface, promotes cell adhesion to a solid surface (Sheng et al., 2010), and helps the development of nitrifying biofilm (Bassin et al., 2012). EPS protects bacteria from sudden environmental changes, exposure to heavy metals, and other potential dangers (Sheng et al., 2010). However, too much EPS production can result in viscous bulking (van den Akker et al., 2010), which might lead to the collapse of the reactor performance. This research showed the different characteristics of EPS in the two types of bacterial aggregates (attached biofilm and suspended activated sludge flocs).





**Figure 3.7.** (a) EPS protein and polysaccharide content per gVSS for both biofilm biomass and activated sludge in three different C/N conditions. In Phase1 the C/N = 10:1, in Phase 2 the C/N = 5:1, and in Phase 3, the C/N = 3:1. (b) Polysaccharide/protein ratio in EPS for both biofilm biomass and activated sludge under three different C/N conditions. PN and PS refer to protein and polysaccharide, respectively. Error bars show the standard deviations.

The production of EPS in biofilm in Phases 1 and 2 was similar ( $92.9 \pm 11.5$  mg/reactor in Phase 1 and  $89.7 \pm 19.2$  mg/tank in Phase 2). In Phase 3, only  $68.1 \pm 4.0$  mg/reactor EPS was produced. A higher EPS production may be related to a higher biomass on the biocarriers. However, the EPS production per VSS (Figure 3.7a) was the highest in Phase 3 when the biomass on carriers was the least ( $P=0.010$ ). On the other hand, in suspended sludge (flocs), EPS production were the highest ( $187.6 \pm 8.7$  mg/reactor) in Phase 2, lowest ( $114.8 \pm 9.8$  mg/reactor) in Phase 3, and  $129.3 \pm 6.7$  mg/reactor in Phase 1. The production of EPS per gVSS in activated sludge increased significantly from Phase 1 to Phase 2, then decreased from Phase 2 to Phase 3, indicating the EPS production was affected by the C/N ratio. The bacteria might have secreted more EPS to protect

themselves when the C/N ratio dropped from 10:1 to 5:1; that could account for the larger EPS production in Phase 2. When the C/N ratio dropped to 3:1 in Phase 3, the COD provided could not support the growth of bacteria, so bacteria started to consume the EPS as a carbon source (Flemming et al., 2007), leading to a decrease in EPS production detected in Phase 3. All EPS production results showed that these two types of bacterial aggregate were influenced in different ways by the C/N ratio. When analyzing the EPS production in an IFAS system, separated analysis on different aggregate types (i.e., biofilms vs. flocs) was necessary. The effects of the C/N ratio on EPS production are complex and require further studies.

#### 3.3.7. EPS composition

The polysaccharide/protein ratio in EPS affects the settleability of sludge (Shin et al., 2001). Settling volume index (SVI) is commonly used to evaluate the settleability of sludge. The sludge volume index (SVI) is positively related to the carbohydrate/protein ratio. Van den Akker et al., (2010) pointed out that a high carbohydrate concentration reduced the compressibility of mixed liquid and adversely affected the settling of sludge.

In this study, the compositions of EPS in the two aggregates (flocs and biofilm) were found to be different. As shown in Figure 3.7b, the polysaccharide/protein (PS/PN) ratio in the biofilm was greater than that in the suspended activated sludge, This result agrees with other studies (Zhang et al., 2014). The different characteristics of EPS in biofilm and activated sludge may be associated with their different settleability, flocculation capacity, and dewatering ability (Zhang et al., 2014). For instance, the high PS/PN ratio for biofilm EPS observed in this study might be attributed to the fact that polysaccharides help bacteria to adhere to solid surfaces (Tsuneda et al., 2003). Furthermore, the PS/PN ratio also changed differently for different bacterial aggregate types (flocs

and biofilm). In the biofilm, the PS/PN ratio decreased from Phase 1 to Phase 2 (from  $17.1 \pm 0.1$  to  $10.2 \pm 4.6$ ) and increased from Phase 2 to Phase 3 (from  $10.2 \pm 4.6$  to  $20.7 \pm 2.5$ ). In the activated sludge, a slightly decreasing trend in the PS/PN ratio was observed when the C/N ratio decreased. Similar results were found in previous research (Ye et al., 2011). Nonetheless, changes in the PS/PN ratio in activated sludge were smaller than those in biofilm, which may be attributed to two possible reasons. Firstly, the PS/PN ratio in activated sludge may affect sludge settling (Shin et al., 2001). If the high PS/PN biofilm EPS detached from the biocarriers and stay in the suspended flocs, there would be a sudden increase of PS/PN ratio in sludge EPS as the C/N decreased. However, the high PS/PN sludge might have been washed out from the reactor. The observed decrease of biomass in activated sludge when the C/N ratio decreased supports this hypothesis. Secondly, the polysaccharides in EPS, either from the detached biofilm or from the suspended flocs, might have been consumed by the suspended activated sludge as carbon sources (Flemming et al., 2007). Because the PS/PN ratio is highly dependent on EPS extraction methods, cation exchange resin, EDTA, and steaming extraction methods have been used in other studies to extract EPS. Different methods will lead to variations in EPS composition. However, a comparison of the PS/PN ratio at different stages of a wastewater treatment study is still very important.

### **3.4. Conclusions**

The IFAS-SBR was robust in removing COD and ammonia-nitrogen in reactor wastewater influent. About 99% ammonia-nitrogen removal and 92–98% COD removal was achieved during reactor operation. However, the nitrate concentration remained high when C/N ratio was lower than 5:1. It can be explained by the insufficient microbial denitrification activity in the reactor when the C/N ratio was low. The COD concentration and the length of settling time might be important factors

in denitrification. Adjusting the reaction and settling time or creating favorable conditions for denitrifiers would promote nitrate removal.

The results show that ammonium utilization by microorganisms is strongly related to the influent C/N ratio. The ammonium uptake rate was high ( $18.25 \text{ mg NH}_4^+ \text{-N/gVSS} \cdot h$ ) when the influent C/N ratio was low (3:1). Even though the biomass concentration was the lowest in both activated sludge and biofilm during Phase 3, the ammonium uptake rate was highest in Phase 3. This result may be attributed to (i) a reduced biofilm thickness, which facilitated oxygen diffusion and material transfer in the biofilm, or (ii) reduced competition pressure among bacteria. The q-PCR results indicated that the biofilm was a more favorable habitat than activated sludge for nitrifying bacteria when the C/N ratio was low. Moreover, percentage of AOB in suspended activated sludge kept dropping when C/N ratio was 3:1, while NOBs were proved to have the ability to thrive in both biofilm and suspended activated sludge. Further study is required to determine whether biofilm or activated sludge has higher nitrifying rate.

EPS works as a double-edged sword in the performance of the IFAS-SBR reactor. On one hand, more EPS produced by heterotrophic bacteria could improve the development of nitrifying biofilm and prevent the detachment of biofilm. On the other hand, thicker biofilm would result in stronger diffusion resistance and lower the mass transfer of nutrients and oxygen in biofilm, compromising the efficient removal of organic compounds and ammonia nitrogen. Therefore, control of the biofilm thickness and the EPS production is important for successful application of an IFAS-SBR to wastewater treatment. Biofilm EPS and activated sludge EPS had different composition and

responded differently to the C/N ratio changes. When analyzing the effects of operation conditions, biofilm and activated sludge EPS should be analyzed separately.

### 3.5. References

- Bassin, J.P., Kleerebezem, R., Rosado, A.S., van Loosdrecht, M.C.M., Dezotti, M., 2012. Effect of Different Operational Conditions on Biofilm Development, Nitrification, and Nitrifying Microbial Population in Moving-Bed Biofilm Reactors. *Environ. Sci. Technol.* 46, 1546–1555. <https://doi.org/10.1021/es203356z>
- Bella, G.D., Trapani, D.D., Freni, G., Torregrossa, M., Viviani, G., 2014. Analysis of biomass characteristics in mbr and mb-mbr systems fed with synthetic wastewater: influence of a gradual salinity increase. *Chem. Eng. Trans.* 445–450. <https://doi.org/10.3303/CET1438075>
- Bradford, M.M., 1976. A rapid and sensitive method for the quantitation of microgram quantities of protein utilizing the principle of protein-dye binding. *Anal. Biochem.* UK.
- Brdjanovic, D., Slamet, A., Van Loosdrecht, M.C.M., Hooijmans, C.M., Alaerts, G.J., Heijnen, J.J., 1998. IMPACT OF EXCESSIVE AERATION ON BIOLOGICAL PHOSPHORUS REMOVAL FROM WASTEWATER. *Water Res.* 32, 200–208. [https://doi.org/10.1016/S0043-1354\(97\)00183-8](https://doi.org/10.1016/S0043-1354(97)00183-8)
- Choi, J., Hwang, G., Gamal El-Din, M., Liu, Y., 2014. Effect of reactor configuration and microbial characteristics on biofilm reactors for oil sands process-affected water treatment. *Int. Biodeterior. Biodegrad.* 89, 74–81. <https://doi.org/10.1016/j.ibiod.2014.01.008>
- Copithron, R.R., Sturdevant, J., Farren, G., Sen, D., 2006. Case study of an IFAS system-Over 10 years of experience. *Water Environ. Found.* 4309–4324.
- Di Trapani, D., Christensson, M., Torregrossa, M., Viviani, G., Ødegaard, H., 2013. Performance of a hybrid activated sludge/biofilm process for wastewater treatment in a cold climate

- region: Influence of operating conditions. *Biochem. Eng. J.* 77, 214–219.  
<https://doi.org/10.1016/j.bej.2013.06.013>
- DuBois, M., Gilles, K.A., Hamilton, J.K., Rebers, P.A., Smith, F., 1956. Colorimetric Method for Determination of Sugars and Related Substances. *Anal. Chem.* 28, 350–356.  
<https://doi.org/10.1021/ac60111a017>
- Esparza-Soto, M., Westerhoff, P., 2003. Biosorption of humic and fulvic acids to live activated sludge biomass. *Water Res.* 37, 2301–2310. [https://doi.org/10.1016/S0043-1354\(02\)00630-9](https://doi.org/10.1016/S0043-1354(02)00630-9)
- Feng, Q., Cao, J., Chen, L., Guo, C.-Y., Tan, J., Xu, H., 2011. Simultaneous nitrification and denitrification at variable C/N ratio in aerobic granular sequencing batch reactors. *J. Food Agric. Environ.* 9, 1131–1136.
- Flemming, H.-C., Neu, T.R., Wozniak, D.J., 2007. The EPS Matrix: The “House of Biofilm Cells.” *J. Bacteriol.* 189, 7945–7947. <https://doi.org/10.1128/JB.00858-07>
- Furumai, H., Rittmann, B.E., 1994. Interpretation of bacterial activities in nitrification filters by a biofilm model considering the kinetics of soluble microbial products. *Water Sci. Technol.* U. K.
- Haandel, A. van, Lubbe, J. van der, 2012. *Handbook of biological wastewater treatment*, 2. ed. ed. IWA Publ, London.
- Hempel, M., Grossart, H., Gross, E., 2009. Community composition of bacterial biofilms on two submerged macrophytes and an artificial substrate in a pre-alpine lake. *Aquat. Microb. Ecol.* 58, 79–94. <https://doi.org/10.3354/ame01353>
- Huang, C., Shi, Y., Gamal El-Din, M., Liu, Y., 2015. Treatment of oil sands process-affected water (OSPW) using ozonation combined with integrated fixed-film activated sludge (IFAS). *Water Res.* 85, 167–176. <https://doi.org/10.1016/j.watres.2015.08.019>
- Johnson, T.L., McQuarrie, J.P., 2002. IFAS BNR Full-scale Design and Performance Challenges. *Proc. Water Environ. Fed.* 2002, 214–226. <https://doi.org/10.2175/193864702784249105>

- Johnson, T.L., Wallis-Lage, C.L., Shaw, A.R., McQuarrie, J.P., 2005. IFAS OPTIONS – WHICH ONE IS RIGHT FOR YOUR PROJECT? *Proc. Water Environ. Fed.* 2005, 6290–6300. <https://doi.org/10.2175/193864705783815069>
- Kim, H., Schuler, A.J., Gunsch, C.K., Pei, R., Gellner, J., Boltz, J.P., Freudenberg, R.G., Dodson, R., 2011. Comparison of Conventional and Integrated Fixed-Film Activated Sludge Systems: Attached- and Suspended-Growth Functions and Quantitative Polymerase Chain Reaction Measurements. *Water Environ. Res.* 83, 627–635. <https://doi.org/10.2175/106143010X12851009156448>
- Kim, Y.M., Lee, D.S., Park, C., Park, D., Park, J.M., 2011. Effects of free cyanide on microbial communities and biological carbon and nitrogen removal performance in the industrial activated sludge process. *Water Res.* 45, 1267–1279. <https://doi.org/10.1016/j.watres.2010.10.003>
- Lee, L., 2004. Biofilm morphology and nitrification activities: recovery of nitrifying biofilm particles covered with heterotrophic outgrowth. *Bioresour. Technol.* 95, 209–214. <https://doi.org/10.1016/j.biortech.2003.05.004>
- Liu, H., Fang, H.H.P., 2002. Extraction of extracellular polymeric substances (EPS) of sludges. *J. Biotechnol.* 95, 249–256. [https://doi.org/10.1016/S0168-1656\(02\)00025-1](https://doi.org/10.1016/S0168-1656(02)00025-1)
- Mahendran, B., Lishman, L., Liss, S.N., 2012. Structural, physicochemical and microbial properties of flocs and biofilms in integrated fixed-film activated sludge (IFFAS) systems. *Water Res.* 46, 5085–5101. <https://doi.org/10.1016/j.watres.2012.05.058>
- Onnis-Hayden, A., Dair, D., Johnson, C., Schramm, A., Gu, A.Z., 2007. Kinetics and Nitrifying Populations in Nitrogen Removal Processes at a Full-Scale Integrated Fixed-Film Activated Sludge (IFAS) Plant. *Proc. Water Environ. Fed.* 2007, 3099–3119. <https://doi.org/10.2175/193864707787973789>
- Onnis-Hayden, A., Majed, N., Schramm, A., Gu, A.Z., 2011. Process optimization by decoupled control of key microbial populations: Distribution of activity and abundance of



- polyphosphate-accumulating organisms and nitrifying populations in a full-scale IFAS-EBPR plant. *Water Res.* 45, 3845–3854. <https://doi.org/10.1016/j.watres.2011.04.039>
- Pérez, J., Picioreanu, C., van Loosdrecht, M., 2005. Modeling biofilm and floc diffusion processes based on analytical solution of reaction-diffusion equations. *Water Res.* 39, 1311–1323. <https://doi.org/10.1016/j.watres.2004.12.020>
- Risgaard-Petersen, N., Nicolaisen, M.H., Revsbech, N.P., Lomstein, B.A., 2004. Competition between Ammonia-Oxidizing Bacteria and Benthic Microalgae. *Appl. Environ. Microbiol.* 70, 5528–5537. <https://doi.org/10.1128/AEM.70.9.5528-5537.2004>
- Sheng, G.-P., Yu, H.-Q., Li, X.-Y., 2010. Extracellular polymeric substances (EPS) of microbial aggregates in biological wastewater treatment systems: A review. *Biotechnol. Adv.* 28, 882–894. <https://doi.org/10.1016/j.biotechadv.2010.08.001>
- Shin, H.S., Kang, S.T., Nam, S.Y., 2001. Effect of carbohydrate and protein in the EPS on sludge settling characteristics. *Water Sci. Technol. J. Int. Assoc. Water Pollut. Res.* 43, 193–196.
- Stricker, A.-E., Barrie, A., Maas, C.L.A., Fernandes, W., Lishman, L., 2009. Comparison of Performance and Operation of Side-By-Side Integrated Fixed-Film and Conventional Activated Sludge Processes at Demonstration Scale. *Water Environ. Res.* 81, 219–232. <https://doi.org/10.2175/106143008X325692>
- Tsuneda, S., Aikawa, H., Hayashi, H., Yuasa, A., Hirata, A., 2003. Extracellular polymeric substances responsible for bacterial adhesion onto solid surface. *FEMS Microbiol. Lett.* 223, 287–292. [https://doi.org/10.1016/S0378-1097\(03\)00399-9](https://doi.org/10.1016/S0378-1097(03)00399-9)
- Tsuneda, S., Park, S., Hayashi, H., Jung, J., Hirata, A., 2001. Enhancement of nitrifying biofilm formation using selected EPS produced by heterotrophic bacteria. *Water Sci. Technol. J. Int. Assoc. Water Pollut. Res.* 43, 197–204.
- van den Akker, B., Beard, H., Kaeding, U., Giglio, S., Short, M.D., 2010. Exploring the relationship between viscous bulking and ammonia-oxidiser abundance in activated sludge: A

- comparison of conventional and IFAS systems. *Water Res.* 44, 2919–2929. <https://doi.org/10.1016/j.watres.2010.02.016>
- Xia, S., Li, J., Wang, R., 2008. Nitrogen removal performance and microbial community structure dynamics response to carbon nitrogen ratio in a compact suspended carrier biofilm reactor. *Ecol. Eng.* 32, 256–262. <https://doi.org/10.1016/j.ecoleng.2007.11.013>
- Ye, F., Peng, G., Li, Y., 2011. Influences of influent carbon source on extracellular polymeric substances (EPS) and physicochemical properties of activated sludge. *Chemosphere* 84, 1250–1255. <https://doi.org/10.1016/j.chemosphere.2011.05.004>
- Ye, J., McDowell, C.S., Koch, K., Koch, K., Kulick, F.M., Rothermel, B.C., 2009. Pilot Testing of Structured Sheet Media IFAS for Wastewater Biological Nutrient Removal (BNR). *Proc. Water Environ. Fed.* 2009, 4427–4442. <https://doi.org/10.2175/193864709793954015>
- Zeng, R.J., Lemaire, R., Yuan, Z., Keller, J., 2003. Simultaneous nitrification, denitrification, and phosphorus removal in a lab-scale sequencing batch reactor. *Biotechnol. Bioeng.* 84, 170–178. <https://doi.org/10.1002/bit.10744>
- Zhang, P., Fang, F., Chen, Y.-P., Shen, Y., Zhang, W., Yang, J.-X., Li, C., Guo, J.-S., Liu, S.-Y., Huang, Y., Li, S., Gao, X., Yan, P., 2014. Composition of EPS fractions from suspended sludge and biofilm and their roles in microbial cell aggregation. *Chemosphere* 117, 59–65. <https://doi.org/10.1016/j.chemosphere.2014.05.070>
- Zhou, X.-H., Liu, J., Song, H.-M., Qiu, Y.-Q., Shi, H.-C., 2012. Estimation of Heterotrophic Biokinetic Parameters in Wastewater Biofilms from Oxygen Concentration Profiles by Microelectrode. *Environ. Eng. Sci.* 29, 466–471. <https://doi.org/10.1089/ees.2010.0456>

## CHAPTER 4. IMPACTS OF AMMONIUM LOADING ON NITRITATION STABILITY AND MICROBIAL COMMUNITY DYNAMICS IN THE INTEGRATED FIXED-FILM ACTIVATED SLUDGE SEQUENCING BATCH REACTOR (IFAS-SBR)<sup>2</sup>

### 4.1. Introduction

Economical treatment of high ammonia wastewater, such as those collected from digester supernatants or thickening lagoon supernatants, is of urgent needs in many cities around the world. In recent decades, several technologies, such as SHARON, CANON, DEMON, and OLAND (Hellenga et al., 1998; Kuai and Verstraete, 1998; Nhu Hien et al., 2017; Nielsen et al., 2005; Sliemers et al., 2003), have been explored to treat the high ammonium content wastewater. These technologies differ in operational conditions and tools for controlling microbial communities that drive the de-ammonification. That is, the process could contain a combination of ammonia oxidizing bacteria (AOB) nitritation and heterotrophic denitrifiers denitrification, a combination of AOB nitritation and anammox, or a combination of nitritation and denitrification by the autotrophic nitrifiers. The common step in all these technologies is the nitritation process in which ammonium is oxidized to nitrite by ammonia oxidizing bacteria (AOB)—a process also called “partial nitrification”. Nitrite, instead of nitrate, is the product. Compared to conventional nitrification-denitrification, nitritation can save up to 25% oxygen. If the nitritation was combined with denitrification (nitrite to N<sub>2</sub>), the combined processes may save up to 40% of the external carbon source addition (Peng and Zhu, 2006).

Elimination of nitrite oxidizing bacteria (NOB) and enrichment of ammonia oxidizing bacteria (AOB) are key to achieving stable partial nitrification (nitritation). Previous researchers have tried to inhibit NOB by controlling temperature, pH, dissolved oxygen (DO),

<sup>2</sup>This chapter has been published: Shao, Y., Yang, S., Mohammed, A., Liu, Y., 2018. Impacts of ammonium loading on nitritation stability and microbial community dynamics in the integrated fixed-film activated sludge sequencing batch reactor (IFAS-SBR). *International Biodeterioration & Biodegradation* 133, 63–69.

free ammonia (FA) and solids retention time (SRT) (Ali et al., 2016; Hellinga et al., 1998; Kuai and Verstraete, 1998; Nielsen et al., 2005; Sliemers et al., 2003). Although high temperature (>30°C) has been observed to successfully inhibit NOB, as AOB outcompetes NOB at temperatures above 25 °C (Brouwer et al., 1996), high-energy input is associated with high temperature. To date, the most effective NOB inhibition approach under temperature conditions below 25°C has been the control of free ammonia (FA) and free nitrous acid (FNA) concentrations (Gabarró et al., 2012). FA and FNA are the two inhibitors of AOB and NOB. A high FA concentration favors AOB growth over NOB growth. However, the inhibition of NOB by free ammonia is reversible, which means that NOB might recover activity over time. FNA inhibits nitrifying bacteria by donating a proton as an un-coupler under intracellular environment. This donated proton can affect the transmembrane pH gradient for adenosine triphosphate (ATP) synthesis (Glass et al., 1997). The feasibility of the partial nitrification for the treatment of high ammonia strength wastewater were discussed in this study. The inhibition of FA or FNA on the NOB were also be elucidated.

To date, most of the existing technologies, that had been applied for high ammonium content wastewater treatment, are sludge based (Ahn, 2006). The others, for example, the moving bed biofilm reactor (MBBR), relies on biofilm only. Integrated fixed film activated sludge (IFAS) system had been approved to improve the nitrification efficiency in the mainstream municipal wastewater treatment. Use of moving bed carriers with appropriate retention grids in an IFAS system mitigates the risk of losing active biomass. Suspended sludge further improves the ammonia removal efficiency. Even though the floc based SBR systems have been proven to be successful for high strength wastewater treatment, the addition of biofilm carriers can help to provide system stability and improve process capacity (Nze et al., 2018). IFAS system are extensively used in treating low strength wastewater. Investigating the microbial community structure is the key to understand the functions of the two major biomass aggregates, suspended sludge and attached

biofilm (Huang et al., 2016; Shao et al., 2017). A small amount of studies investigated the microbial structure of partial nitrification related reactors treating high strength wastewater (Kouba et al., 2014; Wang et al., 2016; Wen et al., 2017). Different molecular microbiology techniques were applied. Quantitative polymerase chain reaction (qPCR) and next generation PCR became more and more trendy in microbial community study because these technologies are cost and time effective (Wen et al., 2017). However, among the literatures the authors reviewed, none of them comprehensively present the different functions and the microbial community dynamics of the sludge and biofilm during the establishment of nitrification in an IFAS reactor. Such information was discussed in this study.

This study systematically investigates the impact of reactor influent ammonium concentrations on the establishment of a stable nitrification process at room temperature. To better understand the transformation of nitrogen species in IFAS systems under various influent ammonium concentrations, two aggregates—attached biofilm and suspended sludge—are investigated with respect to the ammonium removal kinetics. The microbial population dynamics in these two aggregates for partial nitrification are also well elucidated using the combination of qPCR and next generation sequencing techniques for the first time. The relationship between the ammonia removal kinetics and the microbial community structure is also well demonstrated in this study.

## **4.2. Methods and materials**

### **4.2.1. Reactor operation**

A bench top reactor (6 L) was operated in sequencing batch mode and filled with 40% polyethylene biocarriers. These polyethylene biofilm carriers have cylindrical shape with a diameter of 15mm and a height of 9mm. The effective specific surface area of these carriers is about  $463\text{m}^2/\text{m}^3$ . The

reactor was operated for about 500 days. Synthetic wastewater based on the recipe in Shao et al. (2017) was used as reactor influent.  $\text{NH}_4\text{Cl}$  was used as the ammonium source and sodium acetate was used as a chemical oxygen demand (COD) source. The COD concentration in the influent was kept at around 200 mg/L. The  $\text{NH}_4^+\text{-N}$  concentration in the reactor feed was stepwise increased from 100 mg/L to 800 mg/L (Table 4.1). Each cycle of the sequencing batch reactor (SBR) was 12 hours, which included 15 min of feeding, 10 h and 40 min of reaction, 40 min of settling, 5 min of withdrawal, and 20 min of idling. The volume exchange ratio was 50%. The hydraulic retention time was 24 hr. Air was pumped and diffused to the bottom of the reactor to provide oxygen to the reactor. An airflow meter was used to adjust the airflow. During the reaction, the dissolved oxygen (DO) in the reactor was maintained at 0.5–0.8 mg/L by an air flowmeter. A ribbon like impeller was installed to ensure biocarriers were well mixed in the reactor liquid. The reactor was operated at room temperature (20–23°C).

#### 4.2.2. Analytical methods

The system was considered stable if the effluent characteristics and the mixed liquid volatile suspended solids (MLSS) were unchanged for one week. Reactor influent and effluent were sampled by collecting and filtering 15mL of the liquid samples using 0.45 $\mu\text{m}$  filter at least three times per week. Water chemistry ( $\text{NH}_4^+\text{-N}$ ,  $\text{NO}_3^- \text{-N}$ , and  $\text{NO}_2^- \text{-N}$  and alkalinity concentrations) was analyzed three times per week using the Hach kits (Methods 8038, 10206, 10237, and 10239, Hach Company, Loveland, Colorado).

Cycle tests were applied to elucidate the transformation of nitrogen species in the reactor under different conditions. During the cycle test, the concentrations of  $\text{NH}_4^+\text{-N}$ ,  $\text{NO}_3^- \text{-N}$ , and  $\text{NO}_2^- \text{-N}$  were measured, and the reaction rates under different ammonium loadings were calculated for comparison.

Mixed liquor suspended solids (MLSS) and mixed liquor volatile suspended solids (MLVSS) were measured weekly using *Standard Methods* 2540B (APHA, 2011). The biomass attached to carriers was measured using methods in Shao et al. (2017). The biofilm thickness was measured with a confocal microscope (Zeiss LSM 710). Extracellular polymeric substances (EPS) were also extracted from samples under different conditions. The extraction and analysis of EPS samples were included in the supplementary material (Appendix A-4).

#### 4.2.3. DNA extraction and molecular microbiology analysis

Duplicates of the sludge and biofilm samples were collected from the reactor at different ammonium concentrations. Biofilm biomass was removed from the carriers and suspended in milli-Q water before DNA extraction. DNA samples were extracted with MO BIO PowerSoil® DNA Isolation Kits (MoBio Laboratories Inc., Carlsbad, California). Total bacteria, AOB, NOB, and denitrification bacteria were analyzed with the qPCR (Bio-Rad Laboratories (Canada) Ltd., Mississauga, Ontario). Information about the primers and target genes is available in the supplementary material (Appendix B-2). Triplicates for each sample were measured in qPCR. The quantity of the functional gene copies that obtained from the qPCR results were then normalized by the dry weight of biomass (VSS), as copies/mg biomass. The functional genes copies under different conditions were analyzed using ANOVA. Extracted DNA samples were further sequenced on the Illumine Miseq platform by Research and Testing Laboratory (Lubbock, TX, USA) to investigate the diversity and community structure. The primer set used in the sequencing is 357wF (CCTACGGGNGGCWGCAG) and 785R (GACTACHVGGGTATCTAATCC). Sequencing data processing and taxonomic classification were completed with QIIME software (Caporaso et al., 2010) using Silva database. Taxonomic classification of the microbial communities was completed at phylum, class, order, family, and genus levels. The raw data was accessible through the accession number included in the supplementary material (Appendix B-3,4,5). The diversity analysis was based on the alpha rarefaction curves, which were plotted based

on the metrics calculated in QIIME: Chao 1 metric, the observed OTUs, and phylogenetic diversity metric.

#### 4.2.4. Batch test and kinetics analysis

Batch tests were conducted to determine the nitrification rates of the different aggregates (attached biofilm and suspended sludge). Four sets of batch tests were conducted in parallel: suspended sludge, attached biofilm, suspended sludge + attached biofilm, and a control (no biofilm and no sludge). (1) A set of bottles (900mL) were filled with 40 biocarriers from the reactor (attached biofilm) in each bottle; (2) a second set of bottles were filled with 270 mL of washed suspended sludge; (3) a third set of bottles were filled with 40 biocarriers and 270 mL sludge (attached biofilm + suspended sludge); and (4) a control set of bottles were filled with synthetic wastewater only. All tests were performed in triplicates. Sludge and biofilm were washed before being used for batch tests to remove residual compounds. Briefly, at the end of the reaction, 270 mL sludge was collected from the IFAS reactor and was settled for 40 min. The supernatant was drained and the sludge was washed with 1× phosphate buffered saline (PBS) three times before being used in subsequent experiments. All bottles were filled with 270 mL synthetic wastewater substrate. The substrate had a concentration of 400 mg/L  $\text{NH}_4^+\text{-N}$  and 390 mg/L  $\text{NO}_2^-\text{-N}$ , mimicking the condition of the reactor at the beginning of the reaction. Other compounds of the substrate were listed in (Appendix A-6). All the bottles were then transferred into a shaker. To ensure there was enough oxygen in the batch bottles, the shaking speed was set at 150 rpm. Samples were collected as the reaction progressed. All samples were filtered (0.45  $\mu\text{m}$  pore) right after collection.  $\text{NH}_4^+\text{-N}$ ,  $\text{NO}_2^-\text{-N}$ , and nitrate-N in all samples were measured using Hach kits. The ammonium uptake rate and the nitrite accumulation rate in the different aggregates were compared. The ammonium uptake rate was determined using the method in Bassin et al. (2012), which measured the linear regression of  $\text{NH}_4^+\text{-N}$  concentration over time divided by the biomass in the reactor. More specifically, the



specific rate of  $\text{NH}_4^+\text{-N}$  removal was calculated as the changing rate of  $\text{NH}_4^+\text{-N}$  concentration divided by the dry weight of biomass (VSS). The specific nitrite accumulation rate was calculated in a similar way, but in terms of  $\text{mg NO}_2^-\text{-N}/(\text{hr}\cdot\text{g biomass})$ .

The biosorption capacity of the biomass in the batch tests was defined as the quantity of  $\text{NH}_4^+\text{-N}$  removed by biosorption in 5 min (Guellil et al., 2001; Jacobsen et al., 1996).

$$\text{Biosorption capacity} = \frac{\text{NH}_4^+\text{-N in the original substrate} - \text{NH}_4^+\text{-N in the substrate}_{t=5\text{min}}}{\text{total biomass in the batch}(g)} \quad \text{Where}$$

the unit for capacity is  $\text{mg NH}_4^+ - \text{N}/\text{L} \cdot \text{g biomass}$  (Equation 1)

#### 4.2.5. Statistical analysis

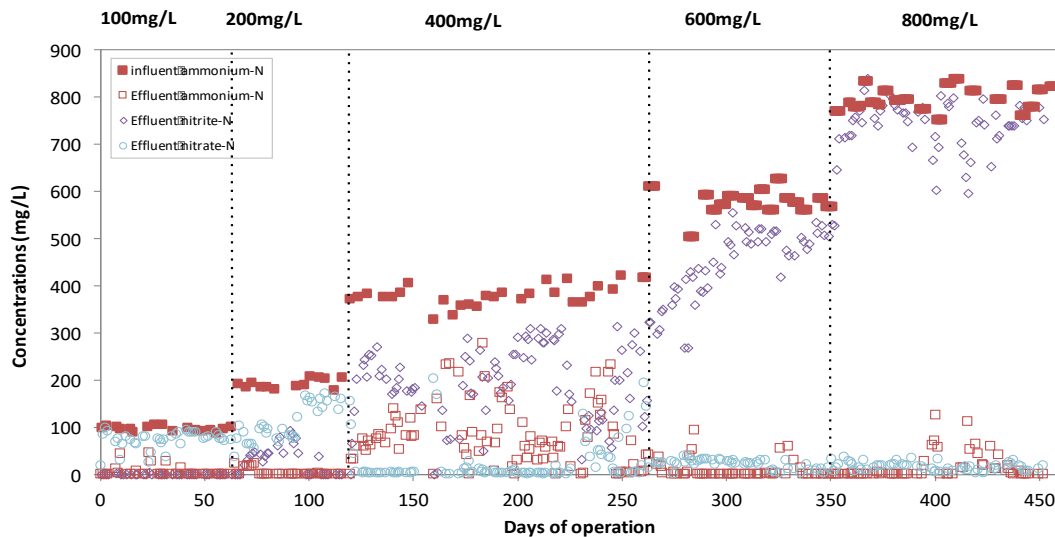
Statistical analyses were performed using t-test and single factor analysis of variance (ANOVA) at 5% probability level with Microsoft Excel® software and reported as p-values. A p-value smaller than 0.05 represents a statistically significant difference.

### 4.3. Results and Discussion

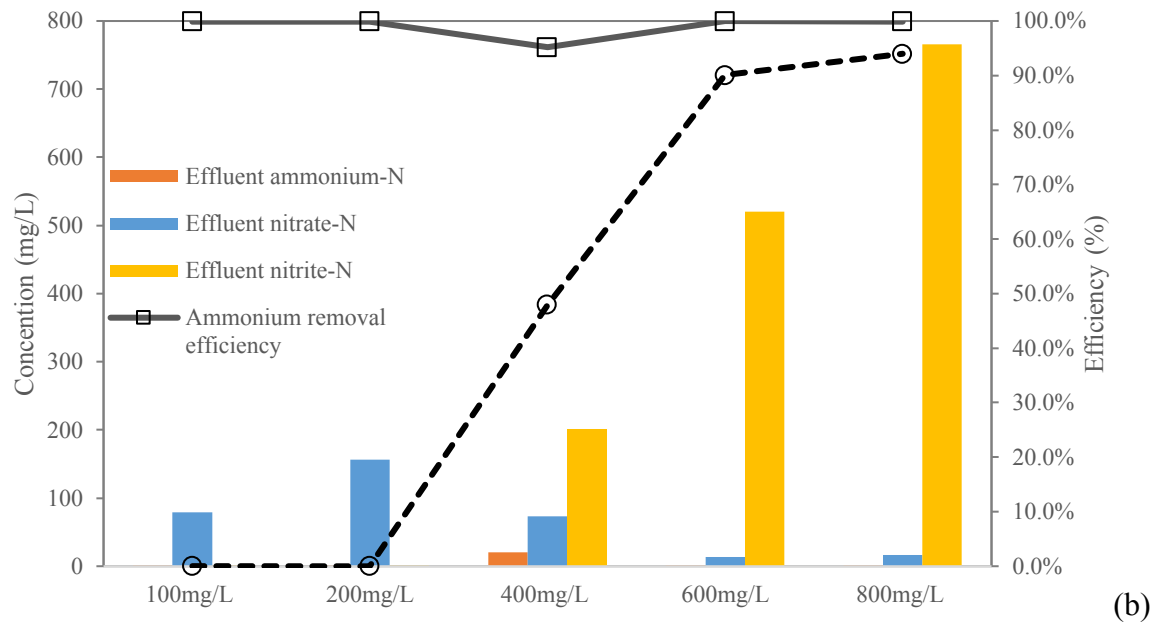
#### 4.3.1. Reactor performance results

According to the measurements (Figure 4.1a), at 100 and 200 mg/L  $\text{NH}_4^+\text{-N}$  feed conditions, complete nitrification was achieved as a high concentration of  $\text{NO}_3^-\text{-N}$  was in the effluent. More than 99% of the  $\text{NH}_4^+\text{-N}$  was oxidized, but no  $\text{NO}_2^-\text{-N}$  accumulated in the reactor (Figure 4.1b). It can be noted that when the condition was first changed from 100 to 200 mg/L  $\text{NH}_4^+\text{-N}$  feed, a short period of nitrite accumulation was observed (Figure 4.1a). However, the nitrite accumulation did not last long as the  $\text{NO}_3^-\text{-N}$  became dominant again under 200 mg/L  $\text{NH}_4^+\text{-N}$  feeding condition, after an extended time of operation (after around 100 days). When the concentration of  $\text{NH}_4^+\text{-N}$

further increased to 400 mg/L, there was an increase of  $\text{NO}_2^-$ -N in the effluent, indicating the nitrite accumulation occurred under this condition. About 48% of the incoming  $\text{NH}_4^+$ -N was converted to  $\text{NO}_2^-$ -N under 400mg/L feed condition, and this percentage increased to 90% (600 mg/L  $\text{NH}_4^+$ -N feed) and 94% (800 mg/L  $\text{NH}_4^+$ -N feed) with an increase of influent  $\text{NH}_4^+$ -N concentration (Figure 4.1b). The 400 mg/L  $\text{NH}_4^+$ -N feed condition seemed to be the turning point from complete nitrification to partial nitrification. At 600 mg/L  $\text{NH}_4^+$ -N feed, partial nitrification was established quickly (within 50 days). Under 600 mg/L and 800 mg/L  $\text{NH}_4^+$ -N feed conditions, stable partial nitrification well maintained in the reactor. In addition, the colour of the reactor changed from a light brownish colour to dark orange-brownish colour before and after partial nitrification establishment.



(a)



**Figure 4.1.** IFAS-SBR reactor performance in the reactor during reactor operation. (a) shows the influent and effluent water quality along time. Ammonium nitrogen concentrations in the reactor feed in different phases are listed on top of the figure and each phase is divided by dashed lines. (b) shows the average effluent quality and the ammonium removal and nitrite accumulation efficiency during the stable phase (last 10 days) of each stage.

Free ammonia (FA) and free nitrous acid (FNA) played important roles in inhibiting NOB. FA and FNA concentrations were calculated based on Anthonisen et al.'s (1976) equations under different  $\text{NH}_4^+\text{-N}$  loading conditions and are listed in Table 4.1. Under 400 mg/L condition, FA and FNA concentrations were 9.61 mg/L and  $14.5 \cdot 10^{-3}$  mg/L, respectively (Table 4.1.). Previous studies reported that the inhibition of *Nitrosomonas* by FA ranged from 10–150 mg/L and the inhibition of *Nitrobacter* by FA was about 0.1–1 mg/L. FNA inhibited nitrification at 0.22–2.8 mg/L (Anthonisen et al., 1976). When the  $\text{NH}_4^+\text{-N}$  concentration in the reactor feed was 400 mg/L, the results indicate that free ammonia (FA) seemed to be the major inhibitor of NOB, as the FNA concentration in the reactor is much lower than reported inhibition threshold. It is noted that studies

reported that FA inhibition of NOB was reversible (Peng and Zhu, 2006). However, long-term stable nitrification in the reactor was achieved.

	100	200	400	600	800
<b>NH<sub>4</sub><sup>+</sup>-N in feeding</b>	100	200	400	600	800
<b>FA (mg/L)</b>	0.97	1.83	9.61	18.70	15.84
<b>FNA (10<sup>-3</sup>mg/L)</b>	0.52	2.50	14.50	18.60	38.60
<b>MLSS (mg/L)</b>	940	1050	1270	2330	2520
<b>SVI (mL/g)</b>	787	638	168	225	238
<b>Biofilm thickness (μm)</b>	80.3±2.8	76.9±14.3	60.4±15.6	122.8±45.8	133.9±29.5
<b>Alkalinity addition as CaCO<sub>3</sub> (mg/L)</b>	543.3±48.8	1050.1±169.9	1871.7±131.4	3765.0±234.4	5147.5±399.3

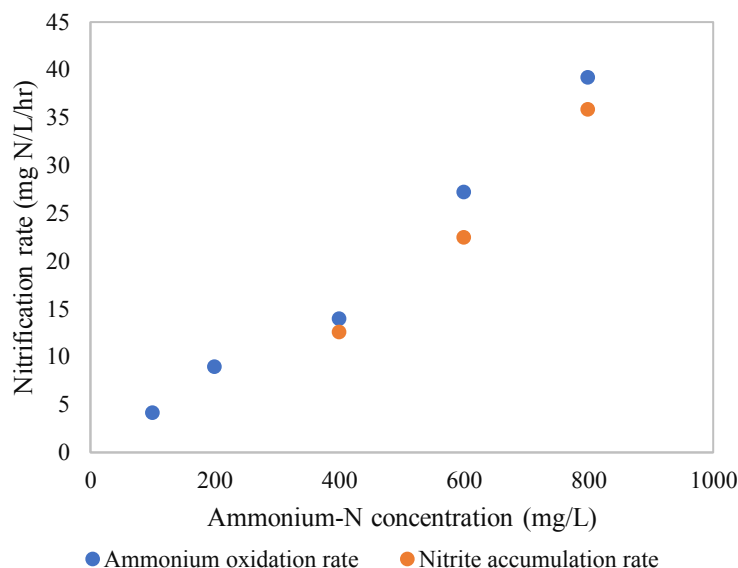
Another reason for stable nitrite accumulation in the reactor might have been inhibition of NOB by Free Hydroxylamine (FH) (Yang and Alleman, 1992). FH inhibition of NOB is irreversible as suggested by previous researchers (Hao and Chen, 1994). It was pointed out that FH proposes an acute toxicity to NOB bacteria and result in the nitrite accumulation in the reactor (Hu, 1990). FH is an intermediate product of nitrification by AOB. As the nitrification in the reactor was extensive, the production of FH could be high under oxygen deficient condition, allowing it to successfully inhibit NOB activity. With the inhibition of NOB, the nitrate concentration in the reactor decreased. Most of the NH<sub>4</sub><sup>+</sup> in the reactor feed was converted to NO<sub>2</sub><sup>-</sup>. The reactor achieved more than 97% ammonium removal under all conditions except for the 400 mg/L NH<sub>4</sub><sup>+</sup>-N feed condition under which the reactor was not stabilized.

An IFAS system can prevent the production of excessive biomass. The MLSS in the reactor increased from 940 to 2520 mg/L as the NH<sub>4</sub><sup>+</sup>-N concentration increased (Table 4.1). A clear increase in biofilm thickness was observed when the NH<sub>4</sub><sup>+</sup>-N concentration increased from 400 to 600 mg/L (Table 4.1). The SVI was high (787 at 100mg/L and 638 at 200mg/L condition) when

the reactor was performing nitrification. As partial nitrification gradually developed in the reactor, the SVI decreased to about 240. It might be due to the fact that the AOB abundance is negatively correlated to the SVI (van den Akker et al., 2010). The sludge settleability improved when the  $\text{NH}_4^+\text{-N}$  concentration increased.

#### 4.3.2. Impact of ammonia loading on ammonia conversion kinetics

Ammonia removal kinetics is another important parameter to evaluate the performance of the reactor. The ammonium and nitrite are the two key components in the nitrification process. Results show that the nitrite accumulation rate is slightly lower than the ammonium reduction rate (Figure 4.2). The discrepancy may be attributed to small amount nitrate production and nitrogen conversion for cells synthesis. Under low  $\text{NH}_4^+\text{-N}$  loading conditions (100 and 200 mg/L  $\text{NH}_4^+\text{-N}$  feed), there was no nitrite accumulation and most of the ammonium was converted to nitrate as described in last section. The nitrite accumulation rates under these low  $\text{NH}_4^+\text{-N}$  loading conditions were zero. As the ammonia loading increased, the ammonium reduction rate and the nitrite accumulation rate increased (Figure 4.2). This might be related to the increasing population and activities of ammonium oxidizing bacteria (AOB), as the condition favours the growth and activities of AOB.

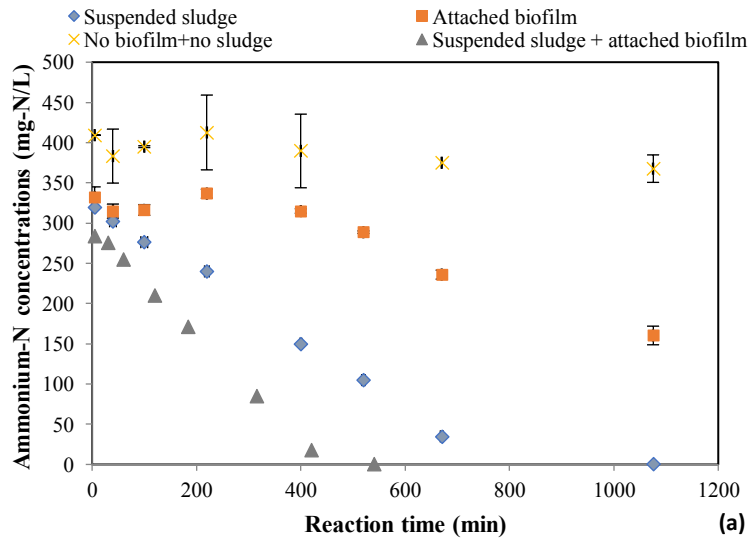


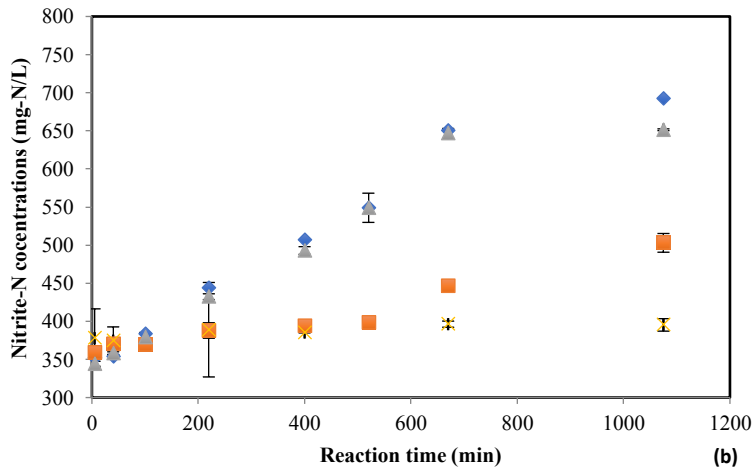
**Figure 4.2.** The impact of ammonium nitrogen concentration on the nitrite accumulation rate and the ammonium removal rate.

#### 4.3.3. Ammonium removal by biofilms and flocs

To investigate the conversion of nitrogen species in the reactor by different microbial aggregates, batch tests were performed. Figure 4.3a compares the removal of ammonium by suspended sludge, attached biofilm, and combined suspended and attached biomass. At the starting point, the concentration of the  $\text{NH}_4^+\text{-N}$  in the controls was about 400mg/L. While the concentrations in the other bottles, that were inoculated with biomass, were less than 400mg/L. Also, more biomass inoculated in the bottle, lower the concentration of  $\text{NH}_4^+\text{-N}$  at the starting point (Data available in supplementary material Appendix B-1). The low ammonium concentration (except for the control) in batch bottles at the starting point may be explained by the fast biosorption of ammonium to biomass (Wei and Hong, 2010). The biosorption of ammonium was associated with the EPS secreted by cells (Sheng et al., 2010). Strong binding between functional groups in the biofilm and flocs EPS, such as carboxyl, hydroxyl, phosphoric, sulfhydryl, phenolic groups, and heavy metals

or other organic compounds has been reported to contribute to the biosorption. As shown in Figure 4.4, results showed that the attached biofilm had higher biosorption capacity ( $85.0 \pm 15.8 \text{ mg NH}_4^+ \text{-N/g biomass}$ ), as compared to the suspended sludge ( $66.4 \pm 5.7 \text{ mg mg NH}_4^+ \text{-N/g biomass}$ ). This coincided with EPS results (Appendix Fig. C-3), which showed slightly higher EPS content/biomass in the biofilm than that in the suspended sludge. However, suspended sludge oxidized ammonium and accumulated nitrite at a rate of  $21.1 \text{ mg NH}_4^+ \text{-N/hr} \cdot \text{g biomass}$ . While the rates were  $11.6 \text{ mg NH}_4^+ \text{-N/hr} \cdot \text{g biomass}$  in biofilm. The variances were related to the microbial community structure which were explained in detail in next section. The ammonium oxidizing rate of this reactor was higher than the rate in Nhat et al.'s (2017) study, in which the feed water was lack of alkalinity; and lower than what was found by Gabarró et al. (2012), in which the reactor was added with alkalinity and operated under higher temperature ( $25 \& 30^\circ \text{C}$ ).

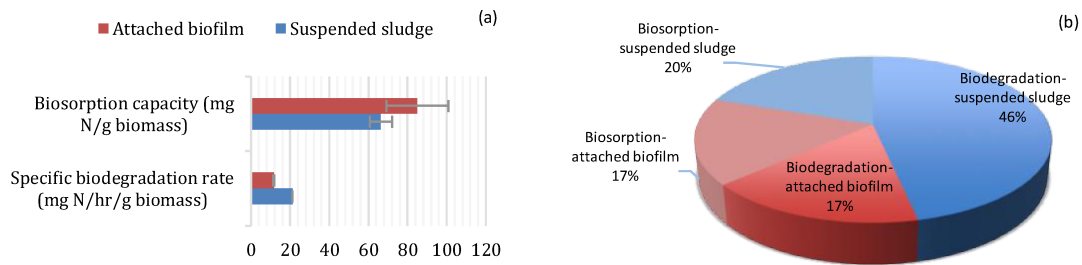




**Figure 4.3.** Batch tests results show the conversion of nitrogen species by different biomass aggregates: (a) oxidation of ammonium, (b) accumulation of nitrite in the same batch test. Control groups are the no biofilm and no sludge groups. The attached biofilm means the test with biofilm only. The suspended sludge represents the test with suspended sludge only, and the suspended sludge + attached biofilm means the group with both the suspended sludge and attached biofilm. Error bars show the standard deviations of replicates.

Based on the biosorption capacity and ammonium oxidation rates, the biosorption and biodegradation were the two main mechanisms for the ammonium reduction in the reactor. Among 37% of ammonium reduced by biosorption, 20% was from the sludge and 17% was from the biofilm. While among the rest 63% of ammonium reduced by biodegradation, 46% was contributed by sludge and 17% was contributed by biofilm (Figure 4.4b). By comparing the suspended sludge and attached biofilm, the suspended sludge was playing a more important role in ammonium reduction because about 66% of ammonium was removed by the sludge and the rest 34% was removed by the biofilm.





**Figure 4.4.** Figure (a) gives the specific ammonium-N biodegradation rates and biosorption capacity of suspended sludge and attached biofilm. Figure (b) shows the two mechanisms (biodegradation and biosorption) of ammonium reduction and the contributions from sludge and biofilm through these two mechanisms.

#### 4.3.4. Microbial community analysis- Real-time polymerase chain reaction (PCR)

In this study, qPCR and NGS methods were used to explore the ecology of the whole microbial community, which were commonly used for microbial structure studies for partial nitrification (Ali et al., 2016; Steuernagel et al., 2018). The comparison of the methods was included in the supplementary material (Appendix A-5).

Real-time PCR analysis, also known as q-PCR, was employed to explore the quantity of nitrogen reduction related functional genes in the reactor. Two major nitrifiers in the reactor, AOB and NOB were focused in this study. Denitrification and anammox genes were also investigated in this study. As shown in Table 4.2, the amount of AOB functional genes increased as the  $\text{NH}_4^+\text{-N}$  concentration increased up to 800 mg/L ( $p=3\times 10^{-6}$  for sludge samples and  $p=1.67\times 10^{-17}$  for biofilm samples). *Nitrosomonas spp.* are the dominant AOB detected in this study. In other studies, *Nitrosomonas europea* / *N. mobilis* lineage was the dominant AOB detected in the WWTP (Koops et al., 2006). *N. europea* was extensively detected in a WWTP treating low strength domestic wastewater, while *N. mobilis* was detected in a WWTP treating industrial wastewater, revealing its tolerance to high salinity (Prosser et al., 2014). Researchers also detected a high amount of *Nitrosomonas oligotropha* in laboratory scale experiments treating industrial wastewater with high heavy metals

content (Stehr et al., 1995). To further understand the diversity of AOB in this nitrification reactor, more genetic analysis is required.

The results showed that *Nitrospira* functional genes per mg biomass decreased by more than 2 logs when the reactor feed increased from 200mg/L to 400 mg/L NH<sub>4</sub><sup>+</sup>-N (Table 4.2) ( $p=3.72 \times 10^{-25}$  for sludge samples and  $p=6.2 \times 10^{-20}$  for biofilm samples). This confirmed that nitrification was established at this high ammonium condition. Previous study by Blackburne et al. (2007) pointed out that the *Nitrospira* has a low inhibition threshold concentration for free ammonia (0.04 to 0.08mg NH<sub>3</sub>-N/L). However, in the reactor, the inhibition of *Nitrospira* became evident only when the free ammonia concentration was in range of 1.83-9.61mg NH<sub>3</sub>-N /L (Table 4.2).

**Table 4.2. Quantification of functional genes per mg biomass in the sludge and biofilm**

	NH <sub>4</sub> <sup>+</sup> -N in feeding	Functional genes					
		amoA (AOB functional gene)	NSR (NOB functional gene)	nirK	nosZ	narG	AMX
Sludge	100mg/L	1.91E+08	1.67E+08	3.90E+08	2.35E+08	1.06E+08	2.36E+07
	200mg/L	3.85E+08	2.17E+08	4.78E+08	2.40E+08	1.70E+08	3.66E+07
	400mg/L	1.48E+09	8.37E+05	1.38E+08	3.10E+08	1.15E+08	1.18E+07
	600mg/L	7.47E+08	3.51E+05	9.43E+07	1.71E+08	8.59E+07	1.68E+07
	800mg/L	9.08E+08	4.92E+05	2.59E+08	2.40E+08	1.41E+08	2.94E+07
Biofilm	100mg/L	8.14E+07	9.02E+07	1.24E+08	9.62E+07	5.01E+07	5.30E+06
	200mg/L	1.21E+08	1.59E+08	2.64E+08	1.81E+08	8.90E+07	1.18E+07
	400mg/L	2.85E+08	1.38E+06	1.08E+08	2.19E+08	7.19E+07	7.64E+06
	600mg/L	5.95E+08	6.45E+05	8.98E+07	1.47E+08	6.50E+07	5.87E+06
	800mg/L	5.39E+08	5.94E+05	1.55E+08	2.36E+08	1.05E+08	1.49E+07

Note: The units for all numbers are gene copies/mg biomass. amoA is the targeted functional gene for AOB; NSR is for *Nitrospira*; nirK, nosZ, and narG are for denitrifiers' functional genes; AMX is for the 16s rRNA gene of *Anammox*.

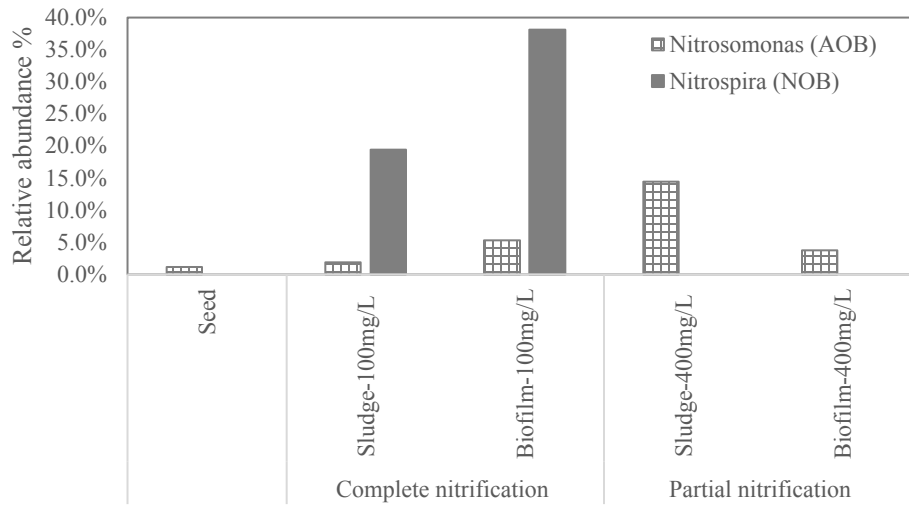
*nosZ* and *narG* denitrification genes were not affected by the high ammonium concentration, whereas *nirK* genes were inhibited at 400 mg/L NH<sub>4</sub><sup>+</sup>-N and adapted to the new condition quickly. The reductase that reduces nitrite to NO is coded by *nirK* genes. Nevertheless, it was reported that some AOB species may carry the *nirK* gene, such as *Nitrosomonas europaea*-a gene cluster (*ncgABC-nirK*) that encodes the Cu containing nitrite reductase (Prosser et al., 2014). The relationship between the increasing *nirK* genes and AOB population in this study is unknown, more detailed study on the origin of nitrification genes is required. Moreover, small amounts of anammox genes were also detected in the reactor.

The bacterial community structures in suspended sludge and biofilm were similar. Similar numbers of AOB functional gene per mg of suspended sludge and biofilm biomass were found. As the suspended sludge shared more biomass than biofilm in the reactor, the total number of AOB functional gene was higher in the sludge than in the biofilm. This result suggested that the sludge was playing an important role in ammonium degradation, which agreed with the batch test results. The results do not agree with those of Onnis-Hayden et al. (2011) and Kim et al. (2011), in which more nitrifiers were present on the carrier media (biofilm) than those in flocs (suspended sludge). However, in van den Akker et al.(2010), equal amounts of AOB were detected on biofilm and sludge. All these studies involved the treatment of low ammonia strength wastewater with high C/N ratios in a continuous mode. Since AOB are slow growers, they tend to stay in biofilm that provides a longer SRT. In the present study, the SRT for suspended sludge was long (about 30 days), which explains the presence of AOB in suspended sludge.

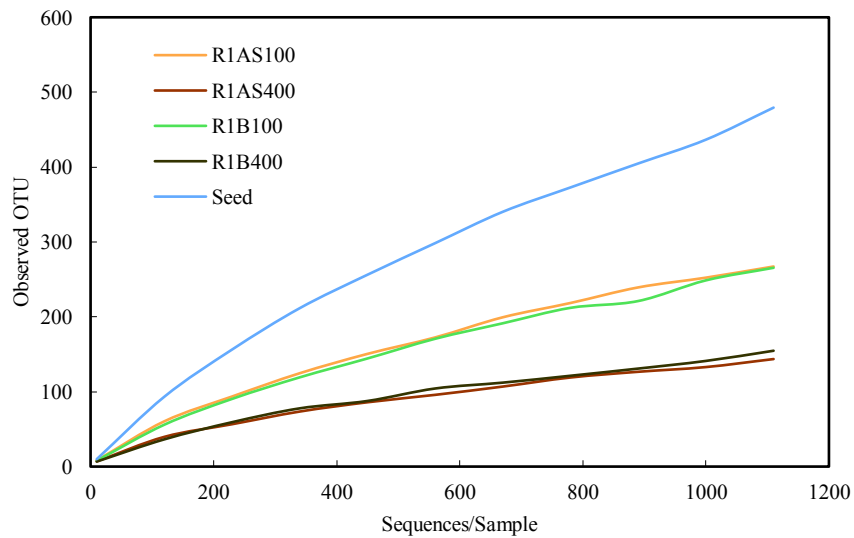
Comparing the sludge and biofilm data, the changes in the microbial community structure in response to different ammonia loadings were different in these two biomass aggregates. Biofilm provided more protection for NOB because it contained higher amount of NOB functional genes than the sludge. Moreover, lower AOB functional genes in the biofilm than the sludge during partial nitrification process, emphasizing a higher diffusion resistance and lower substrate availability in the biofilm (Shao et al., 2017).

#### 4.3.5. Microbial community analysis - Next generation sequencing

Next generation sequencing data provide the relative abundance of microbial genus. The Alpha rarefaction curves gave the richness and the diversity of species in different samples. As shown in Figure 4.5a, *Nitrosomonas* was the dominant AOB in all samples. The lowest relative abundance of *Nitrosomonas* was observed in the seed sludge sample from local WWTP. The species diversity was the highest in the seed (Figure 4.5b). When influent  $\text{NH}_4^+\text{-N}$  concentration increased from 100 to 400 mg/L, the relative abundance of *Nitrosomonas* increased from 2% to 14% in sludge samples but changed from 5% to 4% in the biofilm samples. As mentioned in previous sections, NOB got inhibited when the feeding contains greater than 400mg/L  $\text{NH}_4^+\text{-N}$ , which also marked the beginning of partial nitrification. Relative abundance plot showed that *Nitrospira* was the dominant NOB in the reactor before the establishment of partial nitrification. The relative abundance of *Nitrospira* decreased from 19% to 0 % in the sludge, and from 38% to 0% in the biofilm when the increase of  $\text{NH}_4^+\text{-N}$  in the feeding was from 100 to 400mg/L. These results agreed well with the qPCR data that two log units deduction was observed in NOB functional gene when feeding  $\text{NH}_4^+\text{-N}$  increased from 100 to 400mg/L. In addition, the richness of the species (Figure 4.5b) in the samples decreased along with the increase of  $\text{NH}_4^+\text{-N}$  concentration in the feeding, not only in the sludge, but also in the biofilm. It indicated the inhibition of high ammonium loading on the microbial community structure diversity.



(a)



(b)

**Figure 4.5.** (a) shows the comparison of microbial community before (100mg/L condition) and after partial nitrification establishment and in the seed sludge form Gold Bar wastewater treatment plant. Genus at a relative abundance <1% were removed from the figure. Highlighted areas represent *Nitrosomonas* (orange) and *Nitrospira* (Blue), which were the major nitrifiers in the reactor. (b) gives the microbial community richness analysis. R1AS100 represented the community in the sludge that collected under 100mg/L condition (before partial nitrification); R1AS800

indicated the community in the sludge that collected under 800mg/L condition (partial nitrification); R1B100 corresponded to the community in the biofilm under 100mg/L condition (before partial nitrification); R1B800 indicated the community in the biofilm collected under 800mg/L condition (partial nitrification); and the seed represented the community in the seed sludge.

#### **4.4. Conclusions**

Partial nitrification achieved greater than 97% ammonium removal with influent  $\text{NH}_4^+\text{-N}$  concentration of 800 mg/L in a laboratory scale IFAS. NOB was successfully inhibited when influent  $\text{NH}_4^+\text{-N}$  concentration was greater than 400mg/L. Higher ammonium removal was achieved by the suspended sludge (66%) as compared to the biofilm (34%), which may be attributed to the higher AOB density in the sludge. Overall, the ammonium loading rate played a major role in controlling microbial population and ammonium removal kinetics.

#### **4.5. References**

- Ahn, Y.-H., 2006. Sustainable nitrogen elimination biotechnologies: A review. *Process Biochemistry* 41, 1709–1721. <https://doi.org/10.1016/j.procbio.2006.03.033>
- Ali, M., Chai, L.-Y., Min, X.-B., Tang, C.-J., Afrin, S., Liao, Q., Wang, H.-Y., Peng, C., Song, Y.-X., Zheng, P., 2016. Performance and characteristics of a nitrification air-lift reactor under long-term HRT shortening. *International Biodeterioration & Biodegradation* 111, 45–53. <https://doi.org/10.1016/j.ibiod.2016.04.003>
- Anthonisen, A.C., Loehr, R.C., Prakasam, T.B.S., Srinath, E.G., 1976. Inhibition of Nitrification by Ammonia and Nitrous Acid. *J Water Pollut Control Fed* 48, 835–852.

- APHA, 2011. Standard Methods for the Examination of Water and Wastewater. American Public Health Association, Washington, DC.
- Bassin, J.P., Kleerebezem, R., Rosado, A.S., van Loosdrecht, M.C.M., Dezotti, M., 2012. Effect of Different Operational Conditions on Biofilm Development, Nitrification, and Nitrifying Microbial Population in Moving-Bed Biofilm Reactors. *Environmental Science & Technology* 46, 1546–1555. <https://doi.org/10.1021/es203356z>
- Blackburne, R., Vadivelu, V.M., Yuan, Z., Keller, J., 2007. Kinetic characterisation of an enriched *Nitrospira* culture with comparison to *Nitrobacter*. *Water Research* 41, 3033–3042. <https://doi.org/10.1016/j.watres.2007.01.043>
- Brouwer, M., Loosdrecht, M., Heijnen, J., 1996. One reactor system for ammonium removal via nitrite, STOWA. ed. Utrecht, The Netherlands.
- Caporaso, J.G., Kuczynski, J., Stombaugh, J., Bittinger, K., Bushman, F.D., Costello, E.K., Fierer, N., Peña, A.G., Goodrich, J.K., Gordon, J.I., Huttley, G.A., Kelley, S.T., Knights, D., Koenig, J.E., Ley, R.E., Lozupone, C.A., McDonald, D., Muegge, B.D., Pirrung, M., Reeder, J., Sevinsky, J.R., Turnbaugh, P.J., Walters, W.A., Widmann, J., Yatsunenko, T., Zaneveld, J., Knight, R., 2010. QIIME allows analysis of high-throughput community sequencing data. *Nature Methods* 7, 335–336. <https://doi.org/10.1038/nmeth.f.303>
- Gabarró, J., Ganigué, R., Gich, F., Rusalleda, M., Balaguer, M.D., Colprim, J., 2012. Effect of temperature on AOB activity of a partial nitrification SBR treating landfill leachate with extremely high nitrogen concentration. *Bioresource Technology* 126, 283–289. <https://doi.org/10.1016/j.biortech.2012.09.011>
- Glass, C., Silverstein, J., Oh, J., 1997. Inhibition of Denitrification in Activated Sludge by Nitrite. *Water Environment Research* 69, 1086–1093.
- Guellil, A., Thomas, F., Block, J.-C., Bersillon, J.-L., Ginestet, P., 2001. Transfer of organic matter between wastewater and activated sludge flocs. *Water Research* 35, 143–150. [https://doi.org/10.1016/S0043-1354\(00\)00240-2](https://doi.org/10.1016/S0043-1354(00)00240-2)

- Hao, O.J., Chen, J.M., 1994. Factors Affecting Nitrite Buildup in Submerged Filter System. *Journal of Environmental Engineering* 120, 1298–1307. [https://doi.org/10.1061/\(ASCE\)0733-9372\(1994\)120:5\(1298\)](https://doi.org/10.1061/(ASCE)0733-9372(1994)120:5(1298))
- Hellinga, C., Schellen, A., Mulder, J., Vanloosdrecht, M., Heijnen, J., 1998. The sharon process: An innovative method for nitrogen removal from ammonium-rich waste water. *Water Science and Technology* 37, 135–142. [https://doi.org/10.1016/S0273-1223\(98\)00281-9](https://doi.org/10.1016/S0273-1223(98)00281-9)
- Hu, S., 1990. Acute Substrate-intermediate-product Related Inhibition of Nitrifiers. Purdue University.
- Huang, C., Shi, Y., Gamal El-Din, M., Liu, Y., 2016. Optimization of ozonation combined with integrated fixed-film activated sludge (IFAS) in the treatment of oil sands process-affected water (OSPW). *International Biodeterioration & Biodegradation* 112, 31–41. <https://doi.org/10.1016/j.ibiod.2016.04.037>
- Jacobsen, B.N., Arvin, E., Reinders, M., 1996. Factors affecting sorption of pentachlorophenol to suspended microbial biomass. *Water Research* 30, 13–20. [https://doi.org/10.1016/0043-1354\(95\)00108-W](https://doi.org/10.1016/0043-1354(95)00108-W)
- Kim, H., Schuler, A.J., Gunsch, C.K., Pei, R., Gellner, J., Boltz, J.P., Freudenberg, R.G., Dodson, R., 2011. Comparison of Conventional and Integrated Fixed-Film Activated Sludge Systems: Attached- and Suspended-Growth Functions and Quantitative Polymerase Chain Reaction Measurements. *Water Environment Research* 83, 627–635. <https://doi.org/10.2175/106143010X12851009156448>
- Koops, H.-P., Purkhold, U., Pommerening-Röser, A., Timmermann, G., Wagner, M., 2006. The Lithoautotrophic Ammonia-Oxidizing Bacteria, in: Dworkin, M., Falkow, S., Rosenberg, E., Schleifer, K.-H., Stackebrandt, E. (Eds.), *The Prokaryotes*. Springer New York, New York, NY, pp. 778–811. [https://doi.org/10.1007/0-387-30745-1\\_36](https://doi.org/10.1007/0-387-30745-1_36)
- Kouba, V., Catrysse, M., Stryjova, H., Jonatova, I., Volecke, E.I.P., Svehla, P., Bartacek, J., 2014. The impact of influent total ammonium nitrogen concentration on nitrite-oxidizing bacteria



- inhibition in moving bed biofilm reactor. *Water Science & Technology* 69, 1227. <https://doi.org/10.2166/wst.2013.757>
- Kuai, L., Verstraete, W., 1998. Ammonium Removal by the Oxygen-Limited Autotrophic Nitrification-Denitrification System. *Applied and Environmental Microbiology* 64, 4500–4506.
- Nhat, P.T., Biec, H.N., Van, T.T.T., Tuan, D.V., Trung, N.L.H., Nghi, V.T.K., Dan, N.P., 2017. Stability of partial nitrification in a sequencing batch reactor fed with high ammonium strength old urban landfill leachate. *International Biodeterioration & Biodegradation* 124, 56–61. <https://doi.org/10.1016/j.ibiod.2017.06.017>
- Nhu Hien, N., Van Tuan, D., Nhat, P.T., Thi Thanh Van, T., Van Tam, N., Xuan Que, V.O.N., Phuoc Dan, N., 2017. Application of Oxygen Limited Autotrophic Nitrification/Denitrification (OLAND) for anaerobic latex processing wastewater treatment. *International Biodeterioration & Biodegradation* 124, 45–55. <https://doi.org/10.1016/j.ibiod.2017.07.009>
- Nielsen, M., Bollmann, A., Sliemers, O., Jetten, M., Schmid, M., Strous, M., Schmidt, I., Larsen, L.H., Nielsen, L.P., Revsbech, N.P., 2005. Kinetics, diffusional limitation and microscale distribution of chemistry and organisms in a CANON reactor. *FEMS Microbiol. Ecol.* 51, 247–256. <https://doi.org/10.1016/j.femsec.2004.09.003>
- Nze, K., Xu, S., Mohammed, A., Liu, Y., 2018. Effect of a significant increase in flow rate on the performance and bacteria community in a pilot-scale activated sludge biological nutrient removal reactor. *Journal of Environmental Engineering* In press.
- Onnis-Hayden, A., Majed, N., Schramm, A., Gu, A.Z., 2011. Process optimization by decoupled control of key microbial populations: Distribution of activity and abundance of polyphosphate-accumulating organisms and nitrifying populations in a full-scale IFAS-EBPR plant. *Water Research* 45, 3845–3854. <https://doi.org/10.1016/j.watres.2011.04.039>

- Peng, Y., Zhu, G., 2006. Biological nitrogen removal with nitrification and denitrification via nitrite pathway. *Appl. Microbiol. Biotechnol.* 73, 15–26. <https://doi.org/10.1007/s00253-006-0534-z>
- Prosser, J.I., Head, I.M., Stein, L.Y., 2014. The Family Nitrosomonadaceae, in: Rosenberg, E., DeLong, E.F., Lory, S., Stackebrandt, E., Thompson, F. (Eds.), *The Prokaryotes*. Springer Berlin Heidelberg, Berlin, Heidelberg, pp. 901–918. [https://doi.org/10.1007/978-3-642-30197-1\\_372](https://doi.org/10.1007/978-3-642-30197-1_372)
- Shao, Y., Shi, Y., Mohammed, A., Liu, Y., 2017. Wastewater ammonia removal using an integrated fixed-film activated sludge-sequencing batch biofilm reactor (IFAS-SBR): Comparison of suspended flocs and attached biofilm. *International Biodeterioration & Biodegradation* 116, 38–47. <https://doi.org/10.1016/j.ibiod.2016.09.026>
- Sheng, G.-P., Yu, H.-Q., Li, X.-Y., 2010. Extracellular polymeric substances (EPS) of microbial aggregates in biological wastewater treatment systems: A review. *Biotechnology Advances* 28, 882–894. <https://doi.org/10.1016/j.biotechadv.2010.08.001>
- Slikkers, A.O., Third, K., Abma, W., Kuenen, J., Jetten, M.S., 2003. CANON and Anammox in a gas-lift reactor. *FEMS Microbiology Letters* 218, 339–344. [https://doi.org/10.1016/S0378-1097\(02\)01177-1](https://doi.org/10.1016/S0378-1097(02)01177-1)
- Stehr, G., S. Zörner, B. Böttcher, H. P. Koops, 1995. Exopolymers: An Ecological Characteristic of a Floc-Attached, Ammonia-Oxidizing Bacterium. *Microbial Ecology* 115.
- Steuernagel, L., de León Gallegos, E.L., Azizan, A., Dampmann, A.-K., Azari, M., Denecke, M., 2018. Availability of carbon sources on the ratio of nitrifying microbial biomass in an industrial activated sludge. *International Biodeterioration & Biodegradation* 129, 133–140. <https://doi.org/10.1016/j.ibiod.2018.02.001>
- van den Akker, B., Beard, H., Kaeding, U., Giglio, S., Short, M.D., 2010. Exploring the relationship between viscous bulking and ammonia-oxidiser abundance in activated sludge: A

- comparison of conventional and IFAS systems. *Water Research* 44, 2919–2929.  
<https://doi.org/10.1016/j.watres.2010.02.016>
- Wang, Z., Peng, Y., Miao, L., Cao, T., Zhang, F., Wang, S., Han, J., 2016. Continuous-flow combined process of nitrification and ANAMMOX for treatment of landfill leachate. *Bioresour. Technol.* 214, 514–519. <https://doi.org/10.1016/j.biortech.2016.04.118>
- Wei, L., Hong, T., 2010. Biosorption of Organic Pollutants by Activated Sludge: Equilibrium and Kinetic Modeling. *IEEE*, pp. 1–4. <https://doi.org/10.1109/ICBBE.2010.5515043>
- Wen, X., Gong, B., Zhou, J., He, Q., Qing, X., 2017. Efficient simultaneous partial nitrification, anammox and denitrification (SNAD) system equipped with a real-time dissolved oxygen (DO) intelligent control system and microbial community shifts of different substrate concentrations. *Water Research* 119, 201–211.  
<https://doi.org/10.1016/j.watres.2017.04.052>
- Yang, L., Alleman, J.E., 1992. Investigation of batch-wise nitrite build-up by an enriched nitrification culture. *Wat. Sci. Tech.* 26, 997–1005.

# CHAPTER 5. MICROBIAL POPULATION DYNAMICS IN A PARTIAL NITRIFICATION REACTOR TREATING HIGH AMMONIA STRENGTH SUPERNATANT FROM ANAEROBICALLY DIGESTED SLUDGE: ROLE OF THE FEED WATER CHARACTERISTICS

## 5.1. Introduction

Supernatant from lagoons used to thicken anaerobically digested municipal wastewater treatment sludge contains high concentrations of ammonium-N (in the range of 800-1200 mg  $\text{NH}_4^+\text{-N}$  /L). Returning the supernatant to the mainstream treatment processes imposes a heavy burden on the mainstream treatment. As the standards for effluent disposal have become more stringent, the development of environmentally friendly and economically feasible side-stream treatment has become essential. Unlike conventional nitrification, partial nitrification, also known as nitritation, entails the conversion of ammonium to nitrite without the subsequent oxidation of nitrite to nitrate, thereby lowering the oxygen consumption by up to 25% relative to the conventional process (Hellings et al., 1998; Peng and Zhu, 2006). The key to successful partial nitrification is the elimination of nitrite oxidizing bacteria (NOB) and the proliferation of ammonia oxidizing bacteria (AOB). To date, high temperature (30-40°C) operation has been the most common way to maintain stable and efficient partial nitrification (Hellings et al., 1998). In order to reduce energy costs associated with heating nitritation reactors, efforts have been made to develop partial nitrification under lower temperature conditions (Guo et al., 2010; Peng and Zhu, 2006; Yang et al., 2007). In this study, partial nitrification reactors were operated at 21°C. An integrated fixed-film activated sludge (IFAS) system, that cultivated both suspended flocs and biofilm biomass, was utilized to enhance biomass density in the reactor and to improve the process efficiency.

Although the performance efficiency and stability of the partial nitrification reactors at different scales have been extensively studied (Aslan and Dahab, 2008; J. H. Guo et al., 2009; Kulikowska

and Bernat, 2013; Liu et al., 2017; Zhang, 2009), the impacts of various feed water qualities on the microbial community dynamic and reaction kinetics have not been elucidated. Reported studies on partial nitrification microbial community composition have mainly focused on the population of AOB and NOB (Cho et al., 2011; Gong et al., 2008; J. Guo et al., 2009; J. H. Guo et al., 2009; Sun et al., 2017; Yang et al., 2007; Zhang, 2009). Heterotrophic bacteria can compete with these autotrophic bacteria for electron acceptors (Shao et al., 2017; Sinha and Annachhatre, 2007), and thus should be evaluated in the partial nitrification process. To date, only a limited number of studies have reported the composition of the entire microbial community in nitrification process (Liu et al., 2017).

Ammonium concentration is one of the essential parameters to be controlled to achieve partial nitrification. It has been established that the nitrite oxidizing bacteria are inhibited in the presence of high ammonium concentrations, with the primary inhibitors likely being free ammonia, free nitrous acid, and hydroxylamine (Anthonisen et al., 1976). In a benchmark study, Anthonisen et al., (1976) elucidated the conditions under which nitrite oxidation was inhibited. In general, complete nitrification can be achieved in the presence of lower ammonium concentrations, while partial nitrification is more likely to be achieved under high ammonium concentrations. A search of the literature has revealed only two reports that compare microbial community structures under complete and partial nitrification conditions (Ahn et al., 2011; Rodriguez-Caballero et al., 2013). The work of Ahn et al. (2011) focused on the analysis of AOB and NOB using denaturing gradient gel electrophoresis (DGGE), sequencing. The applied reverse transcriptase polymerase chain reaction (RT-PCR) was used to analyze the ammonia oxidation, nitrite and NO reduction for the RNA samples. Dissolved oxygen and solids retention time were the parameters used to shift the reactor environment from complete nitrification to nitrification. The NOB concentration and activity decreased significantly when the environment changed from complete nitrification to nitrification. Microbial communities in sludge samples from a partial nitrification and a complete nitrification reactor were investigated using pyrosequencing by Rodriguez-Caballero et al. (2013). The authors

reported that the *Nitrosomonas* was successfully enriched in a partial nitrification reactor, and the coexistence of *Nitrosomonas* (dominant AOB) and *Nitrobacter* (dominant NOB) was observed in a complete nitrification reactor. In both studies, the impact of ammonium loading on microbial population dynamics was not considered.

Most of the lab-scale partial nitrification studies employed synthetic wastewater (Ahn et al., 2011; Cho et al., 2011; Rodriguez-Caballero et al., 2013; F. Ye et al., 2011; L. Ye et al., 2011; Zhang, 2009), and seldom used real or raw wastewater (Yang et al., 2007). The wastewater to be treated in real-world applications is far more complex and may contain inhibitory substances not found in synthetic wastewater. Therefore, it is crucial to investigate how the nature of the feed water would affect the performance of the reactor and the microbial community composition before full-scale applications.

In this study, the impacts of feed ammonium concentration and the percentage of raw anaerobically digested sludge thickening lagoon supernatant on the dynamics of microbial community composition were investigated in a bench-scale IFAS bioreactor. Biofilm and suspended flocs, as the two primary biomass aggregates in IFAS bioreactors, were compared in terms of their microbial community structure changes and their nitrogen conversion kinetics. This is the first report that investigates the impacts of feed water characteristics on the microbial communities in an IFAS-based partial nitrification system. The results from this study provide essential information for the application of IFAS technology in partial nitrification systems treating high ammonium strength wastewater.

## **5.2. Methodology**

### **5.2.1. Digested sludge supernatant collection**

Samples of anaerobically digested sludge supernatant were collected from the Clover Bar sludge lagoons at Edmonton's waste management center. The lagoons are used to separate digested biosolids and supernatant. The collected supernatant was stored at 4°C to minimize the microbial activity prior to its use.

### 5.2.2. Reactors operation

A 6L bench scale IFAS reactor was operated at 21°C for 800 days under the sequencing batch mode (volume exchange ratio of 50%). Each reaction cycle lasted for 12 hours. Dissolved oxygen concentration was maintained at 0.5 to 0.8 mg/L during the reaction. The detailed operation of each reaction cycle is included in the supplementary material (Appendix C Fig. C-6). The feeding strategies for the reactor are listed in Table 5.1. The schematic diagram of the reactor is also included in the supplementary material (Appendix C Fig. C-1). Polyethylene biocarriers were used as biofilm support media. The diameter and height of these cylindrical biocarriers were 15mm and 9mm, respectively. The total surface area of each biocarrier was 1658mm<sup>2</sup>. The filling percentage of IFAS biocarriers was 40% by volume.

The reactor was operated for about 800 days to test 9 operation stages. The impacts of ammonium concentration on the microbial community structure were tested in stages 1 through 5. During these five stages, the reactor was fed with synthetic feed, the characteristics and composition of the synthetic feed are available in the supplementary material (Appendix A-1). All the ammonium fed into the reactor was in the form of NH<sub>4</sub>Cl. Stages 6 through 9 were used to interpret the impacts of digested sludge lagoon supernatant on the microbial community dynamics. During these four stages, raw lagoon supernatant was introduced to the reactor; and the percentage of raw supernatant increased step by step from 25% to 100%. Detailed composition of reactor feed water at all stages is provided in the supplementary material (Appendix A-1).

**Table 5.1. feeding strategy for the reactor.**

Stage	1	2 <sup>a</sup>	3	4 <sup>a</sup>	5	6	7	8	9
<b>Duration of stages (days)</b>	65	54	143	89	141	81	104	55	62
<b>NH<sub>4</sub><sup>+</sup>-N concentration (mg/L)</b>	100	200	400	600	800	800	800	800	800
<b>Raw supernatant %</b>	0	0	0	0	0	25	50	75	100
<b>Process achieved</b>	CN <sup>b</sup>	CN	PN	PN	PN	PN	PN	PN	PN

a. DNA samples were not sent out for high throughput sequencing.

b. CN means complete nitrification, PN means partial nitrification.

### 5.2.3. Analytical methods

The NH<sub>4</sub><sup>+</sup>-N, NO<sub>2</sub><sup>-</sup>-N, NO<sub>3</sub><sup>-</sup>-N, phosphorus and alkalinity concentrations in the feed water and effluent from the reactors were measured using Hach kits (Methods 8038, 8507, 10206, 10209, 10239, respectively). The total organic carbon (TOC) in the supernatant and in the effluent was measured using a Shimadzu TOC analyzer. The metal cation concentrations in the feed were determined using ion chromatography (IC). The mixed liquor suspended solids (MLSS) and mixed liquor volatile suspended solids (MLVSS) were measured according to *Standard Methods 2540* (APHA, 2011). The attached biomass on biofilm was determined by sonicating down the biomass from the carriers and measured using the same *Standard Methods*. The attached biofilm thickness was measured with a confocal microscope (Zeiss LSM 710).



#### 5.2.4. Cycle tests for nitrogen removal kinetics

Cycle tests were performed in the reactor to determine nitrogen removal kinetics. During each cycle test, liquid samples were collected from reactors at pre-determined time intervals as the reaction progressed. All samples were filtered (0.45  $\mu\text{m}$  pore) right after collection and the concentration of  $\text{NH}_4^+\text{-N}$ ,  $\text{NO}_2^-\text{-N}$  and  $\text{NO}_3^-\text{-N}$  were measured. The specific ammonium conversion rate was determined using the method adapted from Bassin et al. (2012), which measured the linear regression of  $\text{NH}_4^+\text{-N}$  concentration over time. The  $\text{NH}_4^+\text{-N}$  concentration change rate divided by the dry weight of the total biomass (The sum of suspended and attached biomass) in the reactor gives specific conversion rate. The  $\text{NO}_2^-\text{-N}$  accumulation rate was calculated in a similar way. The ammonium conversion rate and the nitrite accumulation rate in the different stages were compared.

#### 5.2.5. DNA extraction and sequencing

DNA was extracted from biofilm and floc using MO BIO PowerSoil® DNA Isolation Kits (MoBio Laboratories Inc., Carlsbad, California). Details of the sample pretreatment process are available in Shao et al. (2017). Extracted DNA samples were further sequenced on the Illumine MiSeq platform by Research and Testing Laboratory (Lubbock, TX, USA) to investigate the diversity and community composition. The V3-V4 regions of the 16S rRNA genes were amplified using primer set 357wF (CCTACGGGNGGCWGCAG) and 785R (GACTACHVGGGTATCTAATCC). Real time quantitative polymerase chain reaction (q-PCR) was also employed to quantify the functional genes of AOB and NOB in the DNA samples. The information about the primers and the qPCR cycles is included in the supplementary material (Appendix B-2).

#### 5.2.6. Data analysis

Sequencing data processing and taxonomic classification were completed with QIIME software (Caporaso et al., 2010) using Silva database. Taxonomic classification of the microbial communities was completed at phylum, class, order, family, and genus levels. The alpha rarefaction curves were plotted based on the metrics calculated in QIIME: Chao 1 metric, the observed OTUs, and phylogenetic diversity metric. The impacts of environmental variables on the community composition were analyzed using canonical correspondence analysis (CCA) with XLSTAT statistical embedded Microsoft Excel® software.

### **5.3. Results and Discussion**

#### **5.3.1. Digested sludge supernatant characteristics**

The ammonium nitrogen concentration in the digested sludge supernatant was  $891.9 \pm 79$  mg/L. The phosphorus concentration was  $185.6 \pm 10.4$  mg/L. The ratio of alkalinity as mg CaCO<sub>3</sub>/mg NH<sub>4</sub><sup>+</sup>-N was in the range of 3.5 to 4.0. The measured C/N ratio was less than 1. The metallic cations concentrations are listed in Table 5.2. Six metals (Cr, Ni, Cu, Zn, Pb and Cd) have been reported to inhibit the nitrification process in bioreactors (Peng and Zhu, 2006). As shown in Table 5.2, four of the six inhibitory metals were detected in lagoon supernatant (i.e., Cr, Ni, Cu, and Zn) and the concentrations of these metals were higher than the threshold inhibition levels reported; indicating these metals may suppress bioreactor performance.

**Table 5.2. Comparison of the reported ranges of heavy metals inhibition threshold in literature and heavy metals concentrations measured in this study.**

Reported range of inhibition threshold, µg/L				
Cr	Ni	Cu	Zn	References
250-1900 (Cr(T)) 1000-10000 (Cr(VI))	250-500	50-480	80-500	(U.S.EPA, 1987)
	>150000 (38% inhibition)	>5000		(Lee et al., 1997)
0.7-785	3-860	3-5730	3-1000	(Peng and Zhu, 2006)
	1900 (50% inhibition)		17290 (50% inhibition)	(Kapoor et al., 2015)
Concentration of metals in this study				
83.4±3.895%(Cr (52)) 65.5±2.617%(Cr (53))	127.6±9.394%	147.7± 6.89%	100.2±14.056 %(Zn (64)) 103.7±10.586 % (Zn 6(6))	

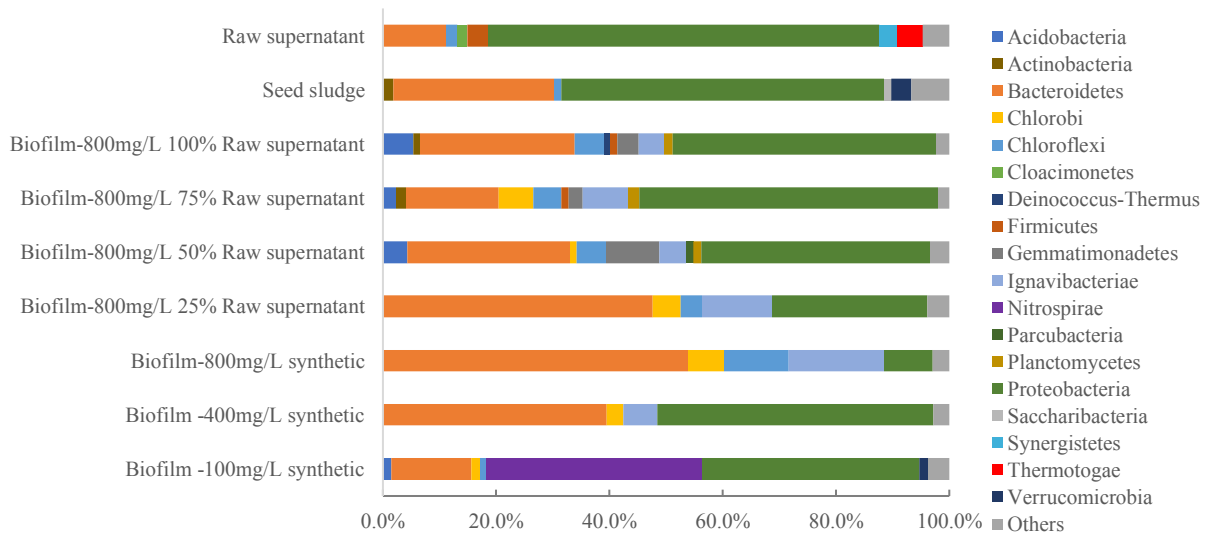
### 5.3.2. Reactor performance

The reactor was operated at around 21°C for about 800 days. Reactor performance in terms of influent and effluent NH<sub>4</sub><sup>+</sup>-N, effluent NO<sub>2</sub><sup>-</sup>-N, and effluent NO<sub>3</sub><sup>-</sup>-N concentrations is provided in the supplementary material (Appendix C Fig.C-7). The reactor achieved complete nitrification when the NH<sub>4</sub><sup>+</sup>-N concentration in the feed was 100 and 200 mg/L (Stage 1 and 2), where most of the ammonium (75 to 90%) was converted to nitrate (information available in supplementary material). The partial nitrification was achieved when the NH<sub>4</sub><sup>+</sup>-N concentration in the reactor feed reached 400 mg/L (information available in Appendix C Fig.C-7). Nitrite started to accumulate in the reactor at this time. Stage 3 (400 mg/L NH<sub>4</sub><sup>+</sup>-N feed condition) seemed to be the turning point from complete nitrification to partial nitrification. Partial nitrification was stable when the NH<sub>4</sub><sup>+</sup>-N concentration in the feed was higher than 400 mg/L (Stages 4 to 9).

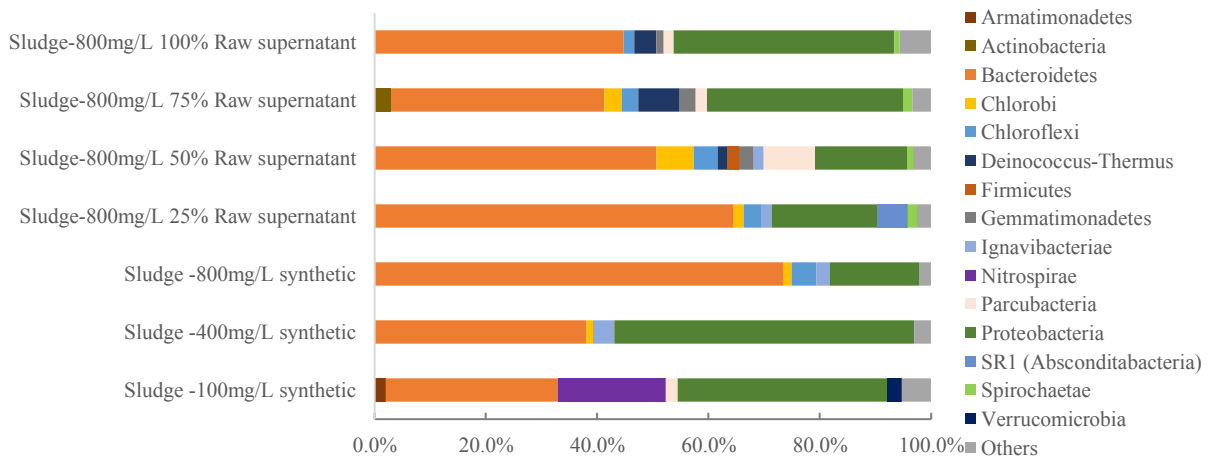
### 5.3.3. Microbial community composition analysis

#### 5.3.3.1. The taxonomic classification of sequencing data at the phylum level

According to the sequencing data, there were 6 major phyla having relative abundances greater than 1% in the seed sludge obtained from the aerobic section of a biological nutrient removal bioreactor (Figure 5.1a). *Proteobacteria* and *Bacteroidetes*, as the two dominant phyla, accounted for 57.0% and 28.4% of the total sequences in the seed sludge, respectively. These numbers were close to the numbers derived in previous studies (Huang et al., 2017). Other phyla included *Verrucomicrobia* (3.5%), *Actinobacteria* (1.8%), *Saccharibacteria* (1.4%) and *Chloroflexi* (1.3%). The number of major phyla increased to 9 when the reactor was fed with synthetic feed containing 100 mg/L  $\text{NH}_4^+\text{-N}$ . Comparing the suspended flocs and biofilm, *Nitrospirae* increased from 0.03% to 19% in the flocs (Figure 5.1b) and to 38% in the biofilm samples (Figure 5.1a). The *Proteobacteria* decreased to 37% in the flocs and to 38% in the biofilm, while the *Bacteroidetes* increased to 31% in the flocs, and decreased to 14% in the biofilm. The further increase of feed  $\text{NH}_4^+\text{-N}$  concentration had an impact on the microbial community structure. The *Bacteroidetes* increased to 73.3% in the floc and to 53.8% in the biofilm, as the feed  $\text{NH}_4^+\text{-N}$  concentration was increased to 800 mg/L. The increase of  $\text{NH}_4^+\text{-N}$  also led to an increase in the prevalence of *Chlorobi*, *Chloroflexi* and *Ignavibacteriae*. However, the increases of these three phyla were more pronounced in the biofilm than in the suspended flocs. *Nitrospirae* disappeared from the community in both flocs and biofilm as the  $\text{NH}_4^+\text{-N}$  concentration reached 400 mg/L. *Nitrospirae* was the dominant NOB detected in the reactor under low ammonium concentration condition. The disappearance of *Nitrospirae* confirmed that the nitrification process was successfully established when the influent ammonia concentration was greater than 400 mg/L. The abundance of *Proteobacteria* increased when the  $\text{NH}_4^+\text{-N}$  concentration increased from 100 to 400 mg/L, but decreased when the  $\text{NH}_4^+\text{-N}$  concentration further increased from 400 mg/L to 800 mg/L.



(a)



(b)

**Figure 5.1.** The relative abundance of sequences at phylum level in biofilm (a) and suspended flocs (b) of reactor 1. Phyla with relative abundance <1% are not shown in the figure.

The percentage of raw supernatant also affected the microbial community structure. The number of major phyla increased to 12 when the reactor started to be fed with raw supernatant. In general, the *Proteobacteria* and *Bacteroidetes* were still the two dominant phyla in the reactor. The higher the percentage of raw supernatant in the feed, the greater was the predominance of *Proteobacteria* and the smaller was the proportion of *Bacteroidetes* in the samples. The raw supernatant seemed

to have had a negative impact on the *Chlorobi* and *Ignavibacteriae*. In addition, no clear trend of *Chloroflex* and *Gemmatimonadetes* response was observed.

### 5.3.3.2 The diversity analysis

The diversity analysis (Table 5.3) demonstrated the impacts of  $\text{NH}_4^+\text{-N}$  concentration and the raw supernatant percentage on the diversity of communities. The higher the OTUs observed, more diverse the community is. The seed sludge from the plant possessed the highest diversity. A similar result was obtained previously (Huang et al., 2017), in which the seed sludge was more diverse than the samples collected from the reactor. The increasing  $\text{NH}_4^+\text{-N}$  concentration negatively affected the diversity (Table 5.3). The increasing percentage of raw supernatant in the feed had a positive impact on the community diversity (Table 5.3). As the reactor was fed with an increasing percentage of raw supernatant, the diversity of the community increased gradually, which may be attributed to the complex water chemistry in lagoon supernatant that enriches a diverse microbial population, and the introduction of lagoon supernatant indigenous microbes into the reactor. The alpha rarefaction plots of all the samples, which confirmed the diversity changes, are also available in the supplementary material (Appendix C Fig. C-8).

There was little difference between the flocs and biofilm communities when the reactor was fed with synthetic feed containing 100 mg/L or 400 mg/L  $\text{NH}_4^+\text{-N}$ . However, when the synthetic feed  $\text{NH}_4^+\text{-N}$  concentration reached 800 mg/L, the floc community became less diverse, while the biofilm community diversity remained relatively unchanged. This result might indicate that the biofilm could provide more protection to the organisms that resided in it from the environmental stresses (*i.e.* the high  $\text{NH}_4^+\text{-N}$  concentration), as compared to the flocs. When the reactor started to be fed with raw supernatant, both biofilm and suspended floc communities became more diverse when the supernatant percentage increased. Again, the biofilm communities were detected to be more diverse than the flocs communities.

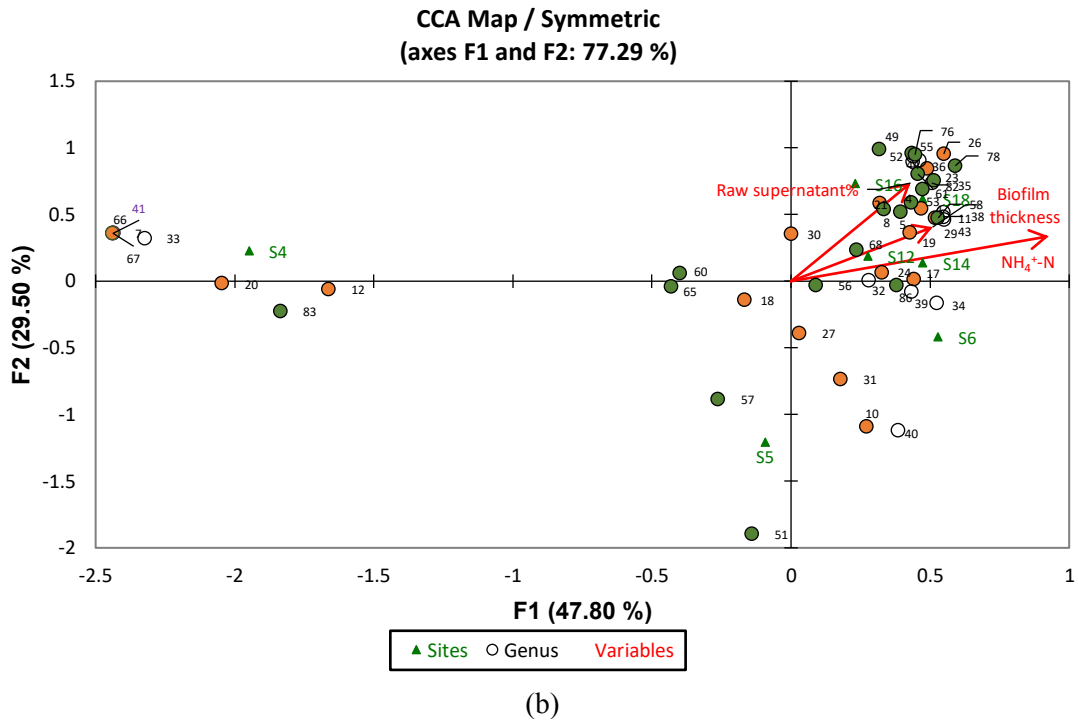
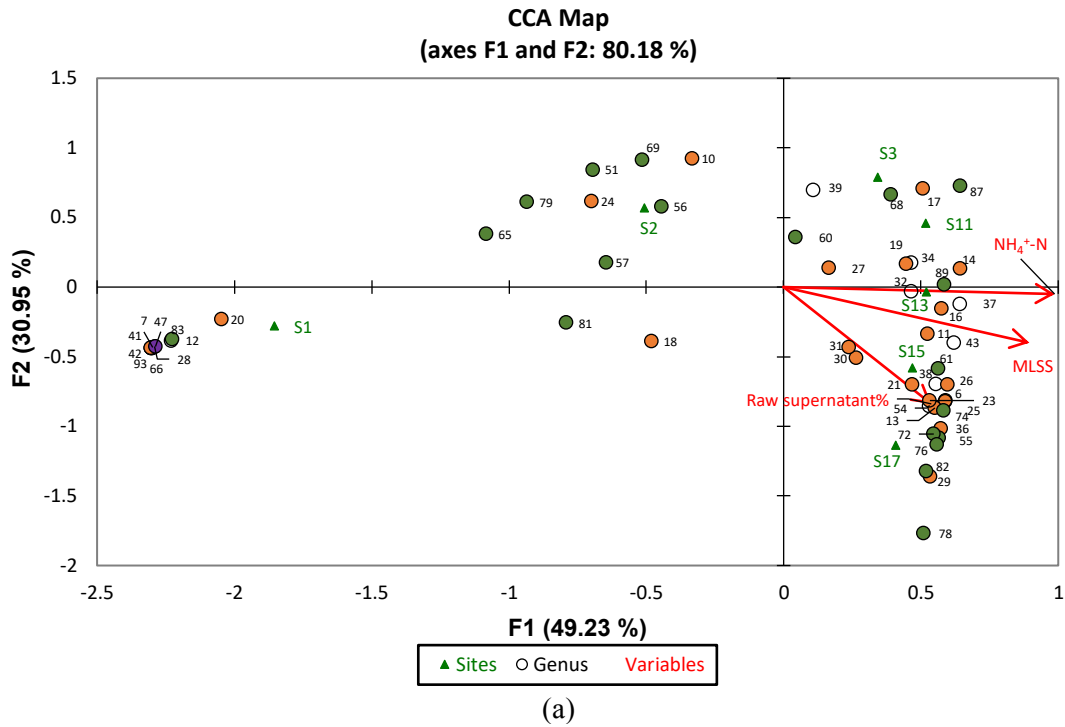
**Table 5.3. The diversity analysis of flocs and biofilm samples.**

Feed characteristics		Samples			
		Flocs		Biofilm	
NH <sub>4</sub> <sup>+</sup> -N concentration (mg/L)	Raw supernatant %	Effective sequences	OTU Observed	Effective sequences	OTU Observed
	100	0	50190	1702	15714
400	0	40415	819	15594	536
800	0	53723	466	26732	558
800	25	41167	666	34545	686
800	50	33046	1004	33246	1484
800	75	31218	1121	34198	1294
800	100	29762	1089	38049	1390
Other samples					
	AS-gold bar	16948	1628		
	Raw supernatant	16845	1015		

#### 5.3.3.3. The CCA analysis

Canonical correspondence analysis (CCA) is a powerful tool to elucidate the relationship between the environmental variables and the variance of a microbial community structure (ter Braak and Verdonschot, 1995). The environmental variables of interest in this study included the NH<sub>4</sub><sup>+</sup>-N concentration and the percentage of raw supernatant in the feed, biofilm thickness, and mixed liquor suspended solids (MLSS). Based on the CCA tri-plots, the directions of the vectors indicate the directions of positive correlations with the environmental variables. The length of an environmental variable's vector indicates the strength of the relationship between the variables and the microbial community structure (Wang et al., 2012). The origin of the tri-plot shows the mean of the environmental parameters (ter Braak and Verdonschot, 1995). The samples are shown in green in the tri-plots with IDs from S1 to S20. The numbers in the plots represent the centroids of the niche for different genera. The projection of a genus along an environmental vector indicates a weighted average of the environmental variable for the genus's niche. A sample identification table with corresponding sample descriptions is in the supplementary material (Appendix B Table B-4). Moreover, the triplot also reveals the correlation between the environmental variables: where the sharp, obtuse and right angles indicate a positive correlation, a negative correlation, and no

correlation between variables, respectively. The projection of one variable on another shows the strength of the correlation (ter Braak and Verdonschot, 1995).





**Figure 5.2.** Canonical correspondence analysis (CCA) analysis of Miseq sequencing data of flocs (a) and biofilm (b). The red vectors represent the environmental variables that affected the microbial community structure. The length of the vectors indicated the strength of the relationship between these variables and the community structure. The green triangles in the plot represent the samples. The circles represent the genus in the community. Genera in *Bacteroidetes* are colored with orange, and Genera in *Proteobacteria* are colored in green. Genera in the other phylum are not colored. Genera with relative abundance <1% were not shown in the plot.

Figure 5.2a is a tri-plot of the CCA analysis for all the flocs samples. Axis F1 explained 49.2% of the community variance, and F2 explained 31.0% of the variance. From Figure 5.2a, all the environmental variables, such as  $\text{NH}_4^+\text{-N}$  concentration, MLSS, and the raw supernatant percentage were strongly correlated to the variance of the community. Compared to the raw supernatant percentage, the  $\text{NH}_4^+\text{-N}$  concentration and the MLSS are the more influential environmental parameters that related to the community variance. The mean value of the environmental variable- $\text{NH}_4^+\text{-N}$  concentration in this tri-plot was ~640mg/L (at the origin of Figure 5.2a). Sample S1 was collected under 100 mg  $\text{NH}_4^+\text{-N}$  /L feed condition, which explained why the projection of the community along  $\text{NH}_4^+\text{-N}$  concentration vector did not appear on the positive side of the ammonium vector. Samples S2 contained community that collected under 400 mg  $\text{NH}_4^+\text{-N}$  /L feed condition. The projection of S2 along the ammonium vector was in an area with moderately low  $\text{NH}_4^+\text{-N}$  concentration. The rest of the communities were collected under high  $\text{NH}_4^+\text{-N}$  concentration conditions, explaining why they were located in regions toward the positive direction of  $\text{NH}_4^+\text{-N}$  concentration vector.

Regarding the location of a specific genus, 93 genera in total were detected for seed sludge, raw supernatant, flocs and biofilm samples (>1%). Detailed genus name and their associated kingdom,

phylum, class, order and family names can be found in the supplementary material (Appendix B Table B-5). The genera from the two dominant phyla (*Proteobacteria* and *Bacteroidetes*) are colored with green and orange, respectively. Genera from these two phyla were widely spread over all conditions, with the majority of the genera being present in the positive direction of the environmental vectors.

In the flocs, 54 genera of interest (accounting for >84% of community sequences) were selected for analysis. The projection of genera shown on the right side of the tri-plot, for example, *Arenimonas* (82), *BDI-7 clade* (76), *Truepera* (36), *Gemmatimonas* (38), *Flluvicola* (13), *Phaeodactylibacter* (26), the uncultured bacterium from *Parcubacteria* (43), the uncultured bacterium from *NS9 marine group* (17), the uncultured candidate division *SRI* bacterium (87), and *Comamonas* (54) along the  $\text{NH}_4^+$ -N concentration vector were the highest, which indicated that these genera dominated under high  $\text{NH}_4^+$ -N concentration. On the other side, the genera *Nitrospira* (41), the uncultured bacterium from *Cytophagaceae* (12), *Dokdonella* (83), and *Zoogloea* (66) presented in the low  $\text{NH}_4^+$ -N concentration condition. It was also interesting that the projection of *Nitrosomonas* (60) along  $\text{NH}_4^+$ -N concentration vector was close to the origin, indicating that the optimal  $\text{NH}_4^+$ -N concentration in the feed for *Nitrosomonas* dominance might be in that range (about 640 mg/L).

The second environmental variable of focus was the raw supernatant percentage. From the tri-plot, the raw supernatant percentage at the origin was around 36% (Figure 5.2a). Using this value as a reference point and the projection of the genera along the raw supernatant vector, it was clear that *Arenimonas* (82), *Pedobacter* (29) and *Halomonas* (78) had the highest tolerances towards raw supernatant in the feed, among all the genera. In addition, genera that also tolerated the high raw supernatant condition included *NS11-12 marine group* (23), *Ottowia* (55), and *BDI-7 clade* (76). While genera *Nitrospira* (41), the uncultured bacterium from *Cytophagaceae* (12), *Dokdonella* (83), *Zoogloea* (66), *Thauera* (65), *Chryseolinea* (51) and other genera nearby were eliminated under raw supernatant conditions.

It was also interesting that genera *Arenimonas* (82), *Halomonas* (78), *BDI-7 clade* (76), *Truepera* (36), *Fluviicola* (13), the uncultured bacterium from *Parcubacteria* (43), *Phaeodactylibacter* (26), *Comamonas* (54), and *Gemmatimonas* (38) were associated with a condition of high MLSS. Most of these genera could either tolerate high  $\text{NH}_4^+$ -N concentration or high raw supernatant percentage in the feed. It was reported that most of these genera could survive under stressful conditions, including high temperature, halophilic, or alkaline conditions (e.g. *Truepera*, *Halomonas*) (Balderrama-Subieta and Quillaguamán, 2013; Milici et al., 2017). Conversely, those genera that could not tolerate under high  $\text{NH}_4^+$ -N concentration and raw supernatant only dominated under low MLSS conditions. This phenomenon could be explained by the positive correlation between the MLSS and  $\text{NH}_4^+$ -N concentration.

Figure 5.2b illustrated the CCA analysis for all the biofilm samples. Axis F1 explained 47.8% of the community variance, and axis F2 explained 29.5% of the variance. For biofilm samples, the biofilm thickness, instead of MLSS, was chosen as the third environmental variable. The biofilm thickness vector was positively correlated to the  $\text{NH}_4^+$ -N concentration vector. The higher the  $\text{NH}_4^+$ -N concentration, the thicker the biofilm in the reactor. As was the case for the tri-plots for the suspended flocs, this tri-plot for biofilm also reveals that  $\text{NH}_4^+$ -N concentration was the most influential environmental parameter on the variance of the microbial community. 50 genera were selected for the plot in Figure 5.2b. They encompassed more than 80% of the sequences in all biofilm samples.

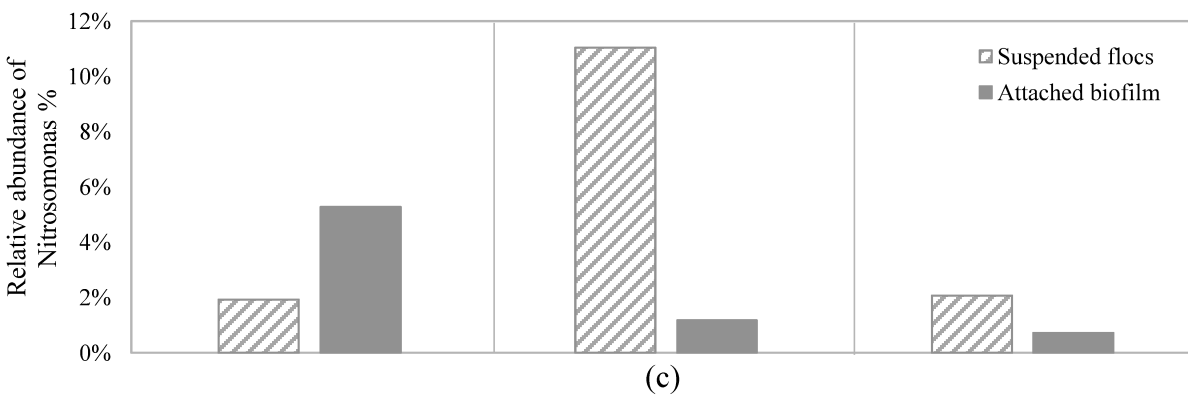
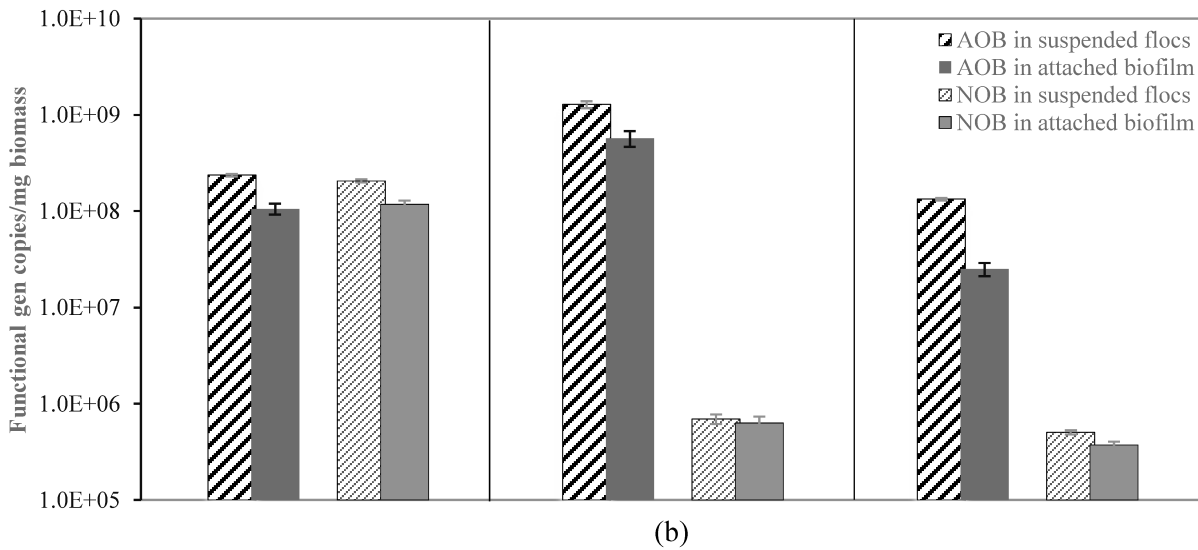
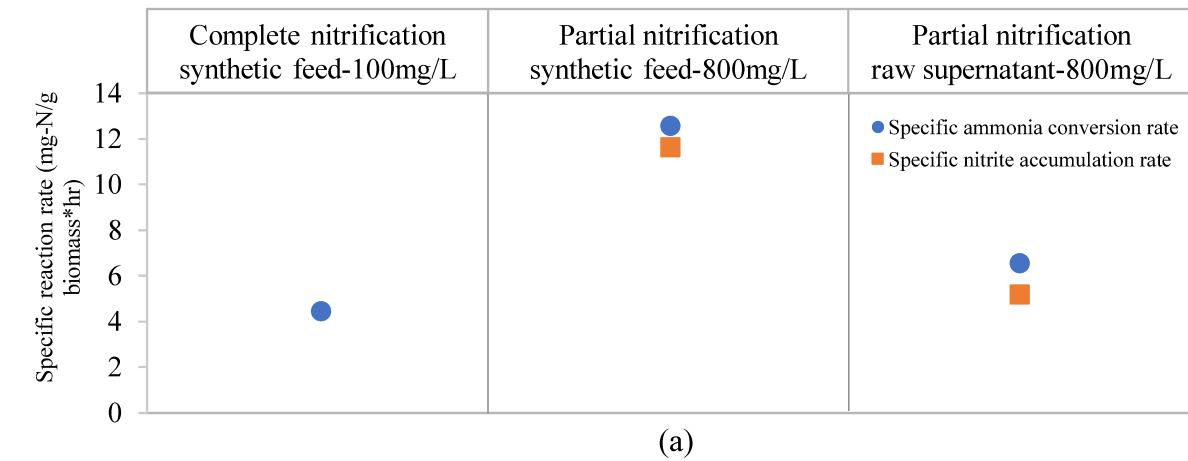
In both Figures 5.2a and 5.2b, more genera were found associated with the high  $\text{NH}_4^+$ -N concentration and high raw supernatant conditions. High ammonium tolerating genera, for example, *Fluviicola* (13), which was found in the floc samples, was excluded from the tri-plot for biofilm. Similarly, some genera that were excluded from the tri-plot for the flocs, were included in the biofilm tri-plot (e.g. *Genus in Chloroflexi* (35) and *Amaricoccus* (49)). The results underlined that under different environmental conditions, the difference in microbial aggregate properties selected different microbial communities. In the IFAS system, the diffusion resistance in biofilm was higher

than that in flocs (Pérez et al., 2005; Shao et al., 2017; Zhou et al., 2012). The differences in diffusion resistance between the biofilm and suspended flocs might contribute to the microbial population difference in these two aggregates.

#### 5.3.4. The impact of feed characteristics on nitrogen removal kinetics and the microbial community structure

The specific ammonium conversion rate increased from 4.5 to 12.6 mg NH<sub>4</sub><sup>+</sup>-N/g biomass·hr when the NH<sub>4</sub><sup>+</sup>-N concentration in the synthetic feed increased from 100 to 800 mg/L. This revealed that the ammonium conversion rate was positively related to the NH<sub>4</sub><sup>+</sup>-N concentration in the feed. In addition, there was no nitrite accumulation when the feed contained 100 mg/L NH<sub>4</sub><sup>+</sup>-N, as partial nitrification was not achieved under this condition. Further, the specific ammonium conversion rates decreased from 12.6 mg NH<sub>4</sub><sup>+</sup>-N/g biomass·hr to 6.6 mg NH<sub>4</sub><sup>+</sup>-N/g biomass·hr when feed water was changed from 100% synthetic feed to 100% raw supernatant.

Figure 5.3a and b demonstrated that there was a positive correlation between the specific ammonium conversion rate and the AOB functional gene copies/mg biomass in the reactor (correlation coefficient R=0.93 and 0.91 for flocs and biofilm, respectively). The AOB functional gene copies/mg biomass in the reactor increased with the increase of the ammonium concentration in the feed. Changing the feed from synthetic to raw supernatant led to a decrease of the AOB functional gene copies in both the flocs and biofilm. These functional genes results confirm the inhibitory effect of raw supernatant on the partial nitrification. The NOB functional gene copies/mg biomass decreased with the increase of NH<sub>4</sub><sup>+</sup>-N concentration and the increase of the raw supernatant in the feed, indicating the inhibitory effect of high NH<sub>4</sub><sup>+</sup>-N concentration and raw supernatant on the NOB.



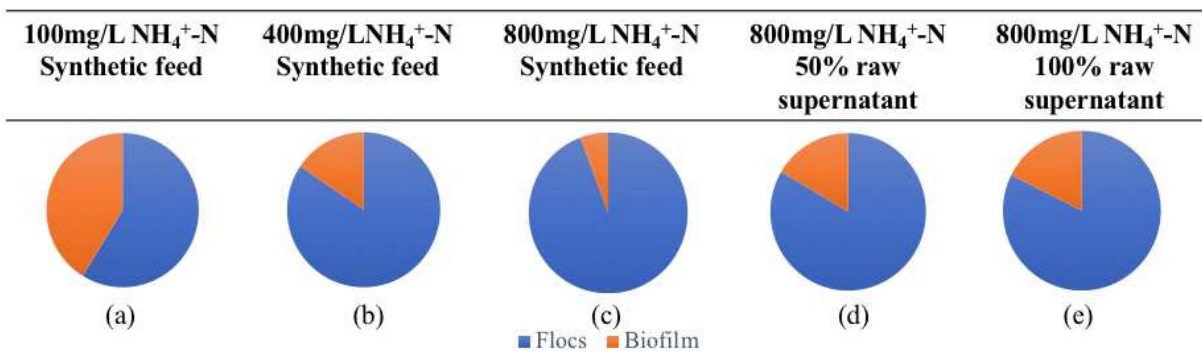
**Figure 5.3.** (a) The change of specific ammonia conversion and nitrite accumulation rate during three different stages: complete nitrification (stage 1), partial nitrification (stage 5), and partial

nitrification when the feed was raw supernatant (stage 9). (b) The AOB and NOB functional genes copies/ mg biomass in both suspended flocs and attached biofilm during these three stages measured by qPCR. (c) The relative abundance of *Nitrosomonas* in % in both flocs and biofilm samples measured by MiSeq analysis.

Figure 5.3c shows the relative abundance of *Nitrosomonas* spp. in the flocs and biofilm communities under different conditions. The *Nitrosomonas* spp. was the dominant AOB detected in the reactor. Under the complete nitrification condition, the proportion of AOB in the biofilm was higher than that in the flocs. These results are similar to reported studies (Onnis-Hayden et al., 2011; Shao et al., 2017). Once the partial nitrification was established under the high ammonium strength condition, the proportion of AOB in the suspended flocs community became higher than that in the biofilm community, which might be attributed to the higher biofilm community diversity that may have been promoted by the greater biofilm thickness and high diffusion limitation in biofilms under high ammonium feed conditions. However, after the feed water was changed to the raw supernatant, the relative abundance of AOB decreased in both flocs and biofilm communities as their community diversities increased. Together with the fact that more diverse community was observed in the reactor when the feed was switched to raw supernatant, the decrease of AOB might be attributed to the inhibition by contaminants in the raw supernatant, and/or the enrichment of other microorganisms.

#### 5.3.5. The comparison of AOB in the flocs and biofilm

To further investigate the microbial population dynamics in the IFAS system, the distribution of AOB functional genes in the flocs and biofilm under different conditions were compared. As shown in Figure 5.4, the flocs contained the majority of the AOB functional genes under all conditions, emphasizing again the importance of the flocs in the IFAS system. It was also observed that the percentage of AOB functional genes in the biofilm increased with the increasing raw supernatant percentage.



**Figure 5. 4.** The distribution of AOB functional genes in the flocs and the biofilm under various feed conditions.

#### 5.4. Conclusions

Partial nitrification was successfully achieved in the reactor when the NH<sub>4</sub><sup>+</sup>-N concentration reached 400 mg/L. The inhibition of *Nitrospira* spp. (the dominant NOB) under such condition confirmed the success of partial nitrification. For both flocs and biofilm in an IFAS reactor, the NH<sub>4</sub><sup>+</sup>-N concentration was the most important environmental variable affecting their community compositions. The ammonium concentration negatively affected the diversity of the microbial community in both biofilm and flocs, while the raw supernatant percentage positively correlated to the diversity of the communities. Besides, the microbial community structure in the suspended flocs differed from that in the biofilm. Different genus of bacteria had different tolerance towards the NH<sub>4</sub><sup>+</sup>-N concentration and the percentage of raw supernatant. The ammonium concentration was positively related to the specific ammonium conversion rate as well as the quantity of AOB functional genes/mg biomass in the reactor; while the raw supernatant percentage was negatively related to the kinetics and quantity of AOB/mg biomass. In the IFAS system, the floc was playing a major role for the partial nitrification, but it was less resistant than the biofilm when raw supernatant was introduced as the feed. The information included in this paper can provide

guidance to better understand the dynamics of the microbial communities under different operational conditions.

## 5.5.References

- Ahn, J.H., Kwan, T., Chandran, K., 2011. Comparison of Partial and Full Nitrification Processes Applied for Treating High-Strength Nitrogen Wastewaters: Microbial Ecology through Nitrous Oxide Production. *Environ. Sci. Technol.* 45, 2734–2740. <https://doi.org/10.1021/es103534g>
- Anthonisen, A.C., Loehr, R.C., Prakasam, T.B.S., Srinath, E.G., 1976. Inhibition of Nitrification by Ammonia and Nitrous Acid. *J. Water Pollut. Control Fed.* 48, 835–852.
- APHA, 2011. Standard Methods for the Examination of Water and Wastewater. American Public Health Association, Washington, DC.
- Aslan, S., Dahab, M., 2008. Nitritation and denitritation of ammonium-rich wastewater using fluidized-bed biofilm reactors. *J. Hazard. Mater.* 156, 56–63. <https://doi.org/10.1016/j.jhazmat.2007.11.112>
- Balderrama-Subieta, A., Quillaguamán, J., 2013. Genomic studies on nitrogen metabolism in *Halomonas boliviensis*: Metabolic pathway, biochemistry and evolution. *Comput. Biol. Chem.* 47, 96–104. <https://doi.org/10.1016/j.compbiolchem.2013.08.002>
- Caporaso, J.G., Kuczynski, J., Stombaugh, J., Bittinger, K., Bushman, F.D., Costello, E.K., Fierer, N., Peña, A.G., Goodrich, J.K., Gordon, J.I., Huttley, G.A., Kelley, S.T., Knights, D., Koenig, J.E., Ley, R.E., Lozupone, C.A., McDonald, D., Muegge, B.D., Pirrung, M., Reeder, J., Sevinsky, J.R., Turnbaugh, P.J., Walters, W.A., Widmann, J., Yatsunenko, T., Zaneveld, J., Knight, R., 2010. QIIME allows analysis of high-throughput community sequencing data. *Nat. Methods* 7, 335–336. <https://doi.org/10.1038/nmeth.f.303>
- Cho, S., Fujii, N., Lee, T., Okabe, S., 2011. Development of a simultaneous partial nitrification and anaerobic ammonia oxidation process in a single reactor. *Bioresour. Technol.* 102, 652–659. <https://doi.org/10.1016/j.biortech.2010.08.031>



- Gong, Z., Liu, S., Yang, F., Bao, H., Furukawa, K., 2008. Characterization of functional microbial community in a membrane-aerated biofilm reactor operated for completely autotrophic nitrogen removal. *Bioresour. Technol.* 99, 2749–2756. <https://doi.org/10.1016/j.biortech.2007.06.040>
- Guo, J., Peng, Y., Huang, H., Wang, S., Ge, S., Zhang, J., Wang, Z., 2010. Short- and long-term effects of temperature on partial nitrification in a sequencing batch reactor treating domestic wastewater. *J. Hazard. Mater.* 179, 471–479. <https://doi.org/10.1016/j.jhazmat.2010.03.027>
- Guo, J., Peng, Y., Wang, S., Zheng, Y., Huang, H., Wang, Z., 2009. Long-term effect of dissolved oxygen on partial nitrification performance and microbial community structure. *Bioresour. Technol.* 100, 2796–2802. <https://doi.org/10.1016/j.biortech.2008.12.036>
- Guo, J.H., Peng, Y.Z., Wang, S.Y., Zheng, Y.N., Huang, H.J., Ge, S.J., 2009. Effective and robust partial nitrification to nitrite by real-time aeration duration control in an SBR treating domestic wastewater. *Process Biochem.* 44, 979–985. <https://doi.org/10.1016/j.procbio.2009.04.022>
- Hellinga, C., Schellen, A., Mulder, J., Vanloosdrecht, M., Heijnen, J., 1998. The sharon process: An innovative method for nitrogen removal from ammonium-rich waste water. *Water Sci. Technol.* 37, 135–142. [https://doi.org/10.1016/S0273-1223\(98\)00281-9](https://doi.org/10.1016/S0273-1223(98)00281-9)
- Huang, C., Shi, Y., Sheng, Z., Gamal El-Din, M., Liu, Y., 2017. Characterization of microbial communities during start-up of integrated fixed-film activated sludge (IFAS) systems for the treatment of oil sands process-affected water (OSPW). *Biochem. Eng. J.* 122, 123–132. <https://doi.org/10.1016/j.bej.2017.03.003>
- Kapoor, V., Li, X., Elk, M., Chandran, K., Impellitteri, C.A., Santo Domingo, J.W., 2015. Impact of Heavy Metals on Transcriptional and Physiological Activity of Nitrifying Bacteria. *Environ. Sci. Technol.* 49, 13454–13462. <https://doi.org/10.1021/acs.est.5b02748>

- Kulikowska, D., Bernat, K., 2013. Nitritation–denitritation in landfill leachate with glycerine as a carbon source. *Bioresour. Technol.* 142, 297–303. <https://doi.org/10.1016/j.biortech.2013.04.119>
- Lee, Y.-W., Ong, S.-K., Sato, C., 1997. Effects of heavy metals on nitrifying bacteria. *Water Sci. Technol.* 36. [https://doi.org/10.1016/S0273-1223\(97\)00730-0](https://doi.org/10.1016/S0273-1223(97)00730-0)
- Liu, T., Mao, Y., Shi, Y., Quan, X., 2017. Start-up and bacterial community compositions of partial nitrification in moving bed biofilm reactor. *Appl. Microbiol. Biotechnol.* 101, 2563–2574. <https://doi.org/10.1007/s00253-016-8003-9>
- Milici, M., Vital, M., Tomasch, J., Badewien, T.H., Giebel, H.-A., Plumeier, I., Wang, H., Pieper, D.H., Wagner-Döbler, I., Simon, M., 2017. Diversity and community composition of particle-associated and free-living bacteria in mesopelagic and bathypelagic Southern Ocean water masses: Evidence of dispersal limitation in the Bransfield Strait: Bacteria in the deep Southern Ocean. *Limnol. Oceanogr.* 62, 1080–1095. <https://doi.org/10.1002/lno.10487>
- Onnis-Hayden, A., Majed, N., Schramm, A., Gu, A.Z., 2011. Process optimization by decoupled control of key microbial populations: Distribution of activity and abundance of polyphosphate-accumulating organisms and nitrifying populations in a full-scale IFAS-EBPR plant. *Water Res.* 45, 3845–3854. <https://doi.org/10.1016/j.watres.2011.04.039>
- Peng, Y., Zhu, G., 2006. Biological nitrogen removal with nitrification and denitrification via nitrite pathway. *Appl. Microbiol. Biotechnol.* 73, 15–26. <https://doi.org/10.1007/s00253-006-0534-z>
- Pérez, J., Picioreanu, C., van Loosdrecht, M., 2005. Modeling biofilm and floc diffusion processes based on analytical solution of reaction-diffusion equations. *Water Res.* 39, 1311–1323. <https://doi.org/10.1016/j.watres.2004.12.020>
- Rodriguez-Caballero, A., Ribera, A., Balcázar, J.L., Pijuan, M., 2013. Nitritation versus full nitrification of ammonium-rich wastewater: Comparison in terms of nitrous and nitric

- oxides emissions. *Bioresour. Technol.* 139, 195–202.  
<https://doi.org/10.1016/j.biortech.2013.04.021>
- Shao, Y., Shi, Y., Mohammed, A., Liu, Y., 2017. Wastewater ammonia removal using an integrated fixed-film activated sludge-sequencing batch biofilm reactor (IFAS-SBR): Comparison of suspended flocs and attached biofilm. *Int. Biodeterior. Biodegrad.* 116, 38–47.  
<https://doi.org/10.1016/j.ibiod.2016.09.026>
- Sinha, B., Annachhatre, A.P., 2007. Partial nitrification—operational parameters and microorganisms involved. *Rev. Environ. Sci. Biotechnol.* 6, 285–313.  
<https://doi.org/10.1007/s11157-006-9116-x>
- Sun, N., Ge, C., Ahmad, H.A., Gao, B., Ni, S.-Q., 2017. Realization of microbial community stratification for single-stage nitrogen removal in a sequencing batch biofilter granular reactor. *Bioresour. Technol.* 241, 681–691. <https://doi.org/10.1016/j.biortech.2017.05.203>
- ter Braak, C.J.F., Verdonschot, P.F.M., 1995. Canonical correspondence analysis and related multivariate methods in aquatic ecology. *Aquat. Sci.* 57, 255–289.  
<https://doi.org/10.1007/BF00877430>
- U.S.Environmental Protection Agency, 1987. Assessment Of Needed Publicly Owned Wastewater Treatment Facilities In The United States, 1986 Needs Survey Report To Congress.
- Wang, X., Hu, M., Xia, Y., Wen, X., Ding, K., 2012. Pyrosequencing Analysis of Bacterial Diversity in 14 Wastewater Treatment Systems in China. *Appl. Environ. Microbiol.* 78, 7042–7047. <https://doi.org/10.1128/AEM.01617-12>
- Yang, Q., Peng, Y., Liu, X., Zeng, W., Mino, T., Satoh, H., 2007. Nitrogen Removal via Nitrite from Municipal Wastewater at Low Temperatures using Real-Time Control to Optimize Nitrifying Communities. *Environ. Sci. Technol.* 41, 8159–8164.  
<https://doi.org/10.1021/es070850f>

- Ye, F., Peng, G., Li, Y., 2011. Influences of influent carbon source on extracellular polymeric substances (EPS) and physicochemical properties of activated sludge. *Chemosphere* 84, 1250–1255. <https://doi.org/10.1016/j.chemosphere.2011.05.004>
- Ye, L., Shao, M.-F., Zhang, T., Tong, A.H.Y., Lok, S., 2011. Analysis of the bacterial community in a laboratory-scale nitrification reactor and a wastewater treatment plant by 454-pyrosequencing. *Water Res.* 45, 4390–4398. <https://doi.org/10.1016/j.watres.2011.05.028>
- Zhang, Y., 2009. Stability of Partial Nitrification and Microbial Population Dynamics in a Bioaugmented Membrane Bioreactor. *J. Microbiol. Biotechnol.* 19, 1656–1664. <https://doi.org/10.4014/jmb.0906.06006>
- Zhou, X.-H., Liu, J., Song, H.-M., Qiu, Y.-Q., Shi, H.-C., 2012. Estimation of Heterotrophic Biokinetic Parameters in Wastewater Biofilms from Oxygen Concentration Profiles by Microelectrode. *Environ. Eng. Sci.* 29, 466–471. <https://doi.org/10.1089/ees.2010.0456>

## CHAPTER 6. COMPARISON OF MICROBIAL COMMUNITY AND EXTRACELLULAR POLYMERIC SUBSTANCE (EPS) IN NITRIFICATION AND NITRITATION BIOREACTORS

### 6.1. Introduction

Compared to conventional nitrification, partial nitrification, also known as nitritation, is an energy saving process to treat the high ammonium content in wastewater. Nitritation utilizes ammonia oxidizing bacteria (AOB) to convert ammonia to nitrite and eliminates the growth of nitrite oxidizing bacteria (NOB) in the bioreactors; the deficiency of NOB prevents the further oxidation of nitrite to nitrate, limiting the need for additional oxygen consumption. The nitrification process is easily achievable under low ammonia loading conditions, while the nitritation process is achievable under high ammonia loading conditions. Extracellular polymeric substances (EPS) secreted by bacterial cells are critical for cell aggregation, flocculation, biofilm development, cell adhesion and biosorption (Flemming et al., 2007; Sheng et al., 2010), but can also cause viscous bulking and biofouling in bioreactors. EPS can be classified into two major structural groups: soluble EPS and bound EPS. Surface bound EPS comprises two layers: loosely bound (LB-EPS) and tightly bound (TB-EPS). TB-EPS envelops the bacterial cell, while LB-EPS covers the TB-EPS, forming an outer layer (Liang et al., 2010). It has been reported that microbial EPS are composed of polysaccharides, protein, humic acids and some DNA. Although, polysaccharides and protein predominate, the reported percentage of each component differs depending on the source of biomass and the extraction method (Frølund et al., 1996; Sheng et al., 2010). It has been reported that organisms vary in their capacity to secrete EPS (Stehr et al., 1995; McIlroy et al., 2015). In general, it is believed that heterotrophic bacteria secrete more EPS than autotrophic bacteria (Tsuneda et al., 2001). Moreover, the abundance of specific organisms also has been related to the composition of EPS. Liang et al. (2010) observed an increased protein/polysaccharide ratio in EPS samples drawn from a nitrifying sludge as its AOB population increased. For studies using

integrated fixed film activated sludge (IFAS) bioreactors, van den Akker et al. (2010) reported that higher AOB abundance was positively related to low polysaccharide content in IFAS suspended flocs. They also detected equal amounts of AOB in the suspended flocs and biofilm. However, the comparison between the EPS from the flocs and from the biofilm was not reported in their study. A different AOB abundance analysis result was reported by Shao et al. (2017). A higher amount of AOB was observed in the biofilm than in suspended flocs of an IFAS treating low ammonium strength wastewater. A lower polysaccharides/protein ratio in the suspended flocs EPS than in the biofilm EPS was also observed in the study. Meanwhile Zhang et al. (2014) reported a in-depth comparison of compositions and functions of EPS from different sources of biomass, but the microbial community analysis was not mentioned. At present, the characteristics of the EPS from nitrification and nitritation integrated fixed-film activated sludge-sequencing batch reactors have not been compared. In depth studies are also required to explore the relationship between EPS characteristics and the microbial structure.

Further, the composition of EPS is related to its function. In the suspended flocs, EPS controls sludge flocculation. It has been reported that flocs having EPS with higher polysaccharides content is more vulnerable to viscous bulking than the flocs containing EPS with lower polysaccharides content (Shin et al., 2001; van den Akker et al., 2010). Other researchers found that the removal of surface protein led to the de-flocculation of microbial aggregates (Higgins and Novak, 1997). The matrix formed by EPS in a biofilm has been referred to metaphorically as “the house of biofilm cells”, emphasizing the importance of EPS to biofilm development (Flemming et al., 2007). In the field of biofilm technology, researchers also point out the importance of biofilm EPS on cell adhesion to a solid surface (Hwang et al., 2013, 2012), and have correlated higher EPS polysaccharides content to a stronger adhesion of bacterial cells to a solid surface (Sweity et al., 2011). However, the stability of nitritation biofilm and its relationship with the EPS composition has not yet been investigated. This relationship might be important for evaluating the stability of biofilm reactors.

In this study, we tested the hypothesis that the differences in the microbial community structure determine the differences in the characteristics of EPS. Moreover, the microbial community and EPS components from different bacterial aggregates (suspended flocs and attached biofilm) were also compared to elucidate the impacts of microbial aggregates' forms on the microbial community structure and EPS characteristics under the both nitrification and nitritation dominant conditions. The impact of EPS composition on their capacity to adhere to a solid surface was also analyzed using Quartz crystal microbalance with dissipation (QCM-D).

## **6.2. Methods and materials**

### **6.2.1. Reactor operation and DNA extraction**

This study employed an integrated fixed-film activated sludge sequencing batch reactor. The reactor had an effective volume of 6 L. It was fed with synthetic wastewater with increasing ammonium loadings, which was achieved by increasing the ammonium concentration in the reactor feed (from 100 mg N/L to 800 mg N/L). The detailed feeding strategy is available in Shao et al. (2018). The COD concentration was held constant at 200 mg/L. The COD source was sodium acetate. EPS samples were extracted when the ammonium nitrogen in the feed was 100 and 800 mg/L. The reactor achieved complete nitrification and stable nitritation under these two conditions, respectively. DNA samples were extracted using MO BIO PowerSoil® DNA Isolation Kits (MoBio Laboratories Inc., Carlsbad, California). Total bacteria, AOB, and NOB gene abundances were analysed with quantitative polymerase chain reaction (qPCR) (Bio-Rad Laboratories (Canada) Ltd., Mississauga, Ontario). The primers information, targeting genes and the qPCR cycles configuration are available in Shao et al. (2017) and are also included in the supplementary material (Appendix B Table B-2).

### 6.2.2. Extracellular polymeric substance extraction

The extraction methods for different components of EPS were based on the methods reported by Liang et al. (2010) with modifications. 10 mL samples of the suspended flocs or biofilm were centrifuged at 2000 g for 15 min at 4 °C. The supernatant was filtered through a 0.2 µm nylon filter and recovered as soluble EPS. The pellet was re-suspended in Milli-Q water to a total volume of 10 mL. Then, 0.04 mL of 36.5% formaldehyde was added to the 10 mL mixture. Formaldehyde was used to prevent cell lysis. Samples were then stored at 4 °C for 1 hr before being centrifuged again at 5000 g for 15 min at 4 °C. After centrifugation, the supernatant was filtered through a 0.2 µm nylon filter and recovered as loosely bound EPS. The pellet was re-suspended in Milli-Q water to a total volume of 10 mL. 4 mL of 1N NaOH was added to each sample and the sample was stored at 4 °C for 3 hr. Samples were centrifuged at 6000 g for 15 min at 4 °C. 6000 g, instead of 10000 g (Liang et al., 2010), was chosen to prevent the lysis of cells. The supernatant was filtered and recovered as tightly bounded EPS. After extraction, EPS samples were purified in a dialysis membrane (3.4 kD) for 24 hr before further analysis. Polysaccharide and protein contents in the EPS were determined by colorimetric analyses (DuBois et al. 1956, Bradford 1976). The composition of functional groups in EPS samples was studied and compared using X-ray photoelectron spectroscopy (XPS), and three-dimensional excitation and emission matrix (3D-EEM) fluorescence. QCM-D was used to investigate the interactions of EPS and EPS surrogates with a sensor surface. Detailed procedures are included in the following sections.

### 6.2.3. X-ray photoelectron spectroscopy (XPS) analysis

All extracted loosely bounded and tightly bounded EPS samples were dry-coated on pre-cleaned copper surface and then analysed by XPS (Kratos AXIS Ultra). XPS data were analysed using CasaXPS software. Classification of the components of C1s peaks is based on the methods proposed by Rouxhet et al. (1994). Briefly, the peak that fixed at 284.8eV (C-(C, H) bond) refers



to the hydrocarbon-like substance. Components at  $286.3 \pm 0.1$  eV (C-(O, N) bond) include alcohol, ether, amide and amine substance. A component at  $288.0 \pm 0.1$  eV (C=O) includes hemiacetal, acetal, amide carboxylate and carbonyl material. The carboxyl bond O=C-OH corresponds to a weak component or shoulder near 289.0 eV. Bar charts for all the EPS samples were generated based on the percentage of each components with corresponding functional groups.

#### 6.2.4. Three-dimensional excitation and emission matrix fluorescence analysis

The dissolved organic material in the purified EPS samples was analysed using excitation-emission matrix (EEM) fluorescence spectroscopy. The scanning wavelength range was from 280 to 500 nm for the emission and was from 200 to 400 nm for the excitation. The EEM data were further analysed using the fluorescence regional integration, a quantitative integration technique adapted from Chen et al. (2003). Briefly, the EEM was separated into 5 different regions according the emission and excitation values: Region I & II are aromatic protein-like material; Region III is fulvic acid-like material; Region IV is soluble microbial by-product-like substances, for example, the tryptophan protein-like substances (Dong et al., 2017); and Region V corresponds to humic acid-like substances.

#### 6.2.5. Quartz crystal microbalance with dissipation analysis

A QCM-D E4 (Q-Sense AB, Gothenburg, SWEDEN) was employed to delineate the adsorption of EPS and EPS surrogates to solid surface. Briefly, the change in frequency ( $\Delta f$ ) correlated to the mass absorbed to the sensor area, according to Sauerbrey relation:  $\Delta m = -C\Delta f/n$ .  $\Delta m$  is the absorbed mass, C is the mass sensitivity constant ( $C=17.7 \text{ ng Hz}^{-1} \text{ cm}^{-2}$  for 5 MHz quartz crystal), and n is the overtone number. All EPS samples were diluted in 10 mM NaCl buffer solution to make sure that the total organic carbon (TOC) concentration for all samples was approximately 20

ppm. We tested the EPS adhesion to the gold coated crystal sensors, which were further coated with polystyrene. Before being mounted to the QCM-D E4 chambers, the crystal sensors were soaked in 1% Deconex solution (Borer Chemie AG, Switzerland), and then rinsed with 99% Milli-Q water and soaked in Milli-Q water for at least 2 hours. After, the sensors were rinsed with 99% ethanol and dried with nitrogen gas. Liquid media were pumped through the E4 chambers (flowrate=150  $\mu$ L/min) in following order: Milli-Q water, 10mM NaCl buffer solution, EPS samples in buffer, 10 mM NaCl buffer solution, and then Milli-Q water. The pumping of each medium lasted for around 20 minutes. The fundamental frequency was set as the default value: 4.95 MHz. The frequency and dissipation shifts of the 3<sup>rd</sup> overtone were chosen for further analysis. To further investigate the functions of different EPS components in adsorption to solid surface (protein and carbohydrates), bovine serum albumin (BSA) and glucose were chosen as the surrogates for protein and carbohydrates components of EPS, respectively. Both the surrogates and the EPS samples have negative zeta potentials in 10 mM NaCl solution (Appendix B Table B-6). These two surrogates were also used as standards for the colorimetric methods in Section 2.2. Five QCM-D trials were conducted using these two surrogates to reveal the functions of the components. These trials included the following ratios: (1) Glucose only; (2) Glucose:BSA ratio of 3:1 ( $TOC_{Glucose}: TOC_{BSA}$ ); (3) Glucose:BSA ratio of 1:1; (4) Glucose:BSA ratio of 1:3; and (5) BSA only. The TOC concentration of all trial samples was 20 mg/L. All QCM-D data were analysed and modelled using QTools software and EXCEL.

#### 6.2.6. Statistical analysis

Statistical analyses were performed using t-test and single factor analysis of variance (ANOVA) at 5% probability level with Microsoft Excel® software and reported as p-values. A p-value smaller than 0.05 represents a statistically significant difference.

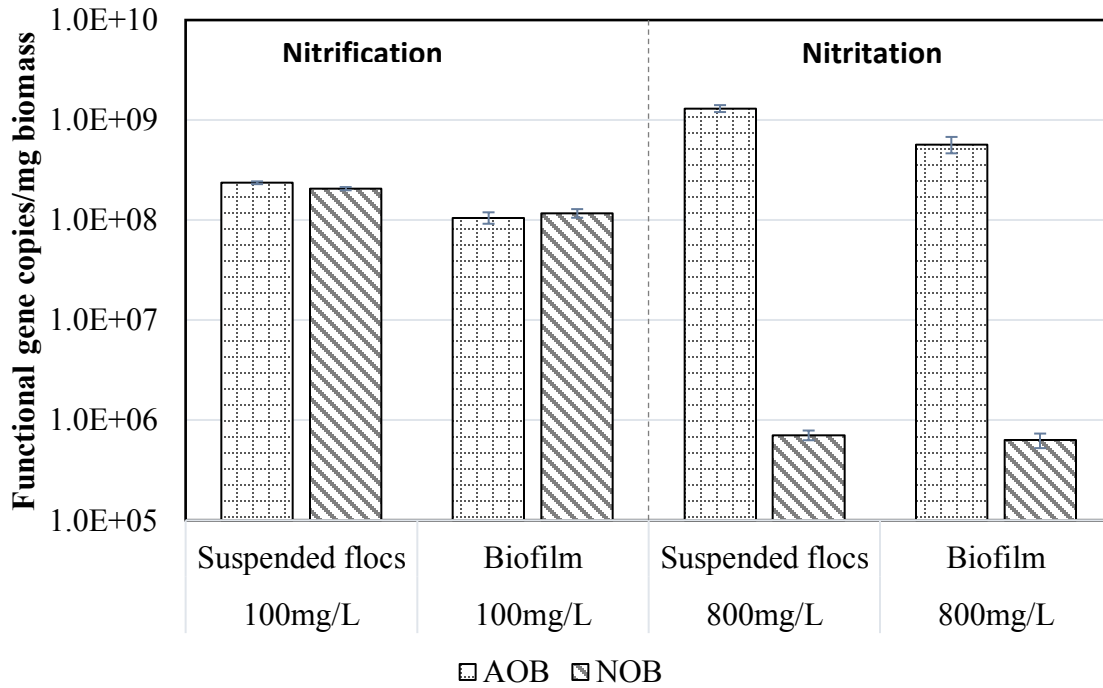
## 6.3. Results and discussions

### 6.3.1. Reactor performance

The reactor performance under the various operating conditions is shown in Figure C-1 (Appendix C). Between 75% and 90% of the feed  $\text{NH}_4^+\text{-N}$  was converted to  $\text{NO}_3^-\text{-N}$  during the 100 mg/L  $\text{NH}_4^+\text{-N}$  feed condition, indicating that essentially complete nitrification was achieved. When the  $\text{NH}_4^+\text{-N}$  in the feed was increased to 800 mg/L, the nitrification process became the dominant process in the reactor. At 800 mg/L  $\text{NH}_4^+\text{-N}$  feed condition, 94% of the  $\text{NH}_4^+\text{-N}$  was converted to  $\text{NO}_2^-\text{-N}$ , instead of  $\text{NO}_3^-\text{-N}$ , indicating that successful nitritation was achieved in the reactor. To simplify our discussion in the following paragraphs, the 100 mg/L feed  $\text{NH}_4^+\text{-N}$  condition is described as the “nitrification” condition, and the 800 mg/L condition is referred to as the “nitritation” condition.

### 6.3.2. Microbial community structure analysis

From the qPCR data, the microbial structure of suspended flocs and biofilm changed before and after the nitritation establishment. As shown in Figure 6.1, the abundance of the AOB functional gene (*amoA*) was lower under the nitrification dominant condition than under the nitritation dominant condition, indicating that the growth of AOB was promoted under high ammonia loading conditions. A significant decrease in abundance of NOB functional genes was also detected when the condition changed from nitrification dominant to nitritation dominant, confirming that NOB was inhibited under nitritation condition. Moreover, the abundance of total bacterial 16S rRNA gene decreased when the condition changed from the nitrification to the nitritation condition (see Appendix C Figure C-9). The detection of a higher abundance of AOB functional genes than the total 16S RNA genes might be due to multiple copies of functional genes existing in one cell (Kim et al., 2011).



**Figure 6.1.** Abundance of functional genes in the suspended flocs and biofilm samples under nitrification and nitritation conditions. The grid patterned blocks represent the AOB functional genes; the slash patterned blocks represent the NOB functional genes.

### 6.3.3. Extracellular polymeric substance production and characteristics

#### 6.3.3.1. Colorimetric data analyses

As shown in Figure 6.2a, when the ammonium concentration increased from nitrification condition (100mg/L NH<sub>4</sub><sup>+</sup>-N) to nitritation condition (800 mg/L NH<sub>4</sub><sup>+</sup>-N), significant decreases in both TB-EPS and LB-EPS production were observed in both suspended and attached biomass.

In the suspended flocs, under both nitrification and nitritation conditions, the TB-EPS was composed of polysaccharides and protein, while the LB-EPS was composed of almost only polysaccharides (Figure 6.2a). These results agreed with the results that reported in Liang et al.'s study (2010), in which protein and polysaccharides were detected in TB-EPS, while no protein was

detected in LB-EPS. In terms of composition, the relative content of polysaccharide in the TB-EPS was more than that of protein under nitrification condition; but no significant difference was observed under nitritation condition ( $P > 0.05$ ).

Similar to the results from the suspended flocs EPS analysis, under both nitritation and nitrification conditions, the TB-EPS in the biofilm was also composed of polysaccharides and protein, and the LB-EPS in the biofilm contained almost no protein. The content of protein and the content of polysaccharides in TB-EPS are not significantly different ( $P > 0.05$ ) under nitrification condition. However, this lack of significance may be due to the relatively large variation in the protein measurement results. While under nitritation conditions, a sharp decrease was observed in the biofilm TB-EPS, with the proportion of its protein being significantly less than that of the polysaccharides ( $P < 0.05$ ).

In general, the production of total EPS in all samples was considerably higher under the nitrification condition (total polysaccharides =  $396.9 \pm 38.6$   $\mu\text{g}/\text{mg}$  MLSS and total protein =  $136.7 \pm 6.3$   $\mu\text{g}/\text{mg}$  MLSS) as compared to the nitritation condition (total polysaccharides =  $82.5 \pm 23.8$   $\mu\text{g}/\text{mg}$  MLSS and total protein =  $24.1 \pm 2.4$   $\mu\text{g}/\text{mg}$  MLSS). The EPS production might be related to the microbial community structure. Commonly found *Nitrosomonas* spp. (AOB) lack EPS production (Stehr et al., 1995; Tsuneda et al., 2001). Commonly found *Nitrospira* spp. (NOB), on the other hand, produce high amounts of EPS if the nitrite oxidation is not inhibited (Nowka et al., 2015). The inhibition of NOB in this reactor might account for the decreased production of EPS when nitritation was established.

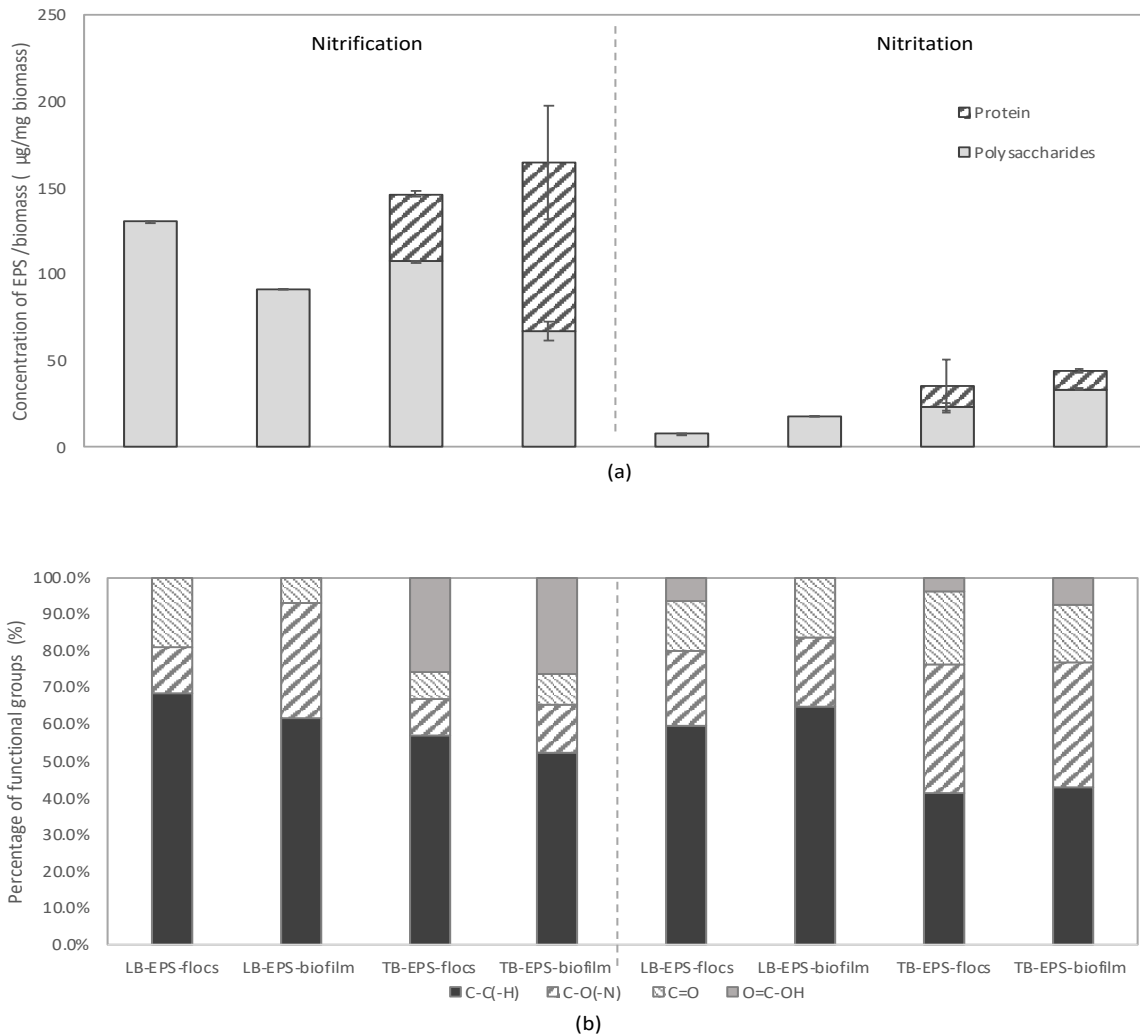
It was interesting that after stable nitrification was achieved, the production of all EPS components showed no significant difference between suspended flocs and biofilm (P values > 0.05), which can be explained by the similar microbial structure in biofilm and flocs under nitrification condition.

#### 6.3.3.2. X-ray photoelectron spectroscopy data analysis

The XPS data analysis reveals differences in the characteristics of LB-EPS and TB-EPS (Figure 2b), confirming the colorimetric results (section 6.3.2.1.). For the EPS produced under nitrification conditions, the main difference is that carboxyl,  $O=C-OH$ , containing substances were absent from LB-EPS, but made up approximately 25% of the floc and biofilm TB-EPS. While carbohydrate-like,  $C-C(-H)$ , substances dominated all forms of the EPS produced under nitrification conditions, the LB-EPS of both the floc and biofilm contained higher percentages of this material than did their TB-EPS. The floc EPS differed from that of the biofilm in that the floc LB-EPS contained a higher percentage of carbonyl,  $C=O$ , containing substances than did the floc TB-EPS; whereas the biofilm LB-EPS contained a greater percentage of amide or amine-like substances,  $C-O(-N)$ , than did the biofilm TB-EPS. It is noteworthy that the composition of TB-EPS produced in the floc was quite similar to that produced in the biofilm under the nitrification conditions.

When the condition changed from nitrification to nitritation dominant, the percentage of hydrocarbon-like substances remained dominant in the floc and biofilm LB-EPS but dropped to 41% and 43% in the floc and biofilm TB-EPS, respectively. The percentage of the carboxyl ( $O=C-OH$ ) substance in the TB-EPS decreased to 4 and 8% in the floc and biofilm TB-EPS, respectively, while it became detectable (6%) in the floc LB-EPS. The percentage of amine or amide like substances containing  $C-O(N)$  bonds increased in all EPS, except the biofilm LB-EPS, and became the second largest component in the floc and biofilm TB-EPS. Meanwhile, the percentage of substances containing a carbonyl,  $C=O$ , functional group also increased in all EPS other than the floc LB-EPS %. Overall, the changes in the composition of LB-EPS were not as great as those of

TB-EPS when the microbial community structure changed in response to the alteration of environmental conditions from nitrification to nitritation.



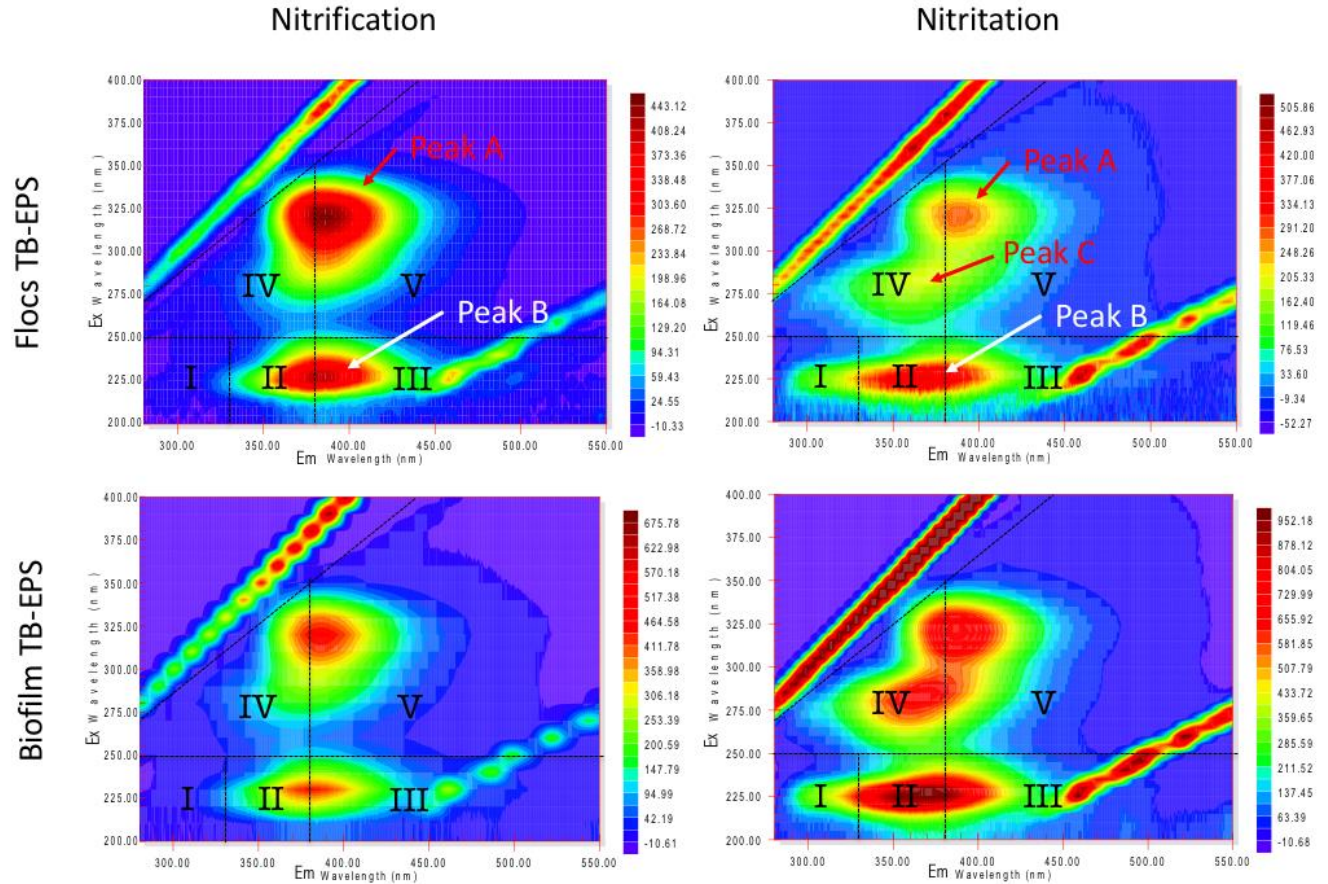
**Figure 6.2.** The characteristics of EPS samples collected from suspended flocs and biofilm under nitrification-dominant and nitritation-dominant conditions. (a) the results for TB-EPS and LB-EPS of suspended flocs and biofilm from nitrification (left) and nitritation dominant (right) conditions. Figure (b) indicates the percentages of substances containing different functional groups in the EPS samples based on the X-ray photoelectron spectroscopy results; the solid fill shows the percentage containing C-C(-H) bonds, thick slashes pattern shows the percentage containing C-O(-N) bonds, the thin slash pattern shows the percentage containing C=O bonds, and the light grey solid pattern shows the percentage containing O=C-OH bonds.

Comparing the qPCR results with XPS results, the content of amide or amine-like substance with C-O(-N) bonds and C=O bonds in the TB-EPS increased when the abundance of AOB increased in the microbial community. This indicates that the existence of AOB was associated with the production of amide or amine like substance in the TB-EPS. Conversely, the dramatic decrease in the abundance of NOB, when conditions changed from nitrification to nitritation conditions, might be responsible for the decrease of the contents of hydrocarbon-like, C-C(-H) bond, and carboxyl O=C-OH , group substances in the TB-EPS.

#### 6.3.3.3. Three-dimensional excitation and emission matrix fluorescence data analysis

The 3D-EEM data (Figure 6.3) further explains the differences between TB-EPS from different biomass aggregates under different ammonium loadings. For both suspended flocs and biofilm collected under nitrification conditions, only two peaks were observed (Peaks A and B). While under the nitritation dominant conditions, three peaks were observed (Peaks A, B, and C) in the EEM plots. Peak A fell in Region V, corresponding to the humic acid-like substances. Peak B was located between Region II and Region III, which corresponds to aromatic protein II and fulvic acid-like material, respectively. Peak C was in region IV, which indicates tryptophan protein-like substances (Dong et al., 2017). The establishment of the nitritation process was associated with the existence of tryptophan protein-like substances (Figure 6.3). The intensity and location information (Ex/Em) of the peaks were listed in Table 6.1.





**Figure 6.3.** 3D-EEM data for biofilm and flocs TB-EPS from nitritation and nitrification dominant conditions.

A higher intensity ratio of Peak A/Peak B (Table 6.1) was observed in the nitrification dominant condition, as compared to the nitritation dominant condition. This indicates a lower content of humic acid-like substance (Region V) and a higher content of aromatic protein-like substances (Region II) in the TB-EPS extracted under the nitritation dominant condition in which lower abundance of NOB bacteria and higher abundance of AOB was observed. In addition, the appearance of Peak C indicates the production of the tryptophan protein-like substances in the TB-EPS collected under the nitritation dominant condition, which may also relate to the high AOB abundance.

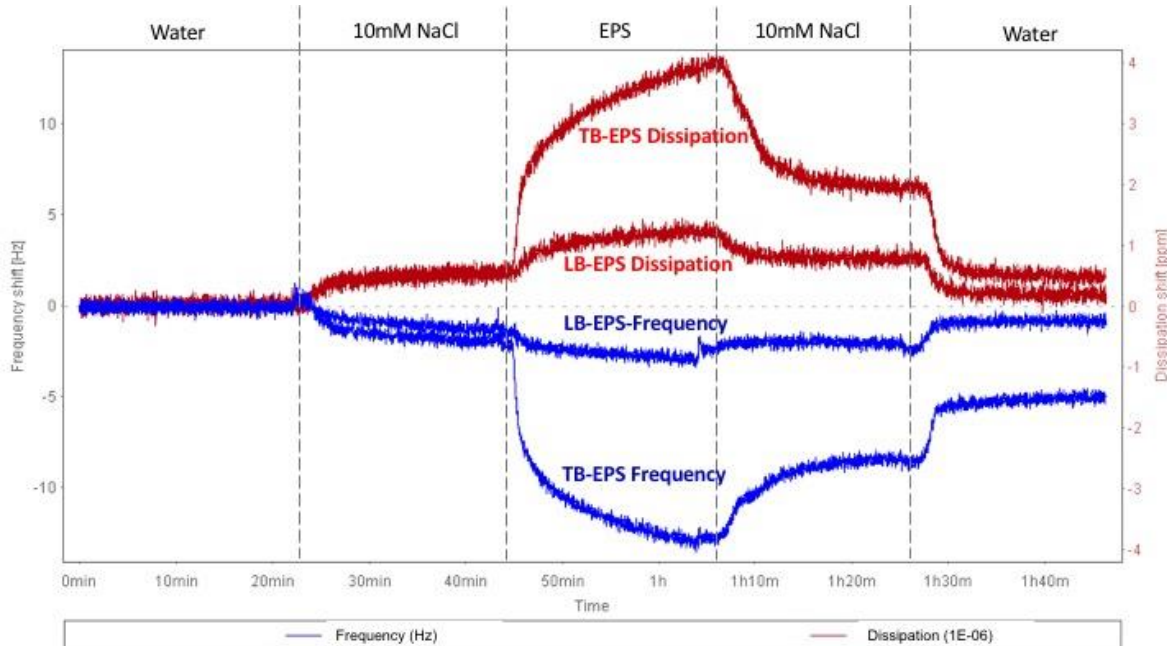
**Table 6.1.** The 3D-EEM fluorescence spectrum parameters for TB-EPS samples from nitrification and nitritation conditions.

Condition	Aggregate type	Peak ID	Intensity	Ex(nm)/ Em(nm)	Composition	A/B
Nitrification	Flocs	Peak A	460.6	320/384	Humic acid-like	1.09
		Peak B	424.3	225/378	Aromatic Protein-like	
	Biofilm	Peak A	486.4	320/388	Humic acid-like	1.06
		Peak B	460.4	230/382	Aromatic Protein-like	
Nitritation	Flocs	Peak A	301.9	320/385	Humic acid-like	0.67
		Peak B	453.9	225/365	Aromatic Protein-like	
		Peak C	216.6	285/374	Tryptophan protein-like	
	Biofilm	Peak A	812.5	320/385	Humic acid-like	0.82
		Peak B	989.2	225/365	Aromatic Protein-like	
		Peak C	702.8	285/366	Tryptophan protein-like	

#### 6.3.3.4 Adsorption of EPS components to solid surface

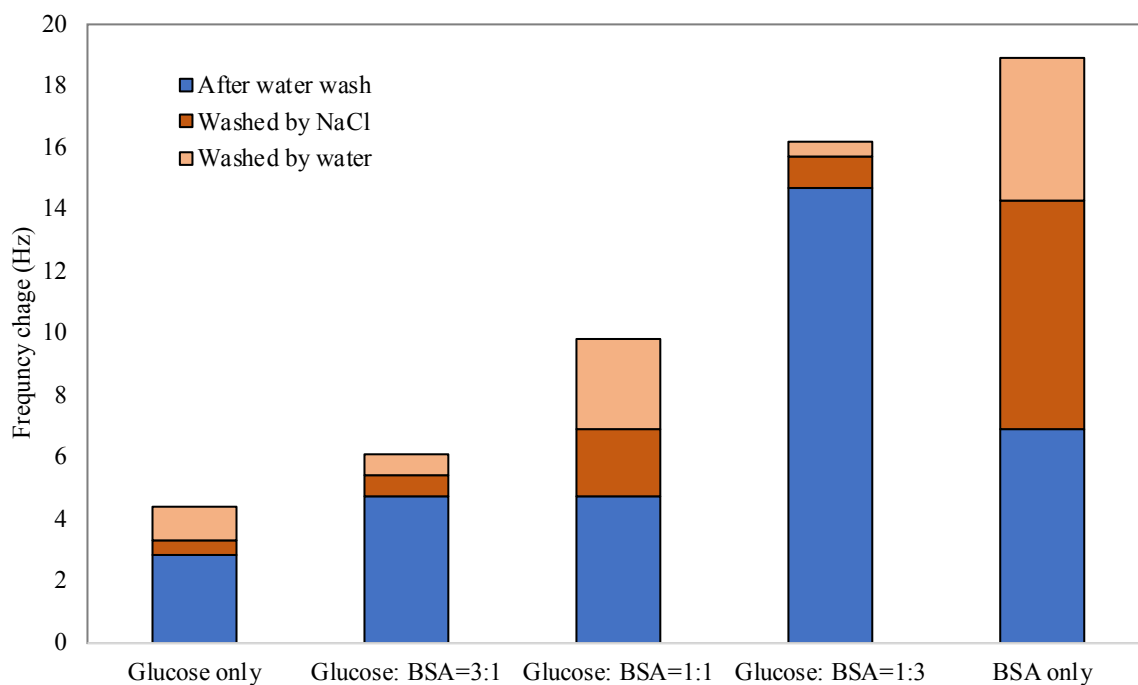
In this part of study, we used polystyrene coated sensors to mimic the surface of the biofilm support carrier (Beneš and Paulenová, 1973). The adsorption characteristics of EPS components were described based on the frequency and dissipation changes detected by QCM-D and were analysed by the Qfind software. The change of the frequency indicated the amount of mass that adsorbed to the sensor.

As shown in Figure 6.4, a considerably higher frequency change was observed for TB-EPS, indicating higher adsorption of TB-EPS to the sensor surface, as compared to the LB-EPS. After the NaCl solution wash and after water wash, a lower frequency change of TB-EPS as compared to LB-EPS was observed, indicating that TB-EPS experienced lower EPS release during the washing process, and thus had a stronger and more stable adsorption to the solid surface. The greater protein content in TB-EPS might have contributed to the greater TB-EPS adsorption to sensor surface. A similar observation has been reported previously (Chandrasekaran et al., 2013).



**Figure 6.4.** the QCMD data for LB-EPS and TB-EPS sample from biofilm that collected under nitrification dominant condition. The deviation of the frequency line (blue line) from the center line (dashed horizontal line) demonstrated the adsorption capacity of EPS samples on to solid surface.

To further evaluate the impacts of EPS composition (especially the proteins/carbohydrates ratio) on their adsorption capability, the adsorption capacities of different ratios of protein and carbohydrate mixtures on solid surfaces were compared. As shown in Figure 6.5, under all conditions, the higher protein content in the mixture, the greater adsorption capacity was found to be. For example, Trial 1 (glucose only) resulted in the least mass adsorption to the sensor. While Trial 5 (BSA only) showed the greatest adsorption capacity to the sensor. These results support the interpretation of the previous EPS experiment that protein in the TB-EPS seems to be the main contributor to the adsorption.



**Figure 6.5.** The frequency changes for five trials with glucose and BSA (as EPS surrogates for polysaccharides and proteins) at different ratios (from left to right: 1. Glucose only; 2. Glucose: BSA=3:1; 3. Glucose: BSA=1:1; Glucose: BSA=1:3; and BSA only). The blue boxes represent the residual attached mass after the NaCl solution wash and water wash. The dark orange parts represent the mass released during the NaCl wash, and the light orange parts represent the mass released during the water wash.

The stability of the attached mass was also analysed by comparing the frequency change after the NaCl solution wash and a water wash. Surprisingly, among all the samples tested, the Trial 4 (glucose: BSA=1:3) resulted in the least amount of mass release during the NaCl solution and water wash. Trial 5 (BSA only), which had the highest adsorption capacity, resulted in the release of most of the mass that previously adsorbed mass during the washing. This result demonstrated that even

though the protein seemed to be the main contributor to the adsorption, the polysaccharides played a role in preventing protein detachment.

#### **6.4. Conclusions**

This study compared the relationship between the EPS production and microbial community characteristics of suspended sludge and attached biofilm from both nitrification dominant and nitritation dominant conditions. Nitritation conditions were established under high ammonium loading conditions, which led to the elimination of NOB, and the reduction in microbial EPS production. A higher AOB abundance was related to higher aromatic protein and tryptophan protein like substances in TB-EPS. EPS adsorption to solid surface relied more on the TB-EPS, rather than the LB-EPS, as the former contained more protein. Further studies are needed to delineate the complex nature of EPS production of specific organisms in the systems.

#### **6.5. References**

- Beneš, P., Paulenová, M., 1973. Surface charge and adsorption properties of polyethylene in aqueous solutions of inorganic electrolytes. *Kolloid-Zeitschrift und Zeitschrift für Polymere* 251, 766–771. <https://doi.org/10.1007/BF01499104>
- Chandrasekaran, N., Dimartino, S., Fee, C.J., 2013. Study of the adsorption of proteins on stainless steel surfaces using QCM-D. *Chemical Engineering Research and Design* 91, 1674–1683. <https://doi.org/10.1016/j.cherd.2013.07.017>
- Chen, W., Westerhoff, P., Leenheer, J.A., Booksh, K., 2003. Fluorescence Excitation–Emission Matrix Regional Integration to Quantify Spectra for Dissolved Organic Matter. *Environmental Science & Technology* 37, 5701–5710. <https://doi.org/10.1021/es034354c>

- Dong, H., Zhang, K., Han, X., Du, B., Wei, Q., Wei, D., 2017. Achievement, performance and characteristics of microbial products in a partial nitrification sequencing batch reactor as a pretreatment for anaerobic ammonium oxidation. *Chemosphere* 183, 212–218. <https://doi.org/10.1016/j.chemosphere.2017.05.119>
- Flemming, H.-C., Neu, T.R., Wozniak, D.J., 2007. The EPS Matrix: The “House of Biofilm Cells.” *Journal of Bacteriology* 189, 7945–7947. <https://doi.org/10.1128/JB.00858-07>
- Frølund, B., Palmgren, R., Keiding, K., Nielsen, P.H., 1996. Extraction of extracellular polymers from activated sludge using a cation exchange resin. *Water Research* 30, 1749–1758. [https://doi.org/10.1016/0043-1354\(95\)00323-1](https://doi.org/10.1016/0043-1354(95)00323-1)
- Higgins, M.J., Novak, J.T., 1997. Characterization of Exocellular Protein and Its Role in Bioflocculation. *Journal of Environmental Engineering* 123, 479–485. [https://doi.org/10.1061/\(ASCE\)0733-9372\(1997\)123:5\(479\)](https://doi.org/10.1061/(ASCE)0733-9372(1997)123:5(479))
- Hwang, G., Kang, S., El-Din, M.G., Liu, Y., 2012. Impact of an extracellular polymeric substance (EPS) precoating on the initial adhesion of *Burkholderia cepacia* and *Pseudomonas aeruginosa*. *Biofouling* 28, 525–538. <https://doi.org/10.1080/08927014.2012.694138>
- Hwang, G., Liang, J., Kang, S., Tong, M., Liu, Y., 2013. The role of conditioning film formation in *Pseudomonas aeruginosa* PAO1 adhesion to inert surfaces in aquatic environments. *Biochemical Engineering Journal* 76, 90–98. <https://doi.org/10.1016/j.bej.2013.03.024>
- Kim, H., Schuler, A.J., Gunsch, C.K., Pei, R., Gellner, J., Boltz, J.P., Freudenberg, R.G., Dodson, R., 2011. Comparison of Conventional and Integrated Fixed-Film Activated Sludge Systems: Attached- and Suspended-Growth Functions and Quantitative Polymerase Chain Reaction Measurements. *Water Environment Research* 83, 627–635. <https://doi.org/10.2175/106143010X12851009156448>
- Liang, Z., Li, W., Yang, S., Du, P., 2010. Extraction and structural characteristics of extracellular polymeric substances (EPS), pellets in autotrophic nitrifying biofilm and activated sludge. *Chemosphere* 81, 626–632. <https://doi.org/10.1016/j.chemosphere.2010.03.043>

- McIlroy, S.J., Saunders, A.M., Albertsen, M., Nierychlo, M., McIlroy, B., Hansen, A.A., Karst, S.M., Nielsen, J.L., Nielsen, P.H., 2015. MiDAS: the field guide to the microbes of activated sludge. Database 2015, bav062. <https://doi.org/10.1093/database/bav062>
- Nowka, B., Off, S., Daims, H., Spieck, E., 2015. Improved isolation strategies allowed the phenotypic differentiation of two *Nitrospira* strains from widespread phylogenetic lineages. FEMS Microbiology Ecology 91. <https://doi.org/10.1093/femsec/fiu031>
- Rouxhet, P.G., Mozes, N., Dengis, P.B., Dufrière, Y.F., Gerin, P.A., Genet, M.J., 1994. Application of X-ray photoelectron spectroscopy to microorganisms. Colloids and Surfaces B: Biointerfaces 2, 347–369. [https://doi.org/10.1016/0927-7765\(94\)80049-9](https://doi.org/10.1016/0927-7765(94)80049-9)
- Shao, Y., Shi, Y., Mohammed, A., Liu, Y., 2017. Wastewater ammonia removal using an integrated fixed-film activated sludge-sequencing batch biofilm reactor (IFAS-SBR): Comparison of suspended flocs and attached biofilm. International Biodeterioration & Biodegradation 116, 38–47. <https://doi.org/10.1016/j.ibiod.2016.09.026>
- Shao, Y., Yang, S., Mohammed, A., Liu, Y., 2018. Impacts of ammonium loading on nitrification stability and microbial community dynamics in the integrated fixed-film activated sludge sequencing batch reactor (IFAS-SBR). International Biodeterioration & Biodegradation 133, 63–69. <https://doi.org/10.1016/j.ibiod.2018.06.002>
- Sheng, G.-P., Yu, H.-Q., Li, X.-Y., 2010. Extracellular polymeric substances (EPS) of microbial aggregates in biological wastewater treatment systems: A review. Biotechnology Advances 28, 882–894. <https://doi.org/10.1016/j.biotechadv.2010.08.001>
- Shin, H.S., Kang, S.T., Nam, S.Y., 2001. Effect of carbohydrate and protein in the EPS on sludge settling characteristics. Water Sci. Technol. 43, 193–196.
- Stehr, G., S. Zörner, B. Böttcher, H. P. Koops, 1995. Exopolymers: An Ecological Characteristic of a Floc-Attached, Ammonia-Oxidizing Bacterium. Microbial Ecology 115.
- Sweity, A., Ying, W., Ali-Shtayeh, M.S., Yang, F., Bick, A., Oron, G., Herzberg, M., 2011. Relation between EPS adherence, viscoelastic properties, and MBR operation: Biofouling

study with QCM-D. *Water Research* 45, 6430–6440.

<https://doi.org/10.1016/j.watres.2011.09.038>

Tsuneda, S., Park, S., Hayashi, H., Jung, J., Hirata, A., 2001. Enhancement of nitrifying biofilm formation using selected EPS produced by heterotrophic bacteria. *Water Sci. Technol.* 43, 197–204.

van den Akker, B., Beard, H., Kaeding, U., Giglio, S., Short, M.D., 2010. Exploring the relationship between viscous bulking and ammonia-oxidiser abundance in activated sludge: A comparison of conventional and IFAS systems. *Water Research* 44, 2919–2929. <https://doi.org/10.1016/j.watres.2010.02.016>



## CHAPTER 7. DENITRITATION AND COMBINED SYSTEM OF PARTIAL NITRIFICATION-DENITRITATION WITH ALKALINITY RECOVERY

### 7.1. Introduction

Like ammonia, high concentration of nitrate or nitrite may also cause environmental problems. If the  $\text{NO}_3^- - \text{N}$  concentration is greater than 10mg/L or the  $\text{NO}_2^- - \text{N}$  concentration is greater than 1mg/L in the drinking water, it may cause diseases, especially for infants, like methemoglobinemia and blue baby. After the ammonia oxidized to nitrite by partial nitrification, high concentration of nitrite, with a small amount of nitrate got accumulated in the wastewater. Further treatment is required to remove the nitrite and the nitrate in the water to meet the regulated total nitrogen limit in the effluent. The biological removal of oxidized nitrogen by denitrifiers is the most common way for nitrite or nitrate removal. This process is termed as “denitrification” process.

Conventional denitrification refers to the conversion of nitrate to nitrite and further to nitrogen gas. If only the nitrite is present, the conversion of nitrite to nitrogen gas would happen, and this process is termed as “denitritation” process. Both the denitrification and denitritation processes are mediated by heterotrophic denitrifiers under anoxic condition, with the supplements of external organic carbon sources. The conversion of nitrite to nitrogen gas consumes 40% less of the organic carbon, as compared to the conventional nitrification process. Together with the partial nitrification process, the pathway for nitrogen removal over nitrite can save 25% of the oxygen and 40% of the organic carbon requirements than the pathway over nitrate. Moreover, the denitritation process was reported to be 1.5 to 2.0 times faster than the denitrification process (Ciudad et al., 2005), which means that the pathway over nitrite can further speed up the overall nitrogen removal process.

The other reason to analyze the denitritation process is the alkalinity deficiency in the raw supernatant. The nitrification and partial nitrification processes consume alkalinity. Theoretically,

for each g of the ammonia-N been oxidized to nitrite, 7.1g of the alkalinity (as CaCO<sub>3</sub>) is required. Our results showed a value of 7g alkalinity per g of ammonia-N oxidized. In the lagoon supernatant collecting from the local treatment plant, the alkalinity/ammonium-N ratio was  $3.4 \pm 0.4$ , which indicated that the supernatant is the lack of alkalinity. However, how the alkalinity deficiency of lagoon supernatant would affect the partial nitrification was not confirmed yet. The addition of chemicals (alkalinity or caustic chemicals) and the proper storage of these chemicals will largely increase the chemicals and operation cost. It was reported that the denitrification process can recover half of the alkalinity utilized by the nitrification process with the addition of external organic carbon. The reported alkalinity recovery from the denitrification process was 3.57g Alkalinity/g N reduced (Savaglio and Puopolo, 2012). Further, as the cost of the organic carbon is much lower than the cost of caustic chemicals, recovering the alkalinity from denitrification process is more economy feasible than direct addition of caustic chemicals.

In addition, studies had revealed that nitrous oxide production would occur during the incomplete denitrification process (Domingo-Félez et al., 2017; Gabarró et al., 2014). Nitrous oxide has 300 times GHG potential than the CO<sub>2</sub> (IPCC, 1995&2012). The production of nitrous oxide during the denitrification process need to be investigated.

The last but not the least, partial nitrification and denitrification process happen under different conditions. Partial nitrification occurred under aerobic condition while the denitrification process happened under anoxic condition (Hellings et al., 1998). Building two separate reactors requires more investments on reactors construction and maintenance. Integrating two processes in the same reactor will be more beneficial and will reduce the capital cost for scale-up. A well-designed sequence that included the aerobic and anoxic conditions was needed to accomplish the partial nitrification and denitrification in a single reactor system.

In order to solve the alkalinity shortage problem in the lagoon supernatant, it was important to understand the inhibition of alkalinity deficiency on the partial nitrification processes and look for alkalinity source which was economy feasible to support the partial nitrification process. Firstly, A denitrification reactor using the acetate as the carbon source was operated in this part of study to 1). verify the feasibility of alkalinity recovery from the denitrification process and to 2). calculate the kinetics of denitrification process and the production of nitrous oxide during the process. Then, a combined partial nitrification and denitrification reactor that operated under a well-designed sequence batch mode was used to investigate the feasibility of combined system.

## **7.2. Methodology**

### 7.2.1. Analytical methods

The pH, DO and temperature of the reactor were monitored. All the liquid samples were first filtered through 0.45 $\mu$ m filters before analysis. The concentrations of  $\text{NH}_4^+ - \text{N}$ ,  $\text{NO}_2^- - \text{N}$  and  $\text{NO}_3^- - \text{N}$  were determined using the Hach kits (Methods 8038, 8153, and 10206). Alkalinity concentration (as  $\text{CaCO}_3$ ) was also determined using Hach kit (Hach Method 10239). The COD concentration was calculated based on the TOC measurement. The calculation was included in Appendix A-7. The TOC concentration was determined using a TOC analyzer From Shimadzu Inc. The nitrous oxide concentrations in the gas samples were analyzed using a gas chromatography with an electron capture detector (GC-ECD) 7890B from Agilent. Mixed liquor suspended solids (MLSS) and mixed liquor volatile suspended solids (MLVSS) were measured weekly using *Standard Methods* 2540B (APHA, 2011). The biomass attached to carriers was measured using methods in Shao et al. (2017).

### 7.2.2. Alkalinity deficiency test

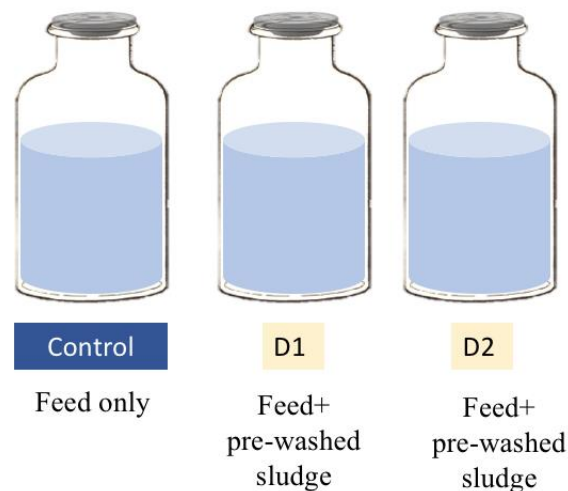
A cycle test was carried out to verify the impact of the alkalinity deficiency on the partial nitrification process. As mentioned in previous chapters, successful partial nitrification process was achieved in an IFAS reactor. The biomass (3L including settled sludge and 900 biofilm carriers) from the reactor was utilized for the test. At the beginning of the reaction, the reactor was feed with 3L of raw supernatant from the thickening lagoon without of any alkalinity addition. During the cycle test, the reactor was provided with aeration at a rate of  $2.4 \times 10^{-5} \text{ m}^3/\text{s}$ . Liquid samples were collected from the reactor once per hour for about 9 hours of reaction. The alkalinity, ammonia, nitrite and nitrate nitrogen concentrations in the liquid samples were analyzed using the analytical methods mentioned above. The pH and DO in the reactor were also monitored on an hourly basis during the reaction.

### 7.2.3. Denitrification kinetics determination

Before determining the denitrification kinetics, a 960mL reactor was set up and inoculated with the sludge from local wastewater treatment plant and operated for more than a month until the denitrification was successfully achieved. The influent into the reactor was the mixture of nitrite feed and sodium acetate feed at a volume ratio of 1:1. The nitrite feed was the effluent from nitrification reactor because the effluent contained high concentration of nitrite. The acetate feed was freshly prepared using sodium acetate (COD concentration in acetate feed was about 2400mg/L) was added into the reactor as carbon source. The mixture was purged with nitrogen gas to lower the dissolved oxygen before being pumped into the reactor. Same as the nitrification reactor, the liquid samples were collected and filtered before analysis. Same analytical methods as mentioned in section 7.2.1 were used for the sample analysis.

After the denitrification was achieved in the reactor (unchanged effluent quality for 2 weeks), sludge (500ml) was collected from a denitrification reactor for the batch test to investigate the denitrification

kinetics. The collected sludge (200mL for two batch bottles) was washed three times with PBS solution to remove residual components before being transferred to pre-autoclaved bottles. The mixture of nitrite feed and sodium acetate feed that used for the denitritation reactor was used again for the batch test. At the beginning of the test, the pre-washed sludge was transferred into the bottles. Then the feed was added to duplicate bottles with sludge (total liquid volume of 100ml each, bottle has a capacity of 170ml) (Figure 7.1). Bottles without sludge addition were also set up as controls. The headspace of each bottle was purged with nitrogen gas to create an anoxic condition. Then the bottles were capped with a rubber stopper and aluminum crimp sealer. The bottles were then placed on a shaker at a speed of 150rpm. The liquid samples (1.5ml each) were collected from each bottle every 15 minutes during the 1.5 hours of reaction. All samples were filtered (0.45  $\mu\text{m}$  pore) before analysis. Without removing the rubber stopper, the liquid samples were collected from the reactor using a syringe and needle. The gas samples (2mL) were also collected from the headspace of each bottle using needles and syringes for GC-ECD analysis.



**Figure 7.1.** the set-up of the denitritation batch test. D1 and D2 are duplicates.

#### 7.2.4. Combined partial nitrification-denitritation cycle test

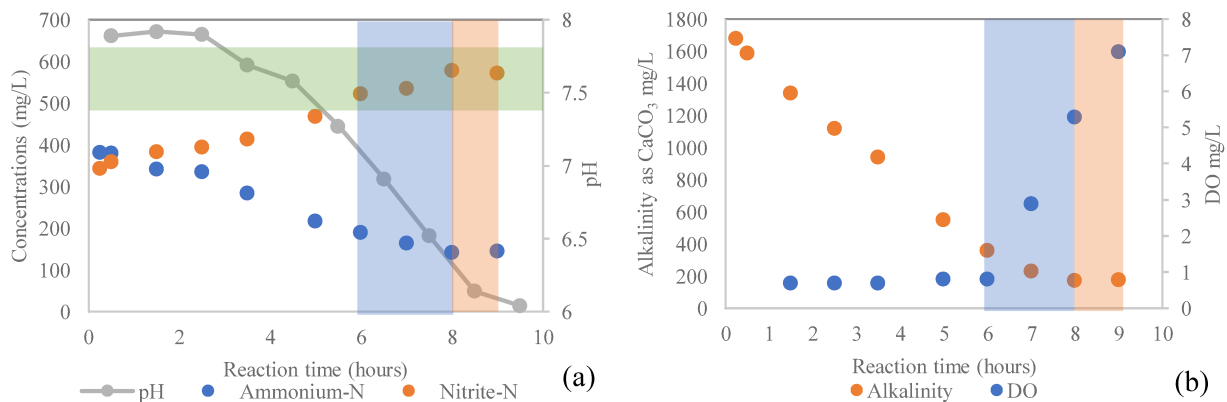
The sequence of the partial nitrification and denitrification processes was determined based on the partial nitrification and denitrification kinetics that determined from previous batch tests. Sludge from a well-established partial nitrification reactor (5.2L sludge and 900 biocarriers) and biomass from a well-established denitrification reactor (500ml) were mixed together for the cycle test. The mixed biomass was prewashed before using. The feed water was the raw supernatant without alkalinity addition. The concentrated COD stock (contains about 100g/L COD) was prepared using sodium acetate. COD stock solution (15ml) was added into the reactor after the aeration stopped. Liquid samples (10ml) were taken from the reactor every hour for 30 hours. All samples were filtered (0.45  $\mu\text{m}$  pore) before the pH, temperature, DO,  $\text{NH}_4^+ - \text{N}$ ,  $\text{NO}_2^- - \text{N}$ ,  $\text{NO}_3^- - \text{N}$ , COD, and alkalinity analysis.

### 7.3. Results and discussion

#### 7.3.1. The impact of alkalinity deficiency on the partial nitrification

The  $\text{NH}_4^+ - \text{N}$  concentration in the raw supernatant was around 900mg/L and the alkalinity concentration (as  $\text{CaCO}_3$ ) was around 3190mg/L. The ratio of alkalinity/ $\text{NH}_4^+ - \text{N}$  was around 3.5. To completely oxidation of the ammonium in the raw supernatant required 6390mg/L of alkalinity (as  $\text{CaCO}_3$ ). The low alkalinity/ $\text{NH}_4^+ - \text{N}$  ratio indicated the lack of alkalinity in the raw supernatant to support the AOB to completely oxidize the ammonium to nitrite. As 3L of the raw supernatant was feed into the 6L reactor, the  $\text{NH}_4^+ - \text{N}$  concentration at the beginning of the reaction ( $t=0\text{min}$ ) was 382.5mg/L. The  $\text{NO}_2^- - \text{N}$  in the settled sludge and biocarriers (bulk liquid quality was the same as the effluent from partial nitrification reactor treating raw supernatant with alkalinity addition) was diluted to about 344 mg/L after the raw supernatant addition. The concentrations of  $\text{NH}_4^+ - \text{N}$  and  $\text{NO}_2^- - \text{N}$  concentrations were similar to the concentrations at the beginning of the partial nitrification that achieved before. The only difference was that no alkalinity

was added into the reactor in this test. After 9 hours of test, the  $\text{NH}_4^+ - \text{N}$  concentration decreased from 382.5 mg/L to 145mg/L and the  $\text{NO}_2^- - \text{N}$  concentration increased from 344 to 578mg/L (Figure 7.2a). The partial nitrification happened slowly at the first three hours ( $t=0-3\text{hrs}$ ). After three hours, the reaction rate became faster from  $t=3\text{hr}$  to  $t=6\text{hr}$ . Then, the partial nitrification was inhibited during  $t=6-8$  hours and completely ceased at  $t=8-9$  hours. The partial nitrification process was considered as completely ceased in the last hour because there was no change in ammonium concentration from  $t=8\text{h}$  to  $t=9\text{h}$ . The inhibition of partial nitrification during  $t=6-8$  hours can be explained by the increase of the DO concentration from 0.8 to 5.3 mg/L during this period (Figure 7.2b), which indicated that the nitrifiers cannot uptake as much oxygen as what they can during  $t=0-6\text{hours}$ . The alkalinity concentration decreased from 1590mg/L to 173mg/L during the first 8 hours of reaction and remained no change during the last hour (Figure 7.2b). Due to the shortage of alkalinity, the pH dropped from 7.9 to 6 after the 9 hours of test. Our results indicates that during  $t=3\text{hr}$  to  $t=5\text{hr}$ , the ammonium conversion was the fastest (47mg/L/hr), and the pH range for this period was coincided with the reported optimal pH range for AOB, which is 7.4 to 7.8 (Claros et al., 2013). The ammonium conversion rate dropped by about 50% to 24mg/L/hr when the partial nitrification was inhibited (from  $t=5\text{hr}$  to  $t=8\text{hr}$ ). The inhibitory pH range was around 6.4 to 7.4. Lower than 6.4, no ammonium conversion was observed and the partial nitrification completely stopped. The results confirmed the inhibition of partial nitrification by the alkalinity deficiency.



**Figure 7.2.** The inhibition of alkalinity shortage on the partial nitrification process. The blue shaded area is the inhibition area and the orange shaded area indicates the complete stop of partial nitrification. The green shaded area is the optimal pH range for AOB.

### 7.3.2 The denitrification kinetics

The denitrification process successfully reduced the concentrations of nitrite and nitrate (Figure 7.3 a,b,c) with the utilization of COD. Based on the kinetics analysis, the specific nitrite reduction rate was around  $37.1 \text{ mg NO}_2^- - \text{N/g biomass}\cdot\text{hr}$ . The specific COD reduction rate was around  $144 \text{ mg/g biomass}\cdot\text{hr}$ . Alkalinity was accumulated during the denitrification process (Figure 7.4d). A specific alkalinity production rate around  $228 \text{ mg/ g biomass}\cdot\text{hr}$  was obtained. The ratio of alkalinity production/ COD utilized was around 1.58. Based on this ratio, the COD dosing can be determined based on the alkalinity requirements. More interesting, the nitrous oxide production was only observed in the control bottle (Figure 7.3e), in which no denitrification sludge was not added. The production of nitrous oxide was attributed by the indigenous microbes in the raw supernatant. It can be explained by the Polyhydroxybutyrate (PHB) production in the controlled bottle (Scherson et al., 2014). The produced PHB during the so-called “Feast” phase, in which the available COD largely exceeded the COD that needed by the microbes. The PHB accumulated inside the microbes reacted with the nitrite to form nitrous oxide. In another word, the formation of PHB was the key to nitrous oxide production and it can only be produced during the “feast” phase. However, a clear threshold to define the “feast” phase was not known. In the bottles that inoculated with the denitrification sludge, the COD concentration was not high enough to be defined as “feast” phase. The PHB less likely accumulated in these bottles. Thus, the nitrous oxide was not produced.



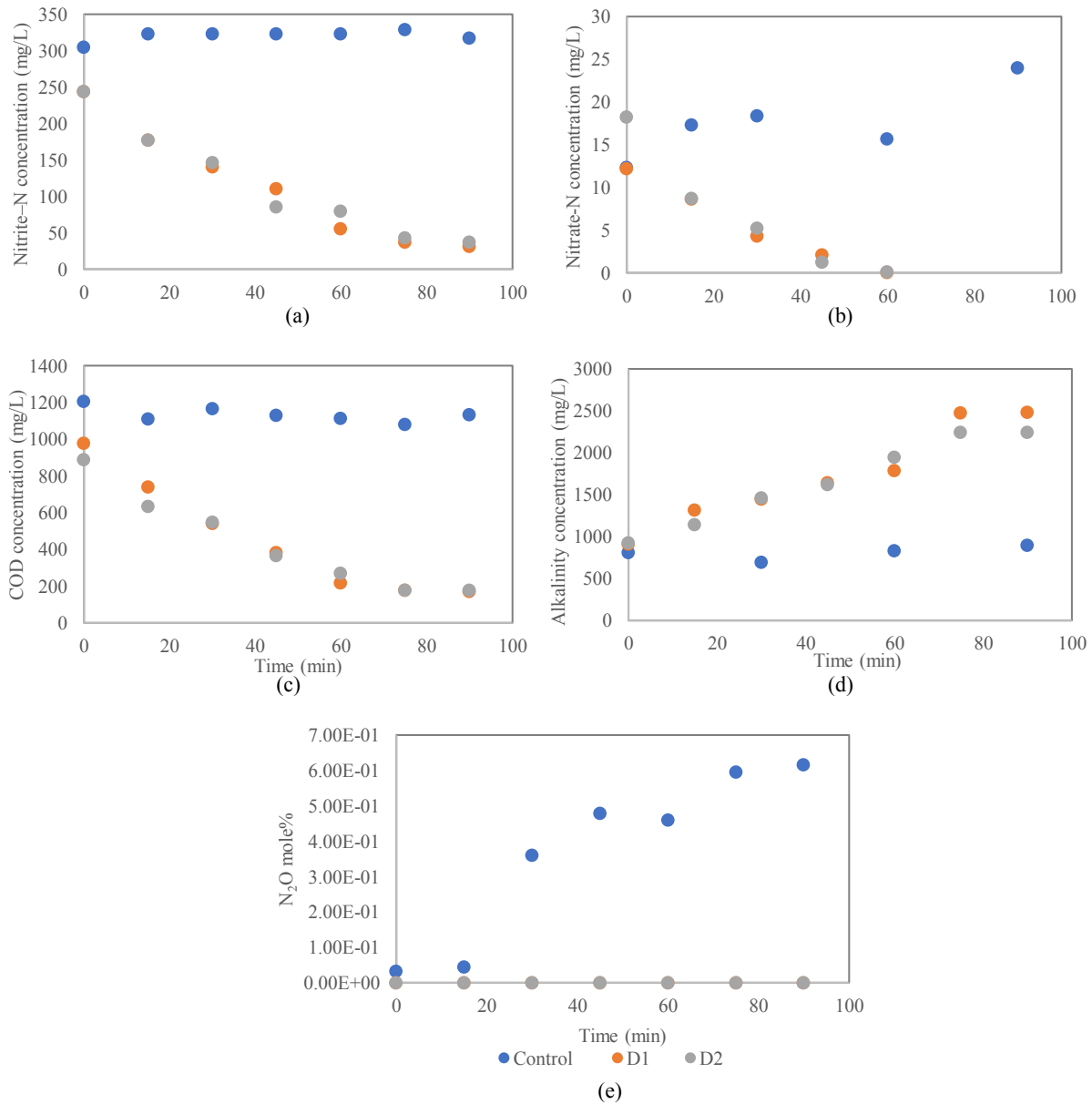


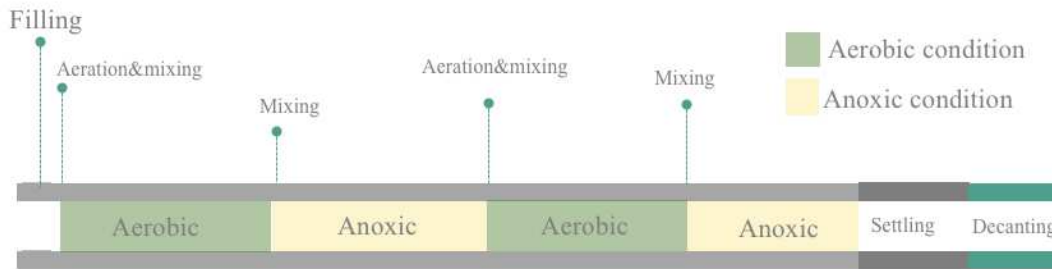
Figure 7.3. The kinetics of denitrification. (a) demonstrated the nitrite-nitrogen concentration changes; (b) demonstrated the nitrate-nitrogen changes; (c) and (d) demonstrated the COD concentration changes; and (e) the nitrous oxide content in the headspace.

### 7.3.3. The cycle test for the combined partial nitrification and denitrification system

To test the feasibility of combined partial nitrification and denitrification system in a single reactor treating raw supernatant without alkalinity addition, a cycle test was conducted. A mixture of

partial nitrification sludge and denitritation sludge was utilized for the cycle test. A combined system consisted of two aerobic-anoxic cycles (Figure 7.4). At the beginning of the reaction, 3L of the raw supernatant without alkalinity addition was added into the reactor. The  $\text{NH}_4^+ - \text{N}$  concentration was around 365 mg/L, the alkalinity concentration was 1330mg/L (Table 7.1). The first sequence of partial nitrification was happening under the aerobic condition, the inert alkalinity in the raw supernatant was utilized by the AOB to support the oxidation of ammonium to nitrite. During this process, the pH decreased. When the alkalinity almost depleted, the aeration was shut down, and the COD stock was added into the reactor. All these steps marked the beginning of the anoxic phase in which denitritation process might happen. During the denitritation process, the COD was utilized as electron donor to reduce the nitrite to nitrogen gas. Alkalinity was recovered during this process and led to the increase of pH. When the nitrite was consumed completely, the aerator was turned on again, and the second round of partial nitrification process started, followed by the second round of denitritation process. The concentrations of the  $\text{NH}_4^+ - \text{N}$ ,  $\text{NO}_2^- - \text{N}$ , alkalinity and COD at the beginning of the reaction and the end of each sequences were listed in Table 7.1. In summary, during the first partial nitrification sequence, 196 mg/L of the ammonium was oxidized, and 170.4 mg/L of nitrite was accumulated. Alkalinity dropped from 1425 to 187mg/L and pH dropped from 8.2 to 7.25 (or 7.1). During the first round of denitritation process, about 185 mg/L of the nitrite was reduced, 643.2 mg/L of COD was utilized, and 1153 mg/L of alkalinity was recovered. pH increased to 10. The second round of partial nitrification oxidized 146.5 mg/L of  $\text{NH}_4^+ - \text{N}$ , and 110mg/L of nitrite was accumulated, and consumed 920 mg/L of alkalinity. The second round of denitritation reactor reduced 91.3 mg/L nitrite, and produced 456mg/L alkalinity, and pH increased to 10. At the end of the second round denitritation process, the  $\text{NH}_4^+ - \text{N}$  concentration dropped to 0.5 mg/L. More than 99.8% of the ammonium was removed.  $\text{NO}_2^- - \text{N}$  concentration at the end of the reaction was about 21.3 mg/L, and no  $\text{NO}_3^- - \text{N}$

detected. The alkalinity concentration was around 875 mg/L (Table 7.1). For the future design of the pilot scale reactor, pH can be used as an effective controlling parameter.



**Figure 7.4.** the sequences of combined nitrification denitrification system.

**Table 7.1.** the changes in  $\text{NH}_4^+\text{-N}$ ,  $\text{NO}_2^-\text{-N}$ , Alkalinity and COD concentrations during the reaction in the combined system.

	Beginning	End of 1st nitrification	End of 1st denitrification	End of 2nd nitrification	End of 2nd denitrification
$\text{NH}_4^+\text{-N}$ (mg/L)	365	169	162	15	0.5
$\text{NO}_2^-\text{-N}$ (mg/L)	20	170	3	130	20
Alkalinity (mg/L)	1425	187	1340	420	875
COD (mg/L)	110	2 increased to 1000	300	24 increased to 248	27

#### 7.4. Conclusion

Due to the nature of the lagoon supernatant, the treatment of the supernatant was inhibited by the alkalinity deficiency. Recovery of alkalinity from the denitrification process would be one of the most economically feasible and environment-friendly option to solve the alkalinity shortage problem. The recovery of alkalinity was achievable by using the combined nitrification and denitrification in a single reactor system. The intermittent aeration created alternative aerobic and anoxic conditions for nitrification and denitrification processes, respectively. The addition of external carbon sources was required to support the denitrification process. More than 99% of the ammonium in the supernatant can be removed through the combined nitrification and denitrification process with

the addition of carbon sources. The results from this study provided guidelines for the construction and operation of larger scale reactors in the short future.

## 7.5. References

- APHA, 2011. Standard Methods for the Examination of Water and Wastewater. American Public Health Association, Washington, DC.
- Ciudad, G., Rubilar, O., Muñoz, P., Ruiz, G., Chamy, R., Vergara, C., Jeison, D., 2005. Partial nitrification of high ammonia concentration wastewater as a part of a shortcut biological nitrogen removal process. *Process Biochem.* 40, 1715–1719. <https://doi.org/10.1016/j.procbio.2004.06.058>
- Claros, J., Jiménez, E., Aguado, D., Ferrer, J., Seco, A., Serralta, J., 2013. Effect of pH and HNO<sub>2</sub> concentration on the activity of ammonia-oxidizing bacteria in a partial nitritation reactor. *Water Sci. Technol.* 67, 2587. <https://doi.org/10.2166/wst.2013.132>
- Domingo-Félez, C., Pellicer-Nàcher, C., Petersen, M.S., Jensen, M.M., Plósz, B.G., Smets, B.F., 2017. Heterotrophs are key contributors to nitrous oxide production in activated sludge under low C-to-N ratios during nitrification-Batch experiments and modeling: N<sub>2</sub>O Production in Nitrifying Batch Experiments. *Biotechnol. Bioeng.* 114, 132–140. <https://doi.org/10.1002/bit.26062>
- Gabarró, J., González-Cárcamo, P., Rusalleda, M., Ganigué, R., Gich, F., Balaguer, M.D., Colprim, J., 2014. Anoxic phases are the main N<sub>2</sub>O contributor in partial nitritation reactors treating high nitrogen loads with alternate aeration. *Bioresour. Technol.* 163, 92–99. <https://doi.org/10.1016/j.biortech.2014.04.019>
- Hellinga, C., Schellen, A., Mulder, J., Vanloosdrecht, M., Heijnen, J., 1998. The sharon process: An innovative method for nitrogen removal from ammonium-rich waste water. *Water Sci. Technol.* 37, 135–142. [https://doi.org/10.1016/S0273-1223\(98\)00281-9](https://doi.org/10.1016/S0273-1223(98)00281-9)

Savaglio, N., Puopolo, R. (Eds.), 2012. Denitrification: processes, regulation and ecological significance. Nova Science Publishers, New York.

Scherson, Y.D., Woo, S.-G., Criddle, C.S., 2014. Production of Nitrous Oxide From Anaerobic Digester Centrate and Its Use as a Co-oxidant of Biogas to Enhance Energy Recovery. Environ. Sci. Technol. 48, 5612–5619. <https://doi.org/10.1021/es501009j>

IPCC's Summary for Policymakers and Technical Summary of the Working Group I Report, 1995.

IPCC's Fourth Assessment Report – Errata, 2012.

## CHAPTER 8. CONCLUSIONS AND RECOMMENDATIONS

### 8.1. Thesis overview

Nitrogen removal is becoming increasingly challenging to meet the more and more stringent standards and regulations in wastewater treatment plants. Technology improvement is one of the options to facilitate the nitrogen removal efficiency. IFAS technology has been proved to be an economical feasible and environment-friendly retrofit option for the mainstream treatment. Upgrading the mainstream treatment to the IFAS system can enhance the nitrogen removal efficiency. 30% of the nitrogen loading to the plant originated from the anaerobically digested sludge liquor lagoon supernatant, due to the high ammonium concentration in the supernatant. Introduction of an effective side stream treatment of the lagoon supernatant can also ease the burden on the main stream treatment.

The capability of IFAS technology to handle the shock loading conditions was not tested in the local treatment plant. It is essential to understand the microbial community dynamics in response to shock loading and understand the relationship between the dynamics and the performance of the reactor. Furthermore, the side stream partial nitrification process was often used for the treatment of rejection water from the dewatering of the digested sludge. The rejection water was usually high temperature wastewater. The commercially available technologies took advantage the high temperature to achieve successful partial nitrification. Compared to the rejection water, the lagoon supernatant has lower temperature, which make the partial nitrification more challenging to achieve.

The research herein, tested the capability of the IFAS technology in handling the shocking loading for the mainstream treatment, and tested the feasibility of partial nitrification and denitrification processes for the side stream treatment using IFAS technology under room temperature. The impacts of feed water characteristics (the ammonium concentration and lagoon supernatant %) on

the establishment of the partial nitrification and microbial community dynamics were evaluated. Besides, the physiochemical properties of EPS samples from conventional nitrification and partial nitrification were also compared. The experience and results that obtained from the project provided valuable information for the application of IFAS technology and partial nitrification and denitrification for the high ammonium strength lagoon supernatant treatment.

## **8.2. Conclusions**

Several conclusions were drawn through this research.

In terms of the IFAS technology, the IFAS-SBR was robust in removing COD and ammonia nitrogen in wastewater. Around 99% ammonia nitrogen removal and 92 to 98% COD removal were achieved during reactor operation.

The ammonium utilization by microorganisms is strongly related to the influent C/N ratio. Lower C/N ratio (<5:1) favors the oxidation of ammonium due to (i) a reduced biofilm thickness, which facilitated oxygen diffusion and material transfer in the biofilm, or (ii) reduced competition pressure among bacteria. However, the denitrification might be negatively affected by the insufficient microbial denitrification activity in the reactor when the C/N ratio was low. The q-PCR results indicated that the biofilm was a more favorable habitat than activated sludge for nitrifying bacteria when the C/N ratio was low.

For the side stream treatment, partial nitrification achieved greater than 97% ammonium removal with influent  $\text{NH}_4^+\text{-N}$  concentration of 800 mg/L in a laboratory scale IFAS. NOB was successfully inhibited when influent  $\text{NH}_4^+\text{-N}$  concentration was greater than 400mg/L. Ammonium removal was achieved mainly by the suspended sludge (66%), as compared to the biofilm (34%), which may be attributed to the higher AOB density in the sludge.

The feed characteristics affected the microbial community composition in an IFAS reactor. The  $\text{NH}_4^+\text{-N}$  concentration in the feed was the most important factor affecting the microbial community compositions in the flocs and biofilm. The ammonium concentration negatively affected the diversity of the microbial community in both biofilm and flocs, while the raw supernatant percentage positively correlated to the diversity of the microbial communities.

Besides, the microbial community structure in the suspended flocs differed from that in the biofilm. The ammonium concentration was positively related to the specific ammonium removal rate and the quantity of AOB functional genes/mg biomass in the reactor; while the raw supernatant percentage was negatively related to the kinetics and quantity of AOB/mg biomass. In the IFAS system, the flocs played a major role for the partial nitrification but was less resistant than the biofilm when raw supernatant was introduced as the feed.

For the mainstream treatment, EPS worked as a double-edged sword in the performance of the IFAS-SBR reactor. On one hand, more EPS produced could improve the development of nitrifying biofilm and prevent the detachment of biofilm. On the other hand, thicker biofilm would result in stronger diffusion resistance and lower the mass transfer of nutrients and oxygen in biofilm and led to inefficient removal of organic compounds and ammonia nitrogen. Therefore, control of the biofilm thickness and the EPS production was important for successful application of an IFAS-SBR to wastewater treatment.

Further, the physiochemical characteristics of EPS from the conventional nitrification and partial nitrification were compared. The relationship between the EPS composition and the microbial community composition of the suspended flocs and attached biofilm was explored. The partial nitrification was attributed to the proliferation of AOB and the elimination of NOB. A higher AOB abundance was related to higher aromatic protein and tryptophan protein like substances in TB-



EPS. EPS adsorption to solid surface relied more on the TB-EPS, rather than the LB-EPS, as the former contained more protein.

The combined single system nitritation-denitritation process was applicable by using alternative aeration and external organic carbon addition. The combined processes can achieve 99% of the ammonium removal with addition of external carbon sources. The alkalinity that recovered from the denitritation can support the nitritation process when treating alkalinity deficient digested sludge liquor lagoon supernatant.

### **8.3. recommendations**

There are some recommendations for future studies:

1. A detailed cost evaluation of the nitritation-denitritation process on treating the high ammonium strength lagoon supernatant in full scale is recommended.
2. Combination of nitritation and anammox processes can save up to more than 60% of the oxygen requirements and 100% of the carbon sources. It is recommended to also test the feasibility of nitritation anammox processes and compare the cost for the nitritation-denitritation and nitritation-anammox processes.
3. Inhibition of raw supernatant on the nitrifiers was detected in this study. The impact of specific heavy metals and solids content on the nitritation processes is recommended for further investigation.
4. Future studies are also recommended focusing on the comparison of different types of carbon sources that added for the denitritation process, especially the volatile fatty acid, due to its complexity and availability at the wastewater treatment plant.

5. Further studies on the impacts of low temperature on the stability of nitrification-denitrification processes and the reaction kinetics are highly recommended, which will be valuable for the application of the processes during Canada's cold weather.
6. Further studies are recommended to delineate the complex nature of EPS production of specific organisms, especially nitrifying organisms, in the nitrifying flocs and biofilm.
7. The model for the combined processes and on the nitrous oxide production is also a recommended topic of future study.

## BIBLIOGRAPHY

- Adair, K.L., Schwartz, E., 2008. Evidence that Ammonia-Oxidizing Archaea are More Abundant than Ammonia-Oxidizing Bacteria in Semiarid Soils of Northern Arizona, USA. *Microb. Ecol.* 56, 420–426. <https://doi.org/10.1007/s00248-007-9360-9>
- Ahn, J.H., Kwan, T., Chandran, K., 2011. Comparison of Partial and Full Nitrification Processes Applied for Treating High-Strength Nitrogen Wastewaters: Microbial Ecology through Nitrous Oxide Production. *Environ. Sci. Technol.* 45, 2734–2740. <https://doi.org/10.1021/es103534g>
- Ahn, Y.-H., 2006. Sustainable nitrogen elimination biotechnologies: A review. *Process Biochem.* 41, 1709–1721. <https://doi.org/10.1016/j.procbio.2006.03.033>
- Alberta, Water Management Division, Alberta, Environmental Sciences Division, 1999. Surface water quality guidelines for use in Alberta. Alberta Environment, Environmental Sciences Division, Edmonton.
- Ali, M., Chai, L.-Y., Min, X.-B., Tang, C.-J., Afrin, S., Liao, Q., Wang, H.-Y., Peng, C., Song, Y.-X., Zheng, P., 2016. Performance and characteristics of a nitrification air-lift reactor under long-term HRT shortening. *International Biodeterioration & Biodegradation* 111, 45–53. <https://doi.org/10.1016/j.ibiod.2016.04.003>
- American Water Works Association (Ed.), 2006. Fundamentals and control of nitrification in chloraminated drinking water distribution systems, 1st ed. ed, AWWA manual. American Water Works Association, Denver, CO.
- Anthonisen, A.C., Loehr, R.C., Prakasam, T.B.S., Srinath, E.G., 1976. Inhibition of Nitrification by Ammonia and Nitrous Acid. *J. Water Pollut. Control Fed.* 48, 835–852.
- APHA, 2011. Standard Methods for the Examination of Water and Wastewater. American Public Health Association, Washington, DC.
- Aslan, S., Dahab, M., 2008. Nitrification and denitrification of ammonium-rich wastewater using fluidized-bed biofilm reactors. *J. Hazard. Mater.* 156, 56–63. <https://doi.org/10.1016/j.jhazmat.2007.11.112>

- Bai, Y., Sun, Q., Wen, D., Tang, X., 2012. Abundance of ammonia-oxidizing bacteria and archaea in industrial and domestic wastewater treatment systems. *FEMS Microbiol. Ecol.* 80, 323–330. <https://doi.org/10.1111/j.1574-6941.2012.01296.x>
- Balderrama-Subieta, A., Quillaguamán, J., 2013. Genomic studies on nitrogen metabolism in *Halomonas boliviensis*: Metabolic pathway, biochemistry and evolution. *Comput. Biol. Chem.* 47, 96–104. <https://doi.org/10.1016/j.compbiolchem.2013.08.002>
- Bartossek, R., Nicol, G.W., Lanzen, A., Klenk, H.-P., Schleper, C., 2010. Homologues of nitrite reductases in ammonia-oxidizing archaea: diversity and genomic context: Nitrite reductase of soil archaea. *Environ. Microbiol.* 12, 1075–1088. <https://doi.org/10.1111/j.1462-2920.2010.02153.x>
- Bartossek, R., Spang, A., Weidler, G., Lanzen, A., Schleper, C., 2012. Metagenomic Analysis of Ammonia-Oxidizing Archaea Affiliated with the Soil Group. *Front. Microbiol.* 3. <https://doi.org/10.3389/fmicb.2012.00208>
- Bassin, J.P., Kleerebezem, R., Rosado, A.S., van Loosdrecht, M.C.M., Dezotti, M., 2012. Effect of Different Operational Conditions on Biofilm Development, Nitrification, and Nitrifying Microbial Population in Moving-Bed Biofilm Reactors. *Environ. Sci. Technol.* 46, 1546–1555. <https://doi.org/10.1021/es203356z>
- Bella, G.D., Trapani, D.D., Freni, G., Torregrossa, M., Viviani, G., 2014. Analysis of biomass characteristics in mbr and mb-mbr systems fed with synthetic wastewater: influence of a gradual salinity increase. *Chem. Eng. Trans.* 445–450. <https://doi.org/10.3303/CET1438075>
- Beneš, P., Paulenová, M., 1973. Surface charge and adsorption properties of polyethylene in aqueous solutions of inorganic electrolytes. *Kolloid-Zeitschrift und Zeitschrift für Polymere* 251, 766–771. <https://doi.org/10.1007/BF01499104>

- Blackburne, R., Vadivelu, V.M., Yuan, Z., Keller, J., 2007. Kinetic characterisation of an enriched Nitrospira culture with comparison to Nitrobacter. *Water Research* 41, 3033–3042. <https://doi.org/10.1016/j.watres.2007.01.043>
- Borchert, J., Hubbell, S., Rupp, H., 2011. Demonstration of IFAS Technology for Cold Temperature Nitrification in Lagoon WWTFs at Clare and Ludington, Michigan. *Proc. Water Environ. Fed.* 2011, 5257–5264. <https://doi.org/10.2175/193864711802765705>
- Bothe, H., Ferguson, S.J., Newton, W.E. (Eds.), 2007. *Biology of the nitrogen cycle*, 1st ed. ed. Elsevier, Amsterdam ; Boston.
- Bradford, M.M., 1976. A rapid and sensitive method for the quantitation of microgram quantities of protein utilizing the principle of protein-dye binding. *Anal. Biochem.* UK.
- Brdjanovic, D., Slamet, A., Van Loosdrecht, M.C.M., Hooijmans, C.M., Alaerts, G.J., Heijnen, J.J., 1998. IMPACT OF EXCESSIVE AERATION ON BIOLOGICAL PHOSPHORUS REMOVAL FROM WASTEWATER. *Water Res.* 32, 200–208. [https://doi.org/10.1016/S0043-1354\(97\)00183-8](https://doi.org/10.1016/S0043-1354(97)00183-8)
- Brouwer, M., Loosdrecht, M., Heijnen, J., 1996. One reactor system for ammonium removal via nitrite, STOWA. ed. Utrecht, The Netherlands.
- Caporaso, J.G., Kuczynski, J., Stombaugh, J., Bittinger, K., Bushman, F.D., Costello, E.K., Fierer, N., Peña, A.G., Goodrich, J.K., Gordon, J.I., Huttley, G.A., Kelley, S.T., Knights, D., Koenig, J.E., Ley, R.E., Lozupone, C.A., McDonald, D., Muegge, B.D., Pirrung, M., Reeder, J., Sevinsky, J.R., Turnbaugh, P.J., Walters, W.A., Widmann, J., Yatsunenko, T., Zaneveld, J., Knight, R., 2010. QIIME allows analysis of high-throughput community sequencing data. *Nat. Methods* 7, 335–336. <https://doi.org/10.1038/nmeth.f.303>
- Chandrasekaran, N., Dimartino, S., Fee, C.J., 2013. Study of the adsorption of proteins on stainless steel surfaces using QCM-D. *Chemical Engineering Research and Design* 91, 1674–1683. <https://doi.org/10.1016/j.cherd.2013.07.017>

- Chen, W., Westerhoff, P., Leenheer, J.A., Booksh, K., 2003. Fluorescence Excitation–Emission Matrix Regional Integration to Quantify Spectra for Dissolved Organic Matter. *Environmental Science & Technology* 37, 5701–5710. <https://doi.org/10.1021/es034354c>
- Cho, S., Fujii, N., Lee, T., Okabe, S., 2011. Development of a simultaneous partial nitrification and anaerobic ammonia oxidation process in a single reactor. *Bioresour. Technol.* 102, 652–659. <https://doi.org/10.1016/j.biortech.2010.08.031>
- Choi, E., 2007. Piggery waste management: towards a sustainable future. IWA Publ, London.
- Choi, J., Hwang, G., Gamal El-Din, M., Liu, Y., 2014. Effect of reactor configuration and microbial characteristics on biofilm reactors for oil sands process-affected water treatment. *Int. Biodeterior. Biodegrad.* 89, 74–81. <https://doi.org/10.1016/j.ibiod.2014.01.008>
- Christensson, M., Ekström, S., Chan, A.A., Le Vaillant, E., Lemaire, R., 2013. Experience from start-ups of the first ANITA Mox Plants. *Water Sci. Technol.* 67, 2677. <https://doi.org/10.2166/wst.2013.156>
- Christensson, M., Ekström, S., Lemaire, R., Le Vaillant, E., Bundgaard, E., Chauzy, J., Stålhandske, L., Hong, Z., Ekenberg, M., 2011. ANITA™ Mox – A BioFarm Solution for Fast Start-up of Deammonifying MBBRs. *Proc. Water Environ. Fed.* 2011, 265–282. <https://doi.org/10.2175/193864711802639309>
- Ciudad, G., Rubilar, O., Muñoz, P., Ruiz, G., Chamy, R., Vergara, C., Jeison, D., 2005. Partial nitrification of high ammonia concentration wastewater as a part of a shortcut biological nitrogen removal process. *Process Biochem.* 40, 1715–1719. <https://doi.org/10.1016/j.procbio.2004.06.058>
- Claros, J., Jiménez, E., Aguado, D., Ferrer, J., Seco, A., Serralta, J., 2013. Effect of pH and HNO<sub>2</sub> concentration on the activity of ammonia-oxidizing bacteria in a partial nitritation reactor. *Water Sci. Technol.* 67, 2587. <https://doi.org/10.2166/wst.2013.132>
- Copithron, R.R., Sturdevant, J., Farren, G., Sen, D., 2006. Case study of an IFAS system-Over 10 years of experience. *Water Environ. Found.* 4309–4324.

- Daims, H., Lebedeva, E.V., Pjevac, P., Han, P., Herbold, C., Albertsen, M., Jehmlich, N., Palatinszky, M., Vierheilig, J., Bulaev, A., Kirkegaard, R.H., von Bergen, M., Rattei, T., Bendinger, B., Nielsen, P.H., Wagner, M., 2015. Complete nitrification by *Nitrospira* bacteria. *Nature* 528, 504–509. <https://doi.org/10.1038/nature16461>
- Desloover, J., De Clippeleir, H., Boeckx, P., Du Laing, G., Colsen, J., Verstraete, W., Vlaeminck, S.E., 2011. Floc-based sequential partial nitritation and anammox at full scale with contrasting N<sub>2</sub>O emissions. *Water Res.* 45, 2811–2821. <https://doi.org/10.1016/j.watres.2011.02.028>
- Desloover, J., Vlaeminck, S.E., Clauwaert, P., Verstraete, W., Boon, N., 2012. Strategies to mitigate N<sub>2</sub>O emissions from biological nitrogen removal systems. *Curr. Opin. Biotechnol.* 23, 474–482. <https://doi.org/10.1016/j.copbio.2011.12.030>
- Di Trapani, D., Christensson, M., Torregrossa, M., Viviani, G., Ødegaard, H., 2013. Performance of a hybrid activated sludge/biofilm process for wastewater treatment in a cold climate region: Influence of operating conditions. *Biochem. Eng. J.* 77, 214–219. <https://doi.org/10.1016/j.bej.2013.06.013>
- Digester Centrate and Its Use as a Co-oxidant of Biogas to Enhance Energy Recovery. *Environ. Sci. Technol.* 48, 5612–5619. <https://doi.org/10.1021/es501009j>
- Domingo-Félez, C., Pellicer-Nàcher, C., Petersen, M.S., Jensen, M.M., Plósz, B.G., Smets, B.F., 2017. Heterotrophs are key contributors to nitrous oxide production in activated sludge under low C-to-N ratios during nitrification-Batch experiments and modeling: N<sub>2</sub>O Production in Nitrifying Batch Experiments. *Biotechnol. Bioeng.* 114, 132–140. <https://doi.org/10.1002/bit.26062>
- Dong, H., Zhang, K., Han, X., Du, B., Wei, Q., Wei, D., 2017. Achievement, performance and characteristics of microbial products in a partial nitrification sequencing batch reactor as a pretreatment for anaerobic ammonium oxidation. *Chemosphere* 183, 212–218. <https://doi.org/10.1016/j.chemosphere.2017.05.119>

- Duan, H., Ye, L., Erler, D., Ni, B.-J., Yuan, Z., 2017. Quantifying nitrous oxide production pathways in wastewater treatment systems using isotope technology – A critical review. *Water Res.* 122, 96–113. <https://doi.org/10.1016/j.watres.2017.05.054>
- DuBois, M., Gilles, K.A., Hamilton, J.K., Rebers, P.A., Smith, F., 1956. Colorimetric Method for Determination of Sugars and Related Substances. *Anal. Chem.* 28, 350–356. <https://doi.org/10.1021/ac60111a017>
- EPA, 1999. Wastewater Technology Fact Sheet Sequencing Batch Reactors.
- EPCOR Water Services Inc., 2017. Gold Bar Wastewater Treatment Plant 2016 Wastewater Treatment Annual Report.
- Esparza-Soto, M., Westerhoff, P., 2003. Biosorption of humic and fulvic acids to live activated sludge biomass. *Water Res.* 37, 2301–2310. [https://doi.org/10.1016/S0043-1354\(02\)00630-9](https://doi.org/10.1016/S0043-1354(02)00630-9)
- Feng, Q., Cao, J., Chen, L., Guo, C.-Y., Tan, J., Xu, H., 2011. Simultaneous nitrification and denitrification at variable C/N ratio in aerobic granular sequencing batch reactors. *J. Food Agric. Environ.* 9, 1131–1136.
- Flemming, H.-C., Neu, T.R., Wozniak, D.J., 2007. The EPS Matrix: The “House of Biofilm Cells.” *J. Bacteriol.* 189, 7945–7947. <https://doi.org/10.1128/JB.00858-07>
- Francis, C.A., Roberts, K.J., Beman, J.M., Santoro, A.E., Oakley, B.B., 2005. Ubiquity and diversity of ammonia-oxidizing archaea in water columns and sediments of the ocean. *Proc. Natl. Acad. Sci.* 102, 14683–14688. <https://doi.org/10.1073/pnas.0506625102>
- Freitag, A., Rudert, M., Bock, E., 1987. Growth of *Nitrobacter* by dissimilatory nitrate reduction. *FEMS Microbiol. Lett.* 48, 105–109. <https://doi.org/10.1111/j.1574-6968.1987.tb02524.x>
- Frison, N., Chiumenti, A., Katsou, E., Malamis, S., Bolzonella, D., Fatone, F., 2015. Mitigating off-gas emissions in the biological nitrogen removal via nitrite process treating anaerobic effluents. *J. Clean. Prod.* 93, 126–133. <https://doi.org/10.1016/j.jclepro.2015.01.017>



- Frølund, B., Palmgren, R., Keiding, K., Nielsen, P.H., 1996. Extraction of extracellular polymers from activated sludge using a cation exchange resin. *Water Research* 30, 1749–1758. [https://doi.org/10.1016/0043-1354\(95\)00323-1](https://doi.org/10.1016/0043-1354(95)00323-1)
- Furumai, H., Rittmann, B.E., 1994. Interpretation of bacterial activities in nitrification filters by a biofilm model considering the kinetics of soluble microbial products. *Water Sci. Technol.* U. K.
- Fux, C., Velten, S., Carozzi, V., Solley, D., Keller, J., 2006. Efficient and stable nitrification and denitrification of ammonium-rich sludge dewatering liquor using an SBR with continuous loading. *Water Res.* 40, 2765–2775. <https://doi.org/10.1016/j.watres.2006.05.003>
- Gabarró, J., Ganigué, R., Gich, F., Rusalleda, M., Balaguer, M.D., Colprim, J., 2012. Effect of temperature on AOB activity of a partial nitrification SBR treating landfill leachate with extremely high nitrogen concentration. *Bioresource Technology* 126, 283–289. <https://doi.org/10.1016/j.biortech.2012.09.011>
- Gabarró, J., González-Cárcamo, P., Rusalleda, M., Ganigué, R., Gich, F., Balaguer, M.D., Colprim, J., 2014. Anoxic phases are the main N<sub>2</sub>O contributor in partial nitrification reactors treating high nitrogen loads with alternate aeration. *Bioresour. Technol.* 163, 92–99. <https://doi.org/10.1016/j.biortech.2014.04.019>
- Ge, S., Peng, Y., Qiu, S., Zhu, A., Ren, N., 2014. Complete nitrogen removal from municipal wastewater via partial nitrification by appropriately alternating anoxic/aerobic conditions in a continuous plug-flow step feed process. *Water Res.* 55, 95–105. <https://doi.org/10.1016/j.watres.2014.01.058>
- Glass, C., Silverstein, J., Oh, J., 1997. Inhibition of Denitrification in Activated Sludge by Nitrite. *Water Environ. Res.* 69, 1086–1093.
- Gong, Z., Liu, S., Yang, F., Bao, H., Furukawa, K., 2008. Characterization of functional microbial community in a membrane-aerated biofilm reactor operated for completely autotrophic

- nitrogen removal. *Bioresour. Technol.* 99, 2749–2756.  
<https://doi.org/10.1016/j.biortech.2007.06.040>
- Guellil, A., Thomas, F., Block, J.-C., Bersillon, J.-L., Ginestet, P., 2001. Transfer of organic matter between wastewater and activated sludge flocs. *Water Research* 35, 143–150.  
[https://doi.org/10.1016/S0043-1354\(00\)00240-2](https://doi.org/10.1016/S0043-1354(00)00240-2)
- Guo, J., Peng, Y., Huang, H., Wang, S., Ge, S., Zhang, J., Wang, Z., 2010. Short- and long-term effects of temperature on partial nitrification in a sequencing batch reactor treating domestic wastewater. *J. Hazard. Mater.* 179, 471–479. <https://doi.org/10.1016/j.jhazmat.2010.03.027>
- Guo, J., Peng, Y., Wang, S., Zheng, Y., Huang, H., Wang, Z., 2009. Long-term effect of dissolved oxygen on partial nitrification performance and microbial community structure. *Bioresour. Technol.* 100, 2796–2802. <https://doi.org/10.1016/j.biortech.2008.12.036>
- Guo, J.H., Peng, Y.Z., Wang, S.Y., Zheng, Y.N., Huang, H.J., Ge, S.J., 2009. Effective and robust partial nitrification to nitrite by real-time aeration duration control in an SBR treating domestic wastewater. *Process Biochem.* 44, 979–985.  
<https://doi.org/10.1016/j.procbio.2009.04.022>
- Gustavsson, D.J.I., 2010. Biological sludge liquor treatment at municipal wastewater treatment plants – a review. *Vatten* 66, 179–192.
- Güven, D., 2009. Effects of Different Carbon Sources on Denitrification Efficiency Associated with Culture Adaptation and C/N Ratio. *CLEAN - Soil Air Water* 37, 565–573.  
<https://doi.org/10.1002/clen.200800198>
- Haandel, A. van, Lubbe, J. van der, 2012. *Handbook of biological wastewater treatment*, 2. ed. ed. IWA Publ, London.
- Hao, O.J., Chen, J.M., 1994. Factors Affecting Nitrite Buildup in Submerged Filter System. *J. Environ. Eng.* 120, 1298–1307. [https://doi.org/10.1061/\(ASCE\)0733-9372\(1994\)120:5\(1298\)](https://doi.org/10.1061/(ASCE)0733-9372(1994)120:5(1298))

- He, J., Shen, J., Zhang, L., Zhu, Y., Zheng, Y., Xu, M., Di, H., 2007. Quantitative analyses of the abundance and composition of ammonia-oxidizing bacteria and ammonia-oxidizing archaea of a Chinese upland red soil under long-term fertilization practices. *Environ. Microbiol.* 9, 2364–2374. <https://doi.org/10.1111/j.1462-2920.2007.01358.x>
- Health Association, Washington, DC.
- Hellinga, C., Schellen, A., Mulder, J., Vanloosdrecht, M., Heijnen, J., 1998. The sharon process: An innovative method for nitrogen removal from ammonium-rich waste water. *Water Sci. Technol.* 37, 135–142. [https://doi.org/10.1016/S0273-1223\(98\)00281-9](https://doi.org/10.1016/S0273-1223(98)00281-9)
- Hempel, M., Grossart, H., Gross, E., 2009. Community composition of bacterial biofilms on two submerged macrophytes and an artificial substrate in a pre-alpine lake. *Aquat. Microb. Ecol.* 58, 79–94. <https://doi.org/10.3354/ame01353>
- Higgins, M.J., Novak, J.T., 1997. Characterization of Exocellular Protein and Its Role in Bioflocculation. *Journal of Environmental Engineering* 123, 479–485. [https://doi.org/10.1061/\(ASCE\)0733-9372\(1997\)123:5\(479\)](https://doi.org/10.1061/(ASCE)0733-9372(1997)123:5(479))
- Hu, S., 1990. Acute Substrate-intermediate-product Related Inhibition of Nitrifiers. Purdue University.
- Huang, C., Shi, Y., Gamal El-Din, M., Liu, Y., 2015. Treatment of oil sands process-affected water (OSPW) using ozonation combined with integrated fixed-film activated sludge (IFAS). *Water Res.* 85, 167–176. <https://doi.org/10.1016/j.watres.2015.08.019>
- Huang, C., Shi, Y., Gamal El-Din, M., Liu, Y., 2016. Optimization of ozonation combined with integrated fixed-film activated sludge (IFAS) in the treatment of oil sands process-affected water (OSPW). *International Biodeterioration & Biodegradation* 112, 31–41. <https://doi.org/10.1016/j.ibiod.2016.04.037>
- Huang, C., Shi, Y., Sheng, Z., Gamal El-Din, M., Liu, Y., 2017. Characterization of microbial communities during start-up of integrated fixed-film activated sludge (IFAS) systems for

- the treatment of oil sands process-affected water (OSPW). *Biochem. Eng. J.* 122, 123–132.  
<https://doi.org/10.1016/j.bej.2017.03.003>
- Hwang, G., Kang, S., El-Din, M.G., Liu, Y., 2012. Impact of an extracellular polymeric substance (EPS) precoating on the initial adhesion of *Burkholderia cepacia* and *Pseudomonas aeruginosa*. *Biofouling* 28, 525–538. <https://doi.org/10.1080/08927014.2012.694138>
- Hwang, G., Liang, J., Kang, S., Tong, M., Liu, Y., 2013. The role of conditioning film formation in *Pseudomonas aeruginosa* PAO1 adhesion to inert surfaces in aquatic environments. *Biochemical Engineering Journal* 76, 90–98. <https://doi.org/10.1016/j.bej.2013.03.024>
- IPCC's Fourth Assessment Report – Errata, 2012.
- IPCC's Summary for Policymakers and Technical Summary of the Working Group I Report, 1995.
- Jacobsen, B.N., Arvin, E., Reinders, M., 1996. Factors affecting sorption of pentachlorophenol to suspended microbial biomass. *Water Research* 30, 13–20. [https://doi.org/10.1016/0043-1354\(95\)00108-W](https://doi.org/10.1016/0043-1354(95)00108-W)
- Jeyanayagam, S., 2005. True confessions of the biological nutrient removal process. *Fla. Water Resour. J.* 37–46.
- Johnson, T.L., McQuarrie, J.P., 2002. IFAS BNR Full-scale Design and Performance Challenges. *Proc. Water Environ. Fed.* 2002, 214–226.  
<https://doi.org/10.2175/193864702784249105>
- Johnson, T.L., Wallis-Lage, C.L., Shaw, A.R., McQuarrie, J.P., 2005. IFAS OPTIONS – WHICH ONE IS RIGHT FOR YOUR PROJECT? *Proc. Water Environ. Fed.* 2005, 6290–6300.  
<https://doi.org/10.2175/193864705783815069>
- Kapoor, V., Li, X., Elk, M., Chandran, K., Impellitteri, C.A., Santo Domingo, J.W., 2015. Impact of Heavy Metals on Transcriptional and Physiological Activity of Nitrifying Bacteria. *Environ. Sci. Technol.* 49, 13454–13462. <https://doi.org/10.1021/acs.est.5b02748>
- Kim, H., Schuler, A.J., Gunsch, C.K., Pei, R., Gellner, J., Boltz, J.P., Freudenberg, R.G., Dodson, R., 2011. Comparison of Conventional and Integrated Fixed-Film Activated Sludge Systems: Attached- and Suspended-Growth Functions and Quantitative Polymerase Chain

- Reaction Measurements. *Water Environ. Res.* 83, 627–635.  
<https://doi.org/10.2175/106143010X12851009156448>
- Kim, H., Schuler, A.J., Gunsch, C.K., Pei, R., Gellner, J., Boltz, J.P., Freudenberg, R.G., Dodson, R., 2011. Comparison of Conventional and Integrated Fixed-Film Activated Sludge Systems: Attached- and Suspended-Growth Functions and Quantitative Polymerase Chain Reaction Measurements. *Water Environment Research* 83, 627–635.  
<https://doi.org/10.2175/106143010X12851009156448>
- Kim, Y.M., Lee, D.S., Park, C., Park, D., Park, J.M., 2011. Effects of free cyanide on microbial communities and biological carbon and nitrogen removal performance in the industrial activated sludge process. *Water Res.* 45, 1267–1279.  
<https://doi.org/10.1016/j.watres.2010.10.003>
- Koops, H.-P., Purkhold, U., Pommerening-Röser, A., Timmermann, G., Wagner, M., 2006. The Lithoautotrophic Ammonia-Oxidizing Bacteria, in: Dworkin, M., Falkow, S., Rosenberg, E., Schleifer, K.-H., Stackebrandt, E. (Eds.), *The Prokaryotes*. Springer New York, New York, NY, pp. 778–811. [https://doi.org/10.1007/0-387-30745-1\\_36](https://doi.org/10.1007/0-387-30745-1_36)
- Kouba, V., Catrysse, M., Stryjova, H., Jonatova, I., Volcke, E.I.P., Svehla, P., Bartacek, J., 2014. The impact of influent total ammonium nitrogen concentration on nitrite-oxidizing bacteria inhibition in moving bed biofilm reactor. *Water Science & Technology* 69, 1227.  
<https://doi.org/10.2166/wst.2013.757>
- Kowalski, M.S., Devlin, T.R., Oleszkiewicz, J.A., 2018. Start-up and long-term performance of anammox moving bed biofilm reactor seeded with granular biomass. *Chemosphere* 200, 481–486. <https://doi.org/10.1016/j.chemosphere.2018.02.130>
- Kozlowski, J.A., Stieglmeier, M., Schleper, C., Klotz, M.G., Stein, L.Y., 2016. Pathways and key intermediates required for obligate aerobic ammonia-dependent chemolithotrophy in bacteria and Thaumarchaeota. *ISME J.* 10, 1836–1845.  
<https://doi.org/10.1038/ismej.2016.2>

- Kuai, L., Verstraete, W., 1998. Ammonium Removal by the Oxygen-Limited Autotrophic Nitrification-Denitrification System. *Appl. Environ. Microbiol.* 64, 4500–4506.
- Kulikowska, D., Bernat, K., 2013. Nitritation–denitritation in landfill leachate with glycerine as a carbon source. *Bioresour. Technol.* 142, 297–303.  
<https://doi.org/10.1016/j.biortech.2013.04.119>
- Lackner, S., Gilbert, E.M., Vlaeminck, S.E., Joss, A., Horn, H., van Loosdrecht, M.C.M., 2014. Full-scale partial nitritation/anammox experiences – An application survey. *Water Res.* 55, 292–303. <https://doi.org/10.1016/j.watres.2014.02.032>
- Lee, L., 2004. Biofilm morphology and nitrification activities: recovery of nitrifying biofilm particles covered with heterotrophic outgrowth. *Bioresour. Technol.* 95, 209–214.  
<https://doi.org/10.1016/j.biortech.2003.05.004>
- Lee, Y.-W., Ong, S.-K., Sato, C., 1997. Effects of heavy metals on nitrifying bacteria. *Water Sci. Technol.* 36. [https://doi.org/10.1016/S0273-1223\(97\)00730-0](https://doi.org/10.1016/S0273-1223(97)00730-0)
- Leininger, S., Urich, T., Schloter, M., Schwark, L., Qi, J., Nicol, G.W., Prosser, J.I., Schuster, S.C., Schleper, C., 2006. Archaea predominate among ammonia-oxidizing prokaryotes in soils. *Nature* 442, 806–809. <https://doi.org/10.1038/nature04983>
- Lemaire, R., Thesing, G., Christensson, M., Zhao, H., Liviano, I., 2013. Experience from Start-up and Operation of Deammonification MBBR Plants, and Testing of a New Deammonification IFAS Configuration. *Proc. Water Environ. Fed.* 2013, 1926–1947.  
<https://doi.org/10.2175/193864713813673857>
- Liang, Z., Li, W., Yang, S., Du, P., 2010. Extraction and structural characteristics of extracellular polymeric substances (EPS), pellets in autotrophic nitrifying biofilm and activated sludge. *Chemosphere* 81, 626–632. <https://doi.org/10.1016/j.chemosphere.2010.03.043>
- Liu, H., Fang, H.H.P., 2002. Extraction of extracellular polymeric substances (EPS) of sludges. *J. Biotechnol.* 95, 249–256. [https://doi.org/10.1016/S0168-1656\(02\)00025-1](https://doi.org/10.1016/S0168-1656(02)00025-1)

- Liu, T., Mao, Y., Shi, Y., Quan, X., 2017. Start-up and bacterial community compositions of partial nitrification in moving bed biofilm reactor. *Appl. Microbiol. Biotechnol.* 101, 2563–2574. <https://doi.org/10.1007/s00253-016-8003-9>
- Mahendran, B., Lishman, L., Liss, S.N., 2012. Structural, physicochemical and microbial properties of flocs and biofilms in integrated fixed-film activated sludge (IFFAS) systems. *Water Res.* 46, 5085–5101. <https://doi.org/10.1016/j.watres.2012.05.058>
- Massara, T.M., Malamis, S., Guisasola, A., Baeza, J.A., Noutsopoulos, C., Katsou, E., 2017. A review on nitrous oxide (N<sub>2</sub>O) emissions during biological nutrient removal from municipal wastewater and sludge reject water. *Sci. Total Environ.* 596–597, 106–123. <https://doi.org/10.1016/j.scitotenv.2017.03.191>
- McIlroy, S.J., Saunders, A.M., Albertsen, M., Nierychlo, M., McIlroy, B., Hansen, A.A., Karst, S.M., Nielsen, J.L., Nielsen, P.H., 2015. MiDAS: the field guide to the microbes of activated sludge. *Database* 2015, bav062. <https://doi.org/10.1093/database/bav062>
- Metcalf, Eddy, 2003. *Wastewater Engineering, Treatment and Reuse*, 4th ed. McGraw-Hill, New York.
- Milici, M., Vital, M., Tomasch, J., Badewien, T.H., Giebel, H.-A., Plumeier, I., Wang, H., Pieper, D.H., Wagner-Döbler, I., Simon, M., 2017. Diversity and community composition of particle-associated and free-living bacteria in mesopelagic and bathypelagic Southern Ocean water masses: Evidence of dispersal limitation in the Bransfield Strait: Bacteria in the deep Southern Ocean. *Limnol. Oceanogr.* 62, 1080–1095. <https://doi.org/10.1002/lno.10487>
- Mulder, J.W., Duin, J.O.J., Goverde, J., Poiesz, W.G., van Veldhuizen, H.M., van Kempen, R., Roeleveld, P., 2006. Full-Scale Experience with the Sharon Process through the Eyes of the Operators. *Proc. Water Environ. Fed.* 2006, 5256–5270. <https://doi.org/10.2175/193864706783763444>

- Mulder, J.W., van Loosdrecht, M.C., Hellinga, C., van Kempen, R., 2001. Full-scale application of the SHARON process for treatment of rejection water of digested sludge dewatering. *Water Sci. Technol. J. Int. Assoc. Water Pollut. Res.* 43, 127–134.
- Nhat, P.T., Biec, H.N., Van, T.T.T., Tuan, D.V., Trung, N.L.H., Nghi, V.T.K., Dan, N.P., 2017. Stability of partial nitrification in a sequencing batch reactor fed with high ammonium strength old urban landfill leachate. *Int. Biodeterior. Biodegrad.* 124, 56–61.  
<https://doi.org/10.1016/j.ibiod.2017.06.017>
- Nhu Hien, N., Van Tuan, D., Nhat, P.T., Thi Thanh Van, T., Van Tam, N., Xuan Que, V.O.N., Phuoc Dan, N., 2017. Application of Oxygen Limited Autotrophic Nitrification/Denitrification (OLAND) for anaerobic latex processing wastewater treatment. *Int. Biodeterior. Biodegrad.* 124, 45–55. <https://doi.org/10.1016/j.ibiod.2017.07.009>
- Nielsen, M., Bollmann, A., Sliemers, O., Jetten, M., Schmid, M., Strous, M., Schmidt, I., Larsen, L.H., Nielsen, L.P., Revsbech, N.P., 2005. Kinetics, diffusional limitation and microscale distribution of chemistry and organisms in a CANON reactor. *FEMS Microbiol. Ecol.* 51, 247–256. <https://doi.org/10.1016/j.femsec.2004.09.003>
- Nifong, A., Nelson, A., Johnson, C., Bott, C.B., 2013. Performance of a Full-Scale Sidestream DEMON® Deammonification Installation. *Proc. Water Environ. Fed.* 2013, 3686–3709.  
<https://doi.org/10.2175/193864713813685700>  
nitrification of high ammonia concentration wastewater as a part of a shortcut biological nitrogen removal process. *Process Biochem.* 40, 1715–1719.  
<https://doi.org/10.1016/j.procbio.2004.06.058>
- Nogueira, R., Melo, L.F., 2006. Competition between *Nitrospira* spp. and *Nitrobacter* spp. in nitrite-oxidizing bioreactors. *Biotechnol. Bioeng.* 95, 169–175.  
<https://doi.org/10.1002/bit.21004>



- Nowka, B., Off, S., Daims, H., Spieck, E., 2015. Improved isolation strategies allowed the phenotypic differentiation of two *Nitrospira* strains from widespread phylogenetic lineages. *FEMS Microbiology Ecology* 91. <https://doi.org/10.1093/femsec/fiu031>
- Nze, K., Xu, S., Mohammed, A., Liu, Y., 2018. Effect of a significant increase in flow rate on the performance and bacteria community in a pilot-scale activated sludge biological nutrient removal reactor. *Journal of Environmental Engineering* In press.
- Onnis-Hayden, A., Dair, D., Johnson, C., Schramm, A., Gu, A.Z., 2007. Kinetics and Nitrifying Populations in Nitrogen Removal Processes at a Full-Scale Integrated Fixed-Film Activated Sludge (IFAS) Plant. *Proc. Water Environ. Fed.* 2007, 3099–3119. <https://doi.org/10.2175/193864707787973789>
- Onnis-Hayden, A., Majed, N., Schramm, A., Gu, A.Z., 2011. Process optimization by decoupled control of key microbial populations: Distribution of activity and abundance of polyphosphate-accumulating organisms and nitrifying populations in a full-scale IFAS-EBPR plant. *Water Res.* 45, 3845–3854. <https://doi.org/10.1016/j.watres.2011.04.039>
- Peng, Y., Zhu, G., 2006. Biological nitrogen removal with nitrification and denitrification via nitrite pathway. *Appl. Microbiol. Biotechnol.* 73, 15–26. <https://doi.org/10.1007/s00253-006-0534-z>
- Peng, Y.Z., Chen, Y., Peng, C.Y., Liu, M., Wang, S.Y., Song, X.Q., Cu, Y.W., 2004. Nitrite accumulation by aeration controlled in sequencing batch reactors treating domestic wastewater. *Water Sci. Technol. J. Int. Assoc. Water Pollut. Res.* 50, 35–43.
- Pérez, J., Picioreanu, C., van Loosdrecht, M., 2005. Modeling biofilm and floc diffusion processes based on analytical solution of reaction-diffusion equations. *Water Res.* 39, 1311–1323. <https://doi.org/10.1016/j.watres.2004.12.020>
- Picioreanu, C., Van Loosdrecht, M.C.M., Heijnen, J.J., 1997. Modelling the effect of oxygen concentration on nitrite accumulation in a biofilm airlift suspension reactor, in:

- Harremoes, P. (Ed.), *Biofilm Systems*. Presented at the WATER SCIENCE AND TECHNOLOGY, Pergamon, pp. 147–156.
- Princic, null, Mahne, null, Megusar, null, Paul, null, Tiedje, null, 1998. Effects of pH and oxygen and ammonium concentrations on the community structure of nitrifying bacteria from wastewater. *Appl. Environ. Microbiol.* 64, 3584–3590.
- Prosser, J.I., Head, I.M., Stein, L.Y., 2014. The Family Nitrosomonadaceae, in: Rosenberg, E., DeLong, E.F., Lory, S., Stackebrandt, E., Thompson, F. (Eds.), *The Prokaryotes*. Springer Berlin Heidelberg, Berlin, Heidelberg, pp. 901–918. [https://doi.org/10.1007/978-3-642-30197-1\\_372](https://doi.org/10.1007/978-3-642-30197-1_372)
- Queiroz, L.M., Aun, M.V., Morita, D.M., Alem Sobrinho, P., 2011. Biological nitrogen removal over nitritation/denitritation using phenol as carbon source. *Braz. J. Chem. Eng.* 28, 197–207. <https://doi.org/10.1590/S0104-66322011000200004>
- Ramos, C., Suárez-Ojeda, M.E., Carrera, J., 2016. Denitritation in an anoxic granular reactor using phenol as sole organic carbon source. *Chem. Eng. J.* 288, 289–297. <https://doi.org/10.1016/j.cej.2015.11.099>
- Randall, C.W., Sen, D., 1996. Full scale evaluation of an integrated fixed-film activated sludge (IFAS) process for enhanced nitrogen removal. *Water Sci. Technol.* 33, 155–161.
- Rikmann, E., Zekker, I., Tenno, T., Saluste, A., Tenno, T., 2018. Inoculum-free start-up of biofilm- and sludge-based deammonification systems in pilot scale. *Int. J. Environ. Sci. Technol.* 15, 133–148. <https://doi.org/10.1007/s13762-017-1374-3>
- Risgaard-Petersen, N., Nicolaisen, M.H., Revsbech, N.P., Lomstein, B.A., 2004. Competition between Ammonia-Oxidizing Bacteria and Benthic Microalgae. *Appl. Environ. Microbiol.* 70, 5528–5537. <https://doi.org/10.1128/AEM.70.9.5528-5537.2004>
- Rodriguez-Caballero, A., Ribera, A., Balcázar, J.L., Pijuan, M., 2013. Nitritation versus full nitrification of ammonium-rich wastewater: Comparison in terms of nitrous and nitric

- oxides emissions. *Bioresour. Technol.* 139, 195–202.  
<https://doi.org/10.1016/j.biortech.2013.04.021>
- Rouxhet, P.G., Mozes, N., Dengis, P.B., Dufrière, Y.F., Gerin, P.A., Genet, M.J., 1994. Application of X-ray photoelectron spectroscopy to microorganisms. *Colloids and Surfaces B: Biointerfaces* 2, 347–369. [https://doi.org/10.1016/0927-7765\(94\)80049-9](https://doi.org/10.1016/0927-7765(94)80049-9)
- Ruiz, G., Jeison, D., Chamy, R., 2003. Nitrification with high nitrite accumulation for the treatment of wastewater with high ammonia concentration. *Water Res.* 37, 1371–1377.  
[https://doi.org/10.1016/S0043-1354\(02\)00475-X](https://doi.org/10.1016/S0043-1354(02)00475-X)
- Savaglio, N., Puopolo, R. (Eds.), 2012. Denitrification: processes, regulation and ecological
- Scherson, Y.D., Woo, S.-G., Criddle, C.S., 2014. Production of Nitrous Oxide From Anaerobic Digester Centrate and Its Use as a Co-oxidant of Biogas to Enhance Energy Recovery. *Environ. Sci. Technol.* 48, 5612–5619. <https://doi.org/10.1021/es501009j>
- Schreiber, F., Wunderlin, P., Udert, K.M., Wells, G.F., 2012. Nitric oxide and nitrous oxide turnover in natural and engineered microbial communities: biological pathways, chemical reactions, and novel technologies. *Front. Microbiol.* 3.  
<https://doi.org/10.3389/fmicb.2012.00372>
- Shao, Y., Shi, Y., Mohammed, A., Liu, Y., 2017. Wastewater ammonia removal using an integrated fixed-film activated sludge-sequencing batch biofilm reactor (IFAS-SBR): Comparison of suspended flocs and attached biofilm. *Int. Biodeterior. Biodegrad.* 116, 38–47.  
<https://doi.org/10.1016/j.ibiod.2016.09.026>
- Shao, Y., Yang, S., Mohammed, A., Liu, Y., 2018. Impacts of ammonium loading on nitrification stability and microbial community dynamics in the integrated fixed-film activated sludge sequencing batch reactor (IFAS-SBR). *International Biodeterioration & Biodegradation* 133, 63–69. <https://doi.org/10.1016/j.ibiod.2018.06.002>

- Sheng, G.-P., Yu, H.-Q., Li, X.-Y., 2010. Extracellular polymeric substances (EPS) of microbial aggregates in biological wastewater treatment systems: A review. *Biotechnol. Adv.* 28, 882–894. <https://doi.org/10.1016/j.biotechadv.2010.08.001>
- Sheng, G.-P., Yu, H.-Q., Li, X.-Y., 2010. Extracellular polymeric substances (EPS) of microbial aggregates in biological wastewater treatment systems: A review. *Biotechnology Advances* 28, 882–894. <https://doi.org/10.1016/j.biotechadv.2010.08.001>
- Shin, H.S., Kang, S.T., Nam, S.Y., 2001. Effect of carbohydrate and protein in the EPS on sludge settling characteristics. *Water Sci. Technol. J. Int. Assoc. Water Pollut. Res.* 43, 193–196.
- Sinha, B., Annachhatre, A.P., 2007. Partial nitrification—operational parameters and microorganisms involved. *Rev. Environ. Sci. Biotechnol.* 6, 285–313.  
<https://doi.org/10.1007/s11157-006-9116-x>
- Slikkers, A.O., Third, K., Abma, W., Kuenen, J., Jetten, M.S., 2003. CANON and Anammox in a gas-lift reactor. *FEMS Microbiol. Lett.* 218, 339–344. [https://doi.org/10.1016/S0378-1097\(02\)01177-1](https://doi.org/10.1016/S0378-1097(02)01177-1)
- Stehr, G., S. Zörner, B. Böttcher, H. P. Koops, 1995. Exopolymers: An Ecological Characteristic of a Floc-Attached, Ammonia-Oxidizing Bacterium. *Microb. Ecol.* 115.
- Stein, L.Y., Klotz, M.G., 2016. The nitrogen cycle. *Curr. Biol.* 26, R94–R98.  
<https://doi.org/10.1016/j.cub.2015.12.021>
- Steuernagel, L., de León Gallegos, E.L., Azizan, A., Dampmann, A.-K., Azari, M., Denecke, M., 2018. Availability of carbon sources on the ratio of nitrifying microbial biomass in an industrial activated sludge. *International Biodeterioration & Biodegradation* 129, 133–140.  
<https://doi.org/10.1016/j.ibiod.2018.02.001>
- Stricker, A.-E., Barrie, A., Maas, C.L.A., Fernandes, W., Lishman, L., 2009. Comparison of Performance and Operation of Side-By-Side Integrated Fixed-Film and Conventional Activated Sludge Processes at Demonstration Scale. *Water Environ. Res.* 81, 219–232.  
<https://doi.org/10.2175/106143008X325692>

- Strous, M., Fuerst, J.A., Kramer, E.H.M., Logemann, S., Muyzer, G., van de Pas-Schoonen, K.T., Webb, R., Kuenen, J.G., Jetten, M.S.M., 1999. Missing lithotroph identified as new planctomycete. *Nature* 400, 446–449. <https://doi.org/10.1038/22749>
- Stüven, R., Vollmer, M., Bock, E., 1992. The impact of organic matter on nitric oxide formation by *Nitrosomonas europaea*. *Arch. Microbiol.* 158. <https://doi.org/10.1007/BF00276306>
- Sun, N., Ge, C., Ahmad, H.A., Gao, B., Ni, S.-Q., 2017. Realization of microbial community stratification for single-stage nitrogen removal in a sequencing batch biofilter granular reactor. *Bioresour. Technol.* 241, 681–691. <https://doi.org/10.1016/j.biortech.2017.05.203>
- Sweity, A., Ying, W., Ali-Shtayeh, M.S., Yang, F., Bick, A., Oron, G., Herzberg, M., 2011. Relation between EPS adherence, viscoelastic properties, and MBR operation: Biofouling study with QCM-D. *Water Research* 45, 6430–6440. <https://doi.org/10.1016/j.watres.2011.09.038>
- ter Braak, C.J.F., Verdonschot, P.F.M., 1995. Canonical correspondence analysis and related multivariate methods in aquatic ecology. *Aquat. Sci.* 57, 255–289. <https://doi.org/10.1007/BF00877430>
- Tokutomi, T., 2004. Operation of a nitrite-type airlift reactor at low DO concentration. *Water Sci. Technol. J. Int. Assoc. Water Pollut. Res.* 49, 81–88.
- Treusch, A.H., Leininger, S., Kletzin, A., Schuster, S.C., Klenk, H.-P., Schleper, C., 2005. Novel genes for nitrite reductase and Amo-related proteins indicate a role of uncultivated mesophilic crenarchaeota in nitrogen cycling: Role of mesophilic crenarchaeota in nitrogen cycling. *Environ. Microbiol.* 7, 1985–1995. <https://doi.org/10.1111/j.1462-2920.2005.00906.x>
- Tsuneda, S., Aikawa, H., Hayashi, H., Yuasa, A., Hirata, A., 2003. Extracellular polymeric substances responsible for bacterial adhesion onto solid surface. *FEMS Microbiol. Lett.* 223, 287–292. [https://doi.org/10.1016/S0378-1097\(03\)00399-9](https://doi.org/10.1016/S0378-1097(03)00399-9)

- Tsuneda, S., Park, S., Hayashi, H., Jung, J., Hirata, A., 2001. Enhancement of nitrifying biofilm formation using selected EPS produced by heterotrophic bacteria. *Water Sci. Technol. J. Int. Assoc. Water Pollut. Res.* 43, 197–204.
- U.S.Environmental Protection Agency, 1987. Assessment of Needed Publicly Owned Wastewater Treatment Facilities In The United States, 1986 Needs Survey Report To Congress.
- U.S.EPA, 2007. Biological nutrient removal processes and cost
- van den Akker, B., Beard, H., Kaeding, U., Giglio, S., Short, M.D., 2010. Exploring the relationship between viscous bulking and ammonia-oxidiser abundance in activated sludge: A comparison of conventional and IFAS systems. *Water Res.* 44, 2919–2929. <https://doi.org/10.1016/j.watres.2010.02.016>
- van Kessel, M.A.H.J., Speth, D.R., Albertsen, M., Nielsen, P.H., Op den Camp, H.J.M., Kartal, B., Jetten, M.S.M., Lücker, S., 2015. Complete nitrification by a single microorganism. *Nature* 528, 555–559. <https://doi.org/10.1038/nature16459>
- Verstraete, W., Philips, S., 1998. Nitrification-denitrification processes and technologies in new contexts. *Environ. Pollut.* 102, 717–726. [https://doi.org/10.1016/S0269-7491\(98\)80104-8](https://doi.org/10.1016/S0269-7491(98)80104-8)
- Walker, C.B., de la Torre, J.R., Klotz, M.G., Urakawa, H., Pinel, N., Arp, D.J., Brochier-Armanet, C., Chain, P.S.G., Chan, P.P., Gollabgir, A., Hemp, J., Hugler, M., Karr, E.A., Konneke, M., Shin, M., Lawton, T.J., Lowe, T., Martens-Habbena, W., Sayavedra-Soto, L.A., Lang, D., Sievert, S.M., Rosenzweig, A.C., Manning, G., Stahl, D.A., 2010. *Nitrosopumilus maritimus* genome reveals unique mechanisms for nitrification and autotrophy in globally distributed marine crenarchaea. *Proc. Natl. Acad. Sci.* 107, 8818–8823. <https://doi.org/10.1073/pnas.0913533107>
- Wang, X., Gao, D., 2016. In-situ restoration of one-stage partial nitrification-anammox process deteriorated by nitrate build-up via elevated substrate levels. *Sci. Rep.* 6. <https://doi.org/10.1038/srep37500>

- Wang, X., Hu, M., Xia, Y., Wen, X., Ding, K., 2012. Pyrosequencing Analysis of Bacterial Diversity in 14 Wastewater Treatment Systems in China. *Appl. Environ. Microbiol.* 78, 7042–7047. <https://doi.org/10.1128/AEM.01617-12>
- Wang, Z., Peng, Y., Miao, L., Cao, T., Zhang, F., Wang, S., Han, J., 2016. Continuous-flow combined process of nitrification and ANAMMOX for treatment of landfill leachate. *Bioresour. Technol.* 214, 514–519. <https://doi.org/10.1016/j.biortech.2016.04.118>
- Wei, L., Hong, T., 2010. Biosorption of Organic Pollutants by Activated Sludge: Equilibrium and Kinetic Modeling. *IEEE*, pp. 1–4. <https://doi.org/10.1109/ICBBE.2010.5515043>
- Wen, X., Gong, B., Zhou, J., He, Q., Qing, X., 2017. Efficient simultaneous partial nitrification, anammox and denitrification (SNAD) system equipped with a real-time dissolved oxygen (DO) intelligent control system and microbial community shifts of different substrate concentrations. *Water Research* 119, 201–211. <https://doi.org/10.1016/j.watres.2017.04.052>
- Wuchter, C., Abbas, B., Coolen, M.J.L., Herfort, L., van Bleijswijk, J., Timmers, P., Strous, M., Teira, E., Herndl, G.J., Middelburg, J.J., Schouten, S., Sinninghe Damste, J.S., 2006. Archaeal nitrification in the ocean. *Proc. Natl. Acad. Sci.* 103, 12317–12322. <https://doi.org/10.1073/pnas.0600756103>
- Xia, S., Li, J., Wang, R., 2008. Nitrogen removal performance and microbial community structure dynamics response to carbon nitrogen ratio in a compact suspended carrier biofilm reactor. *Ecol. Eng.* 32, 256–262. <https://doi.org/10.1016/j.ecoleng.2007.11.013>
- Yang, L., Alleman, J.E., 1992. Investigation of batch-wise nitrite build-up by an enriched nitrification culture. *Wat. Sci. Tech.* 26, 997–1005.
- Yang, Q., Peng, Y., Liu, X., Zeng, W., Mino, T., Satoh, H., 2007. Nitrogen Removal via Nitrite from Municipal Wastewater at Low Temperatures using Real-Time Control to Optimize Nitrifying Communities. *Environ. Sci. Technol.* 41, 8159–8164. <https://doi.org/10.1021/es070850f>

- Ye, F., Peng, G., Li, Y., 2011. Influences of influent carbon source on extracellular polymeric substances (EPS) and physicochemical properties of activated sludge. *Chemosphere* 84, 1250–1255. <https://doi.org/10.1016/j.chemosphere.2011.05.004>
- Ye, J., Chestna, K.L., Kulick, F.M., Rotherme, B., 2010a. Full Scale Implementation, Operation, and Performance of a Structured Sheet Media IFAS System. *Proc. Water Environ. Fed.* 2010, 2555–2565. <https://doi.org/10.2175/193864710798170522>
- Ye, J., Kulick, F.M., McDowell, C.S., 2010b. Effective Biofilm Control on High Surface Density Vertical-Flow Structured Sheet Media for Submerged Applications. *Proc. Water Environ. Fed.* 2010, 4200–4220. <https://doi.org/10.2175/193864710798182402>
- Ye, J., McDowell, C.S., Koch, K., Koch, K., Kulick, F.M., Rothermel, B.C., 2009. Pilot Testing of Structured Sheet Media IFAS for Wastewater Biological Nutrient Removal (BNR). *Proc. Water Environ. Fed.* 2009, 4427–4442. <https://doi.org/10.2175/193864709793954015>
- Ye, L., Shao, M.-F., Zhang, T., Tong, A.H.Y., Lok, S., 2011. Analysis of the bacterial community in a laboratory-scale nitrification reactor and a wastewater treatment plant by 454-pyrosequencing. *Water Res.* 45, 4390–4398. <https://doi.org/10.1016/j.watres.2011.05.028>
- Zeng, R.J., Lemaire, R., Yuan, Z., Keller, J., 2003. Simultaneous nitrification, denitrification, and phosphorus removal in a lab-scale sequencing batch reactor. *Biotechnol. Bioeng.* 84, 170–178. <https://doi.org/10.1002/bit.10744>
- Zhang, C.L., Ye, Q., Huang, Z., Li, W., Chen, J., Song, Z., Zhao, W., Bagwell, C., Inskip, W.P., Ross, C., Gao, L., Wiegel, J., Romanek, C.S., Shock, E.L., Hedlund, B.P., 2008. Global Occurrence of Archaeal amoA Genes in Terrestrial Hot Springs. *Appl. Environ. Microbiol.* 74, 6417–6426. <https://doi.org/10.1128/AEM.00843-08>
- Zhang, P., Fang, F., Chen, Y.-P., Shen, Y., Zhang, W., Yang, J.-X., Li, C., Guo, J.-S., Liu, S.-Y., Huang, Y., Li, S., Gao, X., Yan, P., 2014. Composition of EPS fractions from suspended sludge and biofilm and their roles in microbial cell aggregation. *Chemosphere* 117, 59–65. <https://doi.org/10.1016/j.chemosphere.2014.05.070>



- Zhang, Y., 2009. Stability of Partial Nitrification and Microbial Population Dynamics in a Bioaugmented Membrane Bioreactor. *J. Microbiol. Biotechnol.* 19, 1656–1664. <https://doi.org/10.4014/jmb.0906.06006>
- Zhang, Z., Chen, S., Wu, P., Lin, L., Luo, H., 2010. Start-up of the Canon process from activated sludge under salt stress in a sequencing batch biofilm reactor (SBBR). *Bioresour. Technol.* 101, 6309–6314. <https://doi.org/10.1016/j.biortech.2010.03.040>
- Zhou, X.-H., Liu, J., Song, H.-M., Qiu, Y.-Q., Shi, H.-C., 2012. Estimation of Heterotrophic Biokinetic Parameters in Wastewater Biofilms from Oxygen Concentration Profiles by Microelectrode. *Environ. Eng. Sci.* 29, 466–471. <https://doi.org/10.1089/ees.2010.0456>

## APPENDICES

### Appendix A -Experimental methodology and data analysis

#### A-1 Synthetic wastewater content

The volume of the 2 L of synthetic wastewater feed consisted of 100 mL of solution A and 1.9 L of solution B. Solution A contained, per liter (adapted from Smolders et al., (1994)): 17.53 g  $\text{NaAc}_3 \cdot \text{H}_2\text{O}$ ; 1 g  $\text{MgSO}_4 \cdot 7\text{H}_2\text{O}$ ; 0.45 g  $\text{CaCl}_2 \cdot \text{H}_2\text{O}$ ; 3.3 g  $\text{NH}_4\text{Cl}$ ; and 6 mL of nutrient solution. It was adjusted to pH 5.5 with 2 M HCl and autoclaved. Solution B contained, per liter: 28.5 mg  $\text{KH}_2\text{PO}_4$  and 32.5 mg  $\text{K}_2\text{HPO}_4$ , which was adjusted to pH 10 with 2 M NaOH. One liter of nutrient solution contained (based on Smolders et al. [1994]): 1.5 g  $\text{FeCl}_3 \cdot 6\text{H}_2\text{O}$ ; 0.15g  $\text{H}_3\text{BO}_3$ ; 0.03 g  $\text{CuSO}_4 \cdot 5\text{H}_2\text{O}$ ; 0.18 g KI; 0.12 g  $\text{MnCl}_2 \cdot 4\text{H}_2\text{O}$ ; 0.06 g  $\text{Na}_2\text{MoO}_4 \cdot 2\text{H}_2\text{O}$ ; 0.12 g  $\text{ZnSO}_4 \cdot 7\text{H}_2\text{O}$ ; 0.15 g  $\text{CoCl}_2 \cdot 6\text{H}_2\text{O}$ ; and 10 g ethylene-diamine tetraacetic acid (EDTA). The complete influent contained 400 mg COD/L, 40 mg  $\text{NH}_4\text{-N/L}$ , and 15 mg  $\text{PO}_4\text{-P/L}$ . Stock solutions were prepared based on the information provided above.

#### A-2 Nitrogen balance calculations

Under condition (a), Assume the remaining nitrogen is:

$$N_{\text{Remaining}} = (\text{NH}_4^+ - N_{\text{Remaining}} + \text{NO}_2^- - N_{\text{Remaining}} + \text{NO}_3^- - N_{\text{Remaining}}) \times (1 - 37.5\%)V \text{ (Eq. 1)}$$

Where the nitrogen species represent concentrations and V is the volume of the reactor and the

volume exchange ratio is 37.5% per cycle. Since the influent does not include any organic nitrogen, inorganic nitrogen is the only nitrogen source in the influent. The N in the influent is:

$$N_{in} = NH_4^+ - N_{in} \times 37.5\% V \quad (\text{Eq. 2})$$

Under condition (b), before the reaction started:

The nitrogen species in the reactor is:

$$\begin{aligned} N_{\text{before reaction}} &= N_{\text{Remaining}} + N_{in} \\ &= (NH_4^+ - N_{\text{Remaining}} + NO_2^- - N_{\text{Remaining}} + NO_3^- - N_{\text{Remaining}}) \times (1 - 37.5\%)V + NH_4^+ - N_{in} \times \\ &37.5\% V \quad (\text{Eq. 3}) \end{aligned}$$

the  $NH_4^+ - N$  can be separated into three parts. One part of the  $NH_4^+ - N$  remained in the reactor. The second part of the  $NH_4^+ - N$  was converted to  $NO_2^- - N$  and  $NO_3^- - N$ , and oxidized nitrogen species can be further denitrified to nitrogen gas  $N_2$ . The third part of nitrogen was utilized by cell synthesis. However, this part accounts for less than 2% of the  $NH_4^+ - N$  and usually negligible during the sequencing batch reaction cycle (reference).

Under condition (c), the settling is finished. The nitrogen remained in the system, or the N after the reaction:

$$N_{\text{after reaction}} = N_{\text{Remaining}}' = (NH_4^+ - N_{\text{Remaining}}' + NO_2^- - N_{\text{Remaining}}' + NO_3^- - N_{\text{Remaining}}') \times V \quad (\text{Eq. 4})$$

The remaining nitrogen species concentrations were the same as the effluent nitrogen species, so,

$$N_{\text{after reaction}} = (NH_4^+ - N_{ef} + NO_2^- - N_{ef} + NO_3^- - N_{ef}) \times V \quad (\text{Eq. 5})$$

And if the system is stabilized, the effluent for each cycles are the same. Which means

$$NH_4^+ - N_{Remaining'} = NH_4^+ - N_{Remaining} = NH_4^+ - N_{ef} \quad (\text{Eq. 6})$$

$$NO_2^- - N_{Remaining'} = NO_2^- - N_{Remaining} = NO_2^- - N_{ef} \quad (\text{Eq. 7})$$

$$\text{and } NO_3^- - N_{Remaining} = NO_3^- - N_{Remaining} = NO_3^- - N_{ef} \quad (\text{Eq. 8})$$

Then the molecular nitrogen gas  $N_2$  released from the system is

$$N_2 = N_{\text{before reaction}} - N_{\text{after reaction}}$$

$$= (NH_4^+ - N_{Remaining} + NO_2^- - N_{Remaining} + NO_3^- - N_{Remaining}) \times (1 - 37.5\%)V + NH_4^+ - N_{in} \times 37.5\%V - (NH_4^+ - N_{ef} + NO_2^- - N_{ef} + NO_3^- - N_{ef}) \times V$$

$$= (NH_4^+ - N_{ef} + NO_2^- - N_{ef} + NO_3^- - N_{ef}) \times (1 - 37.5\%)V + NH_4^+ - N_{in} \times 37.5\%V - (NH_4^+ - N_{ef} + NO_2^- - N_{ef} + NO_3^- - N_{ef}) \times V$$

$$= (NH_4^+ - N_{in} - NH_4^+ - N_{ef} - NO_2^- - N_{ef} - NO_3^- - N_{ef}) \times 37.5\%V \quad (\text{Eq. 9})$$

if  $NH_4^+ - N_{in} - NH_4^+ - N_{ef} - NO_2^- - N_{ef} - NO_3^- - N_{ef}$  is greater than 0, then the denitrification happened during one cycle.

### A-3 Calculations of free ammonia (FA) and free nitrous acid (FNA)

Free ammonia (FA) and free nitrous acid (FNA) concentrations can be determined using the following equations (Anthonisen et al., 1976):

$$\text{FA as } NH_3(\text{mg/L}) = \frac{17}{14} \times \frac{\text{total ammonia as N}(\text{mg/L}) \times 10^{pH}}{K_b / K_w + 10^{pH}} \quad (\text{Equation S1})$$

Where  $K_b / K_w = e^{(6344/273 + ^\circ\text{C})}$

$$\text{FNA as } HNO_2(\text{mg/L}) = \frac{46}{14} \times \frac{NO_2^- - N(\text{mg/L})}{K_a \times 10^{pH}} \quad (\text{Equation S2})$$

Where  $K_a = e^{(-2300/273 + ^\circ\text{C})}$

### A-4 Extraction and functions of EPS components

EPS contains soluble EPS (S-EPS) and bound EPS. Bound EPS can be further classified into loosely bound-EPS (LB-EPS) and tightly bound-EPS (TB-EPS). The extraction methods for different components of EPS were based on the methods in Liang et al. (2010) with modifications. 10 mL samples of biofilm or sludge were centrifuged at 2000 g for 15 min at 4 °C. The supernatant

was filtered through a 0.2  $\mu\text{m}$  nylon filter and recovered as soluble EPS (S-EPS). The pellet was re-suspended in milli-Q water to a total volume of 10 mL and 0.04 mL of 36.5% formaldehyde was then added to each sample. Formaldehyde was used to prevent cell lysis. Samples were then stored at 4 °C for 1 hr before being centrifuged again at 5000 g for 15 min at 4 °C. After centrifugation, the supernatant was filtered through a 0.2  $\mu\text{m}$  nylon filter and recovered as loosely bound EPS. The pellet was re-suspended in milli-Q water to a total volume of 10 mL. 4 mL of 1N NaOH was added to each sample and the sample was stored at 4 °C for 3 hr. Samples were centrifuged at 6000 g for 15 min at 4 °C. The supernatant was filtered and recovered as TB-EPS. After extraction, EPS samples were purified in a dialysis membrane (3.4 kD) for 24 hr before further analysis.

The EPS production analysis revealed that the ammonium loading had a negative effect on EPS production (Figure S2), which may be associated with the competition between heterotrophs and autotrophs. The population of nitrifiers, especially AOB, became dominant when the  $\text{NH}_4^+\text{-N}$  in the feeding was above 400 mg/L. Autotrophic nitrifiers produced much less EPS than heterotrophic bacteria. Further, a lower production of EPS contributed to a better-settled sludge. Similar results were obtained in van den Akker et al. (2010), in which a high AOB population was positively correlated with good settleability of suspended sludge. Some studies pointed out that the protein and DNA content in EPS had negative effects on the sludge settleability (Droppo et al., 1998; Liao et al., 2001; Martinez et al., 2000); and that the polysaccharide content in EPS had a positive effect on the SVI (Kim et al., 2010; Shin et al., 2001).

In the batch test, it was observed that biomass aggregates absorbed ammonium. EPS production was directly related to the biosorption capacity of biomass aggregates (Sheng et al., 2010). Our EPS results showed that with a reactor feed of 800 mg/L  $\text{NH}_4^+\text{-N}$ , the attached biofilm produced more EPS than the suspended sludge, as the biosorption capacity of the biofilm was higher than the biosorption capacity of the sludge.

In the present study, the C/N ratios varied from 2 to 0.25. The values were considered low. The reason we choose low C/N ratio is that we were mimicking high ammonium strength wastewater which normally has low C/N ratio (Gustavsson, 2010; Peng and Zhu, 2006). High C/N ratio often promotes the growth of heterotrophs that outcompete autotrophic nitrifiers for oxygen and space. A recent study reported that the abundance of AOB functional genes is higher in attached biofilm than in the suspended sludge when the C/N ratio is low, but is almost equivalent when the C/N ratio is high (Shao et al., 2017). C/N ratio that favors the nitrification process is normally in the range of  $\leq 2$  (Wei et al., 2014).

Besides, COD in the effluent was round 20-30mg/L. Short periods of the COD peaks in the effluent (day 230 to 250 and day 260-280) was observed due to air diffuser blockage.

The DO half saturation coefficients for AOB and NOB range from 0.2-0.4 mg/L and 1.2-1.5 mg/L, respectively (Picioreanu et al., 1997). Previous studies reported that maintaining solution DO below 1mg/L was critical for achieving nitrite accumulation and nitrification. However, some researchers also reported a DO level greater than 1mg/L for optimal nitrification. For instance,

Ciudad et al.(2005) found that nitrification was achieved under a DO level of 1.4mg/L. Peng and Zhu (2006) suggested an DO ranging from 0.5mg/L to 1.5mg/L was suitable for partial nitrification. Ge et al. (2014) reported that 1.5-2.0 mg/L DO was the optimal range for their reactors. These results underlined the importance of controlling other operation factors in addition to DO. Compared with the published values in the literature, the DO range for our reactor is in a reasonable range.

#### **A-5. Comparison of the microbial analysis**

Molecular methods acquired more and more attention in the wastewater treatment field in recent decades. Various methods had been applied to investigate relevant species in wastewater treatment systems of extensive scales. Fluorescent *in situ* hybridization (FISH) technology has been used to identify the spatial distribution of microorganisms in sludge and biofilm samples (Kouba et al., 2014; Wen et al., 2017). qPCR represents a simple and highly effective method to quantify specific genes of interest (Loosdrecht et al., 2016). NGS identifies microbial population structure, and thus can provide revolutionary insights into the ecology of the microbial community and help to evaluate the relationship between the ecology of the microbial community and the functions mediated by the community. Currently, the Illumina platform dominates the NGS market, which was dominated by Roche 454 (pyrosequencing).



Comparing the data obtained from qPCR and NGS, qPCR can provide more detailed information about the absolute quantity of specific nitrogen removal related functional genes, while NGS illuminates the structure of the entire microbial community in the system, and highlight the community shifts under various operation conditions. In the present study, a higher absolute quantity of AOB genes (*amoA*) than *Nitrospira* functional genes was detected using qPCR, while the relative abundance (%) of *Nitrosomonas* was lower than the abundance of *Nitrospira* detected using NGS. Our observation might be explained by that the presence of multiple *amoA* genes in each cell (H. Kim et al., 2011). Also, other bacteria might also contain *amoA* genes (Imhoff, 2016). Further studies are needed to further evaluate the microbial structure during the establishment of nitrification community.

#### **A-6. The preparation of the feed water**

The volume of the 20L of synthetic wastewater feed consisted of 10ml of nutrient, 53.3 mL of solution A (NaAc stock) and 20mL of solution B (KH<sub>2</sub>PO<sub>4</sub> stock), 100mL of solution C (ethylene-diamine tetraacetic acid (EDTA) and FeSO<sub>4</sub> stock), 100ml of solution D (CaCl<sub>2</sub> stock) and 50ml of solution E(MgSO<sub>4</sub> stock). The nutrient solution per 0.5 liter of nutrient solution contained (based on Smolders et al., (1994)): 1.5 g FeCl<sub>3</sub>·6H<sub>2</sub>O; 0.15g H<sub>3</sub>BO<sub>3</sub>; 0.03 g CuSO<sub>4</sub>·5H<sub>2</sub>O; 0.18 g KI; 0.12 g MnCl<sub>2</sub> ·4H<sub>2</sub>O; 0.06 g Na<sub>2</sub>MoO<sub>4</sub>·2H<sub>2</sub>O; 0.12 g ZnSO<sub>4</sub>·7H<sub>2</sub>O; 0.15 g CoCl<sub>2</sub>·6H<sub>2</sub>O; solution A contained 83g NaAc per liter; solution B contained 78.8g KH<sub>2</sub>PO<sub>4</sub> /L; solution C contained 4g

EDTA and 4g of  $\text{FeSO}_4 \cdot 7\text{H}_2\text{O}$ ; solution D contained 9g  $\text{CaCl}_2/\text{L}$ ; solution E contained 20g/L  $\text{MgSO}_4$ . For different phases, the addition of  $\text{NH}_4\text{Cl}$  and  $\text{NaHCO}_3$  (as alkalinity) were different, for phase 1 of R1, the dosage for  $\text{NH}_4\text{Cl}$  and  $\text{NaHCO}_3$  were 7.6g and 24g to 20L of feed to reach a  $\text{NH}_4^+\text{-N}$  concentration of 100mg/L and an alkalinity concentration as  $\text{CaCO}_3$  of 718mg/L. For phase 2, the dosage for  $\text{NH}_4\text{Cl}$  and  $\text{NaHCO}_3$  were 15.2g and 48g; for phase 3, the dosage for them were 30.4g and 96; for phase 4, the dosage were 45.6g and 144g, and for phase 5, the dosage were 60.8g and 192g for 20L of feed.

The feed for nitrification reactor in phase 6 to 8 were prepared by mixing the synthetic wastewater and lagoon supernatant at volumetric ratios of 3:1, 1:1, 1:3. For phase 9, we used pure lagoon supernatant as feed.  $\text{NH}_4\text{Cl}$  and  $\text{NaHCO}_3$  were added into the feed to adjust the ammonium concentration and alkalinity concentration.

#### **A-7. The calculation of COD based on TOC measurements**

The COD/TOC ratio varied for different organic compounds. For the wastewater samples from this study, the COD/TOC ratio varied from 2.84 to 3.12. A COD/TOC=3 was selected for COD calculation based on TOC measurements. A samples calculation is listed below:

If TOC=17 mg/L , as COD/TOC=3, COD=3\*TOC= 3\*17=51mg/L.

## Appendix-B Supporting tables

Table B-1 NH<sub>4</sub><sup>+</sup>-N concentrations during batch test and biomass inoculated into batch bottles.

<b>Table B-1 NH<sub>4</sub><sup>+</sup>-N concentrations during batch test and biomass inoculated into batch bottles.</b>				
<b>Time (min)</b>	<b>Suspended sludge</b>	<b>Attached biofilm</b>	<b>Suspended sludge+attached biomass</b>	<b>Control</b>
<b>5</b>	320.0±2.6	332.3±12.7	257.0±33.2	409.3±33.6
<b>40</b>	302.3±6.4	315.0±8.7	241.3±47.5	383.3±1.2
<b>100</b>	276.3±6.5	316.3±6.7	181.7±23.0	395.0±46.5
<b>220</b>	240±4.6	336.7±5.5	156.7±26.6	412.7±45.8
<b>400</b>	150±2.0	315±2.6	141.3±11.2	389.7±3.8
<b>520</b>	105±3.5	288.7±1.5	81.8±0.9	N/A
<b>670</b>	34.9±2.7	236±5.6	18.3±1.4	375.0±17.1
<b>1075</b>	0.386666667±0.02	160.3±11.6	0.4±0.05	367.7±9.0
<b>1435</b>	0.081666667±0.02	123.7±13.6	0.1±0.03	363.3±4.9
<b>Biomass inoculated (mg)</b>	325.4	216	541.4	0

**Table B-2. Functional genes information and qPCR cycle information**

Target gene	Primer	References	Initial denaturation	Cycle			
				Cycles	Denature	Anneal	Extension (72°C)
AOB amoA	amoA-1F 5'- GGG GTT TCT ACT GGT GGT-3'  amoA-2R-TC 5'- CCC CTC TGC AAA GCC TTC TTC-3'	(Mincer et al., 2007)	95°C 15min	45	95°C, 1min	54°C, 1min	1min
NOB Nitrosospora spp. 16s rDNA	NSR 1113f 5'-CCT GCT TTC AGT TGC TAC CG -3'  NSR 1264r 5'-GTT TGC AGC GCT TTG TAC CG -3'	(Y. M. Kim et al., 2011)	50°C 2min, 95°C 10min	50	95°C 30s	60°C 1min	
nirK gene	nirK 876 5'-ATYGGCGGVCAYGGCGA-3'  nirK 1040 5'-GCCTCGATCAGRTRTRTGTT-3'	(Y. M. Kim et al., 2011)	95°C 30s	30	95°C 15s	58°C 30s	31s
nosZ gene	nosZ 2F 5'-CGC RAC GGC AAS AAG GTS MSS GT-3'  nosZ 2R 5'-CAK RTG CAK SGC RTG GCA GAA-3'	(Y. M. Kim et al., 2011)	95°C 30s	30	95°C 15s	60°C 30s	31s
narG gene	narG 1960m2f 5'-TAYGTSGGGCAGGARAAACTG-3'  narG 2050m2r 5'-CGTAGAAGAAGCTGGTGCTGTT-3'	(Y. M. Kim et al., 2011)	95°C 30s	35	95°C 15s	58°C 30s	31s
Anammox 16s rRNA	Amx809f 5'- GCCGTAAACGATGGGCACT-3'  Amx1066r 5'- AACGTCTCACGACACGAGCTG-3'	(Yin et al., 2016)	95°C 2min	40	95°C 5s	62°C 30s	30s

Table B-3. Total reads of all samples.

Sample ID	Samples	Number of total reads.
S1	sludge -100mg/L	50190
S2	sludge-400mg/L	40415
S4	biofilm-100mg/L	15714
S5	biofilm -400mg/L	15594
S7	seed	16948

**Table B-4. Sample IDs and descriptions**

<b>Sample ID</b>	<b>Sample source</b>	<b>Sample description</b>
<b>S1</b>	R1	Sludge -100mg/L synthetic
<b>S2</b>	R1	Sludge -400mg/L synthetic
<b>S3</b>	R1	Sludge -800mg/L synthetic
<b>S4</b>	R1	Biofilm -100mg/L synthetic
<b>S5</b>	R1	Biofilm -400mg/L synthetic
<b>S6</b>	R1	Biofilm-800mg/L synthetic
<b>S11</b>	R1	Sludge-800mg/L 25% Raw supernatant
<b>S12</b>	R1	Biofilm-800mg/L 25% Raw supernatant
<b>S13</b>	R1	Sludge-800mg/L 50% Raw supernatant
<b>S14</b>	R1	Biofilm-800mg/L 50% Raw supernatant
<b>S15</b>	R1	Sludge-800mg/L 75% Raw supernatant
<b>S16</b>	R1	Biofilm-800mg/L 75% Raw supernatant
<b>S17</b>	R1	Sludge-800mg/L 100% Raw supernatant
<b>S18</b>	R1	Biofilm-800mg/L 100% Raw supernatant

Table B-5. Genus ID and corresponding name

<b>Genus ID</b>	<b>Genus name</b>
1	D_0*_Bacteria;D_1__Acidobacteria;D_2__Blastocatellia;D_3__Blastocatellales;D_4__Blastocatellaceae (Subgroup 4);D_5__11-24
2	D_0__Bacteria;D_1__Acidobacteria;D_2__Blastocatellia;D_3__Blastocatellales;D_4__Blastocatellaceae (Subgroup 4);D_5__Stenotrophobacter
3	D_0__Bacteria;D_1__Acidobacteria;D_2__Blastocatellia;D_3__Blastocatellales;D_4__Blastocatellaceae (Subgroup 4);D_5__uncultured
4	D_0__Bacteria;D_1__Acidobacteria;D_2__Solibacteres;D_3__Solibacterales;D_4__Solibacteraceae (Subgroup 3);D_5__Bryobacter
5	D_0__Bacteria;D_1__Acidobacteria;D_2__Solibacteres;D_3__Solibacterales;D_4__Solibacteraceae (Subgroup 3);D_5__Elev-16S-1166
6	D_0__Bacteria;D_1__Actinobacteria;D_2__Acidimicrobiia;D_3__Acidimicrobiales;D_4__Acidimicrobiales Incertae Sedis;D_5__Candidatus Microthrix
7	D_0__Bacteria;D_1__Armatimonadetes;D_2__Fimbriimonadia;D_3__Fimbriimonadales;D_4__Fimbriimonadaceae;D_5__uncultured bacterium
8	D_0__Bacteria;D_1__Bacteroidetes;D_2__Bacteroidia;D_3__Bacteroidales;D_4__Rikenellaceae;D_5__vadinBC27 wastewater-sludge group
9	D_0__Bacteria;D_1__Bacteroidetes;D_2__Bacteroidia;D_3__Bacteroidales;D_4__Porphyromonadaceae;D_5__Proteiniphilum
10	D_0__Bacteria;D_1__Bacteroidetes;D_2__Cytophagia;D_3__Cytophagales;D_4__Cytophagaceae;D_5__Chryseolinea
11	D_0__Bacteria;D_1__Bacteroidetes;D_2__Cytophagia;D_3__Cytophagales;D_4__Cytophagaceae;D_5__Leadbetterella

Table B-5. Genus ID and corresponding name

<b>Genus ID</b>	<b>Genus name</b>
12	D_0__Bacteria;D_1__Bacteroidetes;D_2__Cytophagia;D_3__Cytophagales;D_4__Cytophagaceae;D_5__uncultured
13	D_0__Bacteria;D_1__Bacteroidetes;D_2__Flavobacteriia;D_3__Flavobacteriales;D_4__Cryomorphaceae;D_5__Fluviicola
14	D_0__Bacteria;D_1__Bacteroidetes;D_2__Flavobacteriia;D_3__Flavobacteriales;D_4__Flavobacteriaceae;D_5__Lutibacter
15	D_0__Bacteria;D_1__Bacteroidetes;D_2__Flavobacteriia;D_3__Flavobacteriales;D_4__Flavobacteriaceae;D_5__Flavobacterium
16	D_0__Bacteria;D_1__Bacteroidetes;D_2__Flavobacteriia;D_3__Flavobacteriales;D_4__Flavobacteriaceae;D_5__Moheibacter
17	D_0__Bacteria;D_1__Bacteroidetes;D_2__Flavobacteriia;D_3__Flavobacteriales;D_4__NS9 marine group;D_5__uncultured bacterium
18	D_0__Bacteria;D_1__Bacteroidetes;D_2__Sphingobacteriia;D_3__Sphingobacteriales;D_4__Chitinophagaceae;D_5__Ferruginibacter
19	D_0__Bacteria;D_1__Bacteroidetes;D_2__Sphingobacteriia;D_3__Sphingobacteriales;D_4__Chitinophagaceae;D_5__Filimonas
20	D_0__Bacteria;D_1__Bacteroidetes;D_2__Sphingobacteriia;D_3__Sphingobacteriales;D_4__Chitinophagaceae;D_5__Terrimonas
21	D_0__Bacteria;D_1__Bacteroidetes;D_2__Sphingobacteriia;D_3__Sphingobacteriales;D_4__Chitinophagaceae;D_5__uncultured
22	D_0__Bacteria;D_1__Bacteroidetes;D_2__Sphingobacteriia;D_3__Sphingobacteriales;D_4__KD3-93;D_5__uncultured bacterium



Table B-5. Genus ID and corresponding name

<b>Genus ID</b>	<b>Genus name</b>
23	D_0__Bacteria;D_1__Bacteroidetes;D_2__Sphingobacteriia;D_3__Sphingobacteriales;D_4__NS11-12 marine group;D_5__uncultured bacterium
24	D_0__Bacteria;D_1__Bacteroidetes;D_2__Sphingobacteriia;D_3__Sphingobacteriales;D_4__PHOS-HE51;D_5__uncultured bacterium
25	D_0__Bacteria;D_1__Bacteroidetes;D_2__Sphingobacteriia;D_3__Sphingobacteriales;D_4__S15A-MN91;D_5__uncultured bacterium
26	D_0__Bacteria;D_1__Bacteroidetes;D_2__Sphingobacteriia;D_3__Sphingobacteriales;D_4__Saprospiraceae;D_5__Phaeodactylibacter
27	D_0__Bacteria;D_1__Bacteroidetes;D_2__Sphingobacteriia;D_3__Sphingobacteriales;D_4__Saprospiraceae;D_5__uncultured
28	D_0__Bacteria;D_1__Bacteroidetes;D_2__Sphingobacteriia;D_3__Sphingobacteriales;D_4__env.OPS 17;D_5__uncultured bacterium
29	D_0__Bacteria;D_1__Bacteroidetes;D_2__Sphingobacteriia;D_3__Sphingobacteriales;D_4__Sphingobacteriaceae;D_5__Pedobacter
30	D_0__Bacteria;D_1__Bacteroidetes;D_2__Sphingobacteriia;D_3__Sphingobacteriales;D_4__uncultured;D_5__uncultured bacterium
31	D_0__Bacteria;D_1__Bacteroidetes;D_2__Sphingobacteriia;D_3__Sphingobacteriales;Other;Other
32	D_0__Bacteria;D_1__Chlorobi;D_2__Chlorobia;D_3__Chlorobiales;D_4__OPB56;D_5__uncultured bacterium
33	D_0__Bacteria;D_1__Chlorobi;D_2__Chlorobia;D_3__Chlorobiales;D_4__OPB56;Other

Table B-5. Genus ID and corresponding name

<b>Genus ID</b>	<b>Genus name</b>
34	D_0__Bacteria;D_1__Chloroflexi;D_2__Anaerolineae;D_3__Anaerolineales;D_4__Anaerolineaceae;D_5__uncultured
35	D_0__Bacteria;D_1__Chloroflexi;D_2__TK10;Other;Other;Other
36	D_0__Bacteria;D_1__Deinococcus-Thermus;D_2__Deinococci;D_3__Deinococcales;D_4__Trueperaceae;D_5__Truepera
37	D_0__Bacteria;D_1__Firmicutes;D_2__Clostridia;D_3__Halanaerobiales;D_4__ODP1230B8.23;D_5__uncultured bacterium
38	D_0__Bacteria;D_1__Gemmatimonadetes;D_2__Gemmatimonadetes;D_3__Gemmatimonadales;D_4__Gemmatimonadaceae;D_5__Gemmatimonas
39	D_0__Bacteria;D_1__Ignavibacteriae;D_2__Ignavibacteria;D_3__Ignavibacteriales;D_4__PHOS-HE36;D_5__uncultured bacterium
40	D_0__Bacteria;D_1__Ignavibacteriae;D_2__Ignavibacteria;D_3__Ignavibacteriales;D_4__PHOS-HE36;Other
41	D_0__Bacteria;D_1__Nitrospirae;D_2__Nitrospira;D_3__Nitrospirales;D_4__Nitrospiraceae;D_5__Nitrospira
42	D_0__Bacteria;D_1__Parcubacteria;Other;Other;Other;Other
43	D_0__Bacteria;D_1__Parcubacteria;D_2__uncultured bacterium;D_3__uncultured bacterium;D_4__uncultured bacterium;D_5__uncultured bacterium
44	D_0__Bacteria;D_1__Planctomycetes;D_2__Planctomycetacia;D_3__Planctomycetales;D_4__Planctomycetaceae;D_5__Pirellula
45	D_0__Bacteria;D_1__Planctomycetes;D_2__Planctomycetacia;D_3__Brocadiales;D_4__Brocadiaceae;D_5__Candidatus Brocadia

**Table B-5. Genus ID and corresponding name**

<b>Genus ID</b>	<b>Genus name</b>
46	D_0__Bacteria;D_1__Proteobacteria;D_2__Alphaproteobacteria;D_3__Rhizobiales;D_4__Hyphomicrobiaceae;D_5__Hyphomicrobium
47	D_0__Bacteria;D_1__Proteobacteria;D_2__Alphaproteobacteria;D_3__Caulobacterales;D_4__Caulobacteraceae;D_5__Brevundimonas
48	D_0__Bacteria;D_1__Proteobacteria;D_2__Alphaproteobacteria;D_3__Parvularculales;D_4__Parvularculaceae;D_5__Amphiplicatus
49	D_0__Bacteria;D_1__Proteobacteria;D_2__Alphaproteobacteria;D_3__Rhodobacterales;D_4__Rhodobacteraceae;D_5__Amaricoccus
50	D_0__Bacteria;D_1__Proteobacteria;D_2__Alphaproteobacteria;D_3__Sphingomonadales;D_4__Sphingomonadaceae;D_5__Sphingopyxis
51	D_0__Bacteria;D_1__Proteobacteria;D_2__Betaproteobacteria;D_3__Burkholderiales;D_4__Comamonadaceae;D_5__Acidovorax
52	D_0__Bacteria;D_1__Proteobacteria;D_2__Betaproteobacteria;D_3__Burkholderiales;D_4__Burkholderiaceae;D_5__Lautropia
53	D_0__Bacteria;D_1__Proteobacteria;D_2__Betaproteobacteria;D_3__Burkholderiales;D_4__Burkholderiaceae;D_5__Limnobacter
54	D_0__Bacteria;D_1__Proteobacteria;D_2__Betaproteobacteria;D_3__Burkholderiales;D_4__Comamonadaceae;D_5__Comamonas
55	D_0__Bacteria;D_1__Proteobacteria;D_2__Betaproteobacteria;D_3__Burkholderiales;D_4__Comamonadaceae;D_5__Ottowia
56	D_0__Bacteria;D_1__Proteobacteria;D_2__Betaproteobacteria;D_3__Burkholderiales;D_4__Comamonadaceae;D_5__uncultured

Table B-5. Genus ID and corresponding name

<b>Genus ID</b>	<b>Genus name</b>
57	D_0__Bacteria;D_1__Proteobacteria;D_2__Betaproteobacteria;D_3__Burkholderiales;D_4__Comamonadaceae;Other
58	D_0__Bacteria;D_1__Proteobacteria;D_2__Betaproteobacteria;D_3__Hydrogenophilales;D_4__Hydrogenophilaceae;D_5__Thiobacillus
59	D_0__Bacteria;D_1__Proteobacteria;D_2__Betaproteobacteria;D_3__Hydrogenophilales;D_4__Hydrogenophilaceae;D_5__uncultured
60	D_0__Bacteria;D_1__Proteobacteria;D_2__Betaproteobacteria;D_3__Nitrosomonadales;D_4__Nitrosomonadaceae;D_5__Nitrosomonas
61	D_0__Bacteria;D_1__Proteobacteria;D_2__Betaproteobacteria;D_3__Rhodocyclales;D_4__Rhodocyclaceae;D_5__Azoarcus
62	D_0__Bacteria;D_1__Proteobacteria;D_2__Betaproteobacteria;D_3__Rhodocyclales;D_4__Rhodocyclaceae;D_5__Dechloromonas
63	D_0__Bacteria;D_1__Proteobacteria;D_2__Betaproteobacteria;D_3__Rhodocyclales;D_4__Rhodocyclaceae;D_5__Denitromonas
64	D_0__Bacteria;D_1__Proteobacteria;D_2__Betaproteobacteria;D_3__Rhodocyclales;D_4__Rhodocyclaceae;D_5__Sulfuritalea
65	D_0__Bacteria;D_1__Proteobacteria;D_2__Betaproteobacteria;D_3__Rhodocyclales;D_4__Rhodocyclaceae;D_5__Thauera
66	D_0__Bacteria;D_1__Proteobacteria;D_2__Betaproteobacteria;D_3__Rhodocyclales;D_4__Rhodocyclaceae;D_5__Zoogloea
67	D_0__Bacteria;D_1__Proteobacteria;D_2__Betaproteobacteria;D_3__Rhodocyclales;D_4__Rhodocyclaceae;D_5__uncultured

Table B-5. Genus ID and corresponding name

<b>Genus ID</b>	<b>Genus name</b>
68	D_0__Bacteria;D_1__Proteobacteria;D_2__Betaproteobacteria;D_3__Rhodocyclales;D_4__Rhodocyclaceae;Other
69	D_0__Bacteria;D_1__Proteobacteria;D_2__Deltaproteobacteria;D_3__Myxococcales;D_4__BIRii41;D_5__uncultured bacterium
70	D_0__Bacteria;D_1__Proteobacteria;D_2__Deltaproteobacteria;D_3__Myxococcales;D_4__Haliangiaceae;D_5__Haliangium
71	D_0__Bacteria;D_1__Proteobacteria;D_2__Deltaproteobacteria;D_3__Myxococcales;D_4__Nannocystaceae;D_5__Nannocystis
72	D_0__Bacteria;D_1__Proteobacteria;D_2__Deltaproteobacteria;D_3__Myxococcales;D_4__P3OB-42;Other
73	D_0__Bacteria;D_1__Proteobacteria;D_2__Deltaproteobacteria;D_3__Myxococcales;D_4__Phaselicytidaceae;D_5__Phaselicystis
74	D_0__Bacteria;D_1__Proteobacteria;D_2__Deltaproteobacteria;D_3__Myxococcales;D_4__Sandaracinaceae;D_5__Sandaracinus
75	D_0__Bacteria;D_1__Proteobacteria;D_2__Epsilonproteobacteria;D_3__Campylobacteriales;D_4__Campylobacteraceae;D_5__Arcobacter
76	D_0__Bacteria;D_1__Proteobacteria;D_2__Gammaproteobacteria;D_3__Cellvibrionales;D_4__Spongiibacteraceae;D_5__BD1-7 clade
77	D_0__Bacteria;D_1__Proteobacteria;D_2__Gammaproteobacteria;D_3__Chromatiales;D_4__Chromatiaceae;D_5__Rheinheimera
78	D_0__Bacteria;D_1__Proteobacteria;D_2__Gammaproteobacteria;D_3__Oceanospirillales;D_4__Halomonadaceae;D_5__Halomonas

Table B-5. Genus ID and corresponding name

Genus ID	Genus name
79	D_0__Bacteria;D_1__Proteobacteria;D_2__Gammaproteobacteria;D_3__Pseudomonadales;D_4__Moraxellaceae;D_5__Acinetobacter
80	D_0__Bacteria;D_1__Proteobacteria;D_2__Gammaproteobacteria;D_3__Pseudomonadales;D_4__Moraxellaceae;D_5__[Agitococcus] lubricus group
81	D_0__Bacteria;D_1__Proteobacteria;D_2__Gammaproteobacteria;D_3__Pseudomonadales;D_4__Pseudomonadaceae;D_5__Pseudomonas
82	D_0__Bacteria;D_1__Proteobacteria;D_2__Gammaproteobacteria;D_3__Xanthomonadales;D_4__Xanthomonadaceae;D_5__Arenimonas
83	D_0__Bacteria;D_1__Proteobacteria;D_2__Gammaproteobacteria;D_3__Xanthomonadales;D_4__Xanthomonadaceae;D_5__Dokdonella
84	D_0__Bacteria;D_1__Proteobacteria;D_2__Gammaproteobacteria;D_3__Xanthomonadales;D_4__Xanthomonadales Incertae Sedis;D_5__Plasticicumulans
85	D_0__Bacteria;D_1__Proteobacteria;D_2__Gammaproteobacteria;D_3__Xanthomonadales;D_4__uncultured;D_5__uncultured bacterium
86	D_0__Bacteria;D_1__Proteobacteria;D_2__Gammaproteobacteria;D_3__Xanthomonadales;D_4__uncultured;D_5__uncultured soil bacterium
87	D_0__Bacteria;D_1__SR1 (Absconditabacteria);D_2__uncultured candidate division SR1 bacterium;D_3__uncultured candidate division SR1 bacterium;D_4__uncultured candidate division SR1 bacterium;D_5__uncultured candidate division SR1 bacterium
88	D_0__Bacteria;D_1__Saccharibacteria;D_2__uncultured bacterium;D_3__uncultured bacterium;D_4__uncultured bacterium;D_5__uncultured bacterium

Table B-5. Genus ID and corresponding name

<b>Genus ID</b>	<b>Genus name</b>
<b>89</b>	D_0__Bacteria;D_1__Spirochaetae;D_2__Spirochaetes;D_3__Spirochaetales;D_4__Leptospiraceae;D_5__Turneriella
<b>90</b>	D_0__Bacteria;D_1__Synergistetes;D_2__Synergistia;D_3__Synergistales;D_4__Synergistaceae;D_5__uncultured
<b>91</b>	D_0__Bacteria;D_1__Thermotogae;D_2__Thermotogae;D_3__Petrotogales;D_4__Petrotogaceae;D_5__SC103
<b>92</b>	D_0__Bacteria;D_1__Verrucomicrobia;D_2__OPB35 soil group;D_3__uncultured bacterium;D_4__uncultured bacterium;D_5__uncultured bacterium
<b>93</b>	D_0__Bacteria;D_1__Verrucomicrobia;D_2__Verrucomicrobiae;D_3__Verrucomicrobiales;D_4__Verrucomicrobiaceae;D_5__Prostheco bacter
<p>Note : *D_0 gives the Kingdom, D_1 gives the Phylum, D_2 gives the class, D_3 is the order, D_4 is the Family that the genus (D_5) belongs to .</p>	

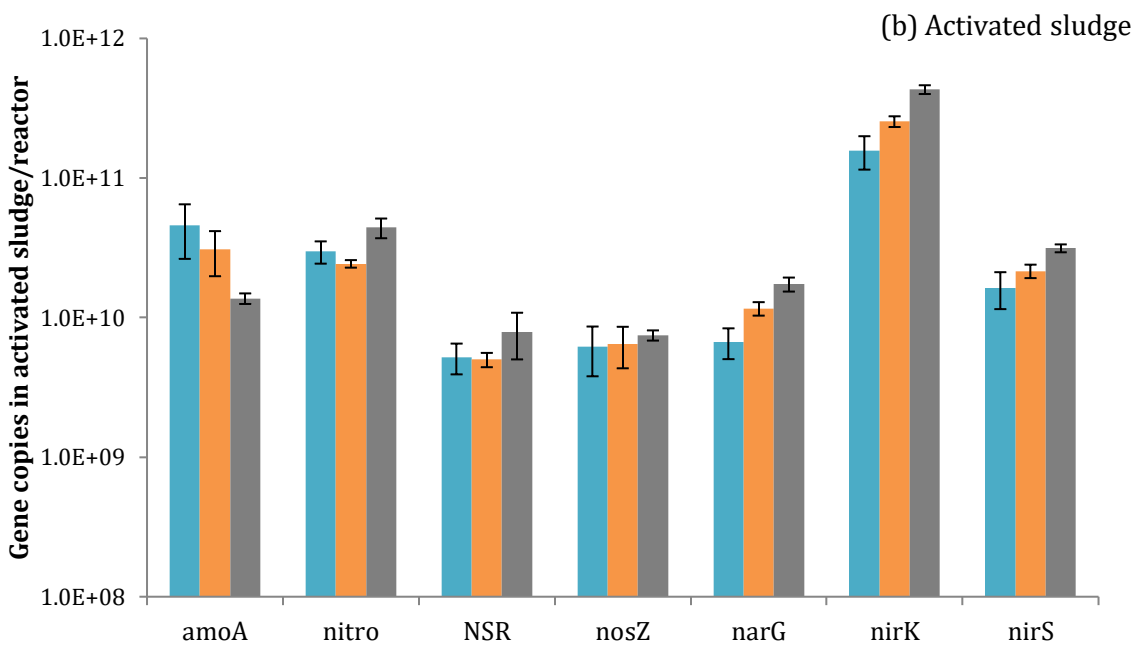
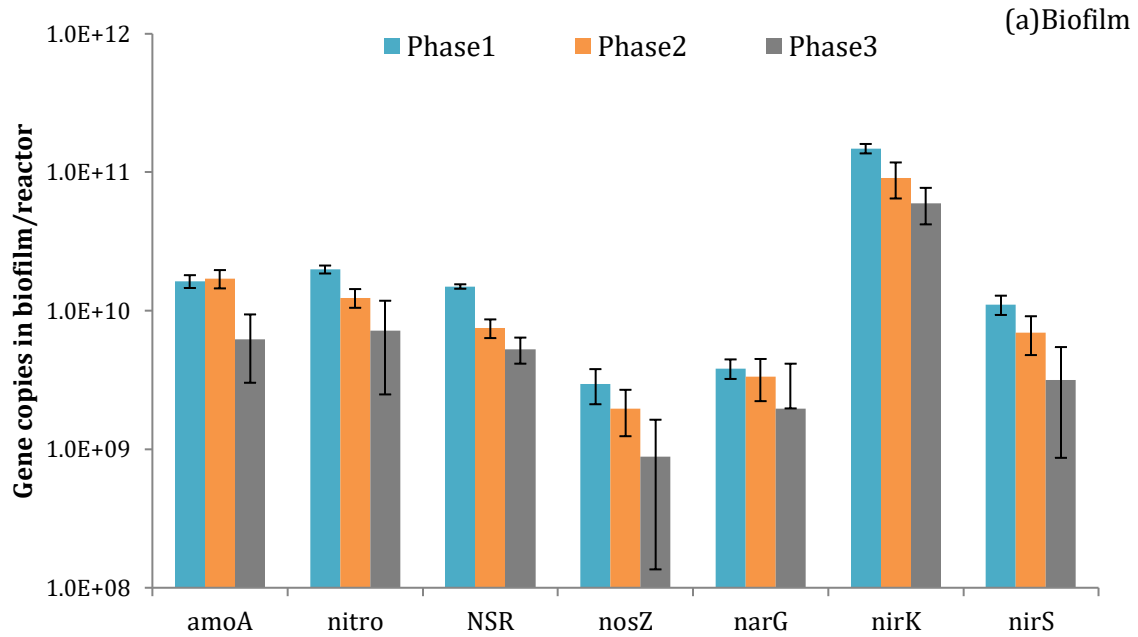
**Table B-6. Zeta potentials of EPS samples and surrogates in 10 mM NaCl**

	Sample description	Zeta-potential
<b>Nitritation</b>	Sludge LB-EPS	$-6.5 \pm 2.2$
	Sludge TB-EPS	$-16.9 \pm 1.2$
	Biofilm LB-EPS	$-14.0 \pm 3.0$
	Biofilm TB-EPS	$-12.5 \pm 0.4$
<b>Nitrification</b>	Sludge LB-EPS	$-25.4 \pm 1.7$
	Sludge TB-EPS	$-13.1 \pm 0.7$
	Biofilm LB-EPS	$-3.8 \pm 0.5$
	Biofilm TB-EPS	$-20.7 \pm 0.3$
<b>Surrogates</b>	Glucose	$-8.3 \pm 1.2$
	BSA	$-7.3 \pm 0.7$

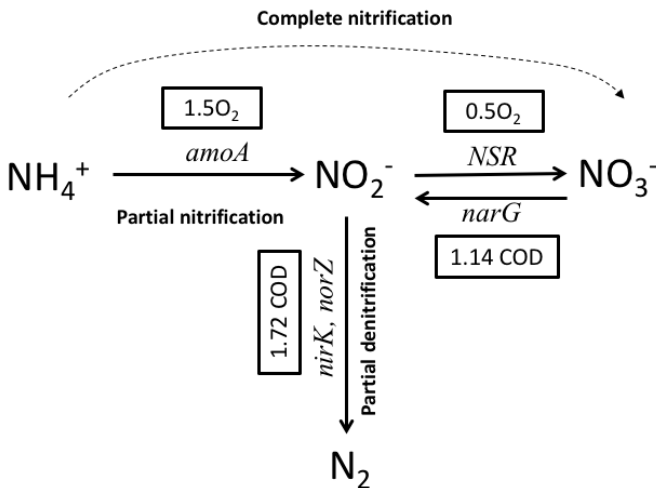


## Appendix C – Supporting figures

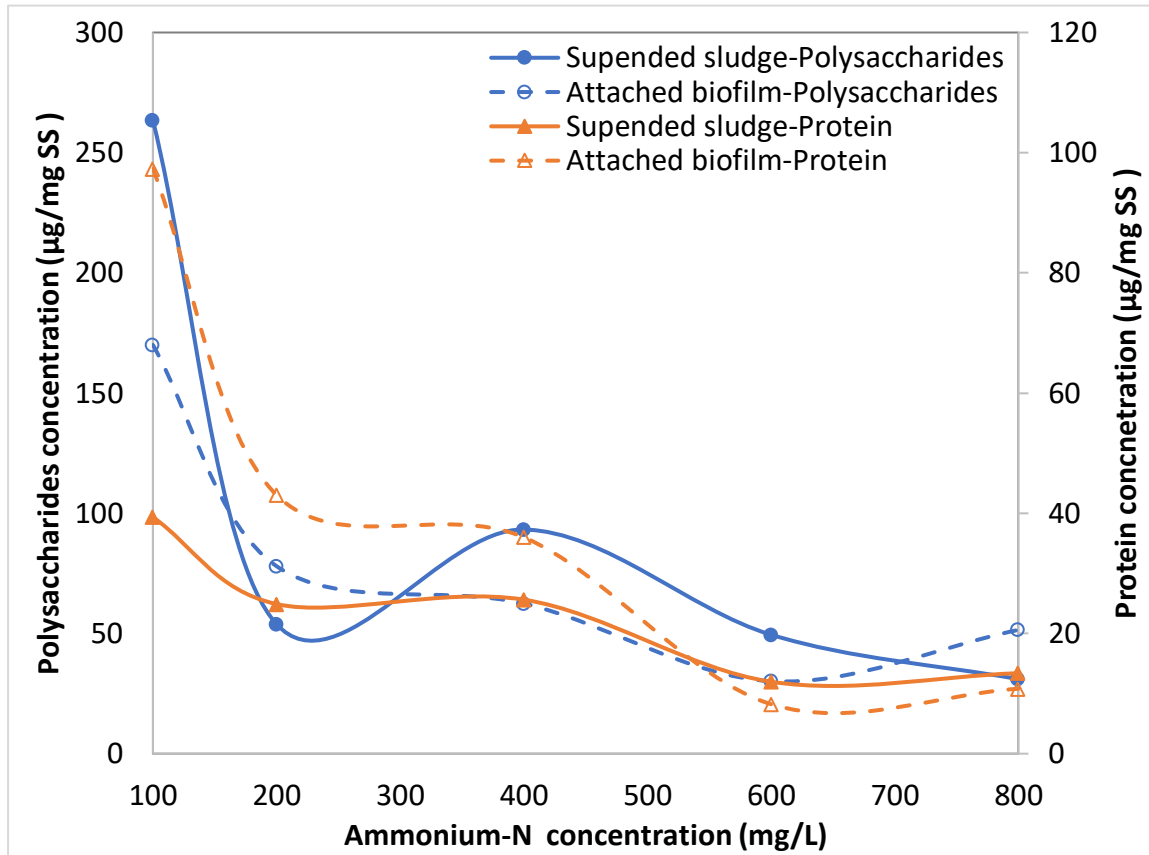
The qPCR results are shown in following figures:



**Figure C-1.** (a) AOB (*amoA* gene), NOB (nitro and NSR gene), and denitrifier gene copies distributions in biofilm and (b) AOB, NOB, and denitrifier gene copies distributions in activated sludge during three reaction phases.



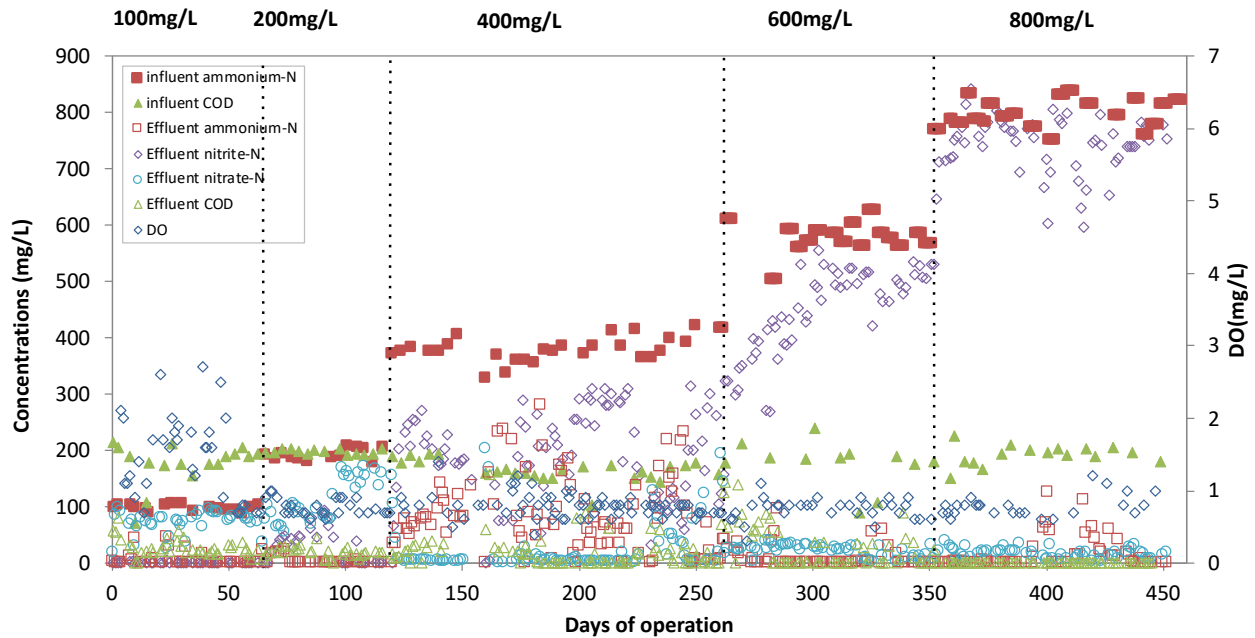
**Figure C-2.** The schematic diagram of complete nitrification, partial nitrification and partial denitrification processes. The genes that encoded the enzyme for each step were displayed in italic, and the oxygen or COD demand for each step were also included in the figure.



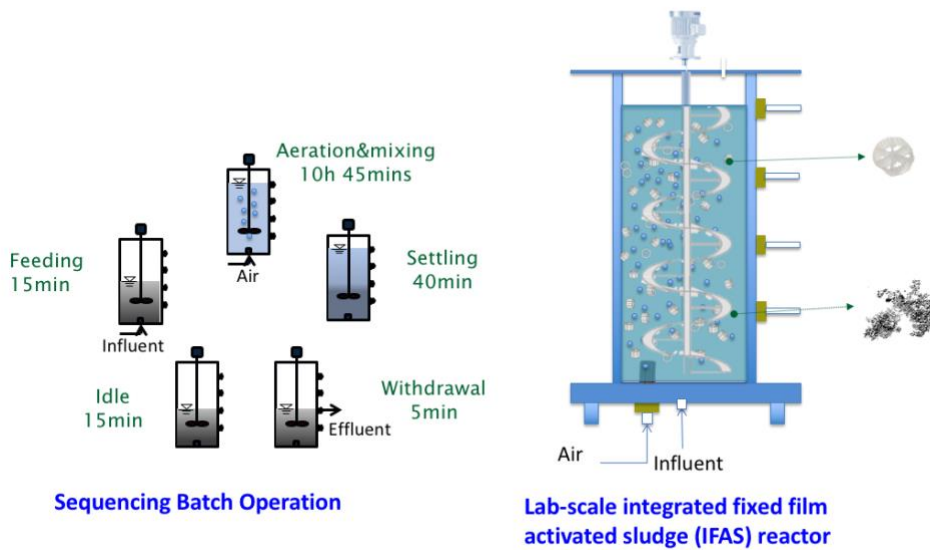
**Figure C-3.** Comparison of EPS from biofilm and suspended sludge. The production of protein is shown in red, and polysaccharides in the EPS are shown in blue. Dashed lines represent biofilm data and solid lines represent suspended sludge data.



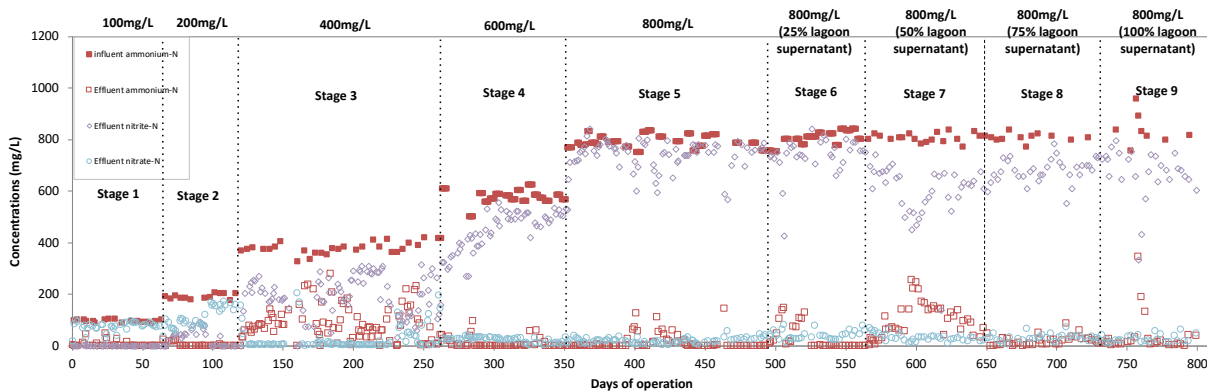
**Figure C-4.** Set up of the batch test bottles, each bottle was in triplicates.



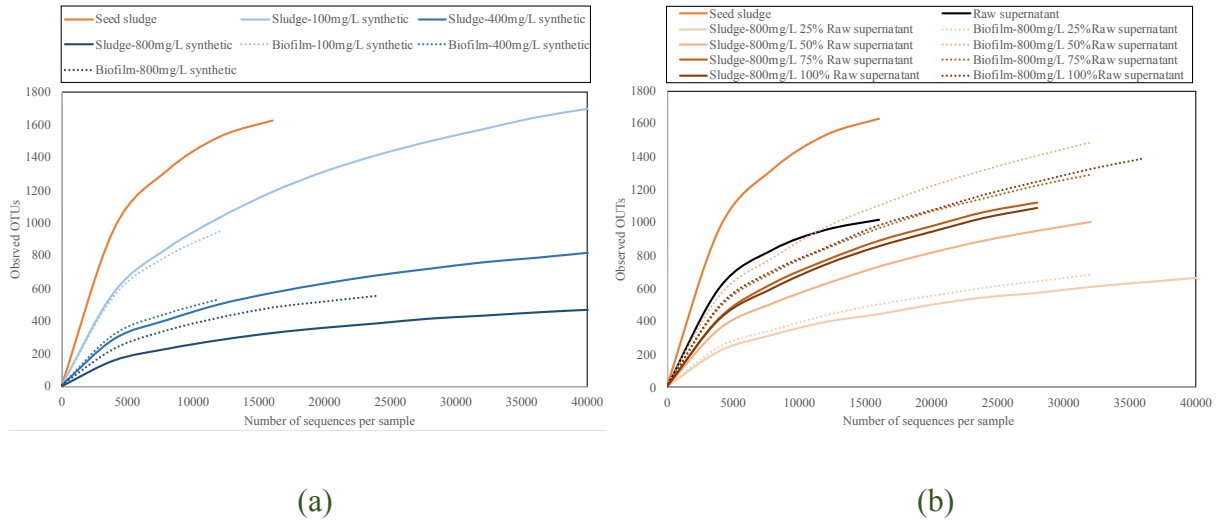
**Figure C-5.** The performance results of the nitritation reactor. The 100mg/L to 800mg/L on the top of the figure give the concentration of  $\text{NH}_4^+\text{-N}$  in the feeding. The solid red squares indicate the  $\text{NH}_4^+\text{-N}$  concentration in the influent; the solid green triangles give the COD concentration in the influent; the empty red squares give the  $\text{NH}_4^+\text{-N}$  concentration in the effluent; the empty purple diamonds indicate the nitrite-N concentration in the effluent; the empty blue circles give the nitrate-N concentration in the effluent, the empty green triangles are the COD concentration in the effluent, and the solid blue diamonds are the DO level in the reactor during reactor.



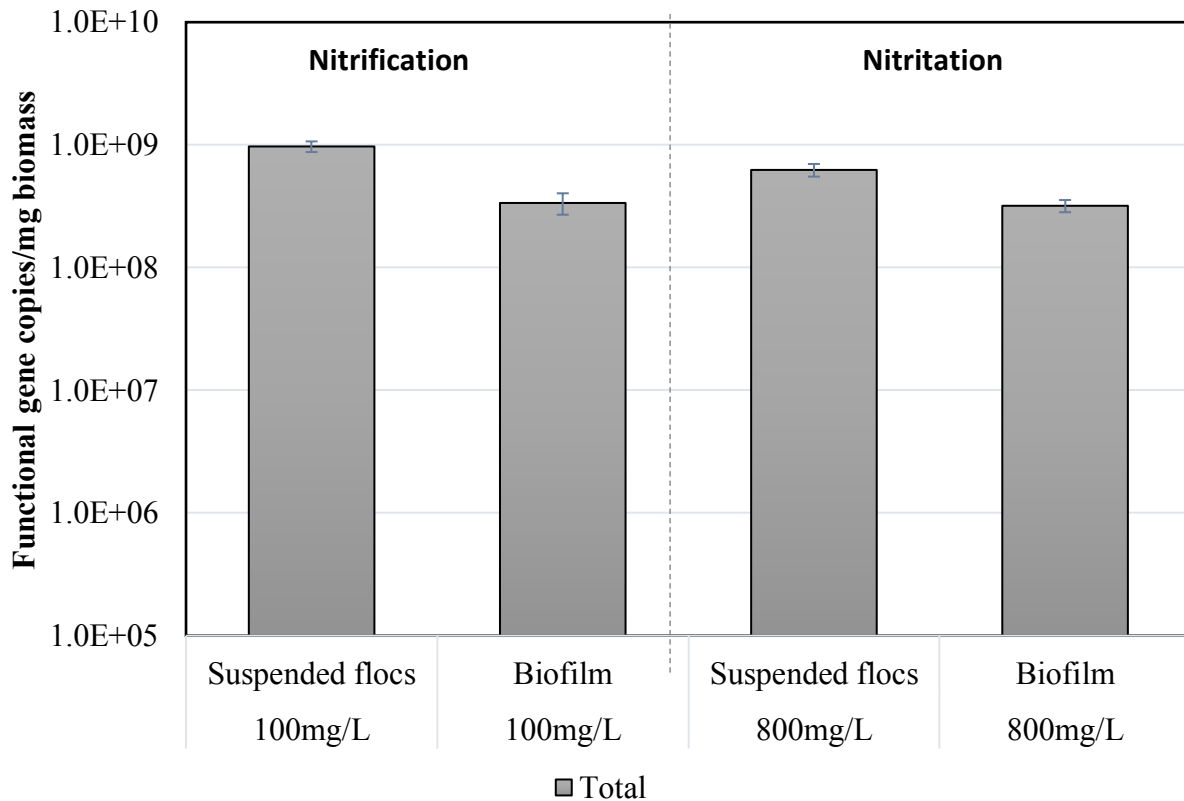
**Figure C-6.** The schematic diagram of the integrated fixed film activated sludge (IFAS) reactor and the time sequences for one cycle of sequencing batch operation.



**Figure C-7.** The performance results for the reactor shows that both reactors achieved partial nitrification when the  $\text{NH}_4^+$ -N concentration in the feed was 400 mg/L.



**Figure C-8.** Rarefaction plot (a) for seed sludge and samples collected during phases 1, 3, 5 from R1. Plot (b) shows the diversity for seed sludge, raw supernatant and samples collected from stages 6-9 from R1. The curves that do not reach the right end of the plot indicating that the sequences detected in the samples were less than 40000.



**Figure C-9.** Abundance of the 16s rRNA genes of total bacteria in the suspended flocs and biofilm samples under nitrification and nitritation conditions.

## References

- Anthonisen, A.C., Loehr, R.C., Prakasam, T.B.S., Srinath, E.G., 1976. Inhibition of Nitrification by Ammonia and Nitrous Acid. *J. Water Pollut. Control Fed.* 48, 835–852.
- Ciudad, G., Rubilar, O., Muñoz, P., Ruiz, G., Chamy, R., Vergara, C., Jeison, D., 2005. Partial nitrification of high ammonia concentration wastewater as a part of a shortcut biological nitrogen removal process. *Process Biochem.* 40, 1715–1719. <https://doi.org/10.1016/j.procbio.2004.06.058>
- Droppo, I.G., Liss, S.N., Cheung, M., Leppard, G.G., Liao, B., Bura, R., Finlayson, J., Lee, B.C., 1998. Composition of extracellular polymeric substances in the activated sludge floc matrix. *Water Sci. Technol.* 37, 325.

- Ge, S., Peng, Y., Qiu, S., Zhu, A., Ren, N., 2014. Complete nitrogen removal from municipal wastewater via partial nitrification by appropriately alternating anoxic/aerobic conditions in a continuous plug-flow step feed process. *Water Res.* 55, 95–105. <https://doi.org/10.1016/j.watres.2014.01.058>
- Gustavsson, D.J.I., 2010. Biological sludge liquor treatment at municipal wastewater treatment plants – a review. *Vatten* 66, 179–192.
- Imhoff, J., 2016. New Dimensions in Microbial Ecology—Functional Genes in Studies to Unravel the Biodiversity and Role of Functional Microbial Groups in the Environment. *Microorganisms* 4, 19. <https://doi.org/10.3390/microorganisms4020019>
- Kim, H., Gellner, J.W., Boltz, J.P., Freudenberg, R.G., Gunsch, C.K., Schuler, A.J., 2010. Effects of integrated fixed film activated sludge media on activated sludge settling in biological nutrient removal systems. *Water Res.* 44, 1553–1561. <https://doi.org/10.1016/j.watres.2009.11.001>
- Kim, H., Schuler, A.J., Gunsch, C.K., Pei, R., Gellner, J., Boltz, J.P., Freudenberg, R.G., Dodson, R., 2011. Comparison of Conventional and Integrated Fixed-Film Activated Sludge Systems: Attached- and Suspended-Growth Functions and Quantitative Polymerase Chain Reaction Measurements. *Water Environ. Res.* 83, 627–635. <https://doi.org/10.2175/106143010X12851009156448>
- Kim, Y.M., Lee, D.S., Park, C., Park, D., Park, J.M., 2011. Effects of free cyanide on microbial communities and biological carbon and nitrogen removal performance in the industrial activated sludge process. *Water Res.* 45, 1267–1279. <https://doi.org/10.1016/j.watres.2010.10.003>
- Kouba, V., Catrysse, M., Stryjova, H., Jonatova, I., Volcke, E.I.P., Svehla, P., Bartacek, J., 2014. The impact of influent total ammonium nitrogen concentration on nitrite-oxidizing bacteria inhibition in moving bed biofilm reactor. *Water Sci. Technol.* 69, 1227. <https://doi.org/10.2166/wst.2013.757>
- Liang, Z., Li, W., Yang, S., Du, P., 2010. Extraction and structural characteristics of extracellular polymeric substances (EPS), pellets in autotrophic nitrifying biofilm and activated sludge. *Chemosphere* 81, 626–632. <https://doi.org/10.1016/j.chemosphere.2010.03.043>



- Liao, B.Q., Allen, D.G., Droppo, I.G., Leppard, G.G., Liss, S.N., 2001. Surface properties of sludge and their role in bioflocculation and settleability. *Water Res.* 35, 339–350.
- Loosdrecht, M.C.M. van, Nielsen, P.H., Lopez-Vazquez, C.M., Brdjanovic, D. (Eds.), 2016. *Experimental methods in wastewater treatment*. IWA Publishing, London.
- Martinez, F., Gomez, J., Favela-Torres, E., 2000. Oscillations of exopolymeric composition and sludge volume index in nitrifying flocs. *Appl. Biochem. Biotechnol.* 87, 177–188.
- Mincer, T.J., Church, M.J., Taylor, L.T., Preston, C., Karl, D.M., DeLong, E.F., 2007. Quantitative distribution of presumptive archaeal and bacterial nitrifiers in Monterey Bay and the North Pacific Subtropical Gyre. *Environ. Microbiol.* 9, 1162–1175. <https://doi.org/10.1111/j.1462-2920.2007.01239.x>
- Muyzer, G.; de waal, E.C. and uittierlinden, A.G. (1993). Profiling of complex microbial populations by denaturing gradient gel electrophoresis analysis of polymerase chain reaction-amplified genes coding for 16S rRNA. *Applied and Environmental Microbiology.* 59 (3), 695-700.
- Muyzer, G.; Teske, A.; Wirsén, C. and Jannasch, H. (1995). Phylogenetic relationships of *Thiomicrospira* species and their identification in deep-sea hydrothermal vent samples by denaturing gradient gel electrophoresis of 16S rDNA fragments. *Archives of Microbiology.* 164(3), 165-172.
- Peng, Y., Zhu, G., 2006. Biological nitrogen removal with nitrification and denitrification via nitrite pathway. *Appl. Microbiol. Biotechnol.* 73, 15–26. <https://doi.org/10.1007/s00253-006-0534-z>
- Picioreanu, C., Van Loosdrecht, M.C.M., Heijnen, J.J., 1997. Modelling the effect of oxygen concentration on nitrite accumulation in a biofilm airlift suspension reactor, in: Harremoës, P. (Ed.), *Biofilm Systems*. Presented at the WATER SCIENCE AND TECHNOLOGY, Pergamon, pp. 147–156.
- Risgaard-Petersen, N., Nicolaisen, M.H., Revsbech, N.P., Lomstein, B.A., 2004. Competition between Ammonia-Oxidizing Bacteria and Benthic Microalgae. *Appl. Environ. Microbiol.* 70, 5528–5537. <https://doi.org/10.1128/AEM.70.9.5528-5537.2004>
- Shao, Y., Shi, Y., Mohammed, A., Liu, Y., 2017. Wastewater ammonia removal using an integrated fixed-film activated sludge-sequencing batch biofilm reactor (IFAS-SBR): Comparison of

- suspended flocs and attached biofilm. *Int. Biodeterior. Biodegrad.* 116, 38–47. <https://doi.org/10.1016/j.ibiod.2016.09.026>
- Sheng, G.-P., Yu, H.-Q., Li, X.-Y., 2010. Extracellular polymeric substances (EPS) of microbial aggregates in biological wastewater treatment systems: A review. *Biotechnol. Adv.* 28, 882–894. <https://doi.org/10.1016/j.biotechadv.2010.08.001>
- Shin, H.S., Kang, S.T., Nam, S.Y., 2001. Effect of carbohydrate and protein in the EPS on sludge settling characteristics. *Water Sci. Technol. J. Int. Assoc. Water Pollut. Res.* 43, 193–196.
- Smolders, G.J.F., van der Meij, J., van Loosdrecht, M.C.M., Heijnen, J.J., 1994. Model of the anaerobic metabolism of the biological phosphorus removal process: Stoichiometry and pH influence. *Biotechnol. Bioeng.* 43, 461–470. <https://doi.org/10.1002/bit.260430605>
- van den Akker, B., Beard, H., Kaeding, U., Giglio, S., Short, M.D., 2010. Exploring the relationship between viscous bulking and ammonia-oxidiser abundance in activated sludge: A comparison of conventional and IFAS systems. *Water Res.* 44, 2919–2929. <https://doi.org/10.1016/j.watres.2010.02.016>
- Wei, D., Du, B., Xue, X., Dai, P., Zhang, J., 2014. Analysis of factors affecting the performance of partial nitrification in a sequencing batch reactor. *Appl. Microbiol. Biotechnol.* 98, 1863–1870. <https://doi.org/10.1007/s00253-013-5135-z>
- Wen, X., Gong, B., Zhou, J., He, Q., Qing, X., 2017. Efficient simultaneous partial nitrification, anammox and denitrification (SNAD) system equipped with a real-time dissolved oxygen (DO) intelligent control system and microbial community shifts of different substrate concentrations. *Water Res.* 119, 201–211. <https://doi.org/10.1016/j.watres.2017.04.052>
- Yin, X., Qiao, S., Zhou, J., 2016. Effects of cycle duration of an external electrostatic field on anammox biomass activity. *Sci. Rep.* 6, 19568. <https://doi.org/10.1038/srep1956>

